3-24-2018

Synthesis, Characterization, and Assessment of Cationic Polypeptoids Toward Gene Delivery and Development of Air Stable N-Substituted N-Thiocarboxyanhydrides

Jessica Michelle Simpson
Louisiana State University and Agricultural and Mechanical College, jsimp28@lsu.edu

SYNTHESIS, CHARACTERIZATION, AND ASSESSMENT OF CATIONIC
POLYPEPTOIDS TOWARDS GENE DELIVERY AND DEVELOPMENT OF AIR STABLE
N-SUBSTITUTED *N*-THIOCARBOXYANHYDRIDES

A Dissertation

Submitted to the Graduate Faculty of the
Louisiana State University and
Agricultural and Mechanical College
in partial fulfillment of the
requirements for the degree of
Doctor of Philosophy

in

The Department of Chemistry

by
Jessica Michelle Simpson
B.S., Fort Valley State University, 2012
May 2018

ACKNOWLEDGEMENTS

TABLE OF CONTENTS

LIST OF ACRONYMS

AEE………………………….............2-[1-(2-Amino-ethoxy)-1-methyl-ethoxy]-ethylamine

AFM ....Atomic force microscopy

Al-NTA…………………………………………………….*N*-Allyl *N*-thiocarboxyanhydride

AMM…………………………………………………….....Activated monomer mechanism

BnNH$_2$..Benzyl amine

CDCl$_3$ ....Deuterated chloroform

CD$_2$Cl$_2$...Deuterated methylene chloride

CHCl$_3$……………………………………………………………Chloroform

COO……………………………………………………………….Carboxy dioxide

COS………………………………………………………………Carboxy oxysulfide

CuAAC…………………………………………….…Copper catalyzed alkyne-azide cycloaddition

CMC…………………………………………………………….Critical micelle concentration

DCM…………………………………………………………….Dichloromethane

De-NCA..*N*-decyl *N*-carboxyanhydride

DI………………………………………………………………….Deionized water

DLS………………………………………………………………Dynamic light scattering

DMEM…………………………………………………………..Dulbecco's modified eagle medium

DMF………………………………………………………….….Dimethylformamide

DNA……………………………………………………………..Deoxyribonucleic acid

DP……………………………………………………….…… Degree of polymerization

DRI………………………………………………………………Differential refractive index

DTT..DL-Dithiothreitol

EB……………………………………………………………………Ethium bromide

ECM……………………………………………………………….Extracellular Matrix

ESI MS……………………………………………………....…Electrospray ionization mass spectroscopy

ABSTRACT

Peptoids are a class of peptidomimetic polymers, which have attracted much attention over the years. Due to their structural similarity to peptides, this group of polymers affords good biocompatibility making them of interest for biomedical applications. This dissertation is largely about the design, synthesis, and characterization of cationic polypeptoids for biological applications, particularly nonviral gene delivery. The dissertation will also cover the development, characterization, and polymerization behavior of a new, air stable *N*-thiocarboxyanhydride (NTA) monomer.

Introducing functionality, such as small biomolecules and organic compounds can provide distinctive properties to the polymers. Chapter 1 introduces gene therapy and concepts pertinent to the topic. Cell transfection and methods and techniques used to carry out the process are described along with their associated advantages and disadvantages.

Chapter 2 provides an overview on the fundamental aspects of polypeptoids as well as previous and recent developments in synthetic strategies, post-polymerization modification, and biological applications in various fields.

Chapter 3 describes the development of cationic polypeptoids by traditional polymerization and post-functionalization methods. Analogue's gene delivery capabilities demonstrated in this chapter establish the potential of this peptidomimetic class of polymers as carriers for gene delivery. Work presented in chapter 4 emphasizes more on the application attribute of cationic polypeptoids via delivery of TNF-α siRNA for effective knockdown of systemic inflammation.

Based upon studies done in chapters 3-4, chapter 5 explores a new direction of varying polymer architectures. The effect of architecture on the nonviral gene delivery of diblock copolypeptoids in serum was assessed.

Research foci of Chapter 6 pertains to the development, characterization, and polymerization of new, *N*-Allyl *N*-thiocarboxyanhydride (Al-NTA), the mercapto analog of the corresponding NCA. The NTA exhibited enhanced moisture-stability but reduced polymerization activities relative to the NCA analogs.

CHAPTER 1: INTRODUCTION TO GENE THERAPY

1.1 Purpose

This chapter will introduce gene therapy and provide an overview of the concepts relevant to the topic and problems in the field, particularly with cell transfection. Aspects essential to the cell transfection process including methods used, carrier types, and associated advantages and disadvantages will be discussed. Recent developments in the design and synthesis of carriers for gene delivery will also be mentioned.

1.2 Overview of Gene Therapy

In the late 20th century, the concept of gene therapy (GT) research was first introduced by pioneers Theodore Friedmann and Richard Roblin in a landmark paper.[1] Initially the primary focus of gene therapy was geared towards correcting inherited genetic disorders. However, as new and rare diseases began to appear, gene therapy becomes increasingly relevant. GT is typically achieved by two technologies, germline and somatic. Whereas germline GT offers a means to correction or the permanent elimination of a genetic abnormality via direct manipulation of germline cells (eggs and sperm), somatic GT involves the insertion of genes into the nonreproductive diploid cells of an individual, thus providing an indirect approach for addressing genetic malfunctions. The major difference among the two methods is that unlike with germline GT, results from somatic therapy are restricted to the patient and are not passed on to their offspring. Though potentially useful, germline gene therapy is considered unethical and has never actually been performed on humans. For this reason, somatic gene therapy is more commonly practiced on individuals with fewer associated risks than the former method.

Within somatic gene therapy, various types of treatment for different disorders are readily available. To access the efficacy of gene therapy under different conditions, gene delivery experiments were conducted under *ex vivo*, *in situ*, and *in vivo* conditions. Under *ex vivo* conditions, experiments and measurements are performed outside of the organism. The *ex vivo* procedures allow the manipulation of cells and tissues to be carried out in an uncontrolled fashion. Fluctuations in cell culture conditions externally (temperature, pH, etc.) are a major disadvantage of *ex vivo* delivery that can possibly lead to disrupted host cell division. *In vitro* delivery is the commonly used type of *ex vivo* experiment where the measurement of gene expression is observed using cells of a specific cell line. In the course of *in situ* experiments, a specific gene or protein is studied in its natural context. This method is advantageous in that a consistent environment for observing is maintained by minimizing the chances of disruption in original conditions. The *in vivo* delivery method is characterized by the use of a live animal to study behavior or how different genes can affect the entire organism. During experiments the transference of genetic material to cells takes place while still inside of the patient or subject's body. *In vivo* delivery is most relevant to assess the efficacy of gene therapy since ultimately the delivery has to occur in an organism. All levels of gene therapy experiments are based on the process of cell transfection as shown in Figure 1.1.
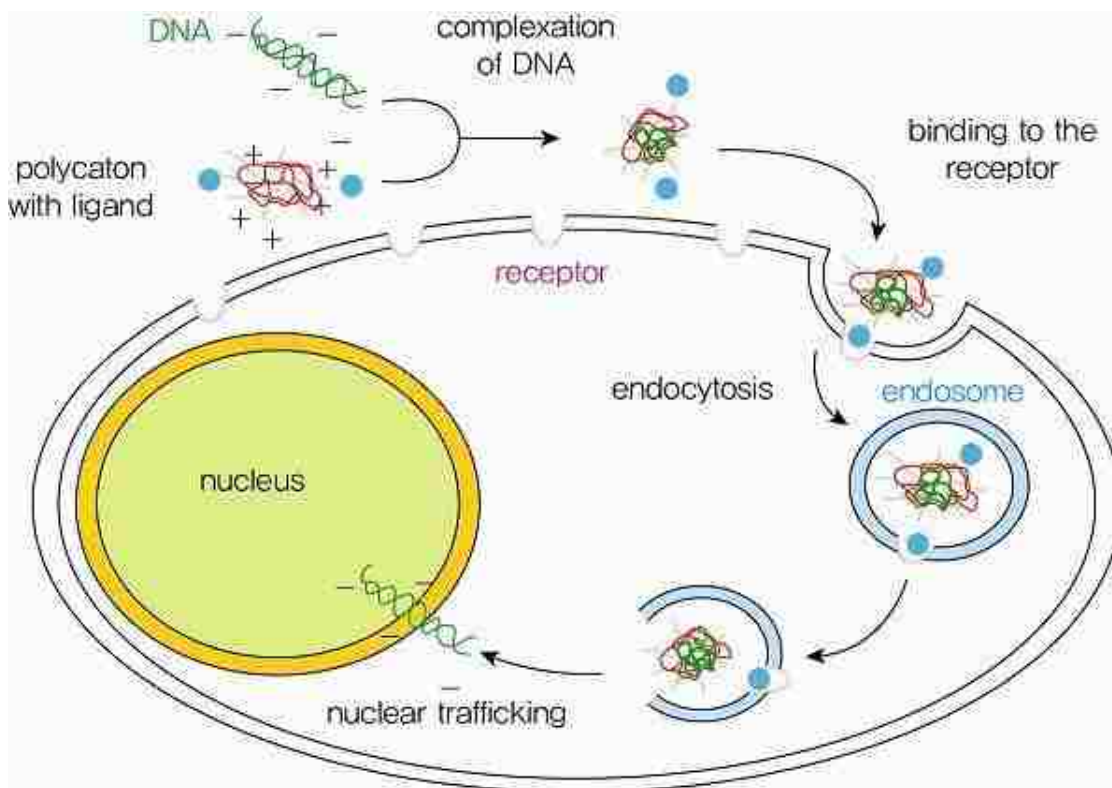
Figure 1.1. Nonviral cell transfection process.

1.3 Cell Transfection Process and Techniques Used

Significant progress has been made in gene therapy over the years including the successful treatment of congenital disease, adenoside deaminase severe combined immunodeficiency (ADA-SCID).[2,3] However, the safe and efficient delivery of intracellular material remains a subject of intensive investigation and great concern. Studies indicate that the gene transfection efficacy to be dependent on multiple factors such as the binding of nucleic acid with transport carrier (complexation), cell recognition, uptake of components by the cell, and the release of genetic material (decomplexation) at targeted sites. Moreover, in the case of treating conditions requiring cell or tissue

specificity (i.e. cancer), incorporation of cell-specific ligands in the carrier design can overcome the challenge of selectivity. Defined by the deliberate act of introducing nucleic acid into eukaryotic cells, cell transfection relies on the proper genome insertion and expression of genetic material. Depending on the nucleic acid being delivered the process of transfection may take place in either the cytosol (for RNA) or nuclear domains (for DNA). Classified into three categories (biological, physical, and chemical), available methods for gene delivery offer a broad range of options for the transport of nucleic acids to subcellular regions in cells.[4] Virus-mediated transfection is the only biological method available for treatment. Considered the most effective for gene delivery due to their biological occurrence, viral carriers easily avoid both extracellular and intracellular barriers presented *in vivo* which enable their excellent gene delivery performance. However, limited cargo loading and the tendency of viruses to simultaneously mutate resulting in cytotoxicity and undesired immune response have restricted their clinical applicability. Physical approaches for transfection include electroporation, gene gun, sonoporation, and magnetofection. Advantages of these methods are the direct transfer of nucleic acids into the cytoplasm or nucleus via noninvasive procedures for transfection. The inability to access internal organs, expensive instrumentation, and sample damage are the major drawbacks that limit the practical use of these methods. In chemical methods for transfection, the transfer of nucleic acids into the cytoplasm or nucleus is achieved by means of a foreign carrier (i.e. biomolecules, lipids, polymers, etc). Among all the approaches, non-viral delivery methods have shown to be very promising due to the inherent synthetic versatility and tunability.

1.4. Nonviral Cell Transfection Carriers and Associated Milestones

Gene carriers for cell transfection have included the use of non-viral based materials such as lipids, peptides, and polymers.[5-7] Each class of carrier materials has presented advantages useful for gene delivery. As one of the most extensively investigated and commonly used nonviral gene delivery method, cationic lipids have the ability to complex with negatively charged nucleic acid to induce cellular uptake and endosomal escape. However, low transfection efficiency, toxicity, colloidal instability, and short duration of gene expression are major hurdles that limit practical use of lipoplex-mediated transfection. Due to their high net positive charge, a systemic elimination of cationic lipids occurs upon formation of larger aggregates via their interactions with the negatively charged serum molecules or cellular components. This drawback of fast clearance from circulation limits their utility in gene delivery to cells located beyond vascular endothelial cells.[28] Polypeptides have been widely used as materials for gene delivery based on their innate ability to adopt ordered conformations (α-helices and β-sheets). This unique characteristic can aid with the effective complexation of DNA.[36] Though highly compatible and effective, issues such as cytotoxicity and proteolytic instability restrict their use in biomedical applications. Strategies such as retroinversion of cell penetrating peptides (CPPs) sequence and/or the conversion to β-peptides have been investigated in order to overcome these challenges.[8] Unfortunately, this development only led to increased cell toxicity. In comparison to synthetic carriers, viral vectors offer excellent transfection efficiency.[9,11] However, viral degradation, repeated dosage, and the risk of attacking non-diseased cells limit the use of viruses as gene delivery vehicles.[9-12] Researchers have since then

navigated towards the conjugation of synthetic oligomers and polymers with bioactive moieties and the synthesis of novel biomimetic polymers in hope to combine the synthetic versatility with biological activities required for efficient gene transfection. Cationic polymers have been widely investigated for gene transfection owing to their ability to condense with and introduce genetic materials into cells.[12] Their success is credited to high density of charged groups and tunability of lipophilicity-and-hydrophilicity balance (HLB). Poly(lysine)[12], Poly(ethylenimine) (PEI)[13,14], chitosan[15], and Poly(amido amine) (PAMAM)[16] are amongst commonly used cationic polymers in DNA complexation and cell transfection (Figure 1.2). Polypeptoids, a class of peptidomimetic polymers, have emerged in cell biology as potential gene delivery agents.[26] Their structural tunability and resistant to proteolytic degradation[17] make polypeptoids attractive for biomedical applications.[26]
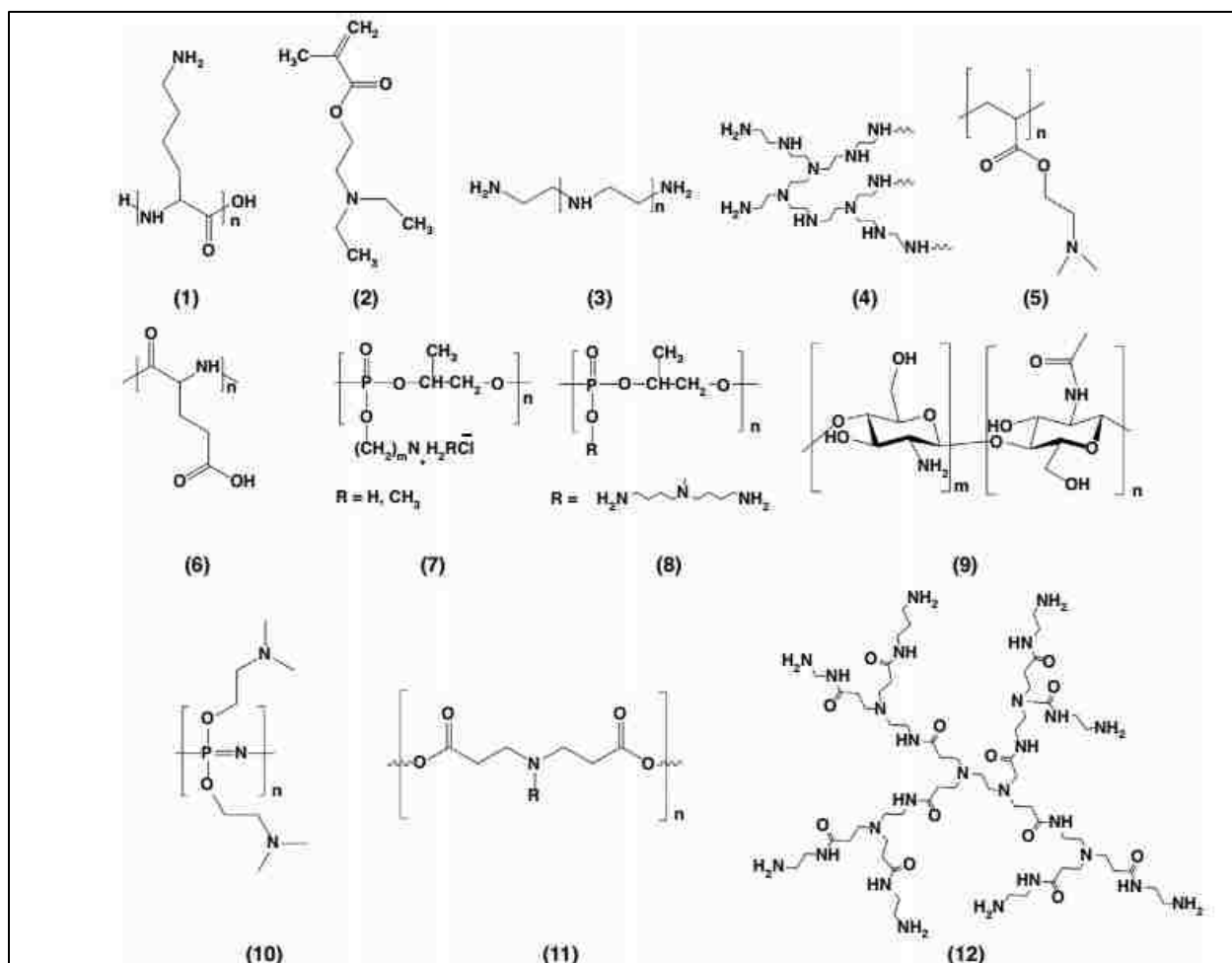
Figure 1.2. Chemical structures of commonly studied synthetic cationic polymers in gene delivery. (Reprinted with permission from reference[38], copyright (2017) Elsevier). **(1)** Poly(L-lysine), **(2)** diethyl aminoethyl methacrylate, **(3)** linear PEI, **(4)** branched PEI, **(5)** poly(dimethylaminoethyl methacrylate), **(6)** poly(L-glutamic acid), **(7)** polyphosphates, **(8)** polyphosphoramidates, **(9)** chitosan, **(10)** poly (DMAE)-phosphazene, **(11)** linear poly(β-amino ester)s, **(12)** polyaminoamine dendrimer.

1.5 Cell Transfection with Amine-based Polymers and Polyammoniums.

Research efforts have focused heavily on the use of amine-containing polymers as nonviral delivery systems for the efficient packing and transport of genetic materials. Ability to condense nucleic acids to form polyplexes for protection and transport of genetic materials into cells has made them practical for biomedical and therapeutic applications. However, correlation between the transfection efficiency and cytotoxicity of

7

amine containing cationic polymers are unsatisfactory.[18,19] This has been attributed to the cytotoxic nature of all cationic polymers above the certain concentration threshold.

In a study by Wetering et al. homopolymers and copolymers based on dimethylaminoethyl methacrylate (DMAMEM) with methyl methacrylate (MMA), ethoxytriethylene glycol methacrylate (triEGMA), or *N*-vinyl-pyrrolidone (NVP) having low molecular weights were synthesized and investigated as transfection agents for pCMV-LacZ and evaluated for their cytotoxicity. Polymer/plasmid polyplexes of the homopolymers and copolymers were tested with different cell lines for their transfection efficiency. DMAMEM copolymers with hydrophilic NVP and amphiphilic triEGMA were found to have the same transfection efficiency and cytotoxicity as the homopolymer with similar molecular weight.[20] By contrast, copolymers containing hydrophobic (MMA) yielded low transfection efficiency as a result of low cell viability suggesting that transfection efficiency and cytotoxicity is greatly dependent on polymer composition. A gene-delivery system with high stability and low cytotoxicity, based on the encapsulation of epsilon-polylysinegrafted-succinic acid-grafted--cyclodextrin-LMW PEI (PPC) and adamantane-functionalized poly-(ethylene glycol) was constructed and explored for its transfection capability by P. Lv et al. (Scheme 1.1).[25] Using HEK293 cells, *in vitro* studies of the polyplexes in 10% serum-supplemented medium using luciferase marker gene revealed comparable transfection efficiencies for the commercial standard PEI-25000 and PEG functionalized PPC. Unmodified PPC carriers produced lower transfection and higher cytotoxicity presumably due to the formation of internalized large aggregates.
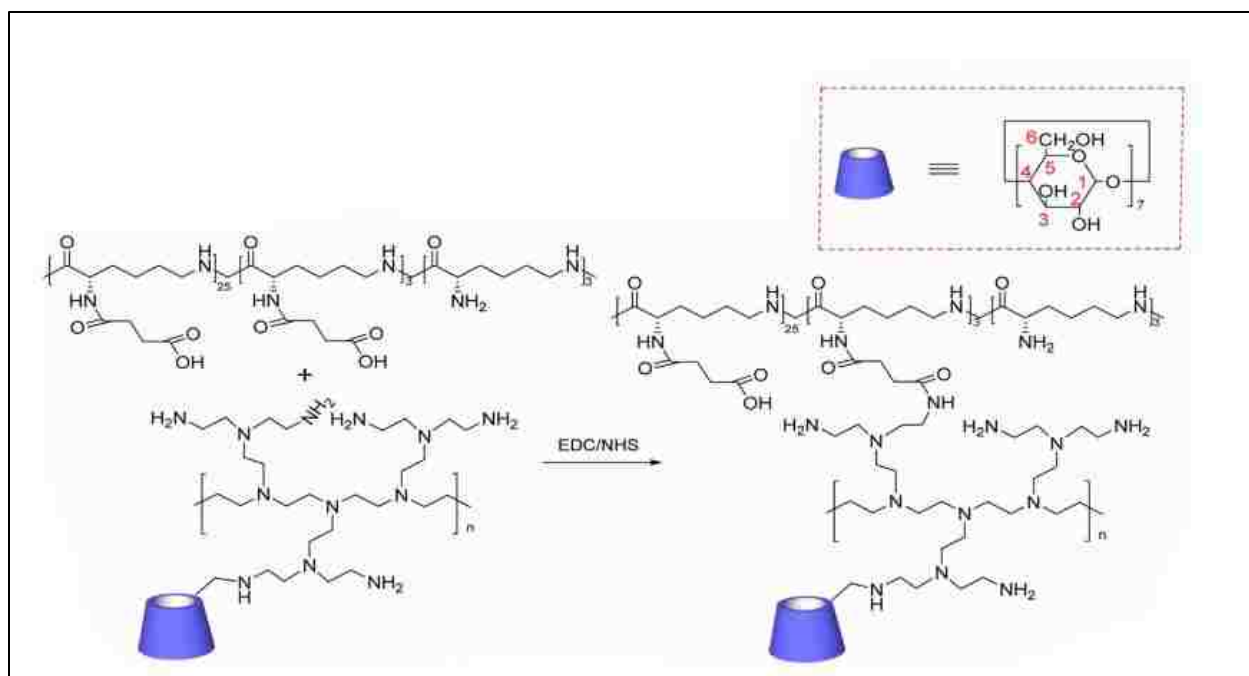
Scheme 1.1. Synthesis of adamantine-PEG modified PPC. (Reprinted with permission from reference[25], copyright (2017) Elsevier).

Efforts to improve nuclear targeting and haemocompatibility of dextran-based carriers during gene delivery via the incorporation of oligoamines have been successfully put forth by Thomas and coworkers.[27] In a study the cationic dextran derivative, Dex-P, was designed by means of combining the innate cationic and nuclear targeting properties of protamine with the biodegradable polysaccharide for a haemocompatible gene carrier. Assessment of the system's ability to facilitate efficient transfection in HepG2 cells resulted in lower levels of gene expression in comparison to bPEI$_{25}$, under serum-free and containing conditions. The highest transfection of Dex-P/DNA complexes was achieved at a low weight ratio (2:1). Increase in polymer/DNA w/w ratio resulted in decreased transfection efficiencies of the nanoplexes. While transfection efficiency in serum free medium was hampered by increasing polymer/DNA weight ratios (2-7) of polymer to DNA due to the shielding effect of polymer, efficiencies in the presence of serum were enhanced demonstrating the haemocompatibility of the

9

cationized dextran carrier. Depiction of nanoplexes in the nuclear region of cells by fluorescence microscopy confirmed that target specificity was introduced to the natural biocompatible polymer (Dextran) by incorporating protamine.[27]

Although very effective in the condensation of DNA for their size, oligomer-based amines are unable to carry out effective transfection alone due to the absence of cationic surface charge following DNA binding.[21] Polymers of larger molecular weight that are capable of sustaining net positive charge upon condensation must be used for effective transfection. However, the increase of molecular weight can result in enhanced cytotoxicity.[22] To address this issue, polymers that can degrade into low molecular species have been developed. For example, H.C. Kang et al. evaluated a series of reducible polycations (RPCs) synthesized from branched polyethyleneimine (bPEI) via thiolation and oxidation for their influence on reducing cytotoxicity and enhancing transfection characteristics in comparison to high molecular weight bPEI (HMW bPEI; 25 kDa). Branched PEIs with varied molecular weights (Mw: 0.8 kDa and Mw: 750 kDa) were used with 2-iminothiolane to prepare four samples of low molecular reducible polycations ([1] 80.3 kDa, [2] 52.7 kDa, [3] 6.3 kDa, and [4] 5.7 kDa).[23] Amongst several factors, the reducible LMW bPEI polymers were mainly anticipated to reduce proton-induced cytotoxicity and effectively condense DNA at relative low charge ratios. RPCs-bPEI$_{0.8}$ 1 and 2 showed higher cytotoxicities than bPEI$_{25kDa}$ in HEK293 cells due to higher molecular weight. However, RPCs 1 and 2 produced an IC$_{50}$ 8-9 fold higher than bPEI$_{25kDa}$. In contrast, RPCs 3 and 4 generated cytotoxicities 14-19 times lower than bPEI$_{25}$. All four polycations demonstrated significantly lowered toxicities in MCF7 cells than bPEI$_{25}$ (9-15 fold) confirming the hypotheses that low molecular weight carriers

10

reduce the tendency to interact with intracellular and extracellular components, thus resulting in reduced cytotoxicities.

The condensation and transfection of DNA using cationic peptoids was first explored by Murphy and coworkers (Table 1.1).[24] A library of oligomeric analogues with varying hydrophobicity, sequence, and main-chain length were synthesized and evaluated for their biological activity against commercial lipid vectors.[24] A 12-mer composed of a repeating triple motif (cationic-hydrophobic-hydrophobic) was the only polyammonium found to demonstrate enhanced DNA complexation and transfection in comparison with cationized homopolymers of higher molecular weight. Additionally, oligomeric peptoid carriers produced higher transfection efficiencies than the commercial lipid vector (DMPE). Under both serum-free and serum containing conditions the nonviral gene delivery of the cationic peptoids were observed to be higher than DMPE. Unlike some cationic systems (e.g., lipids, PLL, etc.) that require catalytic amounts of chloroquine for assistance with lysosomal degradation, peptoid's ability to initiate endosomal release on its own was also elucidated.[24]

Table 1.1. *N*-substituted glycine side chain and designators.[24]
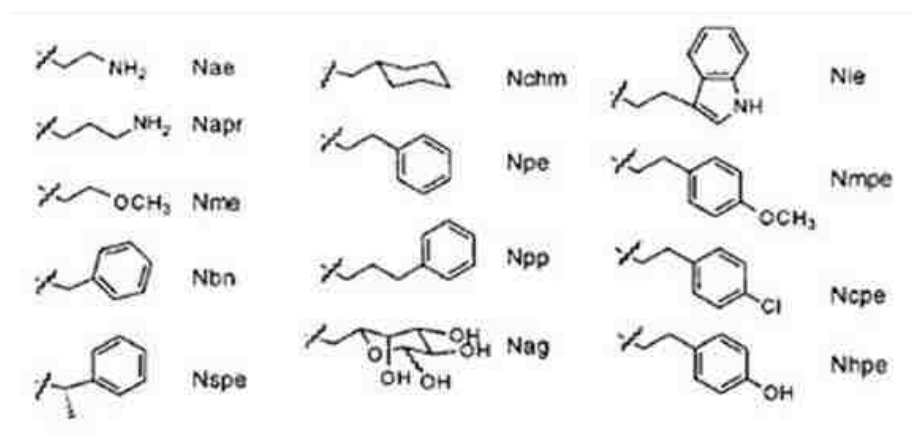
1.6 Current Challenges in the Design of Synthetic Carriers for Nonviral Cell Transfection

The implementation of gene therapy to treat rare genetic diseases and disorders require the continuous innovations in the development of effective gene delivery carriers. Several aspects related to nonviral gene carrier materials need to be properly addressed to ensure their optimal performance. Presently, nonviral vectors encounter various hurdles during *in vitro* and *in vivo* delivery (i.e. cell type-dependent transfection efficiency, post-transfection clearance, cytotoxicity, target delivery) that result in diminished gene transfection.[28,29] One major obstacle for most of the existing nonviral gene delivery vectors is the instability of positively charged complexes caused by plasma proteins. To reduce non-specific interaction with plasma components, strategies such as PEGylation[30-32] have been used. Poly(ethyleneglycol) (PEG) has often been used to shield polyplexes. Because of its hydrophilic and flexible nature, PEG increases steric stability, prevents nonspecific interactions with surrounding molecules, and eventually reduces toxicity. The second major obstacle for carriers is the endosomal entrapment of nonviral vectors following endocytosis. To help facilitate endosomal escape of nonviral vectors, agents such as chloroquine[33,34] or conjugation with fusogenic peptides[35] have been employed. Though chloroquine itself lacks the ability of condensing DNA, chloroquine and its derivatives are known to accumulate in endosomal compartment, buffer endosome acidification, and result in endosome destabilization through a so called "proton sponge" effect. The buffer capacity and electrostatic interaction of charged fusogenic additives with the endosomal membrane mediate the destabilization of endosomes. Together these strategies have alleviated some of the issues associated with the nonviral delivery system and hence attribute the

12

advancement of gene therapy as a whole. Our recent effort in developing cationic

polypeptoids as synthetic carriers for gene transfection will be discussed in chapters 3-

5.

1.7. References

1. Friedmann, T., Roblin, R. Gene therapy for human genetic disease? *Science* **1972**, 175, 4025, 949-955.

2. Hacein-Bey-Abina, S., Hauer, J., Lim, A., Picard, C., Wang, G., Berry, C., Martinache, C., Rieux-Laucat, F., Latour, S., Belohradsky, B., Leiva, L., Sorensen, R., Debré, M., Casanova, J., Blanche, S., Durandy, A., Bushman, F., Fischer, A., Cavazzana-Calvo, M. Efficacy of Gene Therapy for X-Linked Severe Combined Immunodeficiency *N. Engl. J. Med.* **2010**, 363, 4, 355-364.

3. Aiuti, A., Cattaneo, F., Galimberti, S., Benninghoff, U., Cassani, B., Callegaro, L., Scaramuzza, S., Andolfi, G., Mirolo, M., Brigida, I., Tabucchi, A., Carlucci, F., Eibl, M., Aker, M., Slavin, S., Al-Mousa, H., Al Ghonaium, A., Ferster, A., Duppenthaler, A., Notarangelo, L., Wintergerst, U., Buckley, R., Bregni, M., Marktel, S., Valsecchi, M., Rossi, P., Ciceri, F., Miniero, R., Bordignon, C., Roncarolo, M. Gene Therapy for Immunodeficiency Due to Adenosine Deaminase Deficiency. *N. Engl. J. Med.* **2009**, 360, 447–458.

4. Kim, T., Eberwine, J. Mammalian cell transfection: the present and the future *Anal. Bioanal. Chem.* **2010**, 397, 3173-3178.

5. Tang, H., Yin, L., Cheng, J. Water-soluble poly (L-serine)s with elongated and charged side-chains: synthesis, conformations, and cell-penetrating properties *Biomacromolecules* **2012,** 13, 2609–2615.

6. Copolovici, D., Langel, K., Eriste, E., Langel, U., Cell-Penetrating Peptides: Design, Synthesis, and Applications *ACS Nano* **2014,** 8, 1972-1994.

7. Savarala, S., Brailoiu, E., Wunder, S., Ilies, M. Tuning the Self-Assembling of Pyridinium Cationic Lipids for Efficient Gene Delivery into Neuronal Cells *Biomacromolecules* **2013,** 14, 2750-2764.

8. Kolmel, D., Furniss, D., Sustano, S., Lauer, A., Grabher, C., Brase, S., Schepers, U. Cell Penetrating Peptoids (CPPos): Synthesis of a Small Combinatorial Library by Using IRORI MiniKans *Pharmaceuticals* **2012,** 5, 1265-1281.

9. Hahn P., Scanlan E. (**2010**) Gene Delivery into Mammalian Cells: An Overview on Existing Approaches Employed *In Vitro* and *In Vivo*. In: Bielke W., Erbacher

C. (eds) Nucleic Acid Transfection. Topics in Current Chemistry, vol 296. Springer, Berlin, Heidelberg.

10. Lotze, M., Kost, T. Viruses as gene delivery vectors: Application to gene function, target validation, and assay development *Cancer Gene Therapy* **2002,** 9, 692-699.

11. Barua, S., Joshi, A., Banerjee, A., Matthews, D., Sharfstein, S., Cramer, S., Kane, R., Rege, K. Parallel Synthesis and Screening of Polymers for Non-Viral Gene Delivery *Molecular Pharmaceutics* **2008,** 6, 86-97.

12. Fischer, W., Calderon, M., Haag, R., Hyperbranched Polyamines for Transfection *Topics in Current Chemistry* **2010,** 296, 95-129.

13. Boussif, O., Lezoualc'h, F., Zanta, M. A., Mergny, M. D., Scherman, D., Demeneix, B., Behr, J. P. A versatile vector for gene and oligonucleotide transfer into cells in culture and in vivo: polyethylenimine *Proc. Natl. Acad. Sci. U.S.A.* **1995**, 92, 7297–7301.

14. Zanta, M. A., Boussif, O., Adib, A., Behr, J. P. In vitro gene delivery to hepatocytes with galactosylated polyethylenimine *Bioconjugate Chem.* **1997**, *8*, 839–844.

15. Borchard, G. Chitosans for gene delivery *Adv. Drug Delivery Rev.* **2001**, *52*, 145–150.

16. Bielinska, A., Kukowska-Latallo, J. F., Johnson, J., Tomalia, D. A., Baker, J. R. Regulation of in vitro Gene Expression Using Antisense Oligonucleotides or Antisense Expression Plasmids Transfected Using Starburst PAMAM Dendrimers *Nucleic Acids Res.* **1996**, *24*, 2176–2182.

17. Fowler, S., Blackwell, H. Structure–function relationships in peptoids: Recent advances toward deciphering the structural requirements for biological function *Org. Biomol. Chem.* **2009**, 7, 1508–1524.

18. Salcher E.E., Wagner E. (2010) Chemically Programmed Polymers for Targeted DNA and siRNA Transfection. In: Bielke W., Erbacher C. (eds) Nucleic Acid Transfection. Topics in Current Chemistry, vol 296. Springer, Berlin, Heidelberg.

19. Huang, W., Seo, J., Lin, J., Barron, A. Peptoid transporters: effects of cationic, amphipathic structure on their cellular uptake *Mol. Biosyst.,* **2012,** 8**,** 2626-2628.

20.   Wetering. P., Cherng, J., Talsma, H., Crommelin, D., Hennink, W. 2-(dimethylamino)ethyl methacrylate based (co)polymers as gene transfer agents *Journal of Controlled Release,* **1998,** 53, 145 –153.

21.   Chi, W., Shuai Liu, S., Yang, J., Wang, R., Ren, H., Zhou, H., Chen, J., Guo, T. Evaluation of the effects of amphiphilic oligomers in PEI based ternary complexes on the improvement of pDNA delivery *J. Mater. Chem. B*, **2014,** 2, 5387-5396.

22.   Reineke, T., Davis, M. Nucleic Acid Delivery via Polymer Vehicles *Polymer Science A: A comprehensive reference.* **2012,** 9, 497-527.

23.   Kang, H. C., Kang, H. J., Bae, Y. A reducible polycationic gene vector derived from thiolated low molecular weight branched polyethyleneimine linked by 2-iminothiolane *Biomaterials,* **2011,** 32, 1193-1203.

24.   Murphy, J., Uno, T., Hamer, J., Cohen, F., Dwarki, V., Zuckermann, R. A combinatorial approach to the discovery of efficient cationic peptoid reagents for gene delivery *Proc. Natl. Acad. Sci.,* **1998,** 95, 1517–1522.

25.   Lv, P., Zhoua, C., Zhao, Y., Liaoa, X., Yanga, B. Modified-epsilon-polylysine-grafted-PEI--cyclodextrin supramolecular carrier for gene delivery *Carbohydrate Polymers*, **2017**, 168, 103–111.

26.   Zhu, L., Simpson, J., Xu, X., He, H., Zhang, D., Yin, L. Cationic polypeptoids with optimized molecular characteristics toward efficient nonviral gene delivery *ACS Appl. Mater. Interfaces*, **2017**, 9, 23476–23486.

27.   Thomas, J., Rekha, M., Sharma, C. Dextran-protamine polycation: An efficient nonviral and haemocompatible gene delivery system *Colloids and Surfaces B: Biointerfaces*, **2010**, 81, 195-205.

28.   Al-Dosari, M., Gao, X. Nonviral Gene Delivery: Principle, Limitations, and Recent Progress *The AAPS Journal,* **2009**, 4, 671-681.

29.   Charles H. Jones, Chih-Kuang Chen, Anitha Ravikrishnan, Snehal Rane, and Blaine A. Pfeifer Overcoming Nonviral Gene Delivery Barriers: Perspective and Future *Mol. Pharmaceutics* **2013**, 10, 4082−4098.

30.   Harvie, P., Wong, F., Bally, M. Use of poly(ethylene glycol)– lipid conjugates to regulate the surface attributes and transfection activity of lipid–DNA particles. *J Pharm Sci.* **2000**, 89, 652–63.

31.   Petersen, H., Fechner, P. M., Martin, A. L., Kunath, K., Stolnik, S., Roberts, C. J., Fischer, D., Davies, M. C., Kissel, T. *Bioconjugate Chem.* **2002**, 13, 845–854.

32. Mao, S., Neu, M., Germershaus, O., Merkel, O., Sitterberg, J., Bakowsky, U., Kissel, T. Influence of Polyethylene Glycol Chain Length on the Physicochemical and Biological Properties of Poly(ethylene imine)-graft-Poly(ethylene glycol) Block Copolymer/SiRNA Polyplexes *Bioconjugate Chem.* **2006**,17,1209−1218.

33. Ying Xie, Fei Yu, Weimin Tang, Bolutito Oluwole Alade, Zheng-Hong Peng, Yazhe Wang, Jing Li, and David Oupický. Synthesis and Evaluation of Chloroquine-Containing DMAEMA Copolymers as Efficient Anti-miRNA Delivery Vectors with Improved Endosomal Escape and Antimigratory Activity in Cancer Cells *Macromol. Biosci.* **2017**, 1-10.

34. Pack, D., Hoffman, A., Pun, S., Stayton, P., Design and development of polymers for gene delivery *Nat. Rev. Drug Discovery* **2005**, 4, 581.

35. Ayman, E., Futaki, S., Hideyoshi, H. Delivery of Macromolecules Using Arginine-rich Cell-penetrating Peptides: Ways to Overcome Endosomal Entrapment *AAPS Journal* **2009**,11, 13-22.

36. Zhang, R., Song, Z., Yin, L., Zheng, N., Tang, H., Lu, H., Gabrielson, N., Lin, Y., Kim, K., Cheng, J. Ionic α-helical Polypeptides toward Nonviral Gene Delivery *WIREs Nanomed Nanobiotechnol* **2015**, 7, 98–110.

37. Eliyahu, H., Barenholz, Y., Domb, A. Polymers for DNA Delivery *Molecules* **2005**, 10, 34-64.

38. Xiang, Y., Oo, N., Lee, J., Li, Z., Loh, X. Recent development of synthetic nonviral systems for sustained gene delivery *Drug Discovery Today* **2017**, 22, 1318-1335.

CHAPTER 2: OVERVIEW OF POLYPEPTOIDS (POIs)

2.1 Background on Polypeptoids

Since their discovery during the 1980's, polymeric *N*-substituted glycines a.k.a polypeptoids (POIs) have become increasingly investigated in many scientific fields.[1] This special class of psuedo-peptidic polymers bear substituents directly on the nitrogen atom present in the backbone. In contrast to peptides, the presence of alkyl groups on nitrogen prevent peptoids from participating in extensive hydrogen bonding as displayed in Figure 2.1.[7] Additionally, this *N*-substitution affords peptoids with unique physiochemical properties. Enhanced proteolytic stability against enzymatic degradation by these systems is a prime example.[2,3] Polypeptoids are known for their biocompatible and biodegradable properties which make them potential candidates for a variety of biomedical and biotechnological applications such as smart-coatings, drug delivery, and bioseperation.[4-6] In the rest of the discussion, polypeptoids will be used to referred to poly(α-peptoids).
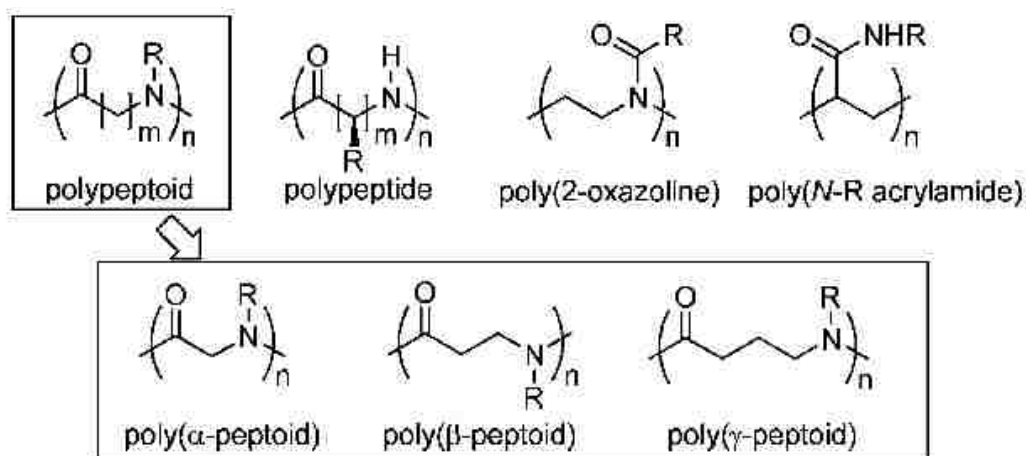
Figure 2.1. Chemical structure of polypeptide, polypeptoids and other peptidomimetic polymers (reproduced from reference 7).

2.2 Significance of POIs as Peptidomimetic Materials: Benefits over Peptides

Peptides have been extensively investigated to gain understanding of their sequence-conformation relationship and enzymatic degradation behavior towards biomedical applications.[8] In spite their proven usefulness as biocompatible and biodegradable materials, peptide based therapeutics often suffer from poor oral bioavailability and short half-life in the body and can induce an immune response.[9] Research in peptidomimetics has gained attraction with the goal to improve the physical-chemical-biological properties of peptides. Strategies such as incorporating one or more peptoid residues to generate peptide-peptoid hybrids (or "peptomers") have been proposed and investigated.[53]

Despite the difference in chemical composition of polypeptoids, their structural similarity to polypeptides has afforded them opportunities in diagnostics, drug-discovery, material science, and fundamental studies involving bio-applications.[5,8] Classified as peptide regioisomers, conformations and properties of POIs are dictated mainly by their appendant side chain (e.g., electronic, sterics).[6-11] Such characteristics are attributed to the absence of a stereogenic center and a lack in hydrogen bonding in polypeptoids. These features are also responsible for peptoids thermal processability.[12] Depending on the N-substituent structure, solubility of polypeptoids in water can be systematically controlled (Figure 2.2).[13]
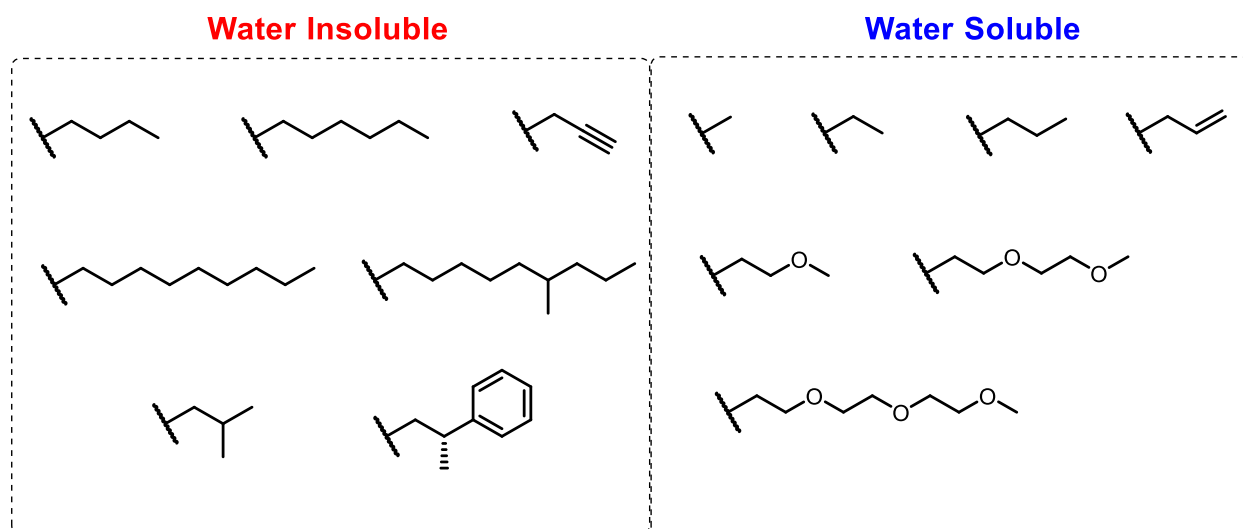
Figure 2.2. Different water solubility of the polypeptoid bearing different *N*-substituents.

2.3. Synthesis of *N*-carboxyanhydride (NCA) Monomers and Polypeptoids

2.3.1 Synthesis of *N*-substituted NCAs

A series of *N*-substituted *N*-carboxyanhydrides (R-NCAs) monomers bearing different *N*-substituents (e.g., ethyl, allyl, propargyl, decyl, etc.) have been developed by means of two general synthetic methods. Starting with glyoxylic acid and the respective primary amine, *N*-substituted glycine precursors were obtained from reductive amination reaction.[14-16] Alkoxycarbonyl protected *N*-substituted glycine was then obtained via the reaction of di-*tert*-butyl dicarbonate and the *N*-substituted glycine precursor (Scheme 2.1).[17] Lastly, cyclization of alkoxycarbonyl protected *N*-substituted glycine with an acylating agent (i.e., PCl$_3$, PBr$_3$, and SOCl$_2$) afforded the desired R-NCAs. Due to their high sensitivity to moisture, purification and storage of R-NCA monomers under inert atmosphere is necessary. In the case of *N*-allyl and *N*-ethyl NCAs that remain as an oil at room temperature, a trace mount of moisture can easily initiate spontaneous polymerization.
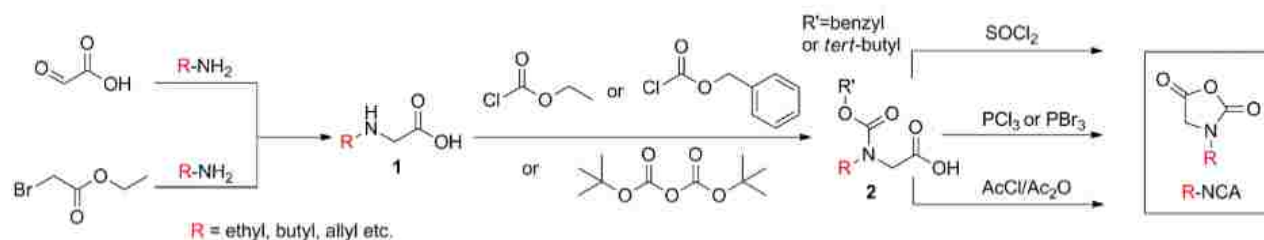
Scheme 2.1. Synthetic routes of R-NCA monomer (copied from reference 17).

2.3.2 Synthesis of polypeptoids by polymerization of R-NCA

Solid-phase submonomer method is commonly used to prepare oligomeric peptoids with well-defined monomer sequences. As a result of two chemical steps (acylation and displacement) this synthetic route allows a variety of commercial available primary amine sources to be used for peptoid synthesis. Sequence-defined structures can be synthesized in this manner. This synthetic advantage has also enabled scientists to gain understanding about monomer sequence in relation to overall polymer conformation and polymer self-assembly in solution or solid state.[18-20] Peptoid therapeutics research has also advanced significantly due to sequence control afforded by this synthetic strategy.[21] Control of the monomer sequence is the key advantage of submonomer synthesis. However, the solid-phase submonomer method has some limitations. The lengthy timeframe it takes to synthesize peptoids via solid-phase submonomer approach has been reported by Zuckerman et al.[22] The submonomer method can only afford short chain polypeptoids (typically less than 30 residues) with relative low molecular weight polymers.

Polymerization strategies are often pursued to access polypeptoids with high molecular weight. The ring-opening polymerization of R-NCAs has been accomplished

with several initiation systems. Various primary amines, organobases (i.e., DBU, TMG), and N-heterocyclic carbenes have been used as initiators in the ROP of R-NCAs to produce polypeptoids having different *N*-substituent structure, molecular architecture (e.g., cyclic or linear) and controlled molecular weights. Recently, Chan et al. also demonstrated the use of alcohols as initiators for ROP of NCAs.[23] Peng et al. have used rare earth borohydrides as initiators for the ROP of NCAs yielding α-hydroxy-ω-aminotelechelic polypeptoids. [24,25]

Primary amines are the most widely used initiators for polypeptoid synthesis due to their convenience for post-functionalization and the variety of structures that are readily available from commercial sources (Scheme 2.2).[26] Benzylamine-initiated ROP of *N*-methyl NCA (Me-NCA) was shown to proceed in a controlled manner without chain transfer or termination events after more than 10 iterative polymerization steps. [47] The produced polysarcosine (PNMG) exhibited narrow Poisson distribution (PDI<1.1-1.3) and controllable molecular weight by simply changing the initial monomer to initiator feed ratios. The living chain end of PNMG was further supported by the chain extension experiment with different monomers (e.g., Et-NCA, Pr-NCA, Bu-NCA and Pe-NCA). The living polymerization character of other monomers (e.g., Et-NCA, Pr-NCA, Bu-NCA) was also reported.[48-49]

Xuan et al. reported the synthesis of a triblock copolypeptoid via the sequential ROP of different R-NCA monomers starting from benzylamine initiator. The ABC triblock copolypeptoids contained hydrophobic, hydrophilic, and thermoresponsive segments.[4] Upon heating, it was observed that the triblock copolypeptoid systems formed free standing gels with narrow sol-to-gel transition windows and that the gels could be

injected through a 24 gauge needle without breaking apart. Likewise using benzylamine initiator, Li et al. recently reported the synthesis of core-crosslinked micelles composed of poly(*N*-ethyl glycine), poly(*N*-propargyl glycine), and poly(*N*-decyl glycine).[27] Crosslinking was achieved via CuAAC (vide supra) using a disulfide crosslinker species which could be degraded using glutathione. The loading and gradual release of doxorubicin, a common anti-cancer drug was also demonstrated.

Initiation
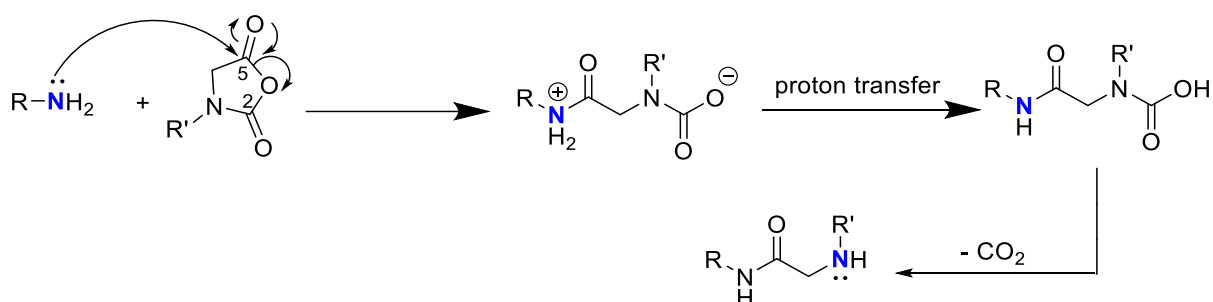
Propagation
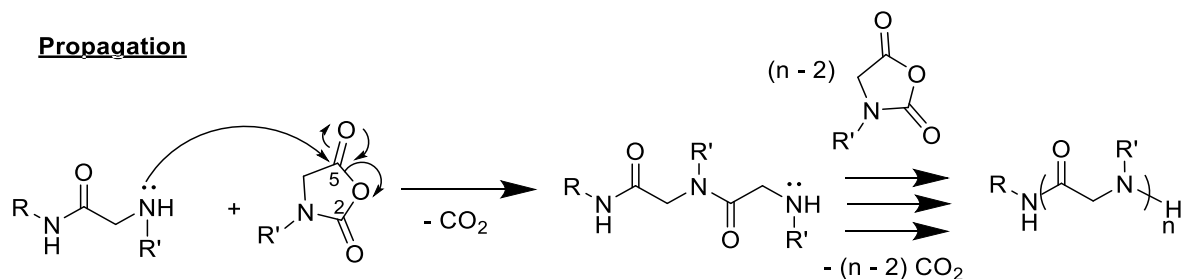
Scheme 2.2. Primary amine-initiated ring-opening polymerization of NCA (via NAM).

2.3.3 Synthesis of polypeptoids via the normal amine mechanism (NAM)

From a mechanistic view point, primary amine-initiated ROP of R-NCAs proceeds by the normal amine (NAM) mechanism (Scheme 2.2). Because R-NCA monomers lack the labile N-H proton that presents in the conventional amino acid derived NCAs, ROP of R-NCA by the normal amine mechanism occurs with minimal

side reactions that often plague the ROP of NCAs bearing N-H protons (e.g., deprotonation of N-H, isocyanate formation). The initiation step of the NAM is a nucleophilic ring-opening addition of primary amine at the C_5 carbonyl of R-NCA. The following proton transfer generates a terminal carbamic acid. Due the thermal instability of the carbamic acid, it subsequently undergoes a decarboxylation step to form a new secondary amine species to complete the initiation step. The newly formed secondary amine reacts with another R-NCA monomer in a similar manner until all monomers are consumed, which constitutes the propagation event (Scheme 2.2). [28]

2.4 Functional Polypeptoids

In order to tailor the property of polypeptoids for different applications, additional synthetic strategies must be developed to further diversify the *N*-substituent structure in polypeptoids. To date, two approaches to synthesize functional polypeptoids exist: the post-polymerization modification method and polymerization of functional R-NCA monomer. The post-polymerization have several advantages. First of all, a variety of different functional groups can be introduced to the polypeptoid backbone by choosing efficient conjugation chemical reactions (e.g., various "click" chemistry). [29,30] Secondary, the sidechain functionalized polypeptoids will have the same molecular weight and molecular weight distribution as the parent polymers. For the functional NCA monomer route, NCA bearing functional *N*-substituent is polymerized via ROP to afford functional polypeptoid.[31,32] However, functional R-NCA monomer synthesis is a tedious and non-trivial task. It entails the design of a new synthetic route, optimization of purification, polymerization conditions, and the careful handling of R-NCAs that may have poor stability. With a well-established synthetic platform, the post-polymerization route offers an efficient and easy for way to obtain functional polypeptoids.

23

2.5 Preparation of Functional Polypeptoids by Post-polymerization Modification Methods

Still considered relatively young in the field of peptidomimetic materials, side chain modification to introduce specific functionalities is important for controlling the properties of polypeptoids for biotechnological, technical, and biomedical applications. To date, very few examples have been reported describing the modification of *N*-substituents in polypeptoids by "click" chemistry.[33] Discovered by Sharpless et al., click chemistry refers to modular reactions that permit the highly efficient chemical bond formation between different types of functionalities under mild conditions.[34,35] Using click chemistry, the incorporation of bioactive groups, targeting moieties, and solubility enhancing groups into polymers have been accomplished.[36,37] In terms of modification, polymers containing side chains with functional groups such as allyl[41] or propargyl[33,39] enable "click" chemistry methods to be used for further structural alteration.

Characteristically, click reactions are denoted by features including high bond-formation efficiency, high yields, easy purification from byproducts, and high stereoselectivity.[34,35] Prime examples of "click" chemistry, thiol-ene reaction and copper catalyzed azide-alkyne cycloaddition (CuAAC), have been heavily used to introduce new moieties to polypeptoids and hence will be discussed here.

A wide range of enes and thiols can undergo thio-ene addition chemistry to afford thioether moieties, making it a versatile method for post-polymerization modification of polymers.[34] Schlaad et al. reported the post-polymerization modification of poly(*N*-allyl glycine) via photoinitiated thiol-ene addition chemistry.[38] Thiol–ene additions of poly(*N*-allyl glycine)s with 1-thioglycerol, 1-thio-β-D-glucose tetraacetate, and 1-thio-β-D-glucose were demonstrated. It was shown that the glycosylation of poly(*N*-allyl glycine)s

was readily achievable under environmentally benign conditions (i.e., in an aqueous solution at room temperature). Moreover, the thiol-ene reaction could be successfully carried out in the presence or absence of a photo initiator hydroxy-4'-(2-hydroxyethoxy)-2-methylpropiophenone (HEMP), though the addition rate was found to be considerably higher in the first instance.

Zhang et al. previously investigated cyclic brush-like polymers which were synthesized by tandem organo-mediated zwitterionic polymerization followed by the CuAAC modification with azido-terminated PEG via a grafting-onto approach.[40] In addition to poly(*N*-propargyl glycine) homopolymer macrocycles, cyclic poly(*N*-propargyl glycine)-ran-poly(*N*-butyl glycine) random copolymers were also studied. As evidenced by AFM analysis, grafting densities in the latter case with the copolymer were noticeably higher (<94%), which was attributed to the reduced aggregation of the polymers in solution and thus enhanced access of the propargyl groups (Figure 2.3).[40] By combining the primary amine-initiated ring-opening polymerization method with CuAAC click chemistry Zhang et al. also reported the first redox-responsive core-cross-linked micelles (CCLMs) based on amphiphilic block copolypeptoids.[41] Sequence-defined peptoids prepared by sequential CuAAC conjugation reactions on a solid support have also been demonstrated by Kirshenbaum et al. (Figure 2.4).[43,44] This on-resin click approach was also applied to glycosylated peptoids for antifreeze applications.[45]
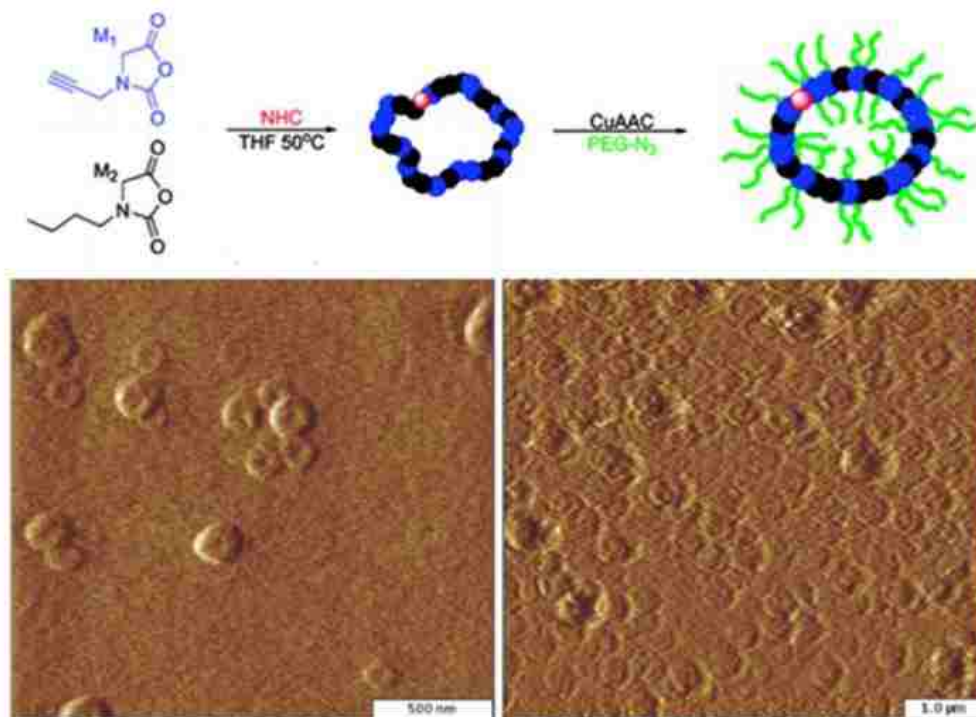
Figure 2.3. Synthesis of cyclic polypeptoid brushes (top) and AFM amplitude images of corresponding donut-shape structures (bottom). (Reprinted (adapted) with permission from reference[40]. Copyright © (2011) American Chemical Society.
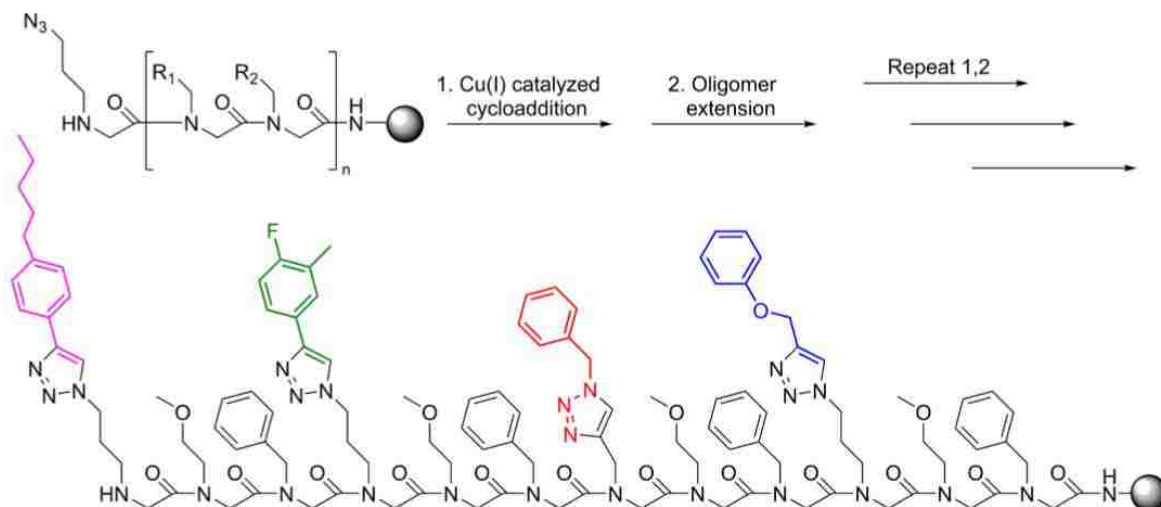
Figure 2.4. Synthesis and modification of oligopeptoids via CuAAC chemistry. (Reproduced from Ref. 43 with permission from The Royal Society of Chemistry).

Schlaad et al. recently described the potential of poly(*N*-propargyl glycine) (PNPgG) as a versatile platform for post-polymerization modification of polypeptoids (Scheme 2.3).[33] Interestingly, the quaternization of triazole linkers with an alkyl halide following CuAAC resulted in the first example of a polypeptoid ionic liquid. In addition, it was shown that acetylide anions produced by deprotonation of the alkyne proton by phosphazene base served as an initiator for the polymerization of ethylene oxide, further highlighting the versatility of propargyl groups for further chemical derivation. The crosslinking of PNPgG by thermal treatment at high temperatures (greater than 190 °C) was also demonstrated, resulting in an insoluble amorphous network which could be useful for a stabilization of bulk materials or films as well as block copolymer aggregates.[33] More recently, use of CuAAC click chemistry was employed to introduce charged moieties onto the homo- and random polypeptoids to access a library of cationic polypeptoids for gene delivery application as shown by Yin et al.[46]
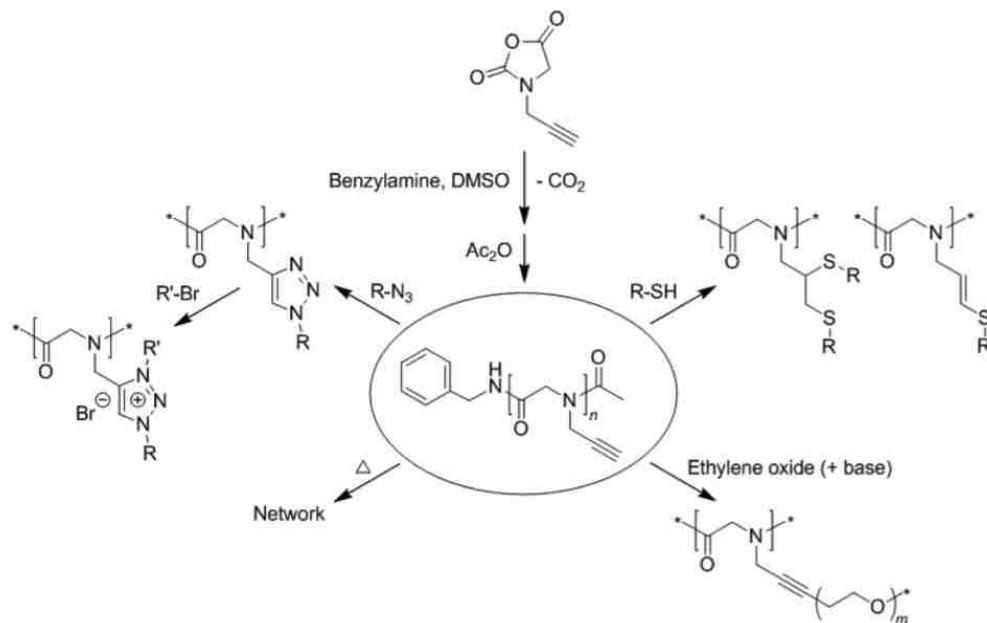
Scheme 2.3. Synthesis of poly(*N*-propargyl glycine) and subsequent modifications of alkyne side chains. (Reprinted with permission from reference 33, copyright (2017) Elsevier).

Synthetic strategies discussed in this chapter have set the stage for the further investigation of the structure-property relationship of polypeptoids. Due to the versatility offered by the post-polymerization modification methods, scientists can now prepare functional polypeptoid materials for different applications.

2.6. References

1.   Zuckermann, R. N. Peptoid Origins. *Peptide Science* **2011,** *96*, 545-555.

2.   Miller, S. M., Simon, R. J., Ng, S., Zuckermann, R. N., Kerr, J. M., Moos, W. H. Proteolytic studies of homologous peptide and N-substituted glycine peptoid oligomers. *Bioorg. Med. Chem. Lett.* **1994**, *4*, 2657-2662.

3.   Miller, S. M., Simon, R. J., Ng, S., Zuckermann, R. N., Kerr, J. M., Moos, W. H. *Drug Dev. Res.* **2004**, *35*, 20-32.

4.   Xuan, S., Gupta, S., Li, X., Bleuel, M., Schneider, G., Zhang, D. Synthesis and Characterization of Well-defined PEGylated Polypeptoids as Protein-resistant Polymers. *Biomacromolecules,* **2017**, 18, 951-964.

5.   Zhang, D., Lahasky, S., Guo, L., Lavan, M. Polypeptoid Materials: Current Status and Future Perspectives. *Macromolecules,* **2012,** 45, 5833-5841.

6.   Guo, L., Zhang, D. Cyclic Poly(a-peptoid)s and Their Block Copolymers from N-Heterocyclic Carbene Mediated Ring-Opening Polymerization of N-Substituted N-Carboxylanhydrides. *J. Am. Chem. Soc.,* **2009,** 131, 18072-18074.

7.   Lahasky, Samuel. *Advancing The Field of Polypeptoids Through The Synthesis of Novel Architectures and Thermoresponsive Polymers.* Diss. Louisiana State University, 2013. Web. 13 Nov. 2017.

8.   Gangloff, N., Ulbricht, J., Lorson, T., Schlaad, H., Luxenhofer, R. Peptoids and Polypeptoids at the Frontier of Supra- and Macromolecular Engineering *Chemical Reviews* **2016**, *116*, 1753-1802.

9.   Kwon, Y., Kodadek, T. Quantitative evaluation of the relative cell permeability of peptoids and peptides *J. Am. Chem. Soc.*, **2007**, *129,* 1508-1509.

10.   Kirshenbaum, K., Barron, A. E., Goldsmith, R. A., Armand, P., Bradley, E. K., Truong, K. T. V., Dill, K. A., Cohen, F. E., Zuckermann, R. N. Sequence-Specific Polypeptoids: A Diverse Family of Heteropolymers with Stable Secondary Structure *Proceedings of the National Academy of Sciences* **1998,** *95*, 4303-4308.

11.   Armand, P., Kirshenbaum, K., Goldsmith, R. A., Farr-Jones, S., Barron, A. E., Truong, K. T. V., Dill, K. A., Mierke, D. F., Cohen, F. E., Zuckermann, R. N., Bradley, E. K. NMR determination of the major solution conformation of a peptoid pentamer with chiral side chains *Proceedings of the National Academy of Sciences* **1998,** *95*, 4309-4314.

12.   Chan, B., Xuan, S., Li, A., Simpson, J. M., Zhang, D., Polypeptoid Polymers: Synthesis, Characterization and Properties. Synthesis and Characterization of Biorelated Polymers for Biomedical Applications. 2017. Print.

13. Knight, A., Zhou, E., Francis, M., Zuckermann, R. Sequence Programmable Peptoid Polymers for Diverse Materials Applications *Adv. Mater*. **2015**, 27, 5665–5691.

14. Fetsch, C., Grossmann, A., Holz, L., Nawroth, J. F., Luxenhofer, R. Polypeptoids from N-Substituted Glycine N-Carboxyanhydrides: Hydrophilic, Hydrophobic, and Amphiphilic Polymers with Poisson Distribution *Macromolecules* **2011,** *44*, 6746-6758.

15. Robinson, J. W., Secker, C., Weidner, S., Schlaad, H. Thermoresponsive Poly(N-C3 glycine)s *Macromolecules* **2013,** *46*, 580-587.

16. Katchalski, E., Sela, M., Synthesis and Chemical Properties of Poly-α-Amino Acids. In *Adv. Protein Chem.*, C.B. Anfinsen, M. L. A. K. B.; John, T. E., Eds. Academic Press: 1958, Vol. Volume 13, pp 243-492.

17. Chan, Brandon A., Xuan, Sunting, Li, Ang, Simpson, Jessica M., Sternhagen, Garrett L., Zhang, Donghui. "Polypeptoid Polymers: Synthesis, Characterization, and Propertiesn *Polymers for Biomedicine: Synthesis, Characterization, and Applications*. Ed. Carmen Scholz. Hoboken: John Wiley & Sons Incorporated, 2017. 77-119. Print.

18. Barz, M., Luxenhofer, R., Zentel, R., Vicent, M. J. Overcoming the PEG-addiction: well-defined alternatives to PEG, from structure–property relationships to better defined therapeutics *Polymer Chemistry* **2011,** *2* (9), 1900-1918.

19. Sun, J., Jiang, X., Lund, R., Downing, K.H., Balsara, N.P., Zuckermann, R.N. Self-assembly of crystalline nanotubes from monodisperse amphiphilic diblock copolypeptoid tiles. *Proc. Natl. Acad. Sci. U.S.A.* **2016, 113**, 3954-3959.

20. Rosales, A., Segalman, R., Zuckermann, R. Polypeptoids: a model system to study the effect of monomer sequence on polymer properties and self-assembly *Soft Matter*, **2013,** 9, 8400-8414.

21. Patch, J. A., Barron, A. E., Mimicry of bioactive peptides via non-natural, sequence-specific peptidomimetic oligomers *Current Opinion in Chemical Biology* **2002,** 6, 872-877.

22. Murphy, J. E., Uno, T., Hamer, J. D., Cohen, F. E., Dwarki, V., Zuckermann, R. N. A Combinatorial Approach to the Discovery of Efficient Cationic Peptoid Reagents for Gene Delivery *Proceedings of the National Academy of Sciences* **1998**, 95, 1517-1522.

23. Chan, B. A., X., S., Horton, M., Zhang, D. 1,3,3-Tetramethylguanidine-Promoted Ring-Opening Polymerization of *N*-Butyl *N*-carboxyanhydride using Alcohol Initiators. *Macromolecules* **2016**, *49*, 2002-2012.

24. Peng, H., Ling, J., Shen, Z. Ring opening polymerization of α-amino acid *N*-carboxyanhydrides catalyzed by rare earth catalysts: Polymerization characteristics and mechanism *J. Polym. Sci., Part A: Polym. Chem.*, **2012**, 50, 1076–1085.

25. Peng, H., Ling, J., Zhu, Y., You, L., Shen, Z. Polymerization of α-amino acid *N*-carboxyanhydrides catalyzed by rare earth tris(borohydride) complexes: Mechanism and hydroxy-endcapped polypeptides *J. Polym. Sci., Part A: Polym. Chem.*, **2012**, 50, 3016–3029.

26. Tao, Xinfeng, Zheng, Botuo, Bai, Tianwen, Zhu, Baoku, and Ling, Jun. Hydroxyl Group Tolerated Polymerization of N-Substituted Glycine N-Thiocarboxyanhydride Mediated by Aminoalcohols: A Simple Way to α-Hydroxyl-ω-aminotelechelic Polypeptoids *Macromolecules* **2017**, 50, 3066−3077.

27. Li, A.; Zhang, D., Synthesis and Characterization of Cleavable Core-CrossLinked Micelles Based on Amphiphilic Block Copolypeptoids as Smart Drug Carriers. *Biomacromolecules* **2016**, 17 (3), 852-861.

28. Cao, Jinbao. *Synthesis of Functional Polypeptides and Development of New Synthetic Strategies Toward Polypeptides.* Diss. Louisiana State University, 2016. Web. 13 Nov. 2017.

29.   Engler, A. C., Shukla, A., Puranam, S., Buss, H. G., Jreige, N., Hammond, P. T., Effects of Side Group Functionality and Molecular Weight on the Activity of Synthetic Antimicrobial Polypeptides. *Biomacromolecules* **2011**, 12, 1666-1674.

30.   Gabrielson, N. P., Lu, H., Yin, L., Li, D., Wang, F., Cheng, J., Reactive and Bioactive Cationic α-Helical Polypeptide Template for Nonviral Gene Delivery. *Angew. Chem. Int. Ed.* **2012**, 51, 1143-1147.

31.   Chen, C., Wang, Z., Li, Z., Thermoresponsive Polypeptides from Pegylated Poly-Lglutamates. *Biomacromolecules* **2011**, 12, 2859-2863.

32.   Kramer, J. R., Deming, T. J., Glycopolypeptides via Living Polymerization of Glycosylated-l-lysine N-Carboxyanhydrides. *J. Am. Chem. Soc.* **2010**, 132, 15068-15071.

33.   Secker, C., Robinson, J. W., Schlaad, H., Alkyne-X modification of polypeptoids. *Eur. Polym. J.* **2015**, 62, 394-399.

34.   Kolb, H. C., Finn, M. G.; Sharpless, K. B., Click Chemistry: Diverse Chemical Function from a Few Good Reactions. *Angew. Chem., Int. Ed.* **2001**, 40, 2004-2021.

35.   Hein, C.D., Xin-Ming, L., and Dong, W. Click Chemistry, a Powerful Tool for Pharmaceutical Sciences. *Pharmaceutical Research* 2008, 25, 2216–2230.

36.   Huang, J., Heise, A. Stimuli responsive synthetic polypeptides derived from N-carboxyanhydride (NCA) polymerisation *Chem. Soc. Rev.* **2013**, 42, 7373-7390.

37.   Krannig, K., Schlaad, H. Emerging bioinspired polymers: glycopolypeptides *Soft Matter* **2014**, 10, 4228-4235.

38. Robinson, J. W., Schlaad, H., A versatile polypeptoid platform based on *N*-allyl glycine. *Chem. Commun.* **2012**, 48, 7835-7837.

39. Lahasky, S. H., Serem, W. K., Guo, L., Garno, J. C., Zhang, D., Synthesis and Characterization of Cyclic Brush-Like Polymers by N-Heterocyclic Carbene-Mediated Zwitterionic Polymerization of N-Propargyl N-Carboxyanhydride and the Grafting-to Approach. *Macromolecules* **2011**, 44 (23), 9063-9074.

40. Lahasky, S. H., Serem W. K., Guo L., Garno J. C., Zhang D. Synthesis and Characterization of Cyclic Brush-Like Polymers by N-Heterocyclic Carbene-Mediated Zwitterionic Polymerization of N-Propargyl N-Carboxyanhydride and the Grafting-to Approach. *Macromolecules* **2011**, 44, 9063-9074.

41. Li, A., Zhang, D. Synthesis and Characterization of Cleavable Core-Cross-Linked Micelles Based on Amphiphilic Block Copolypeptoids as Smart Drug Carriers. *Biomacromolecules* **2016**, *17,* 852–861.

42. Lowe, A. Thiol-ene ''click'' reactions and recent applications in polymer and materials synthesis *Polym. Chem.*, **2010**, 1, 17–36.

43. Holub, J. M., Jang, H., Kirshenbaum, K. Clickity-click: highly functionalized peptoid oligomers generated by sequential conjugation reactions on solid-phase support. *Org. Biomol. Chem.* **2006**, 4, 1497− 1502.

44. Jang, H., Fafarman, A., Holub, J. M., Kirshenbaum, K. Click to Fit: Versatile Polyvalent Display on a Peptidomimetic Scaffold. *Org. Lett.* **2005**, 7, 1951−1954.

45. Norgren, A. S., Budke, C., Majer, Z., Heggemann, C., Koop, T., Sewald, N. On-resin click-glycoconjugation of peptoids. *Synthesis* **2009**, 2009, 488−494.

46. Zhu, L., Simpson, J., Xu, X., He, H., Zhang, D., Yin, L. Cationic Polypeptoids with Optimized Molecular Characteristics toward Efficient Nonviral Gene Delivery. *ACS App. Mater. Inter.* **2017**, 9, 23476-23486.

47. Fetsch, C., Luxenhofer, R. Highly Defined Multiblock Copolypeptoids: Pushing the Limits of Living Nucleophilic Ring-Opening Polymerization. *Macromol. Rapid Commun.* **2012**, 33, 1708-1713.

48. Fetsch, C., Grossmann, A., Holz, L., Nawroth, J. F., Luxenhofer, R. Polypeptoids from N-Substituted Glycine *N*-Carboxyanhydrides: Hydrophilic, Hydrophobic, and Amphiphilic Polymers with Poisson Distribution. *Macromolecules* **2011**, 44, 6746-6758.

49. Robinson, J. W., Secker, C., Weidner, S., Schlaad, H. Thermoresponsive Poly(*N*-C3 glycine)s. *Macromolecules* **2013**, 46, 580-587.

50. Thakkar, A., Cohen, A., Connolly, M., Zuckermann, R., Pei, D. High-throughput sequencing of peptoids and peptide-peptoid hybrids by partial edman degradation and mass spectrometry *J Comb Chem.* **2009**, 11, 294-302.

CHAPTER 3: CATIONIC POLYPEPTOIDS TOWARDS EFFICIENT NON-VIRAL GENE DELIVERY

3.1 Introduction

Gene therapy has been widely regarded as a promising modality to treat various human diseases, including cancer, infectious diseases, and immunodeficiency.[1-7] High transfection efficiency and low toxicity are the two basic requirements for gene delivery vectors.[8-12] Cationic polymers (also referred to as polycations), a major category of non-viral gene vectors, feature potent gene condensation capabilities to promote the cellular internalization, and thus have received wide applications as gene transfection materials.[13-19] However, the relatively low transfection efficiency still remains a critical issue for polycations, which is mainly attributed to the various biological barriers that render the rational design of polycations challenging. Therefore, it is highly demanded that the structure-property relationship of polycations be systemically unraveled, such that their molecular characteristics could be optimized to synergistically overcome the multiple cellular barriers against effective gene transfection.

Because of the sidechain substitution on the nitrogen atom, polypeptoids lack extensive hydrogen bonding and mainchain stereogenic center that are typical for polypeptides. It thus allows the physicochemical properties of polypeptoids (*e.g.*, conformation, solubility, thermal property, and crystallinity) to be tuned by controlling the sequence, sidechain chemistry, and molecular architecture.[20-24] As such, synthetic polypeptoids have been widely applied for non-fouling coating,[25] antimicrobial therapy,[26-28] drug delivery,[29-30] and *etc.*.[31] More importantly, polypeptoids are stable against proteolytic degradation, which allows them to maintain structural integrity under physiological conditions and thus makes them better-suited for certain biomedical

applications *in vivo*.[32-33] There is evidence that polypeptoids are more membrane permeable than structurally analogous peptides.[34-35] However, studies on polypeptoids as gene delivery vectors are limited.[36] While oligopeptoids have been previously explored for gene delivery,[37] they were synthesized by the solid-phase submonomer method which suffered from low yields (less than 20%) and limited chain length.[38]

3.2 Synthesis of Cationic Polypeptoids by Polymerization and Post-polymerization Strategies.

I have pursued the synthesis of cationic polypeptoids by a combination of polymerization and post-polymerization modification using either radical thiol-ene or copper-mediated alkyne-azide cycloaddition (CuAAC) "click" chemistry. This strategy is chosen due to the possibility to access a large library of structurally diverse cationic polypeptoids from a common precursor. This will enable the systematic investigation of structure-function relationship to identify optical molecular motifs for gene transfection application. Specifically, *N*-ally *N*-carboxyanhydride (Al-NCA) has been polymerized to produce the poly(*N*-ally glycine) which is further derivatized by radical thio-ene chemistry to install the cationic moieties on the sidechain. Alternatively, *N*-propargyl *N*-carboxyanhydride (Pg-NCA) monomer was polymerized to yield poly(*N*-propargyl glycine) followed by CuAAC chemistry to access cationic polypeptoids. Both "click" chemistry used in the post-polymerization modification step have successfully led to the desired cationic polypeptoid products. However, the water solubility of the resulting cationic polypeptoids from the two methods is vastly different presumably due to the disparate linker structures (*i.e.*, thioether versus triazole functionality) formed during the "click" chemistry (Scheme 3.1). This has significant implication on their potential uses as

36

non-viral gene delivery carriers. The details of the research findings will be discussed in the following sections.

Radical Thiol-ene Addition:
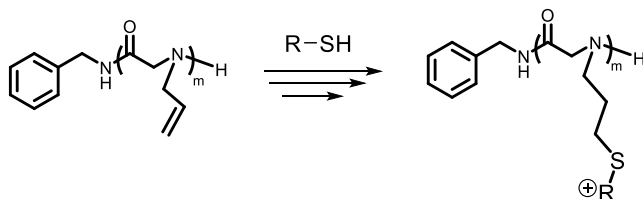
Pros:
 * Tolerant of various solvents
 * Efficient
 * Tolerant of other functional groups

Cons:
 * Poor water solubility of the resulting cationic polymers

Copper Catalyzed Alkyne-Azide Cycloaddition (CuAAC):
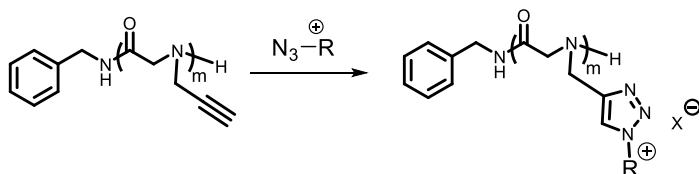
Pros:
 * Tolerant of various functional groups
 * Efficient
 * Versatile reaction conditions
 * Good water solubility of the resulting cationic polymers

Cons:
 * Need for a metal catalyst

Scheme 3.1 Click chemistry that have been investigated to make cationic polypeptoids.

3.3. Synthesis and Characterization of Poly(*N*-allyl glycine) (PNAIG) Polymers

The synthesis and polymerization of *N*-Allyl NCA (Al-NCA) was first reported by Schlaad and coworkers.[43] Briefly, poly(*N*-allyl glycine)s (PNAIG) polymers with M_n in the 1.5–10.5 kg mol^{-1} range and PDI = 1.1–1.4 were synthesized by primary amine-initiated

37

ROP of Al-NCAs. The polymers can be readily dissolved in organic solvents and water. Post polymerization modifications of PNAlGs with unprotected thiosugars by thiol-ene chemistry can be conducted in an aqueous medium. Polymerization of Al-NCA and post-modification by thiol-ene chemistry represents an attractive route to access structurally diverse polypeptoids derivatives. Inspired by Schlaad work, I investigated the synthesis of cationic polypeptoids by a combination of ROP of Al-NCA and post-polymerization modification of the PNAlG polymers by radical thiol-ene chemistry to install the cationic moieties on the *N*-substituent.

Polymerization of Al-NCA using benzylamine initiators in different initial monomer-to-initiator feed ratios ($[M]_0:[I]_0$) have been investigated in THF at 50 $^\circ$C. FT-IR spectroscopy has proven to be a reliable and convenient tool in the monitoring the reaction progress, as the Al-NCA monomer exhibits characteristic carbonyl C=O stretching bands at 1857 cm^{-1} and 1757 cm^{-1} that are distinctly different from the resulting polymer with carbonyl C=O stretching band at ~1654-1659 cm^{-1}. It typically takes 18-24 h for the ROP of Al-NCA to reach quantitative conversion. The resulting polymers were isolated and purified by the addition of excess hexane followed by decantation and drying via high vacuum to afford a white powder. The polymer composition, molecular weight and molecular weight distribution of the resulting polymers have been characterized by ^{1}H NMR spectroscopy and size-exclusion chromatography (SEC) methods (Table 3.1). The polymer chain lengths for PNAlG polymers were determined by the integration of alkene protons of allyl side chains at 5.81 ppm relative to the aromatic protons of the benzyl end group at 7.26 ppm in their respective ^{1}H NMR spectra (Figure 3.1). There was an excellent agreement between

38

the experimental molecular weight (M_n) determined by ^{1}H NMR and SEC with the theoretical prediction in the low molecular weight range ($[M]_0:[I]_0 < 50:1$, $M_n<5$kg/mol)), indicating good control of polymerization. In agreement with earlier reports by Schlaad and Luxenhofer, deviations in M_n were observed with increasing chain lengths of PNAIG above 50 mer (Figure 3.2).[43-44] SEC analysis also revealed fairly broad and multimodal molecular weight distributions for PNAIG samples with PDIs= 1.2-1.4. The presence of high molecular weight shoulders (Table 3.1 and Figure 3.2) is attributed to the aggregation of PNAIG polymers in the DMF/LiBr (0.1M) solvent used in SEC analysis. Schlaad et al. has previously reported that PNAIG along with other poly(C-3 *N*-substituted glycine) polymers can undergo intra-chain hydrogen-bonding, reducing solvation by surrounding solvent by shielding the polymer backbone.[44]
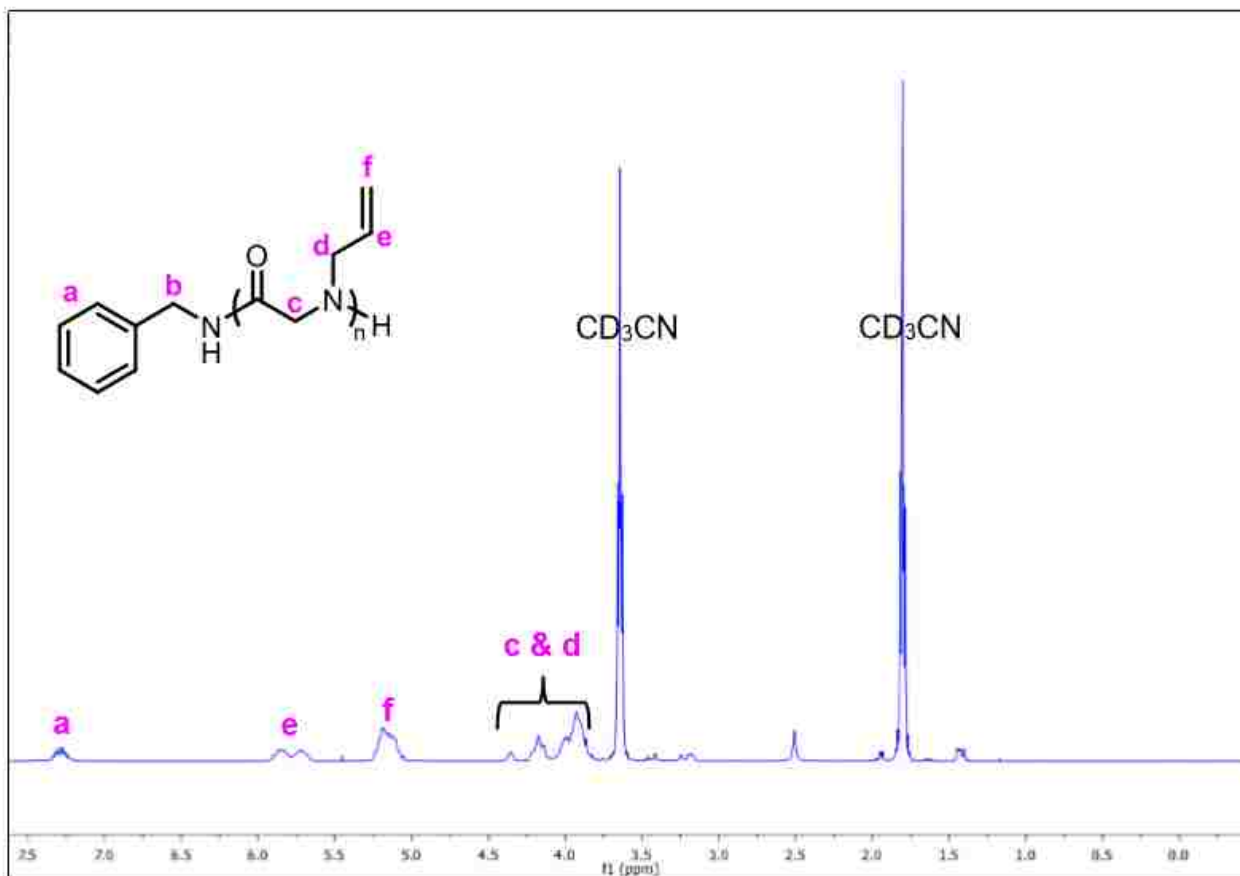
Figure 3.1. Representative ^{1}H NMR spectrum of PNAIG polymers in CD$_3$CN.

Table 3.1 Molecular characteristics of PNAIG polymers obtained by benzylamine–initiated ROP of Al-NCA in THF at 50 °C.

[M]$_0$:[I]$_0$	[M]$_0$	M$_n$ (theor.) (kg/mol^{-1})	M$_n$ (NMR)^a (kg/mol^{-1})	M$_n$ (SEC)^b (kg/mol^{-1})	SEC (PDI)^b
25:1	.5M	2.5	2.1	2.8	1.4
50:1	.5M	4.9	3.7	4.5	1.3
75:1	.5M	7.4	6.6	6.1	1.3
100:1	.5M	9.8	7.4	7.7	1.2

$^{a.}$ Polymer composition determined by integration of alkene protons relative to benzyl end group.
$^{b.}$ Experimental molecular weight and polydispersity index are obtained from a tandem SEC-MALS-DRI system in 0.1 M LiBr/DMF solution dn/dc of 0.0950 mL•g^{-1}.

40
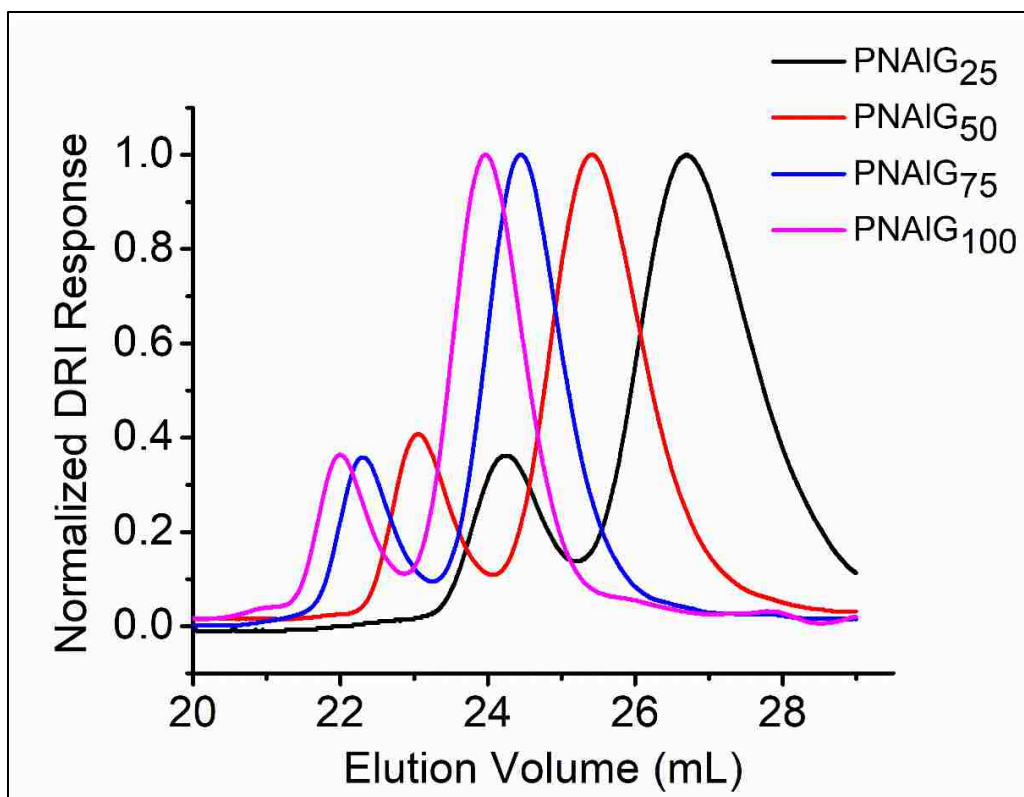
Figure 3.2 Normalized SEC chromatogram (0.1 M LiBr/DMF, 25 °C) of PNAIG polymers. Experimental $M_n s$ (2.8-7.7 kg/mol) and PDIs (1.2.-1.4) of the polymers that were synthesized via benzylamine-initiated ring-opening polymerization of AI-NCA (Table 3.1).

3.4. Grafting of Neutral Thiol Compounds

Free thiols were reacted with PNAIG homopolymers via the photo-initiated radical thiol-ene addition reaction (Scheme 3.2). 1-Chloro-3-propane mercaptan (CPT) was initially investigated in this reaction for the consideration of further derivation by $S_n 2$ substitution chemistry to install various cationic moieties, thus producing a library cationic polypeptoids.
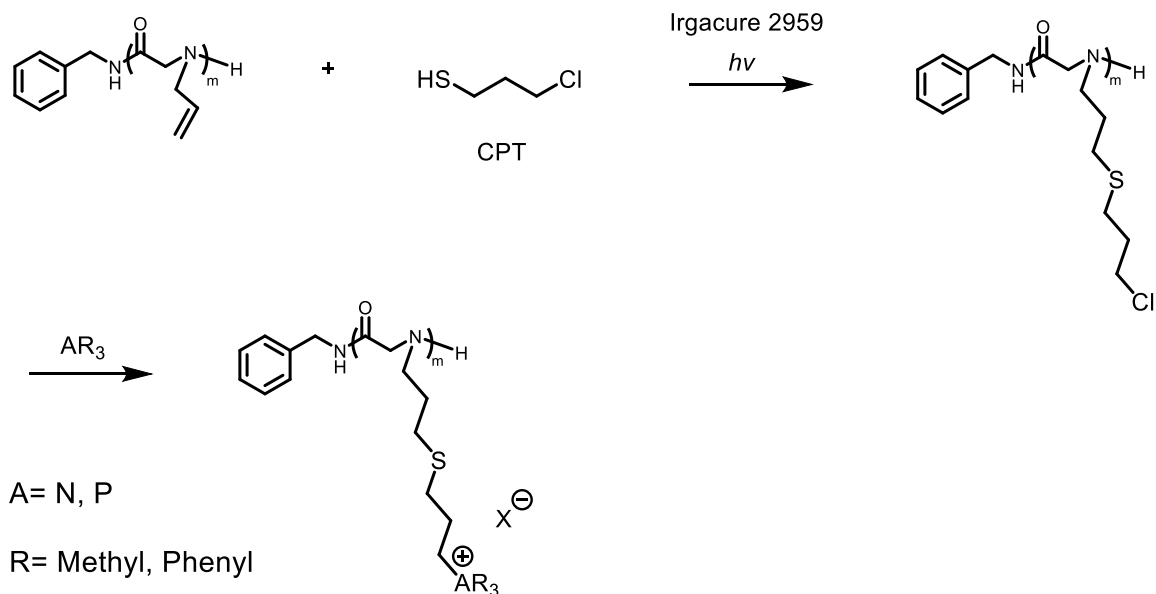
Scheme 3.2. Proposed synthesis of cationic polypeptoids via modification of PNAIG by radical thio-ene addition chemistry with 1-chloro-3-propane thiol (CPT) and nucleophilic substitution (using tertiary heteroatom compounds).

PNAIG polymers were pretreated with methanol and dried prior to thiol conjugation to prevent aggregation.[43] PNAIGs were subjected to UV irradiation In the presence of a photo-initiator and CPT. In all cases quantitative grafting of thiols to the PNAIGs was observed as evident by the disappearance of allylic protons at 5.86 ppm and 5.32 ppm in ^{1}H NMR analysis (Figure A.1). The chain lengths of the resulting polymers were determined by the integration of -CH$_2$ protons of polymer backbone relative to the aromatic protons of the benzyl end group in the ^{1}H NMR spectrum (Figure A.1). Prior to the thiol-ene reaction, the PNAIG polymer is a white powder. Post thiol-ene reaction, the resulting polymers appear yellow and sticky in texture. While PNAIG polymer precursor was fully water soluble, the resulting polymers post thiol-ene addition

become water insoluble, presumably due to the enhanced hydrophobicity of the additional thiol-alkyl ether linkages on the sidechain.

3.5. Grafting of Cationic Thiol Compounds

To improve the water solubility of the polypeptoids bearing the thio-ether sidechain, I investigate the grafting of a positively charged thiol compound by radical thio-lene chemistry. I postulated that presence of cationic groups along polymer side chains would counteract the enhanced hydrophobic character due to the thiol-alkyl ether sidechain, thus resulting in enhanced solubility of the polymers in water. Various cationic alkyl mercaptan compounds were submitted to radical thiol-ene click addition with PNAIGs as depicted in Scheme 3.3. However, this approach led to no reaction with recovery of PNAIG starting material. Because no issues were encountered with the grafting of thiol groups neutral in charge, I presume that charge repulsion between the cationic thiol derivatives following thiyl radical formation occurred. The consequence of this is the suppressed interaction of thiyl radicals with polymer alkene groups for grafting.
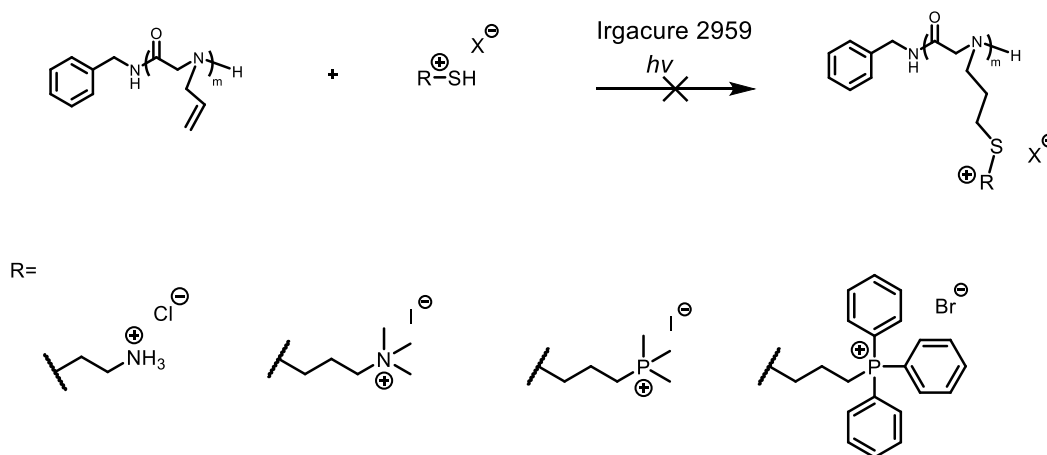
Scheme 3.3 Attempted synthesis of cationic polypeptoids via radical thiol-ene addition reaction using positively charged thiol compounds.

3.6. Synthesis of Thiol Compound with Enhanced Water Solubility

I also investigated the conjugation of PNAIG polymers with 2-mercaptoethanol via radical thiol ene chemistry. The grafting efficiency was quantitative as evidenced by the disappearance of -CH=CH$_2$ proton signals in the allylic region (5.72 ppm and 5.01 ppm) of ^{1}H NMR (Figure 3.3). The backbone degree of polymerization of the resulting polypeptoids can be determined by integration of -CH$_2$ protons of polymer backbone relative to the aromatic protons of the benzyl end group in the ^{1}H NMR spectrum. It is encouraging to find that the resulting polymers are water soluble. It is clear from this result that to enhance the water solubility of polypeptoids bearing thiol-alkyl ether linkages, the relative hydrophilicity and lipophilicity content of the thiol compounds has to be increased.
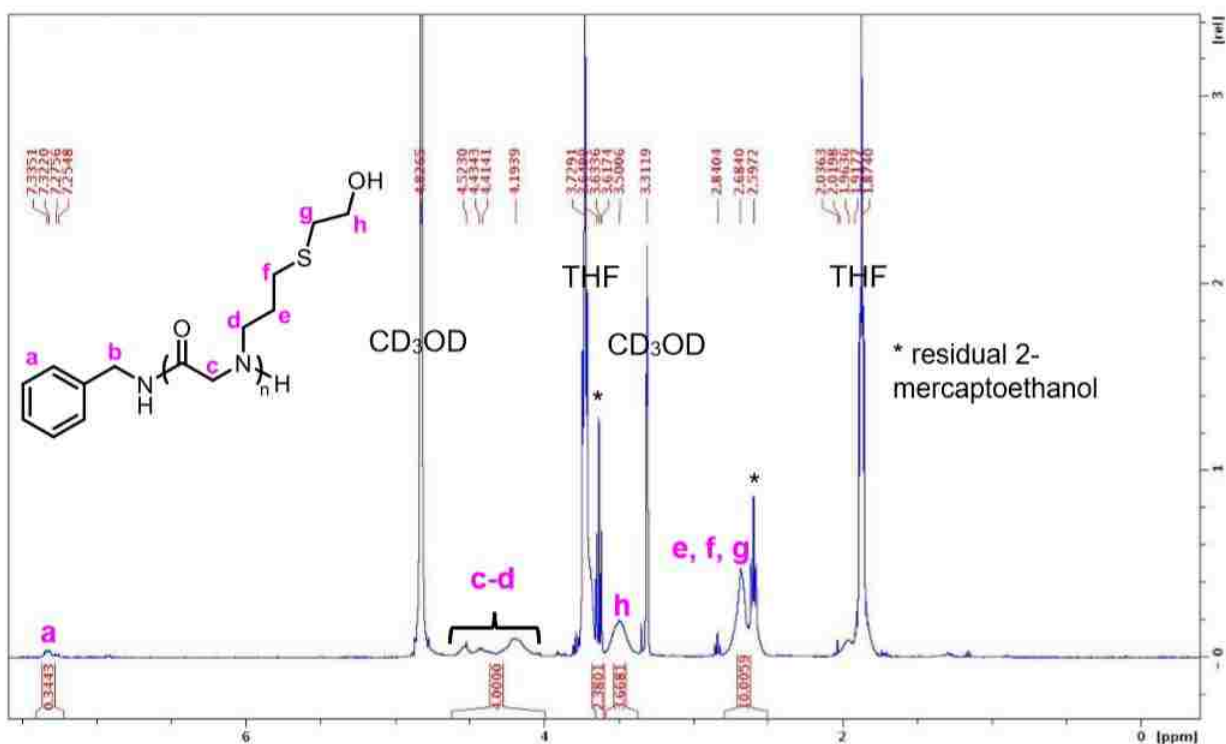
Figure 3.3 Representative ^{1}H NMR spectrum of 2-mercaptoethanol-modified PNAIG in CD$_3$OD.

44

One idea is to use thiols bearing some oligomeric ethylene glycol structure motif and a suitable leaving group (Scheme 3.4) in the thiol-ene reaction with PNAIG. The presence of oligomeric ethylene glycol linker is expected to increase the water solubility of resulting polypeptoids from thiol-ene addition. The leaving group will allow for further installation of cationic moieties by substitution reaction post thiol-ene conjugation. The targeted thiol compound was synthesized in an overall yield of 35.8% by a multi-step reaction scheme as illustrated in Scheme 3.4. All intermediates (Figures A.2-A.5) leading up to the final thiol compound (Figures A.6 and A.7) were characterized by NMR spectroscopy. With the thiol compound in hand, I investigated the radical thiol-ene method to conjugate this moiety to the PNAIG polymer. After multiple attempts, the reaction was unsuccessful in producing the desired polypeptoids bearing thiol-ether sidechains. This is tentatively attributed to the competing radical oligomerization of the thiol compound of its own via the thiol-halide substitution.[45]
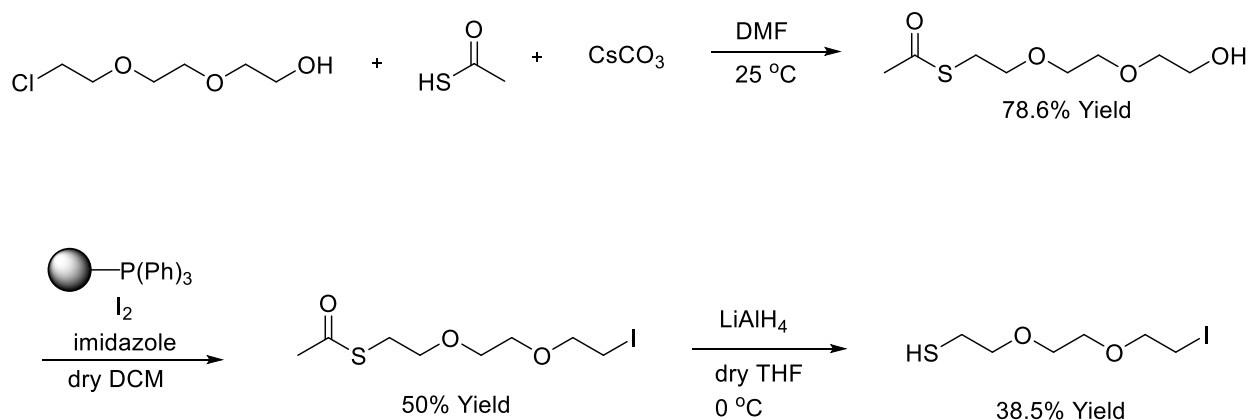
Scheme 3.4 Synthesis of 2-(2-(2-iodoethoxy)ethoxy)ethanethiol.

3.7. Synthesis of PNAIG-*r*-PNMeG Random Copolypeptoids

Having failed at different tactics to develop water-soluble cationic polypeptoid homopolymers, I set to investigate the synthesis of a copolypeptoids precursor that are less hydrophobic than PNAIGs by the copolymerization strategy.[52,53] Polysarcosine polymers obtained from ROP of Me-NCA is highly water soluble and has been studied as biomaterials for various biomedical applications. Hence, I conducted the copolymerization of Al-NCA and Me-NCA using benzylamine initiator, producing a random copolypeptoid to be used in the subsequent thiol-ene addition reaction (Figure A.10).

The random copolypeptoids (PNAIG-*r*-PNMG) can be readily dissolved in water prior to radical thiol-ene coupling as expected, but there are constraints. The water solubility of the resulting polypeptoids was found to be dependent on the composition of allyl segment present in the PNAIG-*r*-PNMG precursors. While PNAIG$_4$-*r*-PNMG$_{39}$ with 9% *N*-allyl glycine content was water-soluble, PNAIG$_{20}$-*r*-PNMG$_{23}$ comprised of 47% *N*-allyl glycine content was insoluble in water. This was a major drawback as carriers for gene delivery need to be water soluble in order to be used. Because of the precursor's inability to dissolve in water, radical thiol-ene addition experiments were carried out using PNAIG$_4$-r-PNMeG$_{39}$. Conjugation of PNAIG$_4$-r-PNMeG$_{39}$ with CPT via radical thiol-ene reaction was successful. Quantitative grafting of CPT thiol to the copolymers by radical thiol-ene chemistry was evidenced by the total disappearance of allylic protons as illustrated in Figure A.10. Subsequently, use of the Sn2 reaction with trimethyl phosphine was performed to obtain the positively charged moiety from PNAIG$_4$-*r*-PNMG$_{39}$-CPT (Figure A.11). Upon conjugation with the tertiary phosphine solvation of

46

the cationic, thiosulfide containing copolymer by water was retained. Unlike the case with CPT-functionalized copolypeptoid precursors, the composition and degree of polymerization of the final cationic random copolypeptoids cannot be accurately determined from ^{1}H NMR spectrum due to the severe overlap of relevant proton peaks (Figure A.11).

While the copolymerization method is viable for the synthesis of water-soluble cationic polypeptoids the low PNAlG content in the copolypeptoids ultimately limit the usefulness of this approach. For a comprehensive understanding of structure-property relationship pertinent to nonviral gene delivery, a synthetic platform that allows for facile and modular tuning of the molecular characteristics is needed.

3.8. Synthesis of Water-Soluble Cationic Polypeptoids by ROP of *N*-Propargyl *N*-carboxyanhydride (Pg-NCA) and Post-Polymerization Modification via Copper Catalyzed Alkyne-azide Cycloaddition (CuAAC) Method

After encountering much difficulty in accessing water-soluble cationic polypeptoids via the post-polymerization modification of PNAlG polymers by radical thio-ene chemistry, I switched my focus to investigate an alternative strategy towards cationic polypeptoids. This involves the polymerization of *N*-propargyl NCA to first afford poly(*N*-propargyl glycine) precursors followed by copper-catalyzed alkyne-azide cycloaddition chemistry to install cationic moieties. This is based on the consideration that triazole linkers resulted from the CuAAC chemistry is more polar than the thio-ether linkages obtained by thio-ene chemistry and will lead to cationic polypeptoids with enhanced water solubility. This strategy proves to be very effective in the synthesis of a variety of water-soluble cationic polypeptoids. The details of the synthesis and

47

characterization of these cationic polypeptoids will be discussed in the following sections.

3.9. Synthesis and ROP of Pg-NCA Monomer

The synthesis of *N*-propargyl NCA was previously reported. It involves the reductive amination of glyoxylic acid with propargyl amine (Scheme 3.5). The reaction appears to be sensitive to the source and purity of glyoxylic acids. In multiple attempts, the reaction stops at the imine intermediate without the formation for the desired *N*-propargyl glycine product. Alternative strategies that involve the substitution of brominated acetyl derivatives[46] with propargyl amine prove to be more reliable in accessing *N*-propargyl glycine in high yield. Subsequent hydrolysis and Boc protection

Route 1:
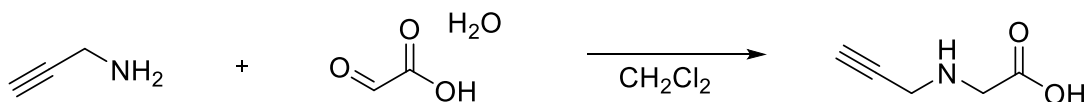
Route 2:
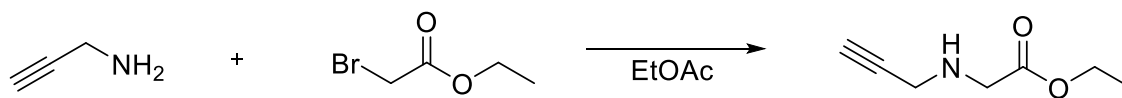
followed by PCl₃-mediated cyclization afforded the desired Pg-NCA in good yields.

Scheme 3.5 Synthetic routes for *N*-propargyl glycine, the precursor to the Pg-NCA monomer.

Ring-opening polymerization of Pg-NCA was investigated using benzyl amine initiators in varying initial monomer-to-initiator feed ratio ($[M]_0:[I]_0$) to access poly(N-

propargyl glycine) (PNPgG) polymers. All reactions were conducted at .5M in THF and 50 °C for 18-24 hours to reach quantitative conversions. The number average degree of polymerization (DP_n) for PNPgG polymers were determined using ^{1}H NMR spectroscopy by integrating the alkyne proton of propargyl side chains at 2.30 ppm relative to the aromatic protons of the benzyl end group at 7.23 ppm (Figure 3.5). The PNPgG polymers were also analyzed by the SEC-MALS-DRI method to determine the absolute polymer molecular weight and molecular weight distribution. The PNPgG with M_n in the range of 2.8-23.9 corresponding to DP= 28-250 and PDI in the 1.03-1.18 range can be obtained by adjusting the $[M]_0:[I]_0$ ratio (Figure 3.4). The SEC traces (Figures 3.4 and 3.6) appear multi-modal for sample samples, which have been attributed to the aggregation of the PNPgG polymers in the SEC solvent (DMF/LiBr (0.1M).[23] It has been found that stirring PNPgG polymers for 18 h at room temperature in DCM, a better solvent than DMF, prior to the SEC analysis can significantly reduce the level of aggregation (Figure 3.6). Copolymerization with other NCAs (e.g., *N*-Decyl NCA) have also shown to be effective in reducing aggregation (Table 3.2 and Figure A.12).

Table 3.2. Cationic polypeptoids with various DPs and sidechain structures.

entry	DP (exp.)[a]	y^d	R[e]	PDI[a]	yield (%)
P1	46	3	$-N(CH_3)_3$	1.08	82
P2	46	3	$-NH(CH_3)_2$	1.08	94
P3	46	3	$-NH_2CH_3$	1.08	96
P4	46	3	$-NH_3$	1.08	75
P5	28	3	$-NH_3$	1.09	60
P6	135	3	$-NH_3$	1.18	80
P7	250	3	$-NH_3$	1.06	70
P8	46	4	$-NH_3$	1.08	76
P9	46	5	$-NH_3$	1.08	95
P10	46	6	$-NH_3$	1.08	91
P11	48 ($m = 39, n = 9$)[b]	6	$-NH_3$	1.03[c]	91

[a]DP and PDI of the PNPgG polymer were obtained from SEC–MALS–DRI. [b]DP of the P(NPgG-r-NDeG) copolymer was determined by ^{1}H NMR. [c]Experimental PDI of polypeptoid copolymer P(NPgG-r-NDeG) was obtained from SEC–MALS–DRI. [d]Number of methylene groups between triazole and charged amine groups. [e]Type of side-chain terminal group.
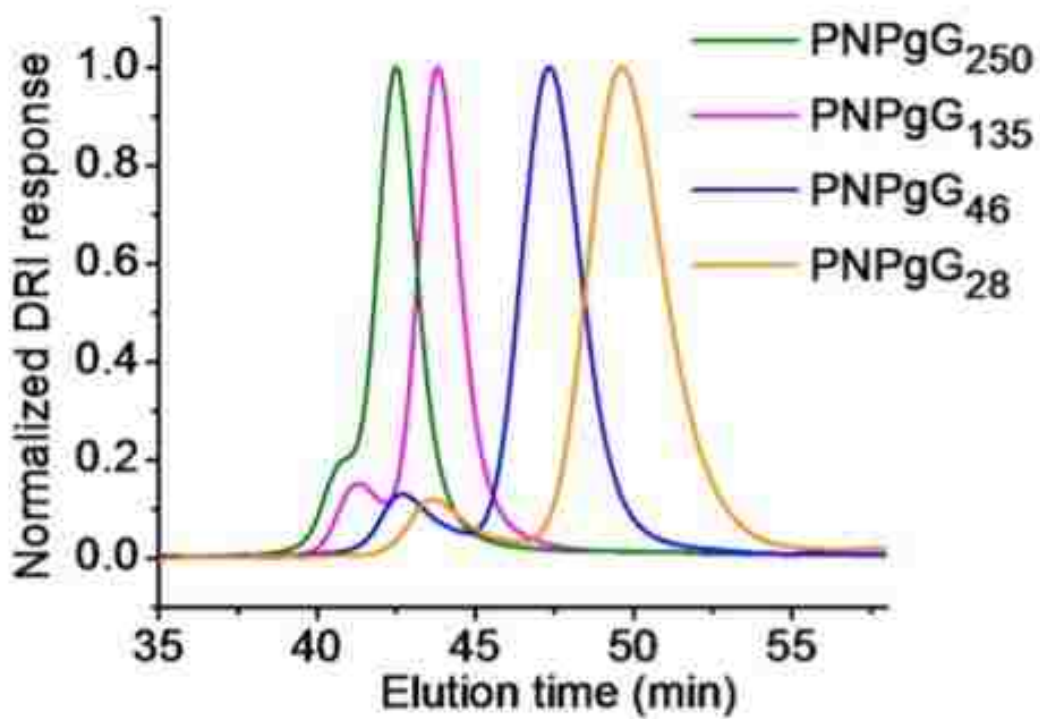
Figure 3.4. Normalized SEC chromatograms (0.1 M LiBr/DMF, 25 °C) of the PNPgG polymer with various backbone lengths (DP = 28, 46, 135, and 250, Mn = 2.8, 4.5, 12.9, and 23.9 kg/mol, PDI = 1.03−1.18) synthesized via the benzylamine-initiated ROP of Pg-NCA.
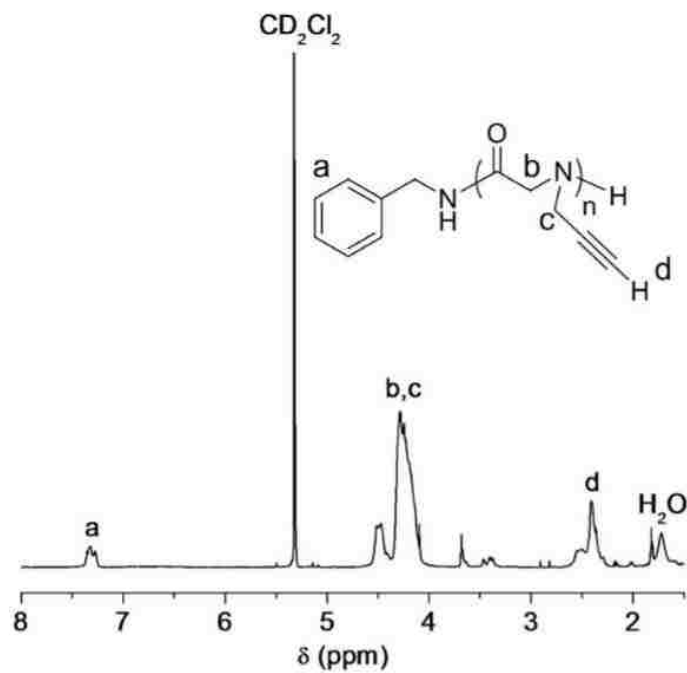
Figure 3.5. Representative ^{1}H NMR spectrum of the poly(N-propargyl glycine) homopolymer (PNPgG) in CD_2Cl_2. (CD_2Cl_2), δ ppm: 7.23−7.19 ppm (br m, −C_6H_5, Ha), 4.67−4.04 ppm (br m, −COCH$_2$N−, −CCH$_2$N−, Hb, Hc), 2.66−2.30 ppm (br m, −CHCCH$_2$−, Hd).
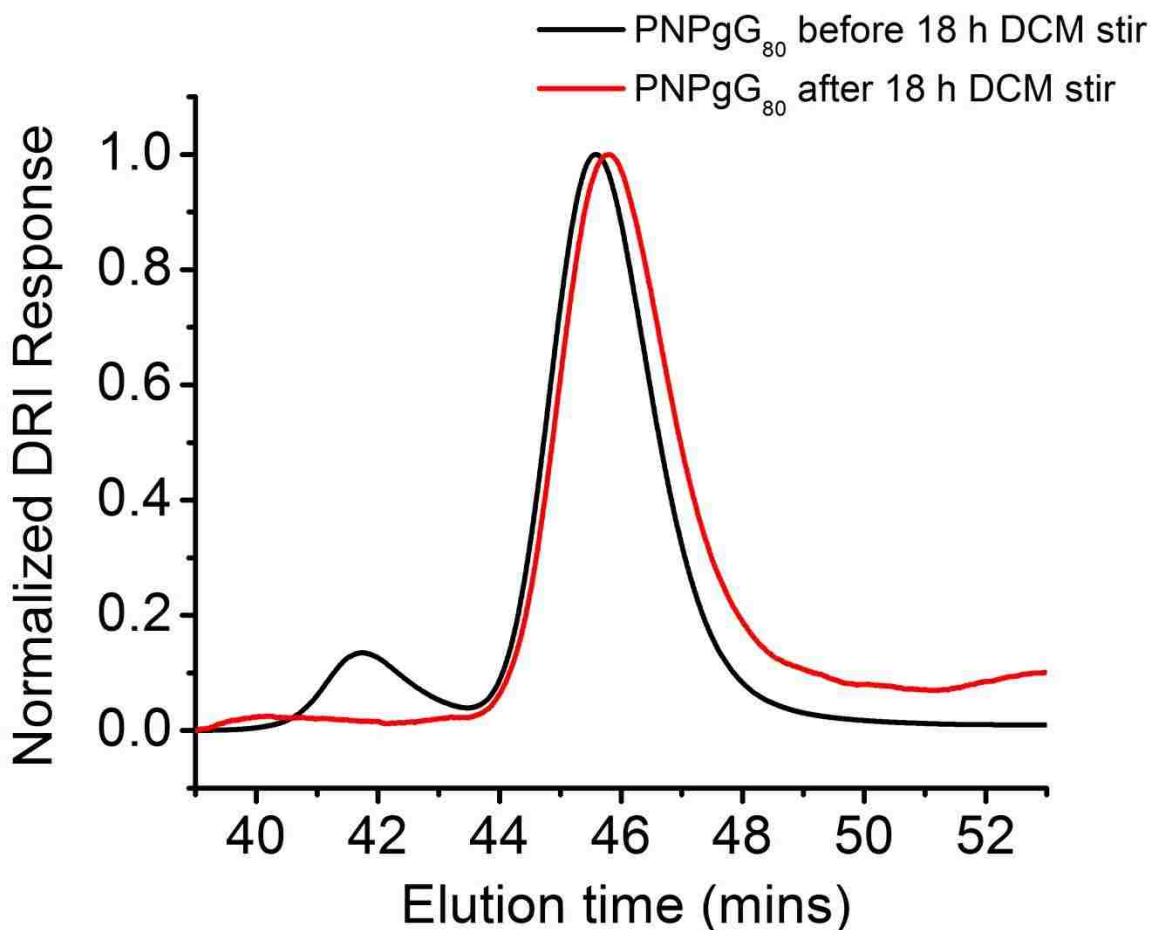
Figure 3.6 SEC chromatograms of PNPgG before and after DCM treatment.

3.10. Post-polymerization Modification of PNPgG with Cationic Azido Compounds by CuAAC Chemistry

With PNPgG polymers having different chain length available, I set to synthesize a series of cationic azido compounds that will be subsequently conjugated to the PNPgG polymers by CuAAC chemistry. I designed a library of cationic molecules bearing one azido group and one cationic ammonium moiety that are separated by a flexible alkyl linker. This structural design allows a variety of cationic moieties to be introduced in a modular manner, as shown in Scheme 3.6. With the presence of cationic groups, it is reasoned that the subsequent conjugation to PNPgG polymers by CuAAC

53

chemistry should be facilitated as the level of aggregation of the resulting polymers should be reduced due to electrostatic repulsion of the charged moieties.
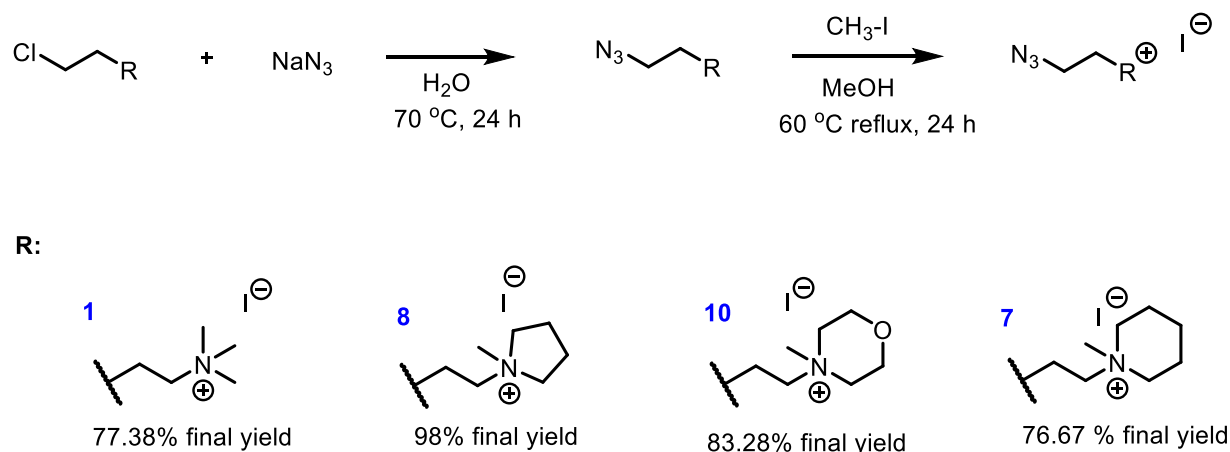
Scheme 3.6 Synthesis of various cationic azido compounds.

I have synthesized a library of cationic azido compounds **1-10** by the method shown in Scheme 3.7 and verified their structures by ^{1}H NMR spectroscopic analysis (Figures A.14-A.17 *Selective structures 1, 7, 8, 10). The conjugation of the cationic azido compounds with PNPgG polymers was then investigated. All reactions were conducted with the propargyl group to azido group in 1: 2 ratio at 50 °C in DMF for 18 h in the presence of 33 mol% CuBr and 33 mol% PMDETA ligand (Scheme 3.7). At completion of cycloaddition, to remove copper from the reaction an aqueous solution of EDTA (9.9 mM, 3 mL), was added directly to a reaction mixture prior to dialysis against DI water for 24-48 h during which the DI water was changed twice a day. Next, the reaction mixture was then lyophilized to yield a light green powder in good yields (~60-95%). To measure copper content of cationic polypeptoids following dialysis Flame Atomic Absorption Spectrometry (FAAS) was performed using a series of solutions for a

calibration curve (1 ppm-10 ppm) that were prepared from copper (II) standard at the concentration of 1 mg/mL. The resulting cationic polypeptoids were readily soluble in water. ^{1}H NMR analysis of the cationic polymers (Figures 3.7 and A.21-A.31) in D_2O revealed the disappearance of the propargyl proton at 2.30 ppm and appearance of the triazole proton at 8.01 ppm, indicative of quantitative conversion by the CuAAC chemistry. The number average degree of polymerization (DP_n) of the resulting cationic polypeptoids can also be determined by the integration of the triazole proton (d) relative to the aromatic protons (a) of the benzyl end group in the ^{1}H NMR spectrum. After CuAAC chemistry, the DP of positively charged polypeptoids often appear reduced as compared to the DP of their neutral polypeptoid precursors. This may be attributed to differential solvation of polypeptoids chains or polymer aggregation in deuterated solvent (D_2O) used in the NMR analysis, resulting in incomplete relaxation of various protons of cationic polypeptoids and rendering errors in the estimation of their DPs. It should be noted that addition of a small aliquot of trifluoroacetic acid (TFA) to D_2O did not affect the relative proton integration for the cationic polypeptoids, even though this has previously been shown to be effectively in reducing aggregation of polypeptides in solution.
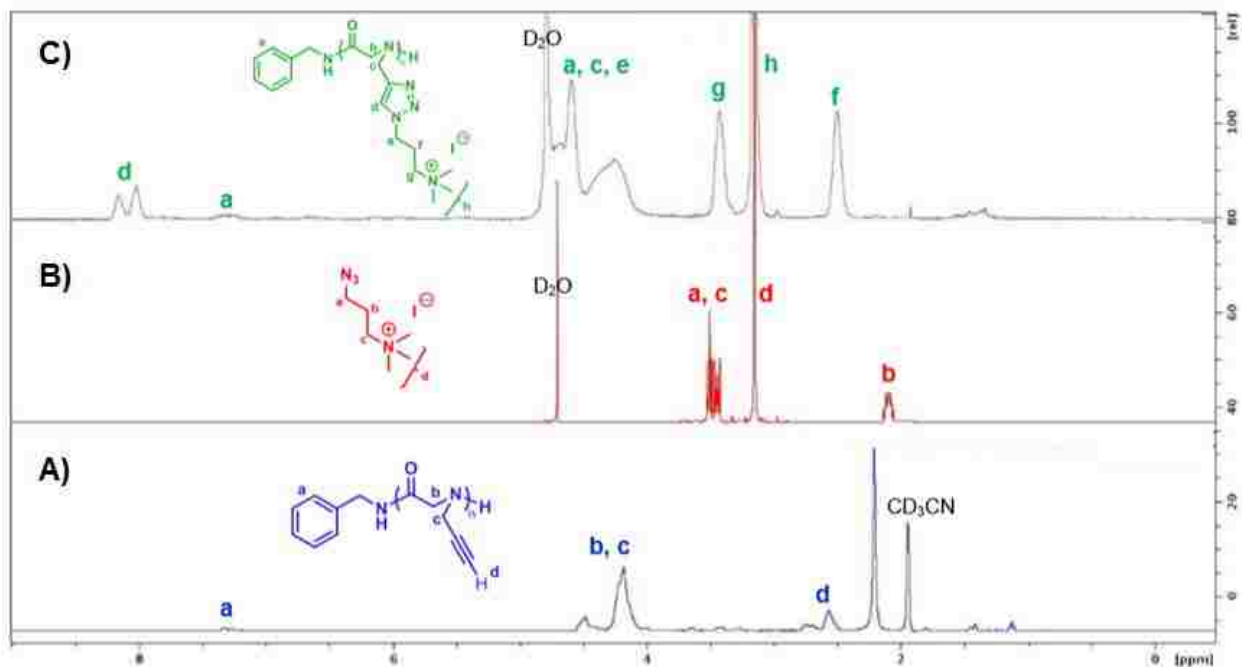
Figure 3.7 Representative ^{1}H NMR spectra of A) PNPgG (before CuAAC), B) cationic alkyl azide compound 2 (Scheme 3.6), C) cationic polypeptoids obtained after CuAAC chemistry.
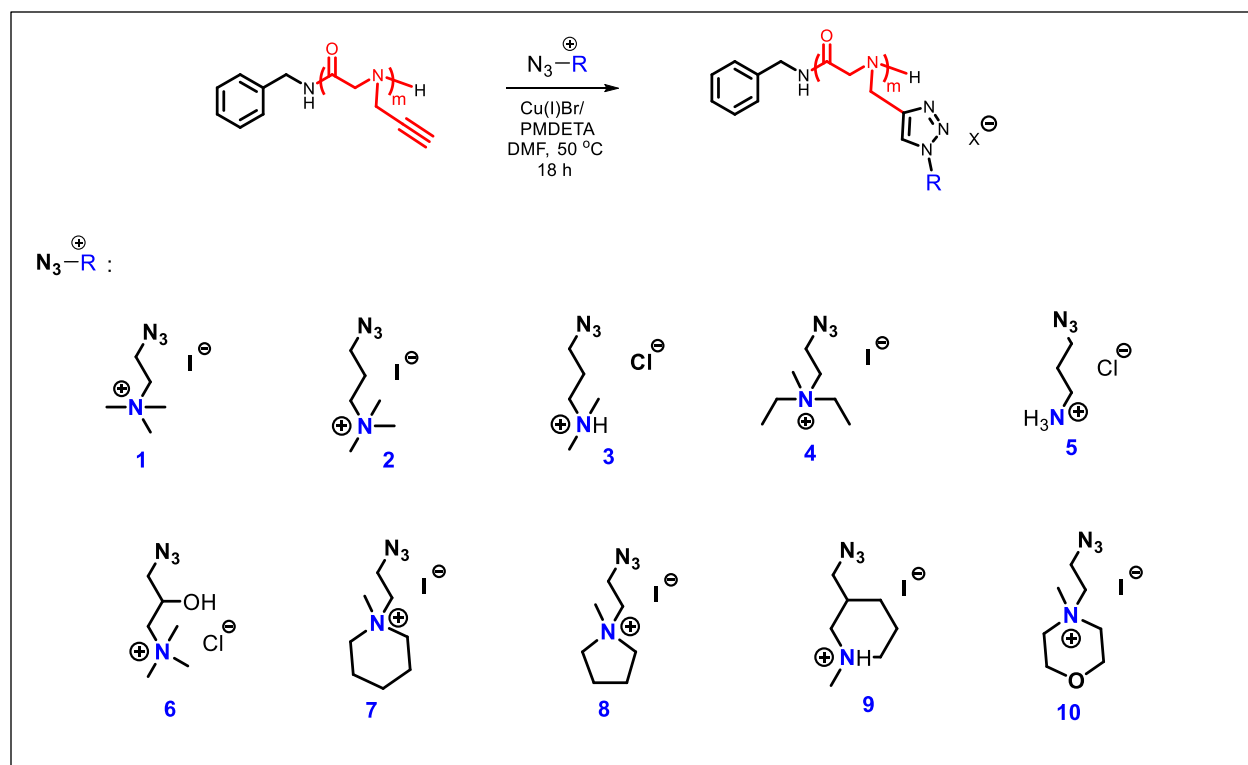
Scheme 3.7 Synthesis of cationic polypeptoids from various cationic alkyl azides and PNPgG polymers using CuAAC chemistry.

3.11. Optimizing the Molecular Characteristics of Cationic Polypeptoids Toward Efficient Non-Viral Gene Delivery

As I have demonstrated that water soluble cationic polypeptoids with tunable molecular characteristics can be accessed by a combination of ring-opening polymerization of Pg-NCA and CuAAC chemistry, a collaboration with the Yin group at Soochow University was initiated to systematically investigate the structure-property relationship towards gene delivery using cationic polypeptoids. In particular, I synthesized a series of polypeptoids with different cationic side-chain terminal groups, degree of polymerization, side-chain lengths, and incorporated aliphatic side chains. Their DNA condensation capability, DNA release, cellular uptake, intracellular kinetics,

transfection efficiency, and cytotoxicity were comprehensively evaluated, in attempt to identify the optimal polypeptoid structure with maximized gene delivery efficiency while minimized cytotoxicity. Herein, my synthetic contributions will be discussed. Results of assessments of cationic polypeptoids for gene transfection will also be mentioned.

3.12. Results and Discussion

3.12.1 Design, Synthesis, and Characterization of Cationic Polypeptoids

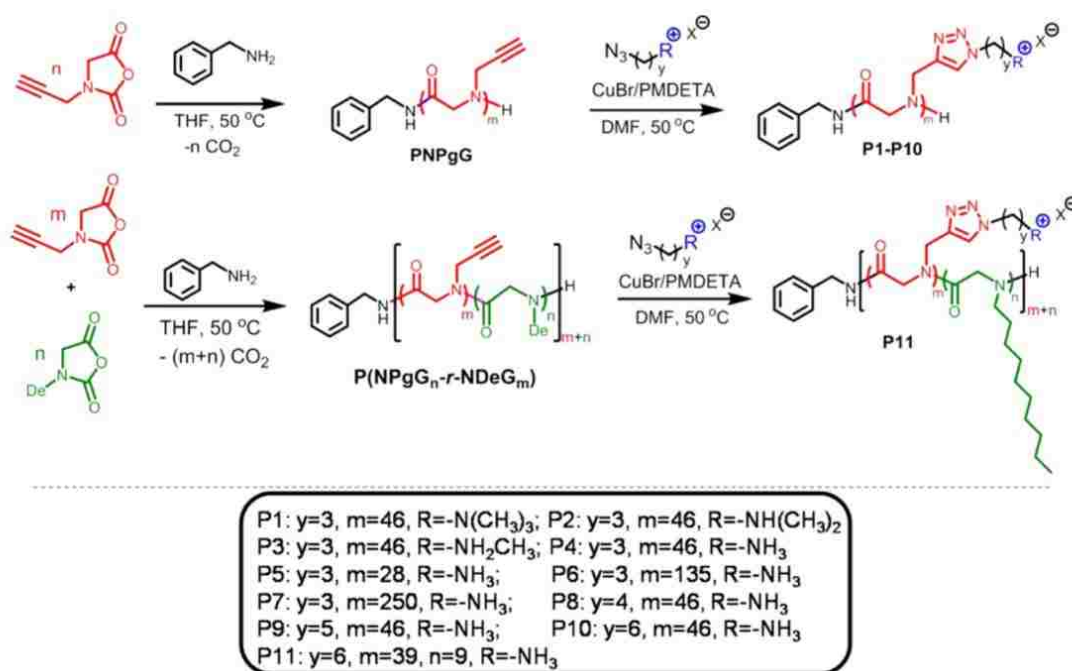I synthesized a series of cationic polypeptoids with varied molecular characteristics (*e.g.*, backbone length, side-chain length, different charged side terminal groups, and incorporated hydrophobicity) (Scheme 3.8 and Table 3.2). PNPgG with different M_ns were first synthesized via benzylamine-initiated controlled ring-opening polymerization (ROP) of the corresponding Pg-NCA monomers (Scheme 3.8). The resulting PNPgG with M_n of 2.8-24 kDa (DP_n = 28-251) and PDI of 1.08-1.48 was obtained, as characterized by SEC-MALS-DRI and NMR analysis (Figure 3.4-3.5, Table 3.2, and Figure A.13). A series of cationic polypeptoids were then synthesized by post-polymerization modification of the PNPgG with various ω-azido alkyl ammonium salts (Scheme A.18) using the "click" chemistry (Scheme 3.7). The side-chain derivation was quantitative in all cases, evidenced by the complete disappearance of the terminal alkyne proton of propargyl group at 2.51 ppm and appearance of the triazole proton at 8.0 ppm from the ^{1}H NMR analysis (Figures A.21-A.31). The cationic polypeptoids were purified by treatment with EDTA to remove copper salts followed by extensive dialysis against DI water. Upon lyophilization, all polymers were obtained as white to pale green powders in good yield (60-96%) with copper ion content in the sub-10 ppm range based on the atomic absorption analysis, which was significantly lower than the concentration

threshold that would otherwise cause potential copper ion-induced cytotoxicity. **P1**-**P4** carried different cationic side-chain terminal groups (primary, secondary, tertiary, and quaternary amine) at the fixed DP of 46; **P4**-**P7** possessed primary amine as the side terminal group while had different DP_n (28, 46, 134, and 251); **P8**-**P10** had the same DP (46) and side terminal group (primary amine), while afforded different spacer lengths between the triazole and amine (3, 4, 5, and 6 methylene groups) (Table 3.3). Chemical structures of the cationic polypeptoids were verified by ^1H NMR spectroscopy. All the resulting cationic polypeptoids afforded desired aqueous solubility, and thus could be readily used to complex DNA and mediate gene transfection in the aqueous medium.

P1: y=3, m=46, R=-N(CH$_3$)$_3$; P2: y=3, m=46, R=-NH(CH$_3$)$_2$
P3: y=3, m=46, R=-NH$_2$CH$_3$; P4: y=3, m=46, R=-NH$_3$
P5: y=3, m=28, R=-NH$_3$;   P6: y=3, m=135, R=-NH$_3$
P7: y=3, m=250, R=-NH$_3$; P8: y=4, m=46, R=-NH$_3$
P9: y=5, m=46, R=-NH$_3$;   P10: y=6, m=46, R=-NH$_3$
P11: y=6, m=39, n=9, R=-NH$_3$

Scheme 3.8. Synthetic routes of a library of cationic polypeptoids bearing different amino groups (**P1−P4**), DPs (**P4−P7**), hydrophobic sidechain lengths (**P4**, **P8**, **P9**, and **P10**), and aliphatic modification of the sidechains (**P11**).

P11 bearing a fraction of hydrophobic *N*-decyl side chains (Figure A.31) was similarly synthesized and characterized via modification of the P(NPgG-*r*-NDeG) random copolymer with ω-azido hexyl ammonium salt using "click" chemistry (Scheme 3.8). The P(NPgG-*r*-NDeG) copolymer precursor was synthesized by copolymerization of Pg-NCA and De-NCA using benzyl amine initiator and characterized by SEC-MALS-DRI and NMR analysis (Figures A.12, A.19 and A.20). **P11**, a random copolypeptoid analogue of **P10**, contained both primary amine groups (with 6 methylene groups between triazole and amine) and hydrophobic decyl groups on side chains, at the DP of 48 that was similar to **P10** (Table 3.2).

3.12.2. Formation and Characterization of Polypeptoid/DNA Polyplexes

DNA condensation by the cationic polypeptoids was first evaluated by the gel retardation assay. All the positively charged polypeptoids were able to condense DNA at the polypeptoid/DNA weight ratio ≥ 2.5, indicating complete condensation of DNA by the positively charged polypeptoids. Such results were further confirmed by a quantitative EB exclusion assay (Figure 3.8), wherein more than 80% of the DNA was condensed at the polypeptoid/DNA weight ratio ≥ 2.5. Polypeptoids with different charged groups (**P1**-**P4**) or with different side-chain length (**P4**, **P8**, **P9**, and **P10**) showed similar DNA condensation profiles.
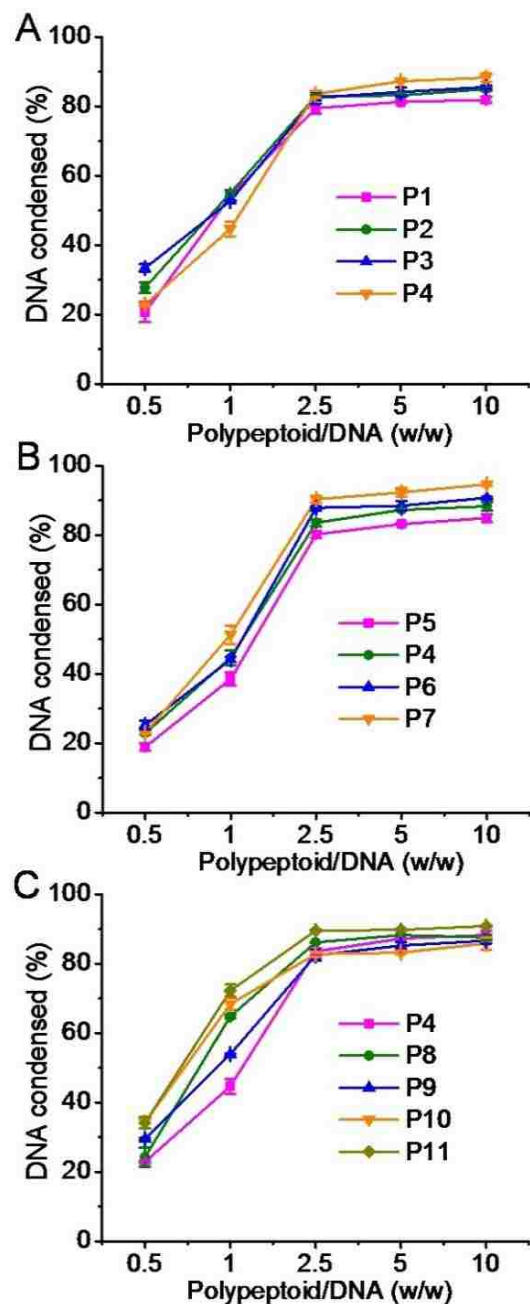
Figure 3.8. DNA condensation efficiencies of polypeptoids at various polypeptoid/DNA weight ratios as evaluated by the EB exclusion assay (n = 3). (A) Polypeptoids with different cationic side-chain terminal groups. (B) Polypeptoids with different DPs. (C) Polypeptoids with different hydrophobic side-chain lengths and incorporated hydrophobic decyl side chains.

In comparison, longer polypeptoid backbone correlated to enhanced DNA condensation level. DNA condensation levels as shown by the EB exclusion assay was represented by the order of **P7**>**P6**>**P4**>**P5**, mainly due to the facilitated entanglement of longer polypeptoids with DNA molecules (Figure 3.8B). Enhanced DNA condensation levels of polypeptoids as a result of presenting hydrophobicity were observed. **P11** with introduced aliphatic decyl side chains afforded higher DNA condensation level than its un-modified analogue **P10** despite its lower content of cationic group (Figure 3.8C), indicating that the hydrophobic interaction with DNA would provide additional forces to drive the assembly between polymer and DNA. As a result of their DNA condensation capabilities, all tested polypeptoid/DNA polyplexes, at the weight ratio higher than 2.5 displayed positive surface charges that would facilitate binding to cell membranes toward effective cellular internalization.

3.12.3. *In Vitro* Gene Transfection with Polypeptoid/DNA Polyplexes

Several molecular characteristics of polypeptoids were adjusted and tested for gene delivery to examine the structure-relationship property on transfection efficiency. Polypeptoids containing fixed DP (46) and side-chain length yet different side charged groups (**P1**, **P2**, **P3** and **P4**) were first evaluated in terms of the transfection efficiency in HeLa cells in serum-free medium (Figure 3.9A). Remarkably higher transfection efficiencies were displayed with analogues bearing primary amine than those containing secondary, tertiary, or quaternary amines. As such, based on the structure of **P4** with primary amine as the optimal cationic charged group, the DP of polymers was varied (**P4**, **P5**, **P6** and **P7**) to explore the effect of backbone length on the gene transfection capabilities. As shown in Figure 3.9B, an increase of polymer DP from 28 (**P5**) to 46

62

(**P4**) resulted in significantly enhanced transfection efficiency, presumably attributed to the enhanced DNA condensation and interactions with cell membranes.

Enhancing hydrophobicity of polymers often facilitates the hydrophobic interaction with cell membranes to promote cellular internalization. To this end, we prepared polypeptoid analogues of **P4** (DP = 46, 3 methylene groups between triazole and primary amine) with increased hydrophobic side chain lengths (**P8**, **P9**, and **P10**, with 4, 5, and 6 methylene groups between triazole and primary amine, respectively). As expected, the transfection efficiencies of polypeptoids in HeLa cells increased when the hydrophobic side-chain length was prolonged (Figure 3.9C), presumably due to enhanced membrane activities of the polymers to facilitate intracellular internalization of DNA cargoes. **P10** showed the highest transfection efficiency at the low polymer/DNA weight ratio of 2.5, outperforming commercial transfection reagent PEI by ~8 fold.

Random copolymers containing both charged side chains and hydrophobic pendant groups have been reported to show improved membrane activities compared to charged homopolymers, presumably due to further increased hydrophobic interactions with cell membranes. We thus went on to explore whether further enhanced gene delivery efficiency can be achieved for polypeptoids through a similar strategy. **P11**, random copolymer analogue of **P10**, was synthesized which contained ~20 mol% of pendent decyl groups. As shown in Figure 3.9D, **P11** displayed significantly improved transfection efficiency over **P10** by ~6 fold and it outperformed PEI by ~45 fold, which substantiated the critical role of introduced hydrophobic aliphatic side chains in promoting intracellular DNA delivery. Both **P10** and **P11** achieved the highest transfection efficiency at relatively low polymer/DNA weight ratio of 2.5 (equals to N/P

ratio of ~3.6 and ~3, respectively), in comparison to majority of polycation-based gene vectors that often require high N/P ratios to achieve effective gene transfection (e.g. N/P = 10 for PEI, N/P = 10 for dendrimers, N/P = 10 for helical polypeptides we developed before). Such desired property could presumably be attributed to the presence of hydrophobic domains that strengthened the membrane interactions, such that excessive cationic polymers are not necessarily required to impose sufficient binding affinities with negatively charged cell membranes.
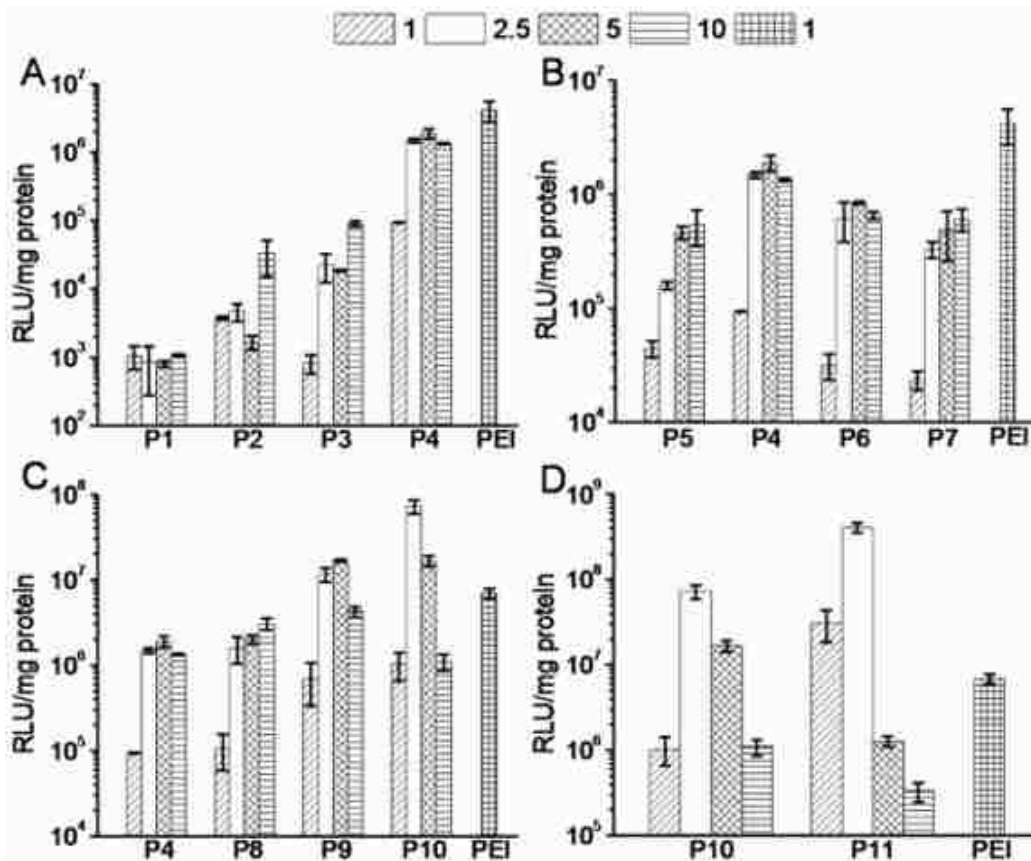

Figure 3.9. Transfection efficiencies of polyplexes at various polypeptoid/DNA weight ratios in HeLa (A−D), B16F10 (E), and COS-7 (F) cells in the absence of serum (n = 3).

Markedly compromised transfection efficiency in serum serves as a critical challenge against polycation-mediated non-viral gene delivery. Therefore, the DNA transfection efficiencies of the top-performing **P10** and **P11** in the presence of 10% FBS were monitored in different cell lines. According to Figure A.32, **P10** and **P11** suffered from compromised gene transfection efficiencies at the same polypeptoid/DNA weight ratio of 2.5 when compared to those under serum-free conditions. However, the transfection efficiencies could be largely recovered at the higher polypeptoid/DNA weight ratio of 10, probably because the additional cationic charges as well as hydrophobicity mediated stronger interactions between DNA and polypeptoids that competitively compensated the DNA replacement by serum. **P11** was still able to maintain high gene transfection efficiencies in the presence of enhanced FBS concentration that were only several fold lower than those under serum-free conditions (Figure A.32C), which indicated their potential utilities toward serum-resistant gene delivery as well as *in vivo* gene delivery.

3.12.4 Cytotoxicity of Polypeptoid/DNA Polyplexes

Cytotoxicity of polypeptoids and polypeptoid/DNA polyplexes was measured by the MTT assay. As shown in Figure 3.10, the cytotoxicity of polypeptoids increased when the polymer concentration or polymer/DNA weight ratio was increased, and polypeptoids with higher membrane activities correlated to higher cytotoxicity. In all, bearing primary amine groups, increasing DP, and enhancing the side-chain hydrophobicity improved cell transfection, but at the expense of elevated cytotoxicities. Particularly, **P11** with pendent decyl groups displayed higher cytotoxicity than its homopolymer analogue **P10** at high concentrations, which further substantiated that the

excessively high membrane activities would cause irreversible damage to cell viability. Based on the above transfection and cytotoxicity results, it could be deduced that a proper balance between membrane affinities and cytotoxicity is demanded to achieve maximal transfection efficiency, and the excessive membrane activities would decrease rather than increase the transfection efficiency by notably compromising the cell viability and transcription/translation functions.

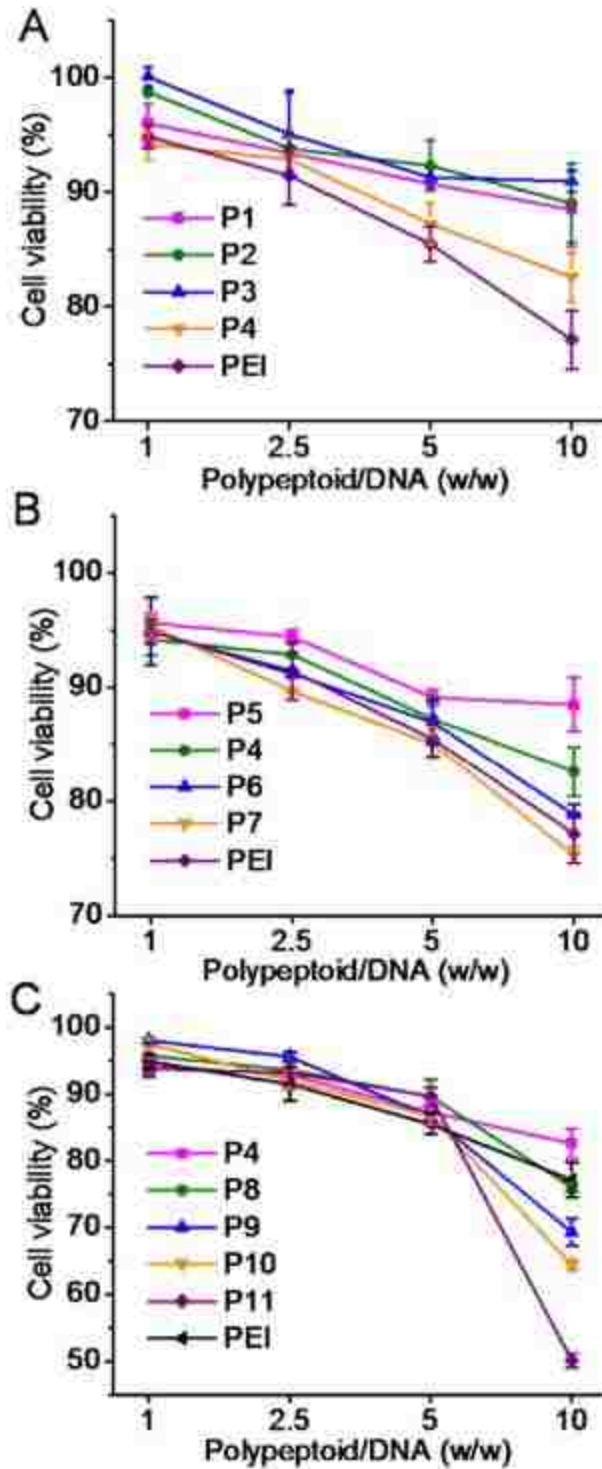Figure 3.10. Cytotoxicity of polyplexes at various polypeptoid/DNA weight ratios (DNA amount was maintained constant at 0.3 µg/well) in HeLa cells as determined by the MTT assay (n = 3). (A) Polypeptoids with different cationic side-chain terminal groups. (B) Polypeptoids with different DPs. (C) Polypeptoids with different hydrophobic side-chain lengths and incorporated hydrophobic decyl side chains.

3.12.5 *In Vivo* Gene Transfection of Polypeptoid/DNA Polyplexes

The high transfection efficiencies of polypeptoids *in vitro* in serum-containing media prompted us to explore the capabilities of these materials toward *in vivo* gene delivery. Thus, we further evaluated the *in vivo* transfection efficiencies of the two top-performing polypeptoids in melanoma-bearing C57/BL6 mice following intratumoral injection. As shown in Figure 3.11, **P11** displayed significantly higher transfection efficiency than **P10**, and PEI by ~20 fold, according well with their *in vitro* transfection capabilities. These results thus suggested the potential utilities of polypeptoids for the topical DNA delivery toward anti-cancer gene therapy.

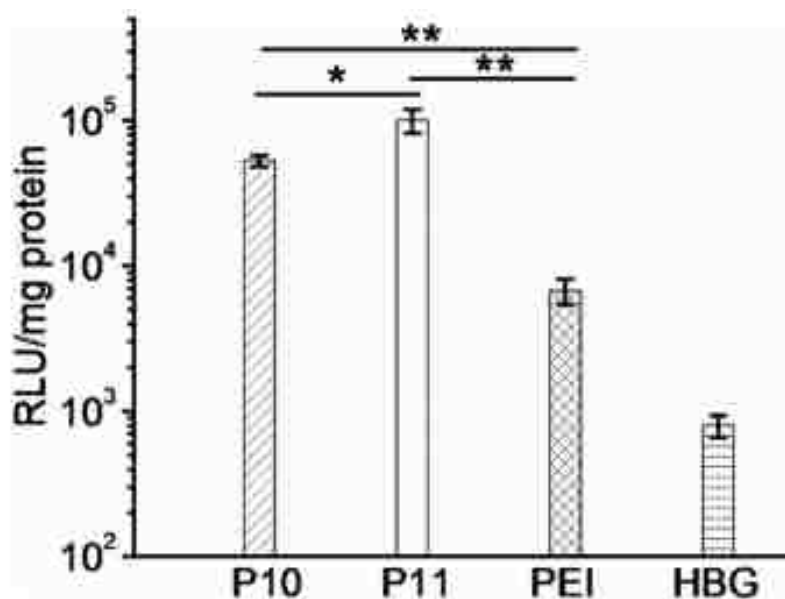Figure 3.11. In vivo transfection efficiencies of polyplexes following intratumoral injection in B16F10 xenograft tumor-bearing mice at 40 μg DNA/mouse (n = 4).

3.13. Conclusion

In summary, a library of cationic polypeptoids with different molecular characteristics were synthesized via the controlled ROP of Pg-NCA and post-modification using Click chemistry, and the structure-property relationship in terms of

non-viral gene delivery was unraveled. Polypeptoid bearing primary amine side terminal groups outperformed its analogues containing secondary, tertiary, or quaternary amines in terms of DNA internalization level and transfection efficiency. Elongating the polypeptoid backbone potentiated DNA condensation and intracellular uptake, while at the meantime induced higher cytotoxicity. As such, polypeptoid with DP of 46 displayed the highest transfection efficiency by achieving an appropriate balance between cellular internalization and cytotoxicity. Enhancing the hydrophobicity of polypeptoids by either elongating the aliphatic spacer between backbone and terminal charged groups or incorporating decyl side chains notably improved the membrane activities and gene transfection efficiencies. Based on these structural optimization, **P11** as the top-performing material was identified which demonstrated potent gene transfection efficiencies in multiple mammalian cell lines under both serum-free and serum-containing conditions, outperforming commercial reagent PEI by several orders of magnitude. These understandings on the structure-property relationship of polypeptoids provide insight into the design of polymeric gene vectors, and the top-performing **P11** may serve as a promising addition to existing gene transfection reagent.

3.14. References

1. Guinn, B. A., Mulherkar, R. International Progress in Cancer Gene Therapy. *Cancer Gene Ther.* **2008**, 15, 765−775.

2. Tan, X., Lu, X., Fei, J., Liu, X., Sun, Y., Logan, J. K., Ke, Z. Blurring the Role of Oligonucleotides: Spherical Nucleic Acids as a Drug Delivery Vehicle. *J. Am. Chem. Soc.* **2016**, 138, 10834−10837.

3. Wu, J. P., Cheng, B., Roffler, S. R., Lundy, D. J., Yen, C. Y., Chen, P., Lai, J. J., Pun, S. H., Stayton, P. S., Hsieh, P. C. Reloadable Multidrug Capturing Delivery System for Targeted Ischemic Disease Treatment. *Sci. Transl. Med.* **2016**, 8, No. 365ra160.

4.   Li, S., Chen, N., Gaddes, E. R., Zhang, X., Dong, C., Wang, Y. A Drosera-Bioinspired Hydrogel for Catching and Killing Cancer Cells. *Sci. Rep.* **2015**, 5, No. 14297.

5.   Won, Y. W., Yoon, S. M., Lim, K. S., Kim, Y. H. Self-Assembled Nanoparticles with Dual Effects of Passive Tumor Targeting and Cancer-Selective Anticancer Effects. *Adv. Funct. Mater.* **2012**, 22, 1199−1208.

6.   Li, C., Hu, J., Li, W., Song, G., Shen, J. Combined BortezomibBased Chemotherapy and p53 Gene Therapy Using Hollow Mesoporous Silica Nanospheres for p53 Mutant Non-Small Cell Lung Cancer Treatment. *Biomater. Sci.* **2016**, 5, 77−88.

7.   Sun, Y., Hu, H., Zhao, N., Xia, T., Yu, B., Shen, C., Xu, F. J. Multifunctional Polycationic Photosensitizer Conjugates with Rich Hydroxyl Groups for Versatile Water-Soluble Photodynamic Therapy Nanoplatforms. *Biomaterials* **2017**, 117, 77−91.

8.   Yang, Y. Y., Hu, H., Wang, X., Yang, F., Shen, H., Xu, F. J., Wu, D. C. Acid-Labile Poly(glycidyl methacrylate)-Based Star Gene Vectors. *ACS Appl. Mater. Interfaces* **2015**, 7, 12238−12248.

9.   Huang, P., Zhao, J., Wei, C., Hou, X., Chen, P., Tan, Y., He, C. Y., Wang, Z., Chen, Z. Y. Erythrocyte Membrane Based Cationic Polymer−mcDNA Complexes as an Efficient Gene Delivery System. *Biomater. Sci.* **2016**, 5, 120−127.

10. Xu, C., Yu, B., Hu, H., Nizam, M. N., Yuan, W., Ma, J., Xu, F. J. PGMA-Based Gene Carriers with Lipid Molecules. *Biomater. Sci.* **2016**, 4, 1233−1243.

11. Chen, Y., Li, Y., Gao, J., Cao, Z., Jiang, Q., Liu, J., Jiang, Z. Enzymatic PEGylated Poly(lactone-co-β-amino ester) Nanoparticles as Biodegradable, Biocompatible and Stable Vectors for Gene Delivery. *ACS Appl. Mater. Interfaces* **2016**, 8, 490−501.

12. Song, H. Q., Dou, X. B., Li, R. Q., Yu, B. R., Zhao, N. N., Xu, F. J. A General Strategy to Prepare Different Types of PolysaccharideGraft-Poly(aspartic acid) as Degradable Gene Carriers. *Acta Biomater.* **2015**, 12, 156−165.

13. Wang, M., Alberti, K., Varone, A., Pouli, D., Georgakoudi, I., Xu, Q. Enhanced Intracellular siRNA Delivery Using Bioreducible Lipid-Like Nanoparticles. *Adv. Healthcare Mater.* **2014**, 3, 1398−1403.

14. Zhang, Q., Shen, C., Zhao, N., Xu, F. J. Redox-Responsive and Drug-Embedded Silica Nanoparticles with Unique Self-Destruction Features for Efficient Gene/Drug Codelivery. *Adv. Funct. Mater.* **2017**, 27, No. 1606229.

15. Wang, M., Sun, S., Alberti, K. A., Xu, Q. A Combinatorial Library of Unsaturated Lipidoids for Efficient Intracellular Gene Delivery. *ACS Synth. Biol.* **2012**, 1, 403−407.

16. Keles, E., Song, Y., Du, D., Dong, W. J., Lin, Y. Recent Progress in Nanomaterials for Gene Delivery Applications. *Biomater. Sci.* **2016**, 4, 1291−1309.

17. Li, Y., Humphries, B., Wang, Z., Lang, S., Huang, X., Hua, X., Jiang, Y., Yang, C. Complex Coacervation-Integrated Hybrid Nanoparticles Increase Plasmid DNA Delivery Efficiency in Vivo. *ACS Appl. Mater. Interfaces* **2016**, 8, 30735−30746.

18. Cutlar, L., Gao, Y., Aied, A., Greiser, U., Murauer, E. M., Zhou, D., Wang, W. A Knot Polymer Mediated Non-Viral Gene Transfection for Skin Cells. *Biomater. Sci.* **2016**, 4, 92−95.

19. Liao, W., Li, W., Zhang, T., Kirberger, M., Liu, J., Wang, P., Chen, W., Wang, Y. Powering up the Molecular Therapy of RNA Interference by Novel Nanoparticles. *Biomater. Sci.* **2016**, 4, 1051− 1061.

20. Sun, J., Zuckermann, R. N. Peptoid Polymers: A Highly Designable Bioinspired Material. *ACS Nano* **2013**, 7, 4715−4732.

21. Zhang, D., Lahasky, S. H., Guo, L., Lee, C.-U., Lavan, M. Polypeptoid Materials: Current Status and Future Perspectives. *Macromolecules* **2012**, 45, 5833−5841.

22. Knight, A. S., Zhou, E. Y., Francis, M. B., Zuckermann, R. N. Sequence Programmable Peptoid Polymers for Diverse Materials Applications. *Adv. Mater.* **2015**, 27, 5665−5691.

23. Rosales, A. M., Segalman, R. A., Zuckermann, R. N. Polypeptoids: A Model System to Study the Effect of Monomer Sequence on Polymer Properties and Self-Assembly. *Soft Matter* **2013**, 9, 8400−8414.

24. Luxenhofer, R., Fetsch, C., Grossmann, A. Polypeptoids: A Perfect Match for Molecular Definition and Macromolecular Engineering? *J. Polym. Sci., Part A: Polym. Chem.* **2013**, 51, 2731−2752.

25. Gangloff, N., Ulbricht, J., Lorson, T., Schlaad, H., Luxenhofer, R. Peptoids and Polypeptoids at the Frontier of Supra- and Macromolecular Engineering. *Chem. Rev.* **2016**, 116, 1753−802.

26. Statz, A. R., Meagher, R. J., Barron, A. E., Messersmith, P. B. New Peptidomimetic Polymers for Antifouling Surfaces. *J. Am. Chem. Soc.* **2005**, 127, 7972−7973.

71

27. Statz, A. R., Park, J. P., Chongsiriwatana, N. P., Barron, A. E., Messersmith, P. B. Surface-Immobilised Antimicrobial Peptoids. *Biofouling* **2008**, 24, 439−448.

28. Chongsiriwatana, N. P., Patch, J. A., Czyzewski, A. M.; Dohm, M. T., Ivankin, A., Gidalevitz, D., Zuckermann, R. N., Barron, A. E. Peptoids that Mimic the Structure, Function, and Mechanism of Helical Antimicrobial Peptides. *Proc. Natl. Acad. Sci. U.S.A.* **2008**, 105, 2794−2799.

29. Kapoor, R., Eimerman, P. R., Hardy, J. W., Cirillo, J. D., Contag, C. H., Barron, A. E. Efficacy of Antimicrobial Peptoids against Mycobacterium Tuberculosis. *Antimicrob. Agents Chemother.* **2011**, 55, 3058−3062.

30. Li, A., Zhang, D. Synthesis and Characterization of Cleavable Core-Cross-Linked Micelles Based on Amphiphilic Block Copolypeptoids as Smart Drug Carriers. *Biomacromolecules* **2016**, 17, 852−861.

31. Birke, A., Huesmann, D., Kelsch, A., Weilbacher, M., Xie, J., Bros, M., Bopp, T., Becker, C., Landfester, K., Barz, M. PolypeptoidBlock-Polypeptide Copolymers: Synthesis, Characterization, and Application of Amphiphilic Block Copolypeptoids in Drug Formulations and Miniemulsion Techniques. *Biomacromolecules* **2014**, 15, 548−557.

32. Sun, J., Stone, G. M., Balsara, N. P., Zuckermann, R. N. Structure−Conductivity Relationship for Peptoid-Based PEO−Mimetic Polymer Electrolytes. *Macromolecules* **2012**, 45, 5151−5156.

33. Bang, J.-K., Nan, Y.-H., Lee, E.-K., Shin, S.-Y. A Novel Trp-Rich Model Antimicrobial Peptoid with Increased Protease Stability. *Bull. Korean Chem. Soc.* **2010**, 31, 2509−2513.

34. Miller, S. M., Simon, R. J., Ng, S., Zuckermann, R. N., Kerr, J. M., Moos, W. H. Proteolytic Studies of Homologous Peptide and NSubstituted Glycine Peptoid Oligomers. *Bioorg. Med. Chem. Lett.* **1994**, 4, 2657−2662.

35. Tan, N. C., Yu, P., Kwon, Y. U., Kodadek, T. High-Throughput Evaluation of Relative Cell Permeability between Peptoids and Peptides. *Bioorg. Med. Chem.* **2008**, 16, 5853−5861.

36. Ovadia, O., Linde, Y., Haskell-Luevano, C., Dirain, M. L., Sheynis, T., Jelinek, R., Gilon, C., Hoffman, A. The Effect of Backbone Cyclization on PK/PD Properties of Bioactive Peptide−Peptoid Hybrids: the Melanocortin Agonist Paradigm. *Bioorg. Med. Chem.* **2010**, 18, 580−589.

37.   Murphy, J. E., Uno, T., Hamer, J. D., Cohen, F. E., Dwarki, V., Zuckermann, R. N. A Combinatorial Approach to the Discovery of Efficient Cationic Peptoid Reagents for Gene Delivery. *Proc. Natl. Acad. Sci. U.S.A.* **1998**, 95, 1517−1522.

38.   Lobo, B. A., Vetro, J. A., Suich, D. M., Zuckermann, R. N., Middaugh, C. R. Structure/Function Analysis of Peptoid/Lipitoid: DNA Complexes. *J. Pharm. Sci.* **2003**, 92, 1905−1918.

39.   Secker, C., Brosnan, S. M., Luxenhofer, R., Schlaad, H. Poly(alpha-Peptoid)s Revisited: Synthesis, Properties, and Use as Biomaterial. *Macromol. Biosci.* **2015**, 15, 881−891.

40.   Guo, L., Zhang, D. Cyclic Poly(alpha-Peptoid)s and their Block Copolymers from *N*-Heterocyclic Carbene-Mediated Ring-Opening Polymerizations of *N*-Substituted *N*-Carboxylanhydrides. *J. Am. Chem. Soc.* **2009**, 131, 18072−18074.

41.   Lahasky, S. H., Serem, W. K., Guo, L., Garno, J. C., Zhang, D. Synthesis and Characterization of Cyclic Brush-Like Polymers by N-Heterocyclic Carbene-Mediated Zwitterionic Polymerization of *N*-Propargyl N-Carboxyanhydride and the Grafting-to Approach. *Macromolecules* **2011**, 44, 9063−9074.

42.   Zhu, H., Wickenden, J. G., Campbell, N. E., Leung, J. C. T., Johnson, K. M., Sammis, G. M. Construction of Carbo- and Heterocycles Using Radical Relay Cyclizations Initiated by Alkoxy Radicals. *Org. Lett.* **2009**, 11, 2019−2022.

43.   Robinson, J.W., Schlaad, H. A versatile polypeptoid platform based on *N*-allyl glycine *Chem. Commun.*, **2012**, 48, 7835–7837.

44.   Robinson, J.W., Secker, C., Weider, S., Schlaad, H. Thermoresponsive Poly(*N*-C3 glycine)s. *Macromolecules* **2013**, 46, 580−587.

45.   Wang, X., Li, Y, Mu, H., Pan, L., Li, Y. Efficient synthesis of diverse well-defined functional polypropylenes with high molecular weights and high functional group contents via thiol–halogen click chemistry. *Polym. Chem.*, **2015**, 6, 1150.

46.   Xuan, S., Gupta, S., Li, X., Bleuel, M., Schneider, G. J., Zhang, D. Synthesis and Characterization of Well-defined PEGylated Polypeptoids as Protein-resistant Polymers. *Biomacromolecules* **2017**, *18*, 951-964.

CHAPTER 4: CATIONIC POLYPEPTOIDS TOWARD TNF-α siRNA DELIVERY

4.1. Introduction

RNA interference (RNAi) has recently emerged as an exciting strategy for the treatment of various genetic disorder-related diseases.[1-8] Small interfering RNA (siRNA), usually 20-25 base pairs in length, is oligonucleotides that can regulate gene expression via site-specific mRNA cleavage and degradation.[9-12] However, naked siRNA hardly enter cells due to its negative charges, high molecular weight, and hydrophilic nature.[13,14] Furthermore, the rapid degradation by nucleases seriously limits it *in vivo* application.[15,16] Hence, a carrier is required to protect siRNA from degradation and facilitate it effective delivery to the cytosol, which could maximize the in *vivo* RNAi efficiency.

Cell penetrating peptides (CPPs), sequence-specific oligopeptides, with exceptional membrane penetrating properties have been extensively applied to deliver various cargos, such as proteins, peptides, nucleic acids, metals, and even nanoparticles.[17-19] However, CPPs only poorly condense siRNA due to their short chain length and lack of sufficient cationic charge density. Additionally, the overall positive charge of CPPs could be neutralized due to condense the negatively charged siRNA, thus reducing interaction with negatively charged cell membranes, resulting in decreased membrane activities and transfection ability.[20,21] As a result, CPPs are often unable to independently mediate effective siRNA delivery.

Polypeptoids, structural analogue of polypeptides, feature facile preparation and enhanced proteolytic stability, which making them attractive for gene delivery.[22-26] To address the drawbacks of CPPs, we recently developed a library of cationic

polypeptoids with different structural characteristics and screened them for DNA delivery.[27] The study has enabled the identification of optimal desired structural motifs that afford high transfection efficiencies for DNA delivery both *in vitro* and *in vivo*. Few studies involving the structure-property relationship in siRNA delivery are available, which would maximize the siRNA delivery efficiency by optimizing their molecular characteristics.[28-33]

Guanidine groups are often abundantly present in the CPPs and play important roles in mediating effective gene delivery by interacting with the sulfate groups of glycosaminoglycans in cell membranes.[34,35] Additionally, the membrane activity of guanidine groups can be enhanced by hydrophobic moieties.[35,36] Meanwhile, It has reported that other synthetic polymers where incorporation of optimal hydrophobicity often leads to enhanced membrane activities.[36,37]

4.2. Design, Synthesis and Characterization of Cationic Polypeptoids with Optimized Molecular Characteristics toward TNF-α siRNA Delivery

In chapter 3, we have systematically investigated the structure-property relationship of cationic polypeptoids towards DNA transfection and identified the molecular features that led to the most optimal gene transfection efficiency for DNA. It was found that the cationic polypeptoids bearing primary ammonium terminus and 6 carbon linker and a small fraction (~20 mol%) of hydrophobic decyl sidechains (introduced via copolymerization) exhibited the most optimal gene transfection efficiency. Based on these early findings, my synthetic focus was shifted towards developing structurally similar homopolypeptoids and random copolypeptoids bearing ammonium or guanidinium cationic moieties towards nonviral gene delivery of TNF-α siRNA to combat systemic inflammation.

I designed and synthesized a series of cationic polypeptoids with different side-chain terminal groups (primary ammonium and guanidinium), degrees of polymerization (DP), and incorporation of aliphatic side chains (Scheme 4.2 and Table 4.1). Random copolypeptoid precursors containing hydrophobic sidechains *i.e.*, PNPgG-*r*-PNDeG, were synthesized by copolymerization of Pg-NCA and De-NCA using benzylamine initiators as previously discussed in Chapter 3 (Section 3.12.1). Cationic azido compounds containing one azido group and one guanidinium or primary ammonium end that are separated by 6 carbon linkers were synthesized using the method shown in Scheme 4.1. The cationic random copolypeptoids bearing ammonium or guanidinium moieties on the sidechains were similarly obtained using the corresponding cationic azido compound and the PNPgG-*r*-PNDeG copolymers by CuAAC chemistry (Scheme 4.2). For the purpose of comparison, cationic homopolymers bearing identical primary ammonium and guanidinium sidechains were also synthesized by a combination of polymerization of Pg-NCA and CuAAC chemistry.

Route 1:
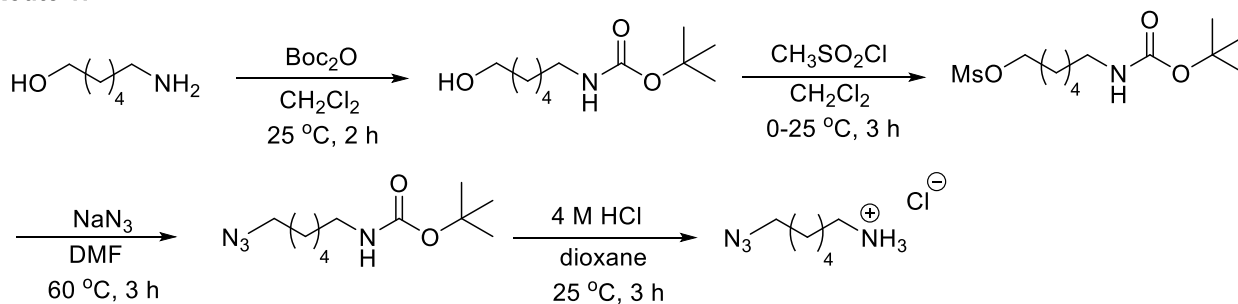
Route 2:
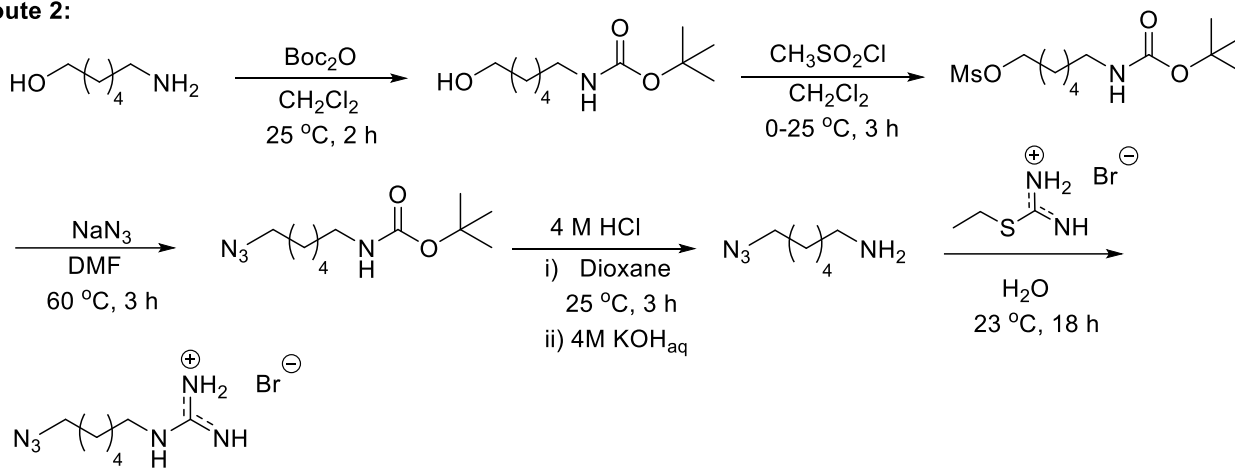
Scheme 4.1. A general synthetic scheme of ω-azido-alkyl ammonium and guanidinium compounds.
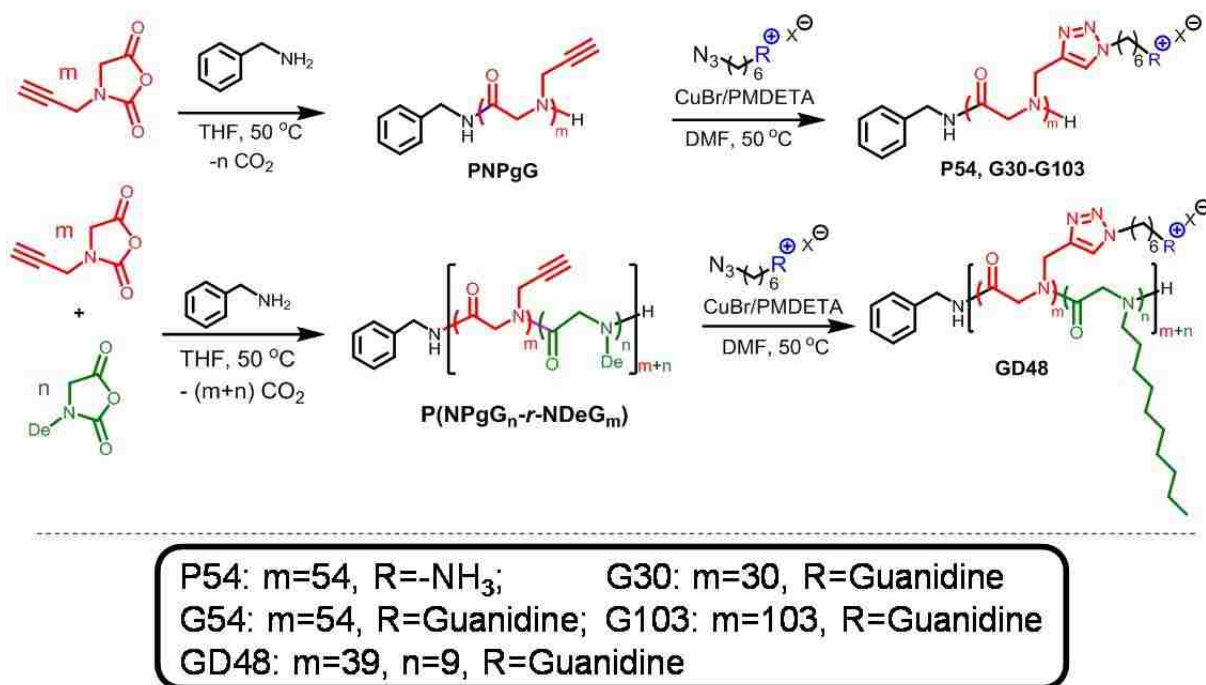
Scheme 4.2. Synthetic routes of a library of cationic polypeptoids bearing different side-chain terminal groups **(P54, G54)**, degrees of polymerization (DP) (**G30**-**G103**), and aliphatic modification of the side chains (**GD48**).

Benzylamine-initiated ROP of Pg-NCA were conducted using different initial monomer to initiator ratio ($[M]_0$:$[I]_0$=25:1, 50:1 and 100:1), yielding the corresponding PNPgG homopolymer with M_n in the 2.9-9.9 kg mol^{-1} range (DP = 30-103) and PDI in the 1.01-1.09 range, as determined by the SEC-MALS-DRI analysis (Figure 4.2). Polymer composition of PNPgG homopolymers were also determined by end-group analysis using well resolved peaks in ^{1}H NMR spectra (Figure 4.1). For example, the number average degree of polymerization (DP_n) for the resulting PNPgG precursor was determined by the integration of the propargyl proton (d) relative to the aromatic protons (a) of the benzyl end group in the ^{1}H NMR spectrum.
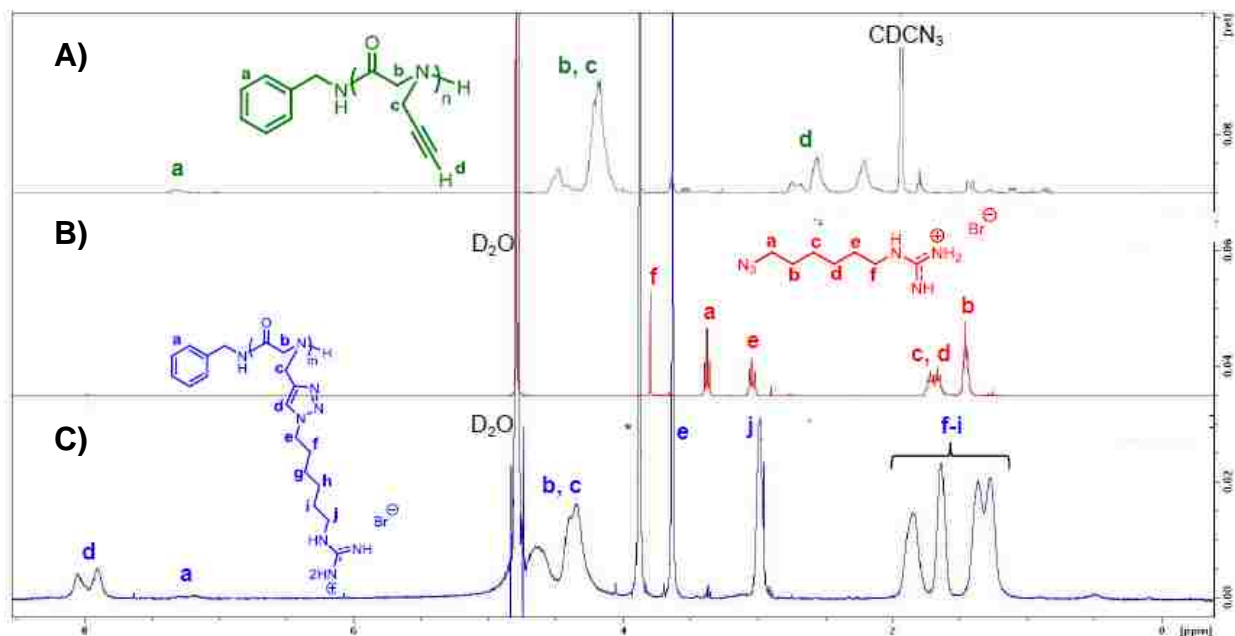
78

Figure 4.1 Representative ¹H NMR spectra of (A) PNPgG homopolymer, (B) ω-azido-alkyl guanidinium compound, and (C) cationic polypeptoids obtained by CuAAC reaction. *Residual dioxane

Table 4.1. Cationic polypeptoids with various DP and side-chain structures.

Entry	DP (SEC) [a]	DP (NMR) [f]	R [e]	PDI [a]	Yield (%)
P54	54	24	-NH$_3$	1.08	91
G30	30	24	Guanidinium	1.09	68
G54	54	37	Guanidinium	1.03	67
G103	103	73	Guanidinium	1.01	79
GD48	48 (m =39 n =9)[b]	27 (m =21 n =6)	Guanidinium	1.03 [c]	80

[a.] DP and PDI of the PNPgG homopolymer were obtained from the SEC-MALS-DRI analysis.

[b.] DP of the PNPgG copolymer was determined by ^{1}H NMR spectroscopy.

[c.] Experimental PDI of polypeptoid copolymer P(NPgG-*r*-NDeG) was obtained from the SEC-MALS-DRI analysis using PS standards.

[d.] DP of the PNPgG copolymer was determined by ^{1}H NMR spectroscopy.

[e.] Types of side-chain terminal groups.

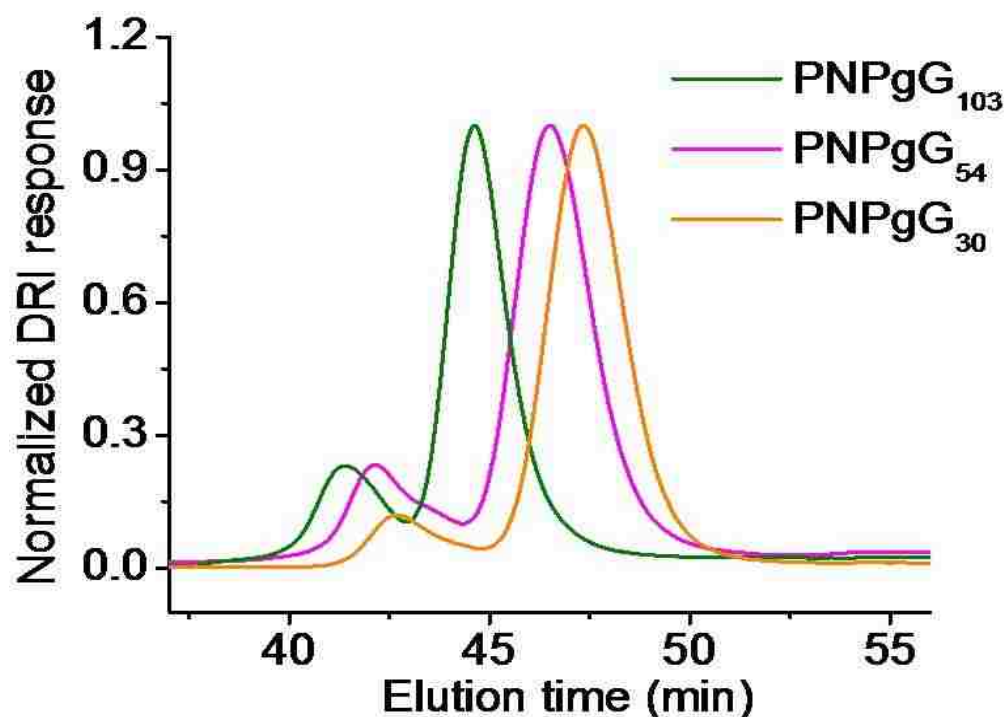[f.] DP of cationic polypeptoids as determined by ^{1}H NMR spectroscopy.

Figure 4.2. Normalized SEC chromatograms (0.1 M LiBr/DMF, 25 °C) of the PNPgG homopolymer with varying chain lengths (DP$_n$= 30, 54, and 103, M_n = 2.96, 6.33, and 9.90 kg/mol, PDI = 1.01-1.09) synthesized by benzylamine-initiated ROPs of Pg-NCA. The M_ns were determined using measured dn/dc of PNPgG (0.1012 ± 0.0007 mL/g). The high molecular weight (MW) shoulders observed are attributed to PNPgG aggregation in the SEC solvent.

Further derivation of PNPgG homopolymers with different cationic azido compounds was quantitative in all cases, evidenced by the complete disappearance of the terminal alkyne proton of propargyl group at 2.51 ppm and appearance of the triazole proton at 8.0 ppm from the ^{1}H NMR analysis (Figure B.1-B.4). The cationic polypeptoids were purified by treatment with EDTA to remove copper salts followed by extensive dialysis against DI water. Upon lyophilization, all polymers were obtained as white to pale green powders in good yield (67-91%) with copper ion content in the sub-10 ppm range based on the atomic absorption analysis. The range of copper content is

significantly lower than the concentration threshold for potential copper ion-induced cytotoxicity.[38]

      P54 and **G54** (Table 4.1) carried different cationic side-chain terminal groups (primary ammonium and guanidinium group) at a constant DP of 54; **G30**-**G103** possessed guanidinium side-chain terminal group while had different DP (30, 54, and 103) (Table 4.1). Chemical structures of these cationic polypeptoid homopolymers were verified by ^{1}H NMR spectroscopy. Compositions for the cationic homopolymers were determined using ^{1}H NMR spectroscopy by integrating the triazole proton relative at 8.01 ppm relative to the aromatic protons of the benzylamine end group at 7.26 ppm. All the resulting cationic polypeptoids exhibited good water solubility and can be used to complex siRNA for gene silencing experiments in the aqueous media.
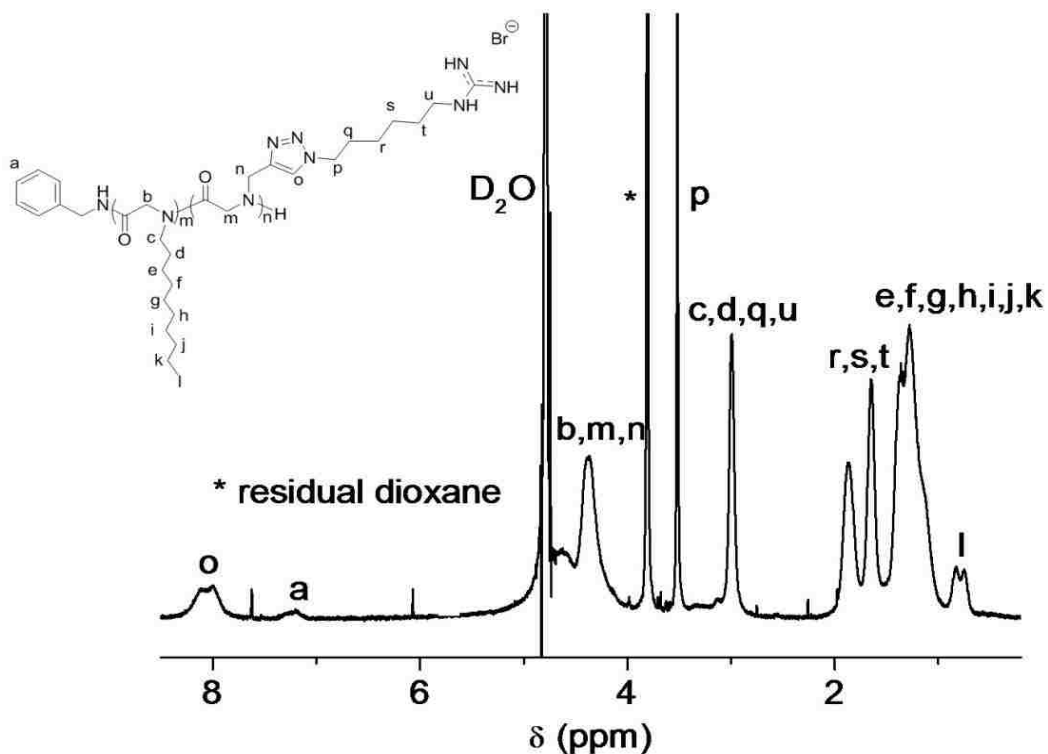
Figure 4.3. Representative ^{1}H NMR spectrum of **GD48** in D$_2$O.

A cationic random copolypeptoid (**GD48**, Table 4.1) bearing a small fraction of hydrophobic *N*-decyl glycine segments (Figure 4.3) was similarly synthesized and characterized via modification of the P(NPgG-*r*-NDeG) random copolymer with ω-azido hexyl ammonium salt using CuAAC chemistry (Scheme 4.2). The P(NPgG-*r*-NDeG) copolymer precursor was synthesized by copolymerization of Pg-NCA and De-NCA in [M]$_0$:[I]$_0$= 40:10 ratio using benzylamine initiator. The P(NPgG-*r*-NDeG) composition was determined using ^{1}H NMR spectroscopy by integrating the terminal methyl protons of the decyl group at 0.79 ppm and the alkyne proton of propargyl group at 2.53 ppm relative to the aromatic protons of benzyl end-group at 7.26 ppm. The molecular weight distribution of P(NPgG-*r*-NDeG) copolymer was determined by the SEC-DRI analysis

using polystyrene standard. Following CuAAC chemistry, the cationic copolymer composition was determined by integrating the newly formed triazole proton at 8.01 ppm and methylene protons of the decyl group at 0.79 ppm relative to the aromatic protons of the benzyl end group at 7.32 ppm in the polymers in the ^{1}H NMR spectrum (Figure 4.4). **GD48**, with ~80% guanidinium side-chain terminal groups and ~20 mol% hydrophobic *N*-decyl sidechains for a backbone DP of 48, was comparable to that of the cationic homopolymer **G54** (DP = 54, Table 4.1).
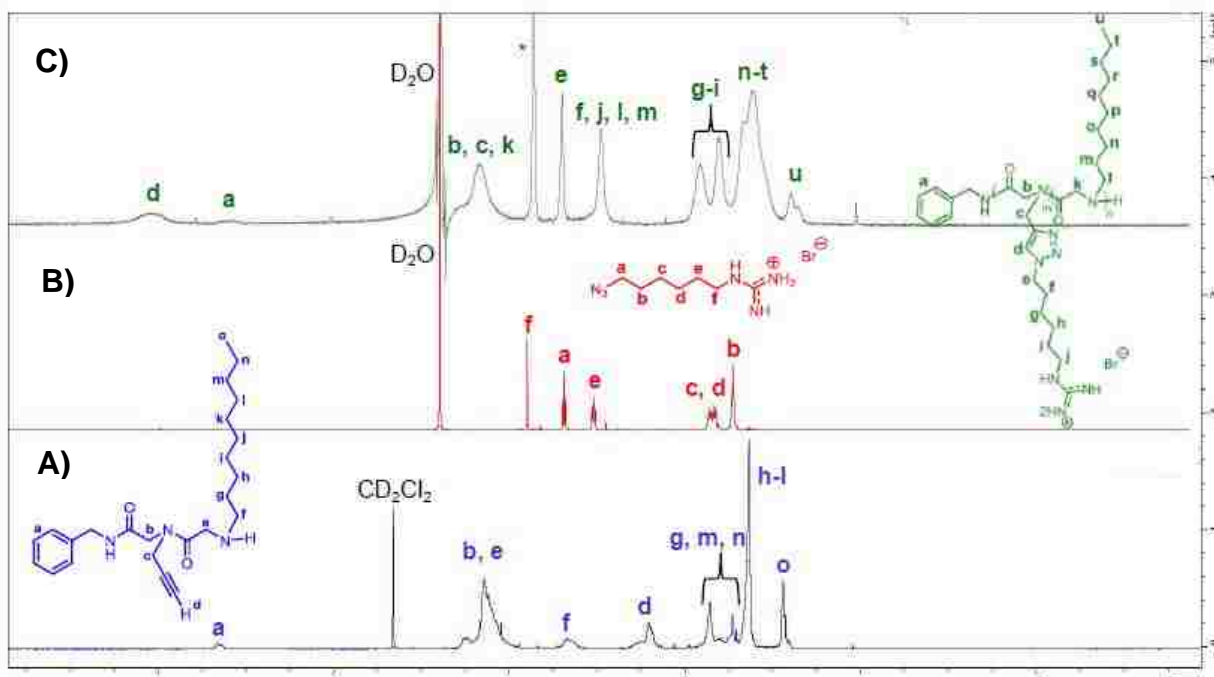
Figure 4.4 Representative ^{1}H NMR spectra of (A) PNPgG-*r*-PNDeG random copolymer, (B) ω-azido-alkyl guanidinium compound, and (C) cationic polypeptoids copolymer obtained by CuAAC reaction. *Residual Dioxane

4.3. Formation and Characterization of Polyplexes

A combination of gel retardation assay and EB exclusion assay indicate high efficiency of siRNA condensation (>80%) with the synthesized cationic polypeptoids at

polypeptoid/siRNA weight ratio ≥ 10. Polypeptoids with different cationic side-chain terminal groups (i.e., ammonium or guanidinium) (**P54** and **G54**) showed similar siRNA binding affinities. In comparison, longer polypeptoid backbone correlated to enhanced siRNA condensation level mainly due to the facilitated entanglement of longer polypeptoids with siRNA molecules, wherein the siRNA condensation level was represented by the order of **G103**>**G54**>**G30**, evidenced by the difference of their EB exclusion efficiencies. In addition, **GD48** bearing a small fraction of *N*-decyl side chains afforded higher siRNA condensation level than analogous **G54** without the aliphatic sidechains. This is presumably because the hydrophobic interaction mediated stronger assembly between siRNA and polymer.

4.4. *In Vitro* Gene Silencing with Polypeptoid/siRNA Polyplexes

TNF-α knockdown efficiencies of polypeptoids with different molecular characteristics were first evaluated in RAW 264.7 cells. The gene-silencing efficiencies of polypeptoids containing a constant DP (54) but different cationic terminal group on the sidechain (**P54** and **G54**) were first evaluated. As shown in Figure B.5, **G54** containing guanidinium terminal groups displayed remarkably higher gene silencing efficiency than its analogues containing primary ammonium terminal groups, suggesting that guanidinium groups played important roles in mediating effective gene delivery presumably due to their membrane activities. Then, based on the structure of **G54** bearing guanidinium charged group, the DP of the polymers was further varied (**G30**, **G54** and **G103**) to allow for investigation of the effect of backbone length on the silencing efficiencies. As shown in Figure B.6, **G54** with an intermediate DP displayed higher silencing efficiency than **G30** having a smaller DP, presumably attributed to the

enhanced siRNA condensation and cellular uptake. However, **G103** having the highest DP exhibited decreased silencing efficiency relative to that of **G54**. This is presumably due to the excessively long polymer backbone leading to restricted intracellular siRNA release and enhanced cytotoxicity. Additionally, the membrane activity of guanidinium groups can be improved by hydrophobic moieties. We thus went on to explore whether gene silencing efficiencies can be further enhanced by introducing a smaller fraction of hydrophobic sidechains to cationic polypeptoids. **GD48,** containing ~20 mol% of pendent *N*-decyl glycine segments and having comparable DP as **G54** has been synthesized and investigated for siRNA delivery. As shown in Figure B.7, **GD48** displayed the highest silencing efficiency, significantly outperforming **G54** and LPF2000, in agreement with the literature reported that the hydrophobic moieties can promote intracellular siRNA delivery.

4.5. *In Vivo* Gene Silencing

In a mouse model of LPS/D-GalN-induced acute liver failure, D-GalN blocks gene transcription in the liver, and LPS in turn induces an acute, cytokine-dependent hepatic inflammation accompanied by massive liver apoptosis and death.[40] Therefore, the extent of TNF-α silencing *in vivo* using **GD48**/TNF-α siRNA polyplexes was investigated. As shown in Figure B.8, i.v. injection of polyplexes significantly depleted TNF-α mRNA levels in macrophage-enriched organs (liver, spleen, and lung), which suggested that the polyplexes had infiltrated and efficiently transfected macrophages in reticuloendothelial tissues to induce significant systemic TNF-α knockdown. Depletion of TNF-α mRNA levels were further reduced as a result of i.v. injection of polyplexes/ TNF-α siRNA at higher dosages, with notably blocked LPS/D-GalN-triggered serum TNF-α

86

production by 74 and 62% respectively (Figure B.8). By contrast, **GD48**/Scr siRNA polyplexes did not evoked any RNAi effect.

4.6. Conclusion

In summary, a sequence of cationic polypeptoids with different molecular characteristics have been synthesized *via* the controlled ROP of Pg-NCA (and De-NCA) and post-modification using the CuAAC "click" chemistry. The structure-property relationship of these cationic polypeptoids in terms of gene silencing was investigated. **GD48**, a cationic polypeptoids copolymer with the guanidinium terminal group on the sidechain, DP of 48 and incorporated aliphatic side chains displayed the highest gene-silencing efficiency, outperforming commercial reagent LPF2000. More importantly, the polypeptoid-based hybrid nanocarrier **GD48** mediated effective TNF-α siRNA delivery *in vivo*. Consequently, **GD48**/TNF-α siRNA polyplexes afforded effective systemic silencing TNF-α and thus demonstrated a potent anti-inflammatory effect to rescue animals from LPS/D-GalN-induced hepatic sepsis. The potent efficacy in systemically downregulation of TNF-α, excellent biocompatibility, and simplicity and reproducibility in formulation of polyplexes would represent an exciting prospect for anti-inflammation therapies.

4.7. References

1. Hannon, G. RNA interference *Nature* **2002***,* 418, 244-251.

2. Siomi, M. Short interfering RNA-mediated gene silencing; towards successful application in human patients *Advanced Drug Delivery Reviews* **2009***,* 61, 668-671.

3.   Shim, M., Bhang, S., Yoon, K., Choi, K., Xia, Y. A bioreducible polymer for efficient delivery of Fas-silencing siRNA into stem cell spheroids and enhanced therapeutic angiogenesis. *Angewandte Chemie* **2012***,* 51, 11899-11903.

4.   Wilson, D., Dalmasso, G., Wang, L., Sitaraman, S., Merlin, D., Murthy, N. Orally delivered thioketal nanoparticles loaded with TNF-α–siRNA target inflammation and inhibit gene expression in the intestines. *Nature Materials* **2010***,* 9, 923.

5.   Aouadi, M., Tesz, G., Nicoloro, S., Wang, M., Chouinard, M., Soto, E., Ostroff, G., Czech, M. Orally delivered siRNA targeting macrophage Map4k4 suppresses systemic inflammation *Nature* **2009***,* 458, 1180.

6.   Dassie, J., Liu, X., Thomas, G., Whitaker, R., Thiel, K., Stockdale, K., Meyerholz, D., McCaffrey, A., Ii, M., Giangrande, P. Systemic administration of optimized aptamer-siRNA chimeras promotes regression of PSMA-expressing tumors *Nature Biotechnology* **2009***,* 27, 839.

7.   Kozielski, K., Tzeng, S., De Mendoza, B., Green, J. Bioreducible Cationic Polymer-Based Nanoparticles for Efficient and Environmentally Triggered Cytoplasmic siRNA Delivery to Primary Human Brain Cancer Cells *Acs Nano* **1936***,* 8, 3232.

8.   Lee, S., Huh, M., Lee, S., Min, S., Lee, S., Koo, H., Chu, J., Lee, K., Jeon, H., Choi, Y. Tumor-Homing Poly-siRNA/Glycol Chitosan Self-Cross-Linked Nanoparticles for Systemic siRNA Delivery in Cancer Treatment *Angewandte Chemie* **2012***,* 51, 7203.

9.   Elbashir, S., Harborth, J., Lendeckel, W., Yalcin, A., Weber, A., Tuschl, T. Duplexes of 21-nucleotide RNAs mediate RNA interference in cultured mammalian cells *Nature* **2001***,* 411, 494.

10.   Ghildiyal, M., Zamore, P. Small silencing RNAs: an expanding universe *Nature Reviews Genetics* **2009***,* 10, 94.

11.   McManus, M., Sharp, P. Gene silencing in mammals by small interfering RNAs *Nature Reviews Genetics* **2002***,* 3, 737.

12.   Castanotto, D., Rossi, J. The promises and pitfalls of RNA-interference-based therapeutics *Nature* **2009***,* 457, 426.

13.   Bumcrot, D., Manoharan, M., Koteliansky, V., Sah, D. RNAi therapeutics: a potential new class of pharmaceutical drugs *Nature Chemical Biology* **2006***,* 2, 711.

14. Oh, Y., Park, T. siRNA delivery systems for cancer treatment *Advanced Drug Delivery Reviews* **2009**, 61, 850.

15. Ballarín-González, B., Howard, K. Polycation-based nanoparticle delivery of RNAi therapeutics: Adverse effects and solutions *Advanced Drug Delivery Reviews* **2012**, 64, 1717.

16. S. S. Min, S. Wong, Y. J. Kwon, *Drug Discov Today Technol* **2012**, 9, e71.

17. Saw, P., Ko, Y., Jon, S. Efficient Liposomal Nanocarrier-mediated Oligodeoxynucleotide Delivery Involving Dual Use of a Cell-Penetrating Peptide as a Packaging and Intracellular Delivery Agent *Macromolecular Rapid Communications* **2010**, 31, 1155.

18. Nakase, I., Akita, H., Kogure, K., Gräslund, A., Ülo, L., Harashima, H., Futaki, S. Efficient Intracellular Delivery of Nucleic Acid Pharmaceuticals Using Cell-Penetrating Peptides *Acc Chem Res* **2016**, 45, 1132.

19. van Asbeck, A., Beyerle, A., McNeill, H., Bovee-Geurts, P., Lindberg, S., Verdurmen, W., Hällbrink, M., Langel, U., Heidenreich, O., Brock, R. Molecular Parameters of siRNA–Cell Penetrating Peptide Nanocomplexes for Efficient Cellular Delivery *ACS Nano* **2013**, 7, 3797.

20. Meade, B., Dowdy, S. Exogenous siRNA delivery using peptide transduction domains/cell penetrating peptides *Adv. Drug Deliv. Rev.* **2007**, 59, 134.

21. Gooding, M., Browne, L., Quinteiro, F., Selwood, D. siRNA Delivery: From Lipids to Cell-penetrating Peptides and Their Mimics *Chemical Biology & Drug Design* **2012**, 80, 787.

22. Sun, J., Zuckermann, R. Peptoid Polymers: A Highly Designable Bioinspired Material *ACS Nano* **2013**, 7, 4715.

23. Zhang, D., Lahasky, S., Guo, L., Lee, C., Lavan, M. Polypeptoid Materials: Current Status and Future Perspectives *Macromolecules* **2012**, 45, 5833.

24. Li, A., Zhang, D. Synthesis and Characterization of Cleavable Core-Cross-Linked Micelles Based on Amphiphilic Block Copolypeptoids as Smart Drug Carriers *Biomacromolecules* **2016**, 17, 852.

25. J.-K. Bang, Y.-H. Nan, E.-K. Lee, S.-Y. Shin, *Bull. Korean Chem. Soc.* **2010**, 31, 2509.

26. S. M. Miller, R. J. Simon, S. Ng, R. N. Zuckermann, J. M. Kerr, W. H. Moos, Walter, H., Proteolytic studies of homologous peptide and N-substituted glycine peptoid oligomers *Bioorg. Med. Chem. Lett.* **1994**, 4, 2657.

27. Zhu, L., Simpson, J., Xu, X., He, H., Zhang, D., Yin, L. Cationic Polypeptoids with Optimized Molecular Characteristics toward Efficient Nonviral Gene Delivery *ACS Appl. Mater. Interfaces* **2017**, 9, 23476−23486.

28. Bishop, C., Ketola, T., Tzeng, S., Sunshine, J., Urtti, A., Lemmetyinen, H., Vuorimaa-Laukkanen, E., Yliperttula, M., Green, J. The effect and role of carbon atoms in Poly(β-amino ester)s for DNA binding and gene delivery *J. Am. Chem. Soc.* **2013**, 135, 6951.

29. Venkataraman, S., Ong, W., Ong, Z., Joachim Loo, S., Ee, P., Yang, Y. The role of PEG architecture and molecular weight in the gene transfection performance of PEGylated poly(dimethylaminoethyl methacrylate) based cationic polymers *Biomaterials* **2011**, 32, 2369.

30. S. S. Parelkar, D. Chan-Seng, T. Emrick, Reconfiguring polylysine architectures for controlling polyplex binding and non-viral transfection *Biomaterials* **2011**, 32, 2432.

31. Hinton, T., Guerrero-Sanchez, C., Graham, J., Le, T., Muir, B., Shi, S., Tizard, M., Gunatillake, P., McLean, K., Thang, S. The effect of RAFT-derived cationic block copolymer structure on gene silencing efficiency *Biomaterials* **2012**, 33, 7631.

32. Ahmed, M., Jawanda, M., Ishihara, K., Narain, R. Impact of the nature, size and chain topologies of carbohydrate–phosphorylcholine polymeric gene delivery systems *Biomaterials* **2012**, 33, 7858.

33. A. A. Eltoukhy, D. J. Siegwart, C. A. Alabi, J. S. Rajan, L. Robert, D. G. Anderson, Effect of molecular weight of amine end-modified poly(β-amino ester)s on gene delivery efficiency and toxicity *Biomaterials* **2012**, 33, 3594.

34. Wender, P., Galliher, W., Goun, E., Jones, L., Pillow, T. The design of guanidinium-rich transporters and their internalization mechanisms *Advanced Drug Delivery Reviews* **2008**, 60, 452-472.

35. Naik, R., Chandra, P., Mann, A., Ganguli, M. Exogenous and Cell Surface Glycosaminoglycans Alter DNA Delivery Efficiency of Arginine and Lysine Homopeptides in Distinctly Different Ways *Journal of Biological Chemistry* **2011**, 286, 18982-18993.

36. Som, A., Reuter, A., Tew, G. Protein Transduction Domain Mimics: The Role of Aromatic Functionality *Angewandte Chemie* **2012**, 124, 1004.

37. Abhigyan, S., Ozgul, T., Gabriel, G., Tew, G. Self-Activation in De Novo Designed Mimics of Cell-Penetrating Peptides *Angewandte Chemie* **2011***,* 50, 6147-6150.

38. Xie, X.X., Ma, Y., Wang, Q., Chen, Z., Liao, R., Pan, Y. Yeast CUP1 Protects HeLa cells against Copper-induced Stress. *Brazilian Journal of Medical and Biological Research*, **2015**, 48, 616-621.

CHAPTER 5: CATIONIC POLYPEPTOID DIBLOCK COPOLYMERS AS POTENTIAL CARRIERS FOR NONVIRAL GENE DELIVERY IN SERUM

5.1 Introduction

The escalated increase in rare diseases and genetic disorders make gene therapy practices highly relevant in the field of medicine. Ultimately, for gene therapy practices to be successful in treating and preventing of diseases and disorders, efficient gene delivery intracellularly to targeted site and expression is essential. Cationic polymers continue to thrive as vectors for nonviral gene delivery. As synthetic compounds, many structural modifications (e.g. MW and ligand attachment) can be easily achieved as an advantage.[1] However, the gene expression efficacy associated with polymeric vectors face various biological barriers such as those in the extracellular body fluid, extracellular matrix (ECM), and at the cellular level (cell entry, escape from endo-lysomal vesicles, cytoplasmic trafficking, DNA unpacking, and nuclear translocation of therapeutic DNA). Research efforts sought to overcome this limitation have included the development of polymers incorporating PEGylation[2-4] and combinatorial chemistry[5]. In many instances, stimuli-responsive polymers for nonviral gene delivery have been demonstrated.

Recently, a new class of polysulfoniums capable of gene delivery via degradation into neutral thioether fragments by triggered reactive oxygen species (ROS) was reported by Zhu and coworkers.[6] It was discovered that a sequence of polysulfoniums (Scheme 5.1) could efficiently complex DNA into nanosized polyplexes in an aqueous medium (80 nm). Taking advantage of the elevated ROS levels in cancer cells, the efficient delivery and release of DNA for gene expression was also achieved. In another report Stayton et al. described how careful tuning of pH profiles for poly(alkyl acrylic

acid) polymers could result in higher transfection efficiencies *in vitro.*[7] The key to optimal cellular uptake and release was found to rely greatly upon the specific choice of monomer and monomer ratios used during polymerization.
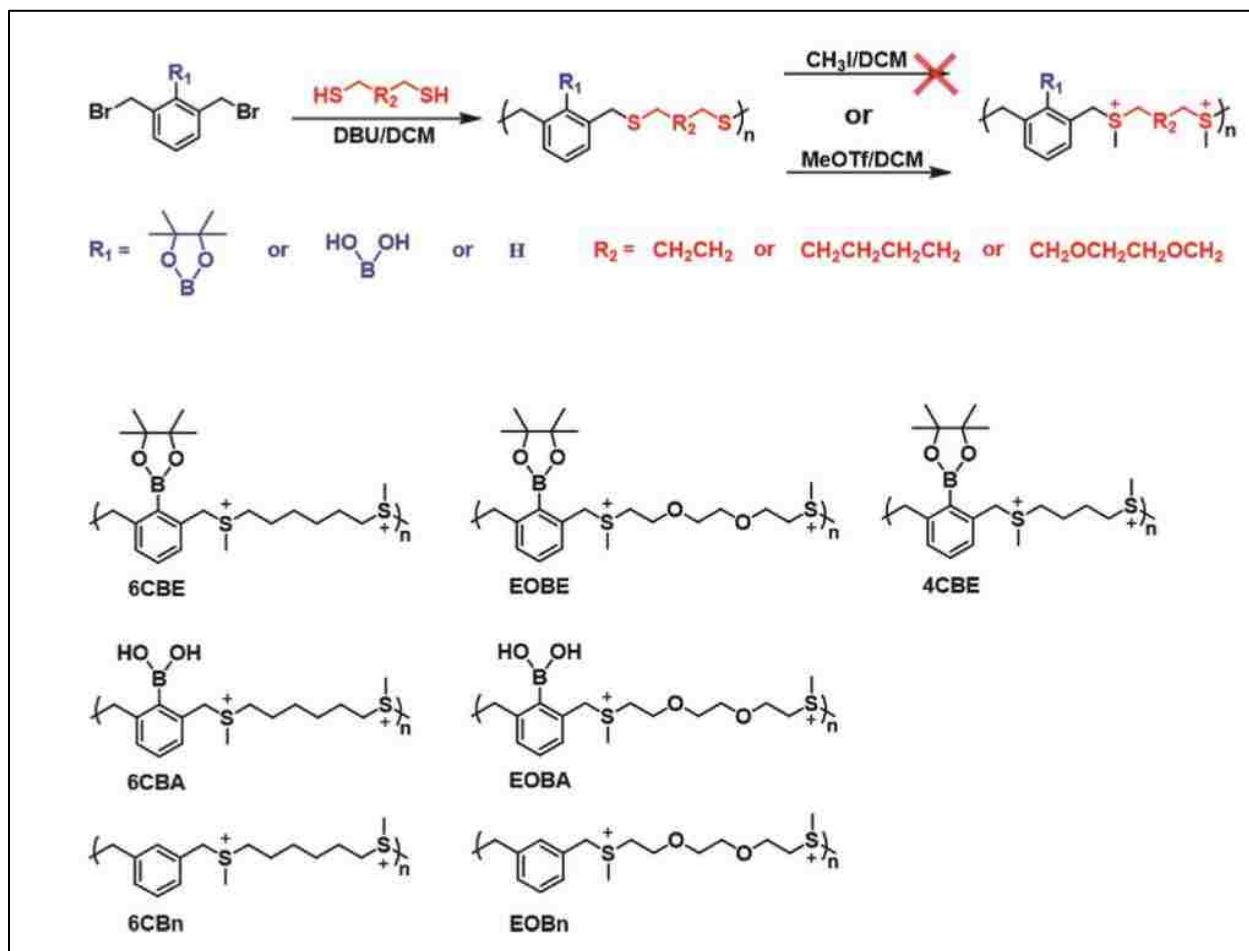
Scheme 5.1. Synthesis and structures of ROS responsive polysulfoniums. (Adapted with permission from reference[6], copyright (2017) John Wiley and Sons).

Interestingly, Yang and coworkers developed polymer systems with a dual response mechanism for the efficient intracellular delivery of DNA *in vitro* and *in vivo.*[8] Octa-arginine peptides (R8)-conjugated cationic polyamino acid derivatives denoted PPCRC-50 and PPCRC-100, synthesized via free radical polymerization and subsequent aminolysis (Scheme 5.2) were assessed and compared to their peptide lacking

analogue (PPCC). From in vitro experiments it was concluded that conjugation of the synthetic polymers with peptides significantly enhanced the transmembrane and nucleus import of DNA. At low N/P ratios the PPCRC polyplexes demonstrated the best transfection efficiency *in vitro* and *in vivo* in comparison to PPCC, presumably due to the ability of the peptides to act as a buffer during endosomal escape. Furthermore, after incubation of the PPCRC polyplexes with a high concentration of DTT (10 mM), it was concluded that the cleavage of the disulfide-linkage would promote the rapid DNA release under conditions mimicking intracellular reducing environments.
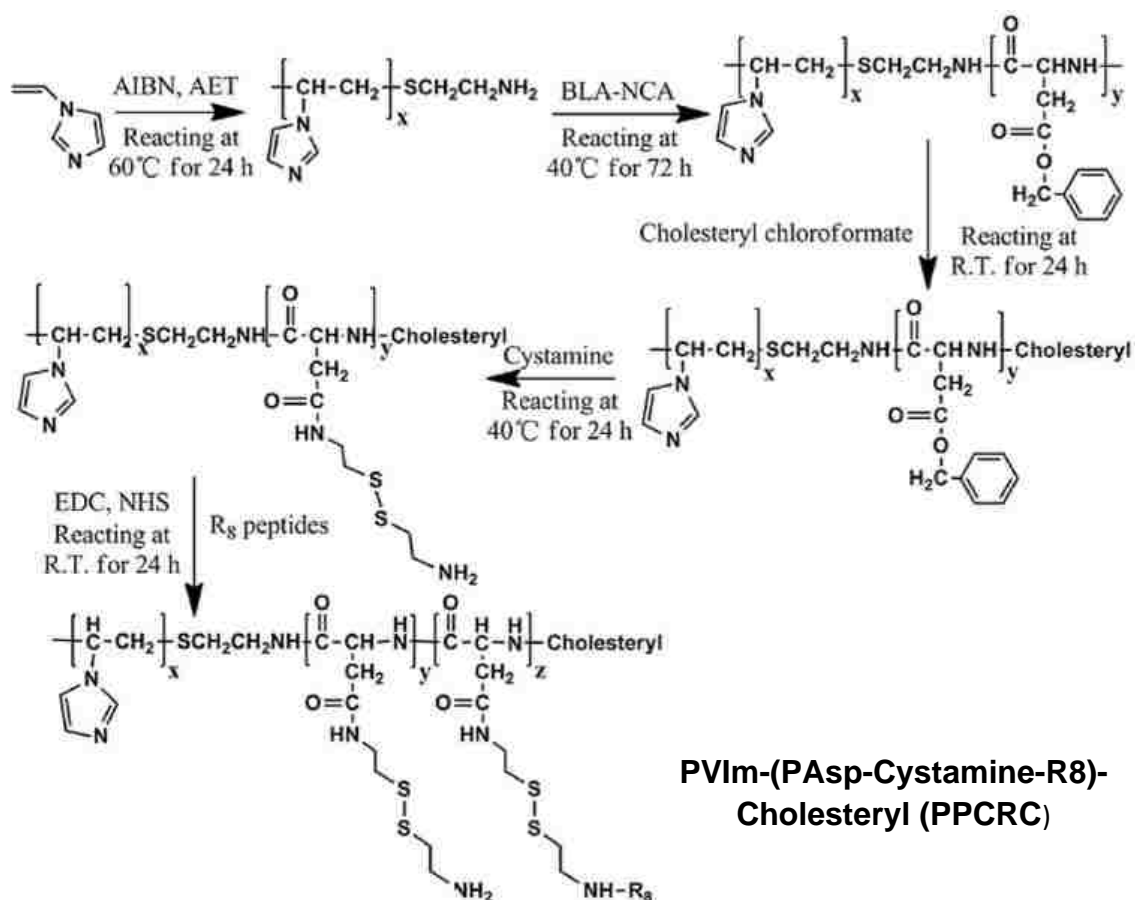
Scheme 5.2. Synthesis of PVIm-(PAsp-Cystamine-R8)-Cholesteryl (PPCRC). (Reprinted with permission from reference[8], copyright (2017) Elsevier).

It is known that transfection efficiencies of cationic polymer systems encounter issues with colloidal stability in serum-containing media.[9] The manifestation of charge shielding, in which interaction with anionic serum components (lipids, albumin, salts, etc.) reduces polyplex surface charge, is mainly responsible for this outcome. As a result of polyplex instability, genetic material becomes displaced throughout cellular transport resulting in a reduced amount delivered to targeted sites hence, poor gene expression.

Cationic homo and random polypeptoids with transfection efficacies surpassing that of high molecular weight polyethylenimine (PEI, a standard gene transfection carrier) in serum-free media has been previously demonstrated (Chapter 3 and 4).[9] To gain a full understanding of their potential contributions to the field of gene therapy we must investigate their transfection behavior under conditions relevant to *in vivo* environment. Based on their structural composition it was postulated that the pH-responsive block copolymers would condense nucleic acids forming an inner charged core with by a charge neutral hydrophilic shell, thus minimizing interactions with extracellular components during transport (Scheme 5.3). The copolymer's core-shell architecture was expected to enhance the overall stability of polyplexes during gene delivery. The hydrophilic shell layer will also contribute to reduced cytotoxicity. Lastly, presence of the acid-labile linker at the core-shell interface will enable the complete dissociation of gene/polymer particle at the extracellular compartment under mildly acidic environment (pH= 5.0) such that the positively charged core can be exposed for cell internalization.[10] It is desirable for dissociation of the core-shell complex to occur after cell entrance via endocytosis so that the charged core can perform endosomal

escape. The alkene functional group present at the end of the hydrophilic segment of the polymer (Scheme 5.4) provides a site for fluorescent labeling and ligand tagging of the gene/polymer micellar complex, thus imparting the capability for site targeting and tracking during the gene delivery process.
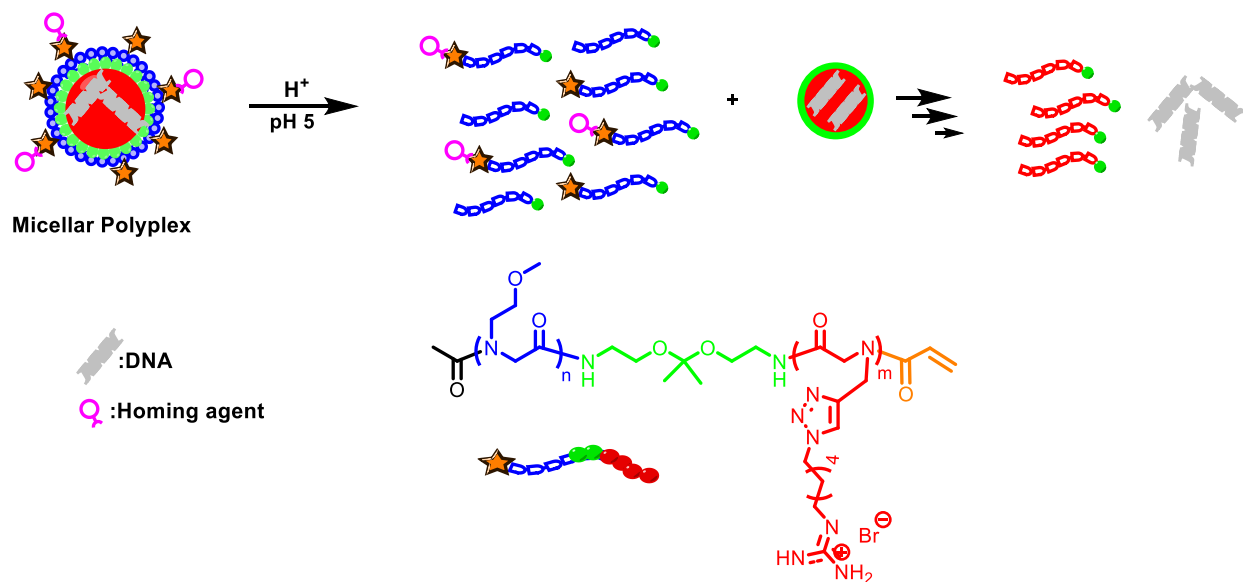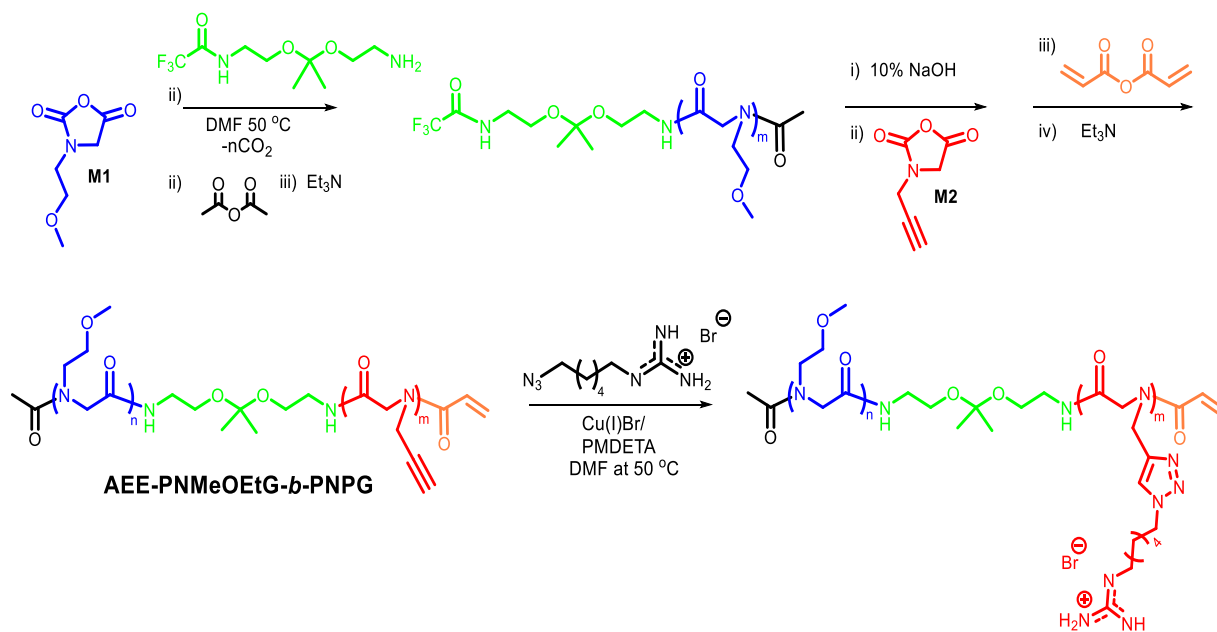

Scheme 5.3. Dissociation of pH-responsive copolypeptoids for gene delivery in serum.

A key aspect in the development of responsive diblock copolypeptoids relied upon the synthesis of an initiator that offered dual functionalities (Scheme 5.6). As depicted in Scheme 5.3, presence of the acetal group within the diamine initiator provided a feature that is expected to undergo rapid cleavage in low pH environment following cellular internalization. As a diamine, the initiator would also enable sequential control over the ring-opening polymerization of NCAs to yield diblock copolypeptoids that would exhibit a core-shell like morphology upon condensation with genetic materials.

For comparison purposes, cationic diblock copolypeptoids which lack a pH-responsive linker between blocks were also synthesized and investigated for their gene

delivery capabilities (Scheme 5.5). As a result of the resemblance of the polymer's chemical makeup, the non-pH responsive copolymers served as a control to assess the effect of pH induced disassembly of micellar carriers on the gene transfection efficiency.

Scheme 5.4. Synthesis and modification of pH responsive block copolypeptoid (AEE-PNMeOEt-*b*-PNPgGs).
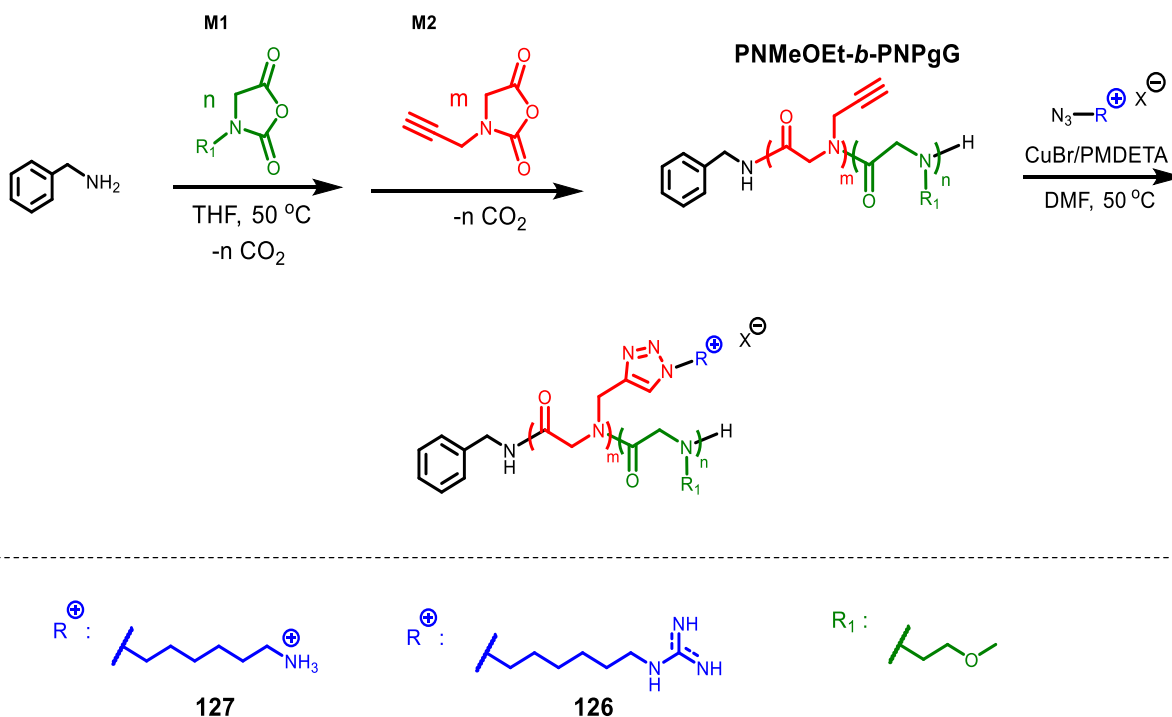
Scheme 5.5. Synthesis and modification of non-pH responsive block copolypeptoid (PNMeOEt-*b*-PNPgGs).

5.2. Materials and Methods

5.2.1 General Considerations

All chemicals were purchased from Sigma-Aldrich and used as received unless specified. All solvents are regular ACS grade solvents and used directly in the reactions without any special drying or purification step unless specified. ^1H and $^{13}C\{H\}$ NMR spectra were recorded on a Bruker AV-400 or AV-500 spectrometer. Chemical shifts in ppm were referenced relative to proton impurities or ^{13}C isotope of deuterated solvents (e.g., CDCl$_3$, CD$_3$CN, THF-d$_8$). SEC-DRI analyses were performed with an Agilent 1200 system equipped with three Phenomenex 5 μm, 300 × 7.8 mm columns [100 Å, 1000 Å and Linear (2)], Wyatt DAWN EOS MALS detector (GaAs 30 mW laser at λ=690 nm) and Wyatt Optilab rEX DRI detector with a 690 nm light source. DMF containing 0.1 M

LiBr was used as the eluent at a flow rate of 0.5 mLm· in^{-1}. The temperature of the column and detector was 25 °C.

5.2.2 Synthesis of Mono-protected pH Responsive Initiator (AEE)

Derivation of starting precursor, 2-[1-(2-Amino-ethoxy)-1-methyl-ethoxy]-ethylamine (AEE), towards the synthesis of the mono-protected responsive initiator was achieved using a modified procedure initially described by Shim and Kwon.[11] N-(2-hydroxyethyl)-phthalimide (25 g, 1 equiv) was added to benzene (400 mL), and the solution was cooled to 0 °C in an ice bath. Next, 2-Methoxy propene (12.5 mL, 1 equiv) was slowly added into the solution followed by the addition of p-toluenesulfonic acid (234.1 mg, 0.01 equiv). After stirring for 1 h at 0 °C, the reaction mixture was heated to evaporate the solvent. Once cooled to room temperature, triethylamine (TEA, 30 mL) and acetic anhydride (7.5 mL) were added to the mixture and allowed to stir overnight. The crude product was precipitated from the solution using excess hexanes and further purified by recrystallization with ethyl acetate for twice to obtain final product compound **4** as whitish-yellow crystals in 30-40% yield (Scheme 5.6).[11]

Compound **4** was deprotected using 6 M NaOH (50 mL) at 100 °C overnight. The solution was extracted with CHCl$_3$/iPrOH (1/1, v/v, 100 mL × 3) and the organic phase was combined and dried over anhydrous Na$_2$SO$_4$.[11] The solution was filtered and concentrated by rotary evaporation. The excess of iPrOH was removed by repeated washing with hexanes and compound **5** was obtained as yellow oil in 80% yield. The mono-protection of AEE (compound **6**) with trifluoroacetate derivative was accomplished using basic conditions.[11] ^{1}H NMR (400MHz, CDCl$_3$): δ 9.08 ppm (br. s, CF$_3$CON*H*CH$_2$CH$_2$OC(CH$_3$)$_2$OCH$_2$CH$_2$-NH$_2$),   7.31   ppm   (br.   s,

CF$_3$CONHCH$_2$CH$_2$OC(CH$_3$)$_2$OCH$_2$CH$_2$-NHCOCF$_3$), 3.59 ppm (s, CF$_3$CONHCH$_2$CH$_2$OC(CH$_3$)$_2$OCH_2CH$_2$-NH$_2$, H$_E$), 3.44 ppm (s, CF$_3$CONHCH_2CH_2OC(CH$_3$)$_2$OCH_2CH_2NHCOCF$_3$, H$_A$, H$_{A'}$, H$_B$, H$_{B'}$), 2.78 ppm (s, CF$_3$CONHCH$_2$CH$_2$OC(CH$_3$)$_2$OCH$_2$CH_2-NH$_2$, H$_D$), 1.77 (br. s, CF$_3$CONHCH$_2$CH$_2$OC(CH$_3$)$_2$OCH$_2$CH$_2$-NH_2), 1.27 ppm (s, CF$_3$CONHCH$_2$CH$_2$OC(CH_3)$_2$OCH$_2$CH$_2$NHCOCF$_3$, H$_C$, H$_{C'}$). Refer to Figure 5.1 for proton labeling.
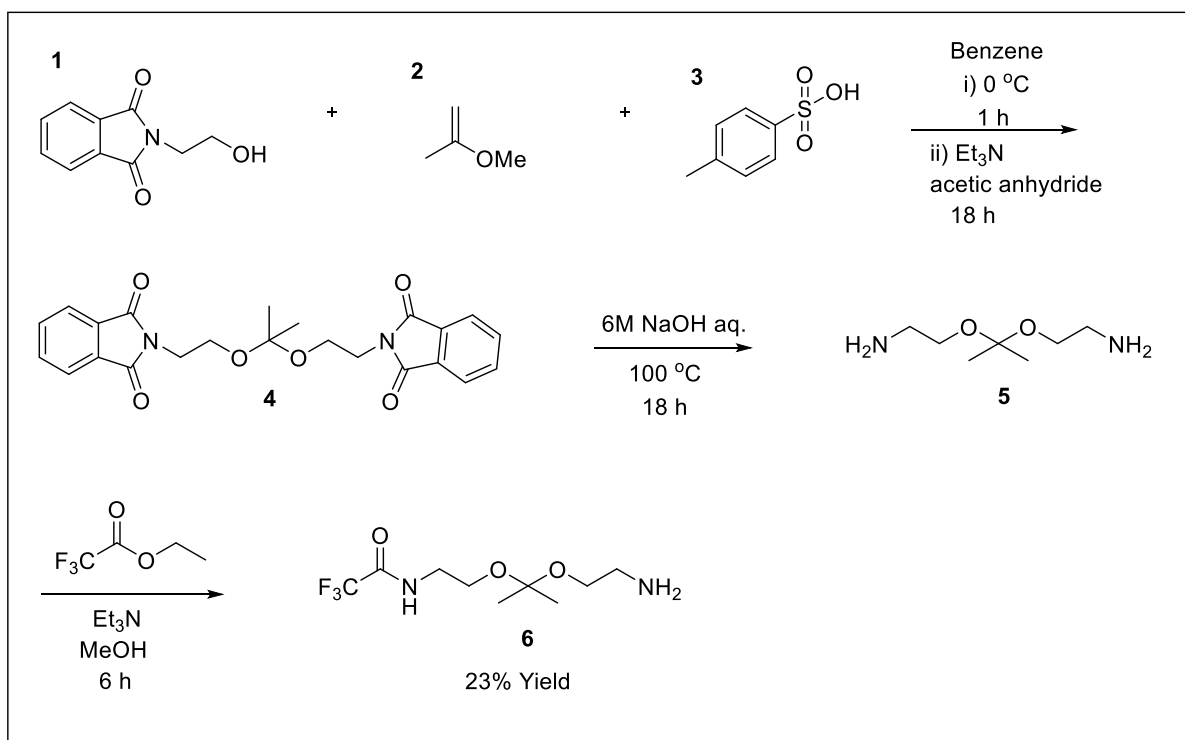
Scheme 5.6. Synthesis of mono-protected pH-responsive initiator (AEE).

5.2.3 Synthesis of pH Responsive Diblock Copolypeptoids (AEE-PNMeOEt-*b*-PNPgG)

In the glovebox, methoxy ethyl-NCA (M1) (55 mg, .346 mmol, [M1]$_0$ = 0.4 M) was dissolved in anhydrous THF (865 µL). A predetermined volume of monoprotected AEE initiator, compound **6,** in a THF stock solution (34.6 µL, 7 µmol, 250 mM,

100

[M1]$_0$:[CF$_3$AEE]$_0$ = 50:1) was added to the monomer solution via syringe. Polymerization was allowed to proceed for 24 h at 50 °C under a nitrogen atmosphere. Aliquots of the reaction mixture were taken and monitored for monomer conversion by FT-IR. Upon completion of the first polymer block the analogue was end capped using acetic anhydride in an equivalent amount to initiator before precipitation with excess hexane. The molecular weight analysis of AEE-PNMeOEtG following precipitation was conducted by size exclusion chromatography. Next, the initial polymer was stirred in a 10% sodium hydroxide solution in methanol for 10 min to remove the trifluoroacetate protective group prior to the sequential addition of propargyl-NCA to the polymerization for generation of the second polymer block. Under nitrogen, propargyl-NCA (M2) (24 mg, .173 mmol, [M2]$_0$ = 0.1 M) was added to AEE-PNMeOEtG re-dissolved in anhydrous THF (173 μL) and stirred at 50 °C for an additional 18 h. Complete monomer conversion was monitored by FT-IR before the polymer chain end was capped with acrylic anhydride. Following precipitation with excess hexane, the final block copolymer's composition and molecular weight was analyzed by ^{1}H NMR spectroscop (Figure S5.1) and SEC method (Table 5.1). ^{1}H NMR (400 MHz, CDCl$_3$), δ ppm: 6.35−6.15 (m, −COCH=CH$_2$, H$_N$), 5.83−5.35 (br. m, −COCH=CH_2, H$_O$), 4.43−4.20 (br. m, −COCH_2N−, H$_B$, H$_K$), 3.50−3.27 (br. m, −CCH_2N−, −N(CH_2)$_2$OCH$_3$, −N(CH$_2$)$_2$OCH_3, −CCH_2N−, H$_C$-H$_E$, H$_L$), 2.43−2.30 (br. m, HC≡CCH_2N−, H$_M$), 2.10−2.01 (br. s, CH_3COCN−, H$_A$), 1.31 (br. m, −NHCH$_2$CH$_2$OC(CH_3)$_2$OCH$_2$CH$_2$NH−, H$_H$). Refer to Figure 5.2 for proton labeling.

5.2.4 Synthesis of Cationic pH-Responsive and Non-pH Responsive Block Copolypeptoids

Post-polymerization modification of the pH responsive diblock copolypeptoids with 6-azidohexane guanidinium for their positively charged derivatives was achieved by CuAAC chemistry as previously reported in chapter 3. The cationic polypeptoids were purified by treatment with EDTA to remove copper salts followed by extensive dialysis against DI water. Upon lyophilization, all polymers were obtained as white to pale green powders in good yield (60-96%) with copper ion content in the sub-10 ppm range as determined by the atomic absorption analysis. The copper ion content is significantly lower than the concentration threshold that would otherwise cause potential copper ion-induced cytotoxicity.[15] Cationic block copolymers were characterized by ^{1}H NMR spectroscopy (Figure 5.4). ^{1}H NMR (400 MHz, D$_2$O), δ ppm: 8.01-7.95 ppm (br. m, −C=CHN−, H$_M$), 4.69-4.18 [(br.m,−COCH_2N−,−CCH_2N−,−CONHCH_2CH$_2$OC(CH$_3$)$_2$OCH$_2$CH_2NHCO−,−CONHCH$_2$C H_2OC(CH$_3$)$_2$OCH_2CH$_2$NHCO−, −NCH_2(CH$_2$)$_5$NHCNH$_3$, H$_B$, H$_F$, H$_G$, H$_I$, H$_L$, H$_N$)], 3.82-2.92 [(br. m, −CCH_2N−, −N(CH_2)$_2$OCH$_3$, −N(CH$_2$)$_2$OCH_3, −NCH$_2$CH_2(CH$_2$)$_4$NHCNH$_3$, −N(CH$_2$)$_4$CH_2CH$_2$NHCNH$_3$, H$_C$-H$_E$, H$_O$, H$_R$)], 2.31-2.23 (br. t, CH_3CON−, −N(CH$_2$)$_5$CH_2NHCNH$_2$, H$_A$, H$_S$), 1.81-1.23 [(br. m, −N(CH$_2$)$_2$CH_2(CH$_2$)$_3$NHCNH$_3$, −N(CH$_2$)$_2$(CH$_2$CH_2)(CH$_2$)$_2$NHCNH$_3$,−N(CH$_2$)$_4$CH_2CH$_2$NHCNH$_3$,−CONHCH$_2$CH$_2$OC(CH_3) $_2$OCH$_2$CH$_2$NHCO−, H$_P$, H$_Q$,H$_H$)]. Refer to Figure 5.6 for proton labeling.

In the glovebox, *N*-methoxy ethyl-NCA (M1) (86 mg, 0.74 mmol, [M1]$_0$ = 0.4 M) was dissolved in anhydrous THF (1.9 mL). A known volume of BnNH$_2$/THF stock solution (168 μL, 11 μmol, 63.2 mM, [M1]$_0$:[BnNH2]$_0$ = 40:1) was added using a syringe. Polymerization was allowed to proceed for 24 h at 50 °C under a nitrogen atmosphere.

Aliquots of the reaction mixture were taken and analyzed for conversion by FT-IR and molecular weights by SEC. An THF solution (2.5 mL) containing *N*-propargyl-NCA (M2) (23 mg, 0.11 mmol, $[M2]_0 = 0.4$ M, $[M2]_0:[BnNH2]_0 = 10:1$) was added into the above reaction mixture, which was heated at 50 °C for additional 24 h to reach complete conversion. The polymer product was precipitated by the addition of cold hexanes and collected by filtration. Following filtration, the polymer was washed with ample hexanes to remove any unreacted monomers or homopolymers, and dried under vacuum (45 mg, 63% yield). The degree of polymerization (DP) of PNMeOEtG and PNPgG blocks was determined by ^{1}H NMR spectroscopy (Figure S5.2). ^{1}H NMR (400 MHz, CD$_3$CN), δ ppm: 7.31−7.27 ppm (br m, −C$_6$H$_5$, H$_A$), 4.80-4.16 (br. m, −CO*CH$_2$*N−, −C*CH$_2$*N−, H$_C$, H$_G$, H$_H$), 3.48-3.25 [(br. m, −C*CH$_2$*N−, −N(C*H$_2$*)$_2$OCH$_3$, −N(CH$_2$)$_2$OC*H$_3$*, H$_D$, H$_E$, H$_F$)], 2.75-2.25 (br. m, *H*C≡C*CH$_2$*N−, H$_I$). Refer to Figure 5.5 for proton labeling.

Post-polymerization modification of the non-pH responsive diblock copolypeptoids with 6-azidohexane ammonium (127) or 6-azidohexane guanidinium (126) was achieved by CuAAC in the same manner that was used to obtain positively charged homopolymers and random copolymers discussed in chapters 3 and 4. The cationic polypeptoids were purified by treatment with an aqueous solution of EDTA (9.9 mM, 2 mL) to remove copper salts followed by extensive dialysis against DI water. Upon lyophilization, all polymers were obtained as white to pale green powders in good yield (60-96%) with copper ion content in the sub-10 ppm range based on the atomic absorption analysis, which was significantly lower than the concentration threshold that would otherwise cause potential copper ion-induced cytotoxicity. ^{1}H NMR (400 MHz, D$_2$O), δ ppm: 8.05-8.01 ppm (br m, −C=C*H*N−, H$_I$), 7.23−7.19 ppm (br m, −C$_6$H$_5$, H$_A$),

4.70-4.33 (br. m, −COCH_2N−, −CCH_2N−, H$_C$, H$_G$, H$_H$), 3.86 (s, −N(CH$_2$)$_5$CH_2NH$_3$), H$_O$),

3.46 (s, −NCH_2(CH$_2$)$_5$NHCNH$_3$, −NCH$_2$CH_2(CH$_2$)$_4$NHCNH$_3$, H$_J$, H$_K$), 3.56-3.09 [(br. m,

−CCH_2N−,   −N(CH_2)$_2$OCH$_3$,   −N(CH$_2$)$_2$OCH_3 ,   H$_D$-H$_F$)],   1.80-1.26   [br.   m,

(−N(CH$_2$)$_2$CH_2(CH$_2$)$_3$NH$_3$, −N(CH$_2$)$_2$ (CH$_2$CH_2)(CH$_2$)$_2$NH$_3$, −N(CH$_2$)$_4$CH_2CH$_2$NH$_3$), H$_L$-

H$_N$]. Refer to Figure 5.7 for proton labeling.

5.2.5. Copolypeptoid/DNA Polyplex Preparation and Characterization

Cationic polypeptoids and pCMV-Luc were dissolved in PBS water at 1 mg/mL

and 0.1 mg/mL, respectively, and mixed at various polypeptoid/DNA weight ratios. The

mixture was vortexed for 10 s and further incubated at 37 °C for 30 min to allow

complete formation of the polyplexes. To qualitatively evaluate the DNA condensation

by the polypeptoids, a gel retardation assay was conducted. Briefly, freshly prepared

polyplexes were loaded in 1% agarose gel followed by electrophoresis at 100 V for 45

min. To quantitatively determine the DNA condensation level, the ethidium bromide (EB)

exclusion assay was adopted. EB solution was mixed with DNA at the DNA/EB weight

ratio of 10:1, and was incubated at room temperature for 1 h. Cationic polypeptoids

were then added to the mixture at various polypeptoid/DNA ratios, before further

incubation at room temperature for 30 min. Quantification of all polyplexes' fluorescence

intensity was carried out by spectrofluorimetry (λ_{ex} = 510 nm, λ_{em} = 590 nm). A pure EB

solution and the DNA/EB solution without any polypeptoids were used as negative and

positive controls, respectively. The DNA condensation efficiency (% DNA condensed)

was defined as the following:

$$\text{DNA condensation efficiency (\%)} = \left(1 - \frac{F - F_{EB}}{F_0 - F_{EB}}\right) \times 100$$

Where F_{EB}, F, and F_0 denote the fluorescence intensity of pure EB solution, DNA/EB solution with polypeptoids, and DNA/EB solution without any polypeptoids, respectively.

5.2.6. Critical Micelle Concentration (CMC) Measurement of Copolypeptoid/DNA Polyplexes

The critical micelle concentration experiment for polyplexes was carried out using pyrene as a fluorescence probe. Fresh stock solutions of copolymer/DNA polyplexes were prepared at 0.1mg/mL. Pyrene was dissolved in acetone at 1 mg/mL. The concentration of copolymer/DNA polyplexes was varied from 1.0×10^{-6} to 0.3 mg/mL by serial dilution with ultrapure water while the concentration of pyrene was fixed at 0.6 µM. The mixture was incubated at 37 °C overnight and acetone was removed for another 4 h. The fluorescence spectra were recorded using the microplate reader with the excitation wavelength of 330 nm. The emission fluorescence at 372 and 383 nm was monitored. The CMC was estimated as the inflection-point when extrapolating the intensity ratio I_{372}/I_{383} at low and high concentration regions.

5.2.7. *In Vitro* Transfection

HeLa cells were seeded on 96-well plates at 2×10^4 cells/well and cultured in DMEM containing 10% FBS for 24 h. The medium was replaced by opti-MEM (100 µL/well), into which polyplexes were added at 0.3 µg DNA/well. After incubation at 37 °C for 4 h, the medium was replaced by DMEM containing 10% FBS, and cells were further incubated for another 20 h. Luciferase expression level was determined in terms of luminescence intensity using the Bright-Glo Luciferase assay kit (Promega), and the cellular protein level was determined using the BCA kit (Pierce). Results were expressed as relative luminescence unit (RLU) associated with 1 mg of pCMV-Luc cellular protein (RLU/mg protein). To evaluate the transfection efficiency of polyplexes in

the presence of serum, cells were incubated with polyplexes in DMEM supplemented with 10% FBS for 4 h. Then the medium was replaced by fresh DMEM containing 10% FBS and cells were further incubated for another 20 h before measurement of luciferase expression levels as described above.

5.2.8. Cytotoxicity Studies

HeLa cells were seeded on 96-well plates at 2×10^4 cells/well and cultured for 24 h. The medium was replaced by opti-MEM (100 µL/well) into which free polypeptoids at various concentrations or polyplexes at 0.3 µg DNA/well and various polypeptoid/DNA weight ratios were added. After incubation at 37 °C for 4 h, the medium was replaced by DMEM containing 10% FBS and cells were further incubated for another 20 h. Cell viability was then evaluated by the MTT assay. Cells without polypeptoid or polyplexes treatment served as the control and results were represented as percentage viability of control cells.

5.3. Results and Discussion

5.3.1 Synthesis of Mono-protected pH-responsive Initiator (AEE) and Cationic pH Responsive and Non-pH Responsive Diblock Copolypeptoids

Synthesis of cationic block peptoid copolymers which contain a pH responsive linker has been investigated. As a result, the mono-protection of pH sensitive AEE was accomplished by means of a multistep synthetic route (Scheme 5.6). Attempts at the selective protection of the diamine under basic conditions with a trifluoroacetate yielded the desired mono-protected and bis-protected product in an inseparable mixture as illustrated in ^{1}H NMR spectrum (Figure 5.1). The mixture was the statistical result of the reaction. The relative integration of protons for the mono to bis protected diamine was

used to determine the relative amount of each species by ^{1}H NMR analysis (peak labels E, C and C' of Figure 5.1).
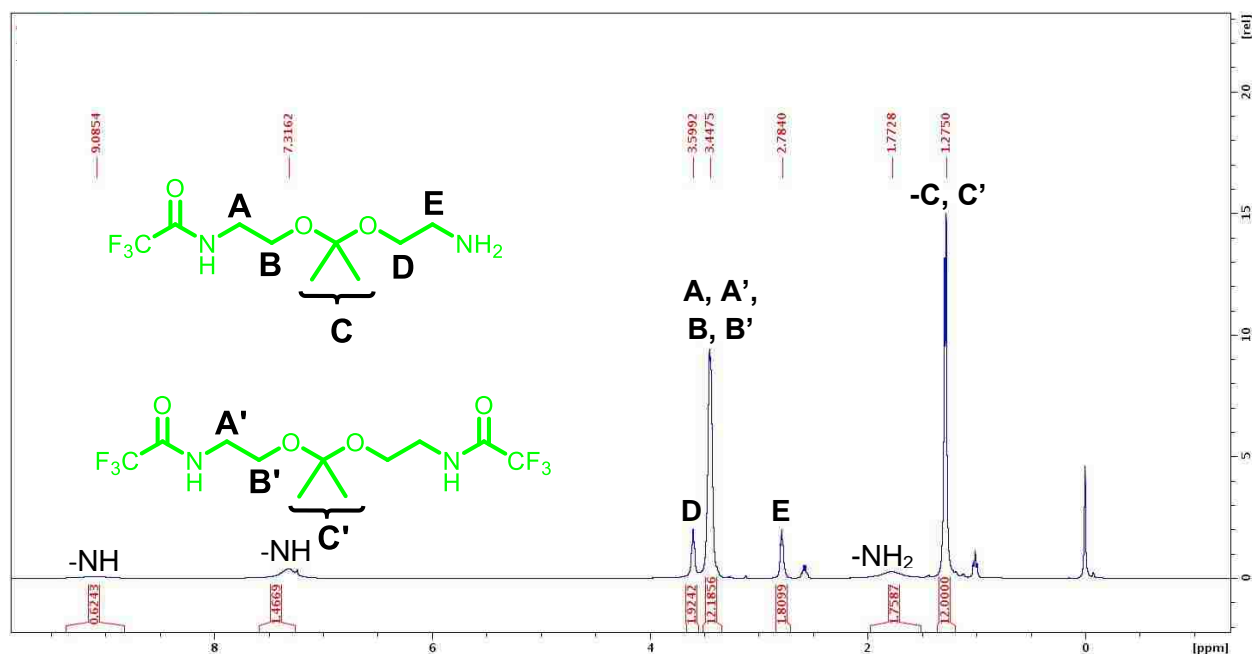
Figure 5.1. ^{1}H NMR spectrum of mono-protected AEE amine initiator in CDCl$_3$.

The primary amine-mediated ROP of Pg-NCA and MeOEt-NCA was used to obtain neutral block copolypeptoid precursors bearing the pH responsive linker (Scheme 5.4). For pH responsive diblock copolymer precursors, where the neutral hydrophilic methoxy ethyl content was varied, the total degree of polymerizations DP = 50 and DP = 75 were targeted. After being synthesized their experimentally determined compositions were determined by ^{1}H NMR analysis and summarized in Table 5.1. The block copolypeptoid composition was determined using the integrations of methyl protons of PNMeOEtG segments and terminal alkyne proton of PNPgG segments relative to the methyl protons in acetal end group in ^{1}H NMR spectra (Figure 5.2). The determined final chain lengths for unmodified pH responsive copolymers appeared to correspond well with initially targeted [M]$_0$:[I]$_0$ ratios. SEC analysis revealed PNMeOEtG

homopolymer precursors with relatively narrow polydispersities, which characteristically suggested minimal molecular weight distribution and good control over ROP with the pH responsive initiator. However, an increase in PDI was observed following generation of the PNPgG block, presumably due to propargyl's innate aggregation behavior in organic solvent. According to Figures 5.3 and 5.4 SEC chromatograms suggested that the diblock copolymer precursors did not suffer from any chain cleavage during the multi-step synthetic route used to in final polymer chain lengths.
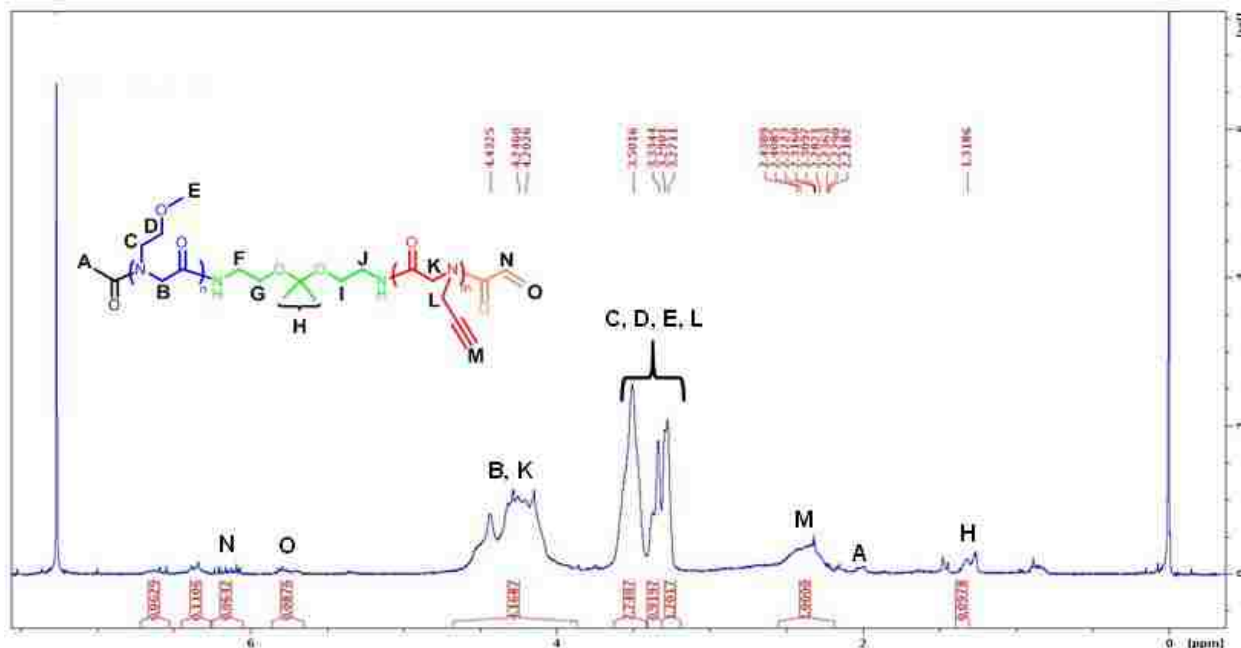
Figure 5.2. Representative ^{1}H NMR spectrum of neutral pH-responsive block copolypeptoid precursor (AEE-PNMeOEtG-b-PNPgG) in CDCl$_3$.

Table 5.1. Molecular weight parameters of neutral block copolypeptoid precursor (AEE-PNMeOEt-b-PNPgG).

Sample #	$[M]_o:[N]_o:[I]_o$	DP (^{1}H NMR)	M_n (SEC)[a] kg·mol^{-1}	M_n (SEC)[b] kg·mol^{-1}	PDI (SEC)[a]	PDI (SEC)[b]	Percent Yield
128	25:25:1	m= 23 n= 31	5.78	6.80	1.09	1.30	100%
129	50:25:1	m= 51 n= 22	8.29	8.83	1.23	1.76	75%

[a]M_n and PDI of PNMeOEt block was determined using a dn/dc of 0.0633mL·g^{-1}.

[b]M_n and PDI of AEE-PNMeOEt-b-PNPgG block of copolymers were determined using polystyrene standards.
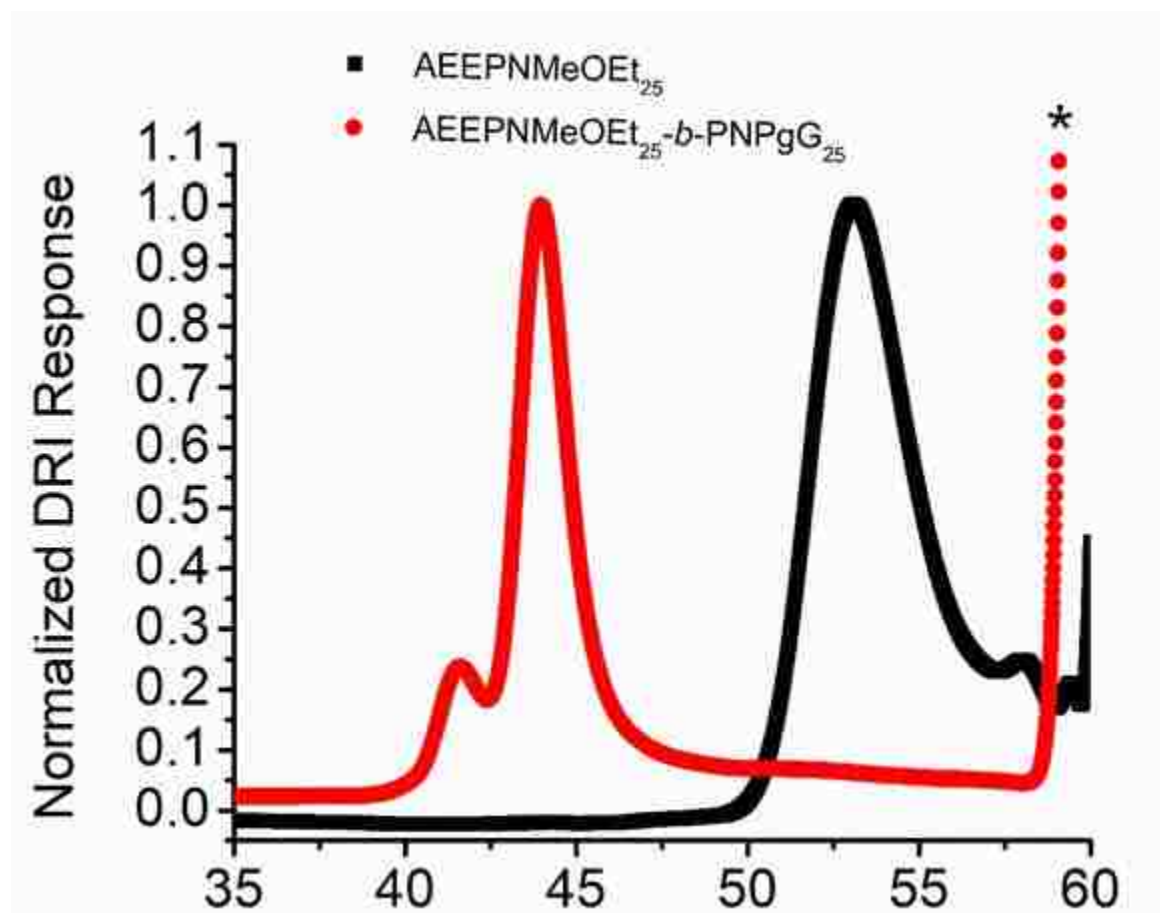
Figure 5.3. SEC chromatograms of the neutral pH-responsive block copolypeptoid precursor (AEE-PNMeOEt$_{25}$-b-PNPgG$_{25}$).* Indicates elution of LiBr/DMF solvent.
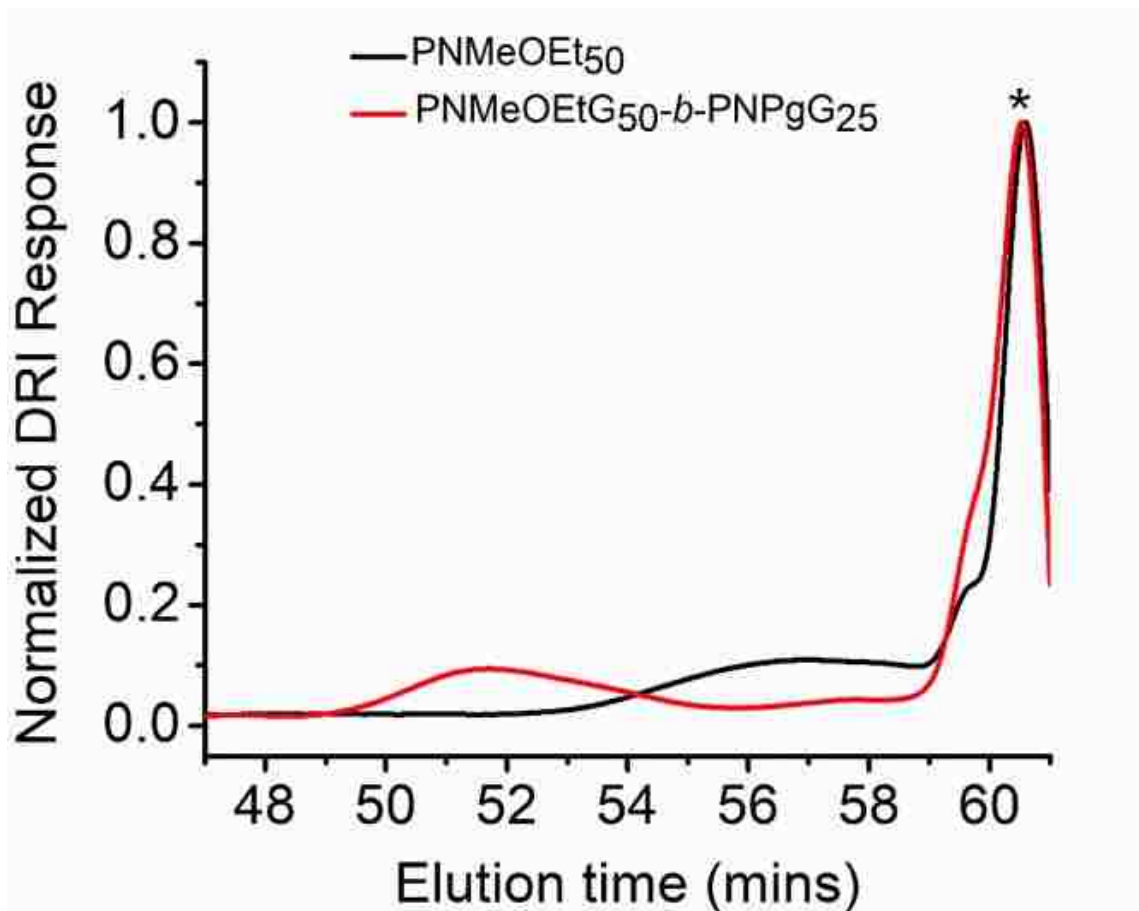
Figure 5.4. SEC chromatograms of the neutral pH-responsive block copolypeptoid precursor (AEE-PNMeOEt$_{50}$-b-PNPgG$_{25}$) copolymer precursors. * Indicates elution of LiBr/DMF solvent.

Scheme 5.5 illustrates the synthetic route to prepare non-pH responsive cationic diblock copolymers. The neutral block copolypeptoid precursors (PNMeOEtG-b-PNPgG) have been similarly prepared as the one to the pH-responsive cationic block copolypeptoid and characterized via ^{1}H NMR spectroscopic analysis prior to CuAAC functionalization to introduce the cationic sidechain (Table 5.2 and Figure 5.5). For the non-pH responsive block copolymer precursor, a total degree of polymerization (DP) of 50 was targeted (Table 5.2). The block copolymer compositions determined from ^{1}H NMR analysis are in good agreement with targeted [M]$_0$:[I]$_0$ ratios, suggesting that the

110

polymerization occurs in a controlled manner (Figure 5.3). The molecular weight distribution (PDI) for the non-pH responsive block copolypeptoid precursors (PNMeOEt-*b*-PNPgG) were not determined due to the malfunctioning of the SEC instruments at the time.
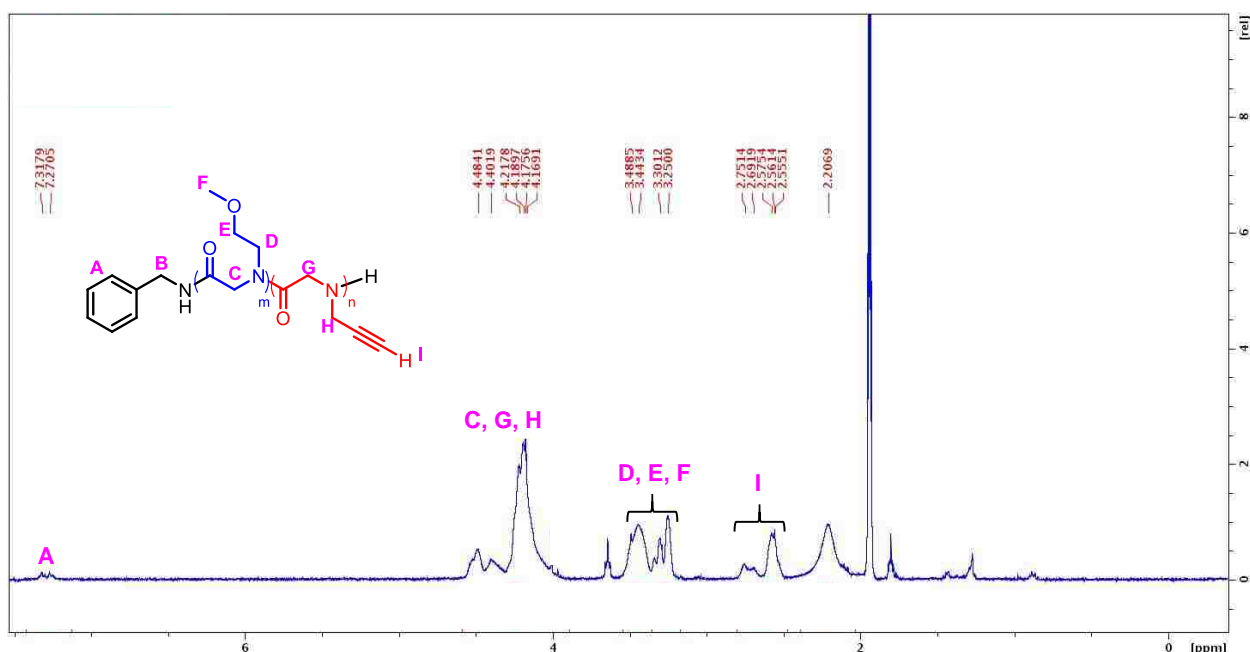
Figure 5.5. ^{1}H NMR spectrum of non-pH responsive neutral block copolypeptoid precursor (PNMeOEtG-*b*-PNPgG) in CD$_3$CN.

Table 5.2. Molecular weight parameters of neutral non-pH responsive block copolypeptoid precursor (PNMeOEt-*b*-PNPgG) and the cationic non-pH responsive block copolypeptoid.

Copolymer	[M]$_o$: [N]$_o$: [I]$_o$	Chain length before CuAAC (^{1}H NMR)	Chain length after CuAAC (^{1}H NMR)	Percent Yield
126	40:10:1	m= 37 n= 12	m= 25 n= 10	89%
127	40:10:1	m= 37 n= 12	m= 31 n= 11	92%

The conjugation of cationic sidechains to the polypeptoid precursors were conducted using CuAAC chemistry. Both pH-responsive and non-pH responsive block copolypeptoids were found to be soluble in common organic solvents (e.g. chloroform,

111

THF) but insoluble in water. The hydrophobic nature of the propargyl side chains is likely to be responsible for the observed solubility property. Upon conjugation with cationic moieties, resulting polypeptoids became water soluble. In all cases successful conversion of neutral block copolymer precursors into cationic block copolypeptoids was evidenced by the complete disappearance of the terminal alkyne proton of propargyl group at 2.51 ppm and appearance of the triazole proton at 8.0 ppm in the ^{1}H NMR spectra, suggesting that the sidechain derivation was quantitative (Figures 5.6 and 5.7). Whereas the determination of the final composition of the non-pH responsive cationic diblock copolypeptoids was feasible by ^{1}H NMR analysis (Table 5.2), the overlap of the polymer peaks with that of AEE initiating moieties in the ^{1}H NMR spectra prevented the composition for the pH responsive cationic copolypeptoid to be unambiguously determined. One possible solution to this issue is to use acid to trigger to cleavage of the cationic block copolymers. The resulting neutral segment (PNMeOEtG) can be independently analyzed by the SEC method (in LiBr/DMF solvent) to determine the chain length, which will allow us to deduce the chain length of the cationic segment in the cationic block copolymer.
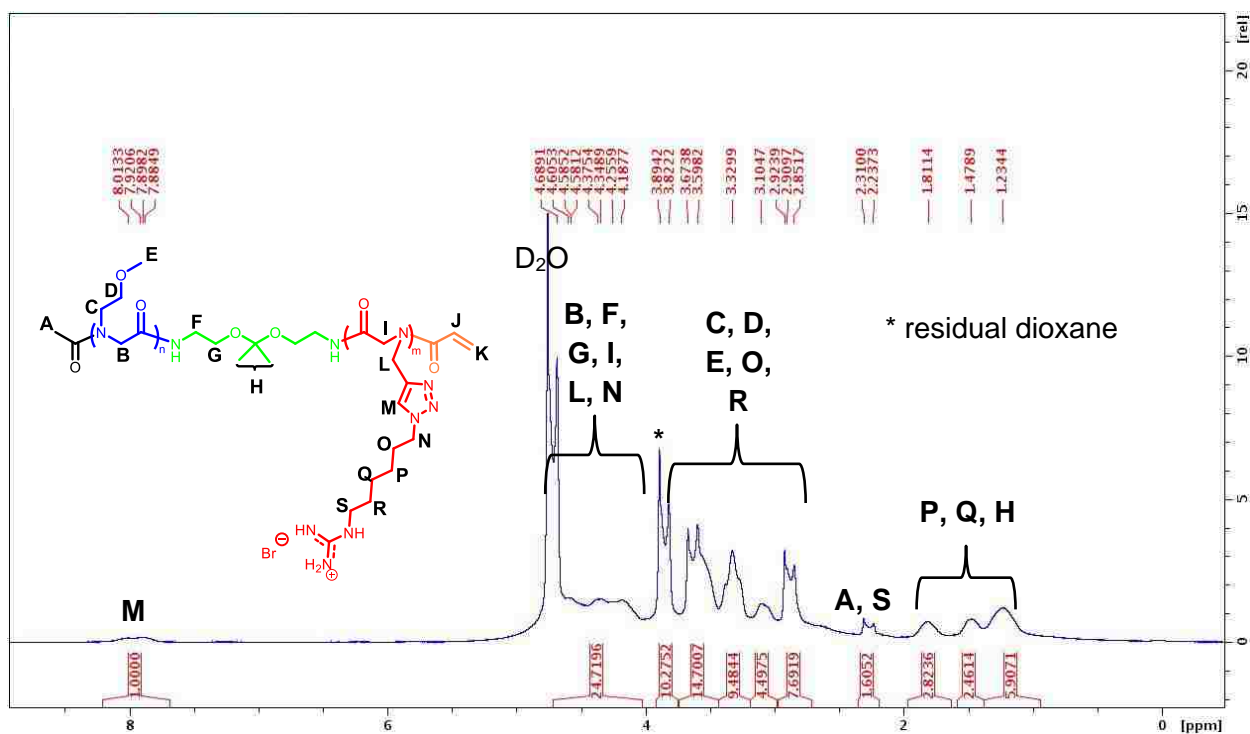
Figure 5.6. Representative ^{1}H NMR spectrum of pH-responsive cationic block copolypeptoid (AEEPNMeOEt-*b*-PNPG) in D$_2$O.
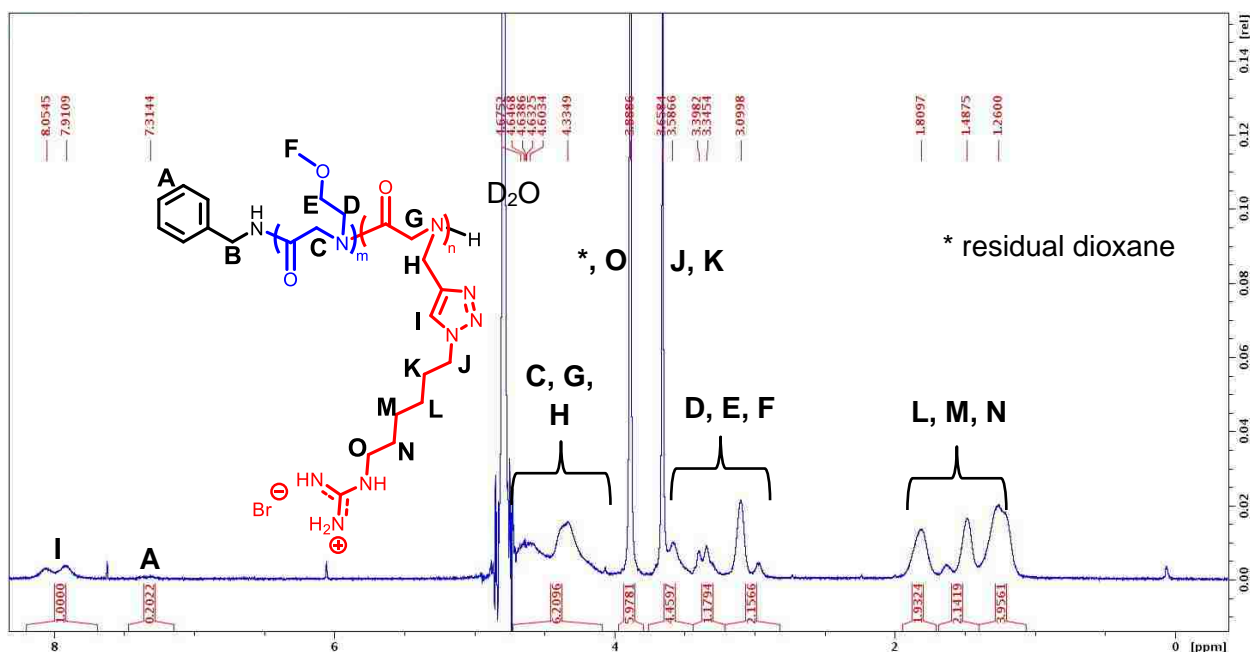
Figure 5.7. ^{1}H NMR spectrum of non-pH responsive cationic block copolypeptoid (PNMeOEt-*b*-PNPG) in D$_2$O.

5.3.2 Characterization of Cationic Block Copolypeptoid/DNA Polyplexes

Each cationic diblock copolypeptoid was qualitatively assessed for their capability to condense DNA via the gel retardation assay (Figure 5.6). All polymers were able to completely condense DNA at varied polypeptoid/DNA weight ratios. Non-pH responsive cationic block copolypeptoids derived from PNMeOEt-*b*-PNPgG (126, 127 in Table 5.2) were able to condense DNA at polymer/DNA weight ratio ≥ 1. This is comparable to cationic polypeptoid homopolymers and random copolymers previously investigated (chapter 3 and 4). By contrast, pH responsive cationic block copolypeptoids derived from (AEE-PNMeOEt-*b*-PNPgG) (Table 5.1) complexed DNA at w/w ratios much higher polymer/DNA ratios (≥ 10). To confirm these findings, a more quantitative EB exclusion assay is required. Furthermore, zeta potential should be measured for the polyplexes formed with the pH-responsive and non-pH responsive diblock copolymers in order to obtain information about their surface charge characteristic. Due to differing chemical compositions of the pH-responsive and non-pH responsive copolymers no direct comparison of condensation profiles can be made.
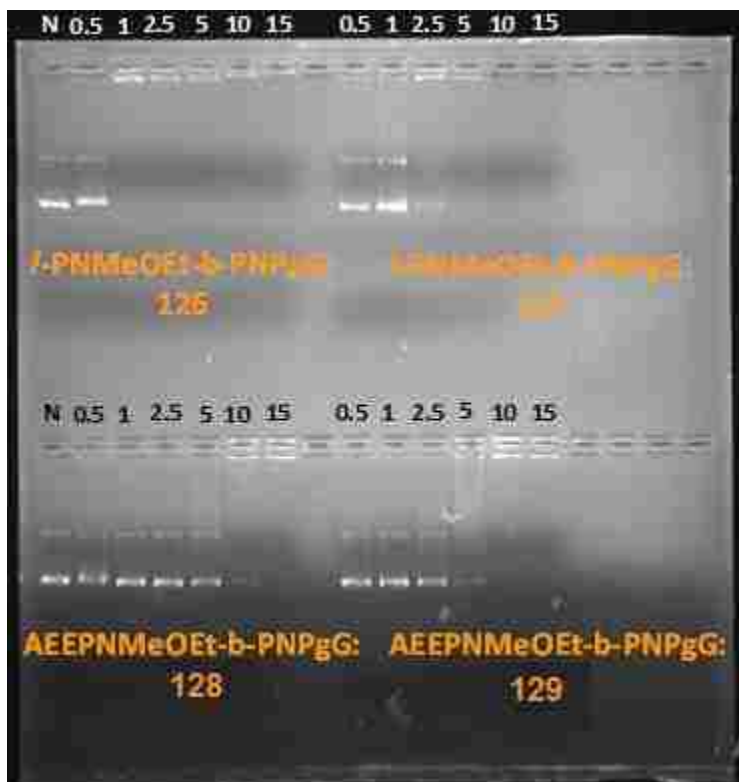
Figure 5.8. DNA condensation by cationic block copolypeptoids derived from the PNMeOEt-*b*-PNPgG precursor (126, 127, Table 5.2) or AEE-PNMeOEtG-*b*-PNPgG precursor (128, 129, Table 5.1) at various polymer/DNA weight ratios as evaluated by the gel retardation assay. "N" represents naked DNA.

Block copolymers consisting of a hydrophilic and hydrophobic segment are known to form micelles above a critical polymer concentration. For gene delivery purposes CMCs can vary based on the polymeric structure.[11-13] Polypeptoid/DNA polyplexes based on the pH responsive and non-pH responsive cationic block copolypeptoids and pCMV-Luc were also measured for a critical micelle concentration (CMC) in deionized water at varying concentrations. Given the double hydrophilic nature presented by polymer side chains within the copolymer design deviating from the general description of what micelles are composed of, it was worthwhile to investigate this aspect. DNA polyplexes with all polypeptoid block copolymers were prepared in

water at the concentration 1 mg·mL^{-1}. To characterize the critical micellar concentration (CMC), a series of aqueous solutions containing a constant concentration of pyrene and varying concentrations of polypeptoid/DNA polyplexes were prepared and measured by fluorescence spectroscopy in the 200-400 nm range with an excitation at λ= 370 nm. Pyrenes are used as fluorophores that exhibits high fluorescence intensity in a hydrophobic environment but low fluorescence intensity in a hydrophilic environment. [14] Plot of fluorescence maximum versus concentration revealed an inflection point where the fluorescence intensity increases sharply. The polymer concentration at the inflection point is defined as the CMC. Because two hydrophilic blocks are contained in my copolymers used, the micellation process would be predominantly driven by complexation between DNA and the cationic copolymer block. If the ionic domain exhibited sufficient hydrophobic character, one would expect to see a difference in the fluorescence intensity as a result of the partitioning of pyrene between the hydrophilic and hydrophobic copolymer domains. It is clear in the 0.1- 1mg/mL concentration range, no obvious trend of the fluorescent intensity was found with the concentration (Figures 5.9 A-D). Either no micelles are formed in this concentration range or the fluorescent method based on pyrene is not suited for the determination of CMC for the micellation of the cationic block copolymer with DNA. As the cationic block copolypeptoid condenses with DNA, the micellar core may still be very hydrophilic due to the abundance of charges. In this case, the fluorescent intensity of pyrene would not change appreciably upon micelle formation. Further experiments are required to determine the CMC in this system
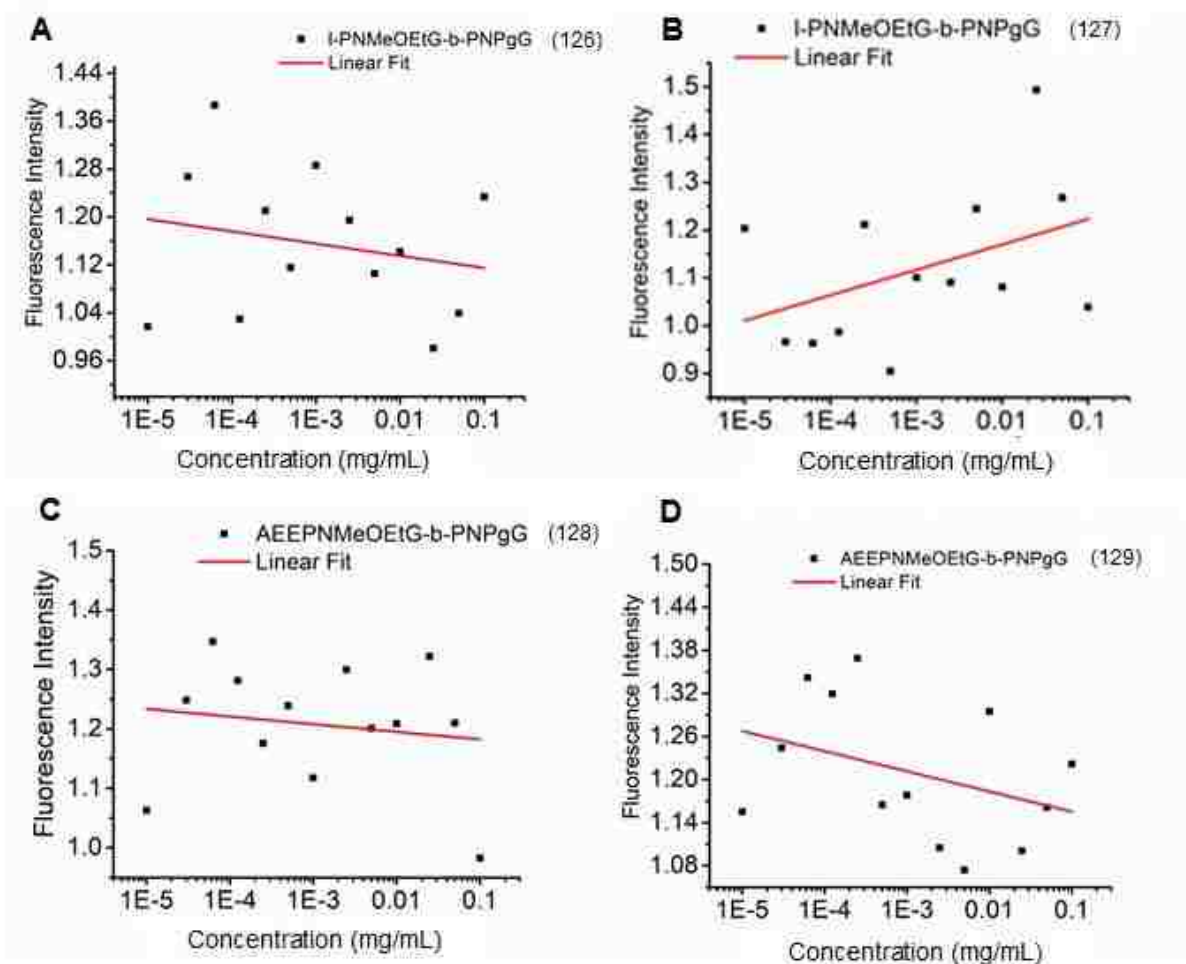
Figure 5.9. Log plot of the maximum fluorescence intensity (λ_{em} = 372 & 383 nm) versus polymer concentrations for cationic copolypeptoid/DNA polyplexes derived from: PNMeOEt-*b*-PNPgG (126, 127, Table 5.2) and AEE-PNMeOEt-*b*-PNPgG (128, 129, Table 5.1).

5.3.3. *In Vitro* Transfection of Polypeptoid/DNA Polyplexes

Using HeLa cells, pH-responsive and non-pH responsive cationic diblock copolypeptoids were assessed for the gene delivery capability. As shown in Figure 5.10, transfection efficiencies for pH-responsive and non-pH responsive block copolypeptoids were considerably lower than PEI, more than ~3 orders of magnitude respectively. In comparison with copolymers containing terminal guanidinium groups, the commercial vector outperformed 126, 128, and 129 by up to 6 orders of magnitude (Figure 5.10 A,

C, D). Though varying the polypeptoid/DNA weight ratio (w/w ratio) of the block copolypeptoids did improve transfection by 1-2 orders overall, efficiencies were still not comparable to that achieved with PEI. However, a trend was observed for the three guanidinum samples upon increasing w/w ratios, with slightly higher efficiencies produced in each case (Figure 5.10 A, C, D). Gene delivery for primary amine bearing copolypeptoid, 127, yielded efficiencies that were also several orders lower (~4 orders) than PEI (Figure 5.10 B). Varying w/w ratios appeared not to have any influence on the transfection profile of 127 as seen with copolymers bearing guanidinum end groups. In terms of transfection performance, no direct comparison can be made between the pH-responsive and non-pH responsive copolypeptoids given their different polymer compositions.

As mentioned in chapter 3, the presence of hydrophobicity in addition to charge is critical to enhanced transfection efficiency of polypeptoids. Findings from gene delivery experiments in this work highly suggest that a lack in one or both of these aspects lead to the consequence of poor transfection. In our earlier studies higher transfection efficiencies were generated for copolymers comprised of hydrophobic side chains in comparison to their corresponding homopolymer as the result of increased membrane activity.[9] In the case for all diblock copolymers, despite the presence of a charged segment that can complex with DNA, the shielding of the polyplex by the hydrophilic poly(*N*-methoxyethyl glycine) (PNOMEG) segments may have contributed to the poor transfection efficiencies (Figures 5.10). The ability of PNOMEG to act as an anti-fouling agent has been previously demonstrated by members of our group.[16] In addition, another factor which may have led to low transfection is the significantly

reduced net positive charge on the surface of the polyplexe micelles due to the shielding by PNOMeG segments. Measurements of zeta potential of the polyplex micelles at different w/w ratios should shine lights on the relative strength of surface charges.
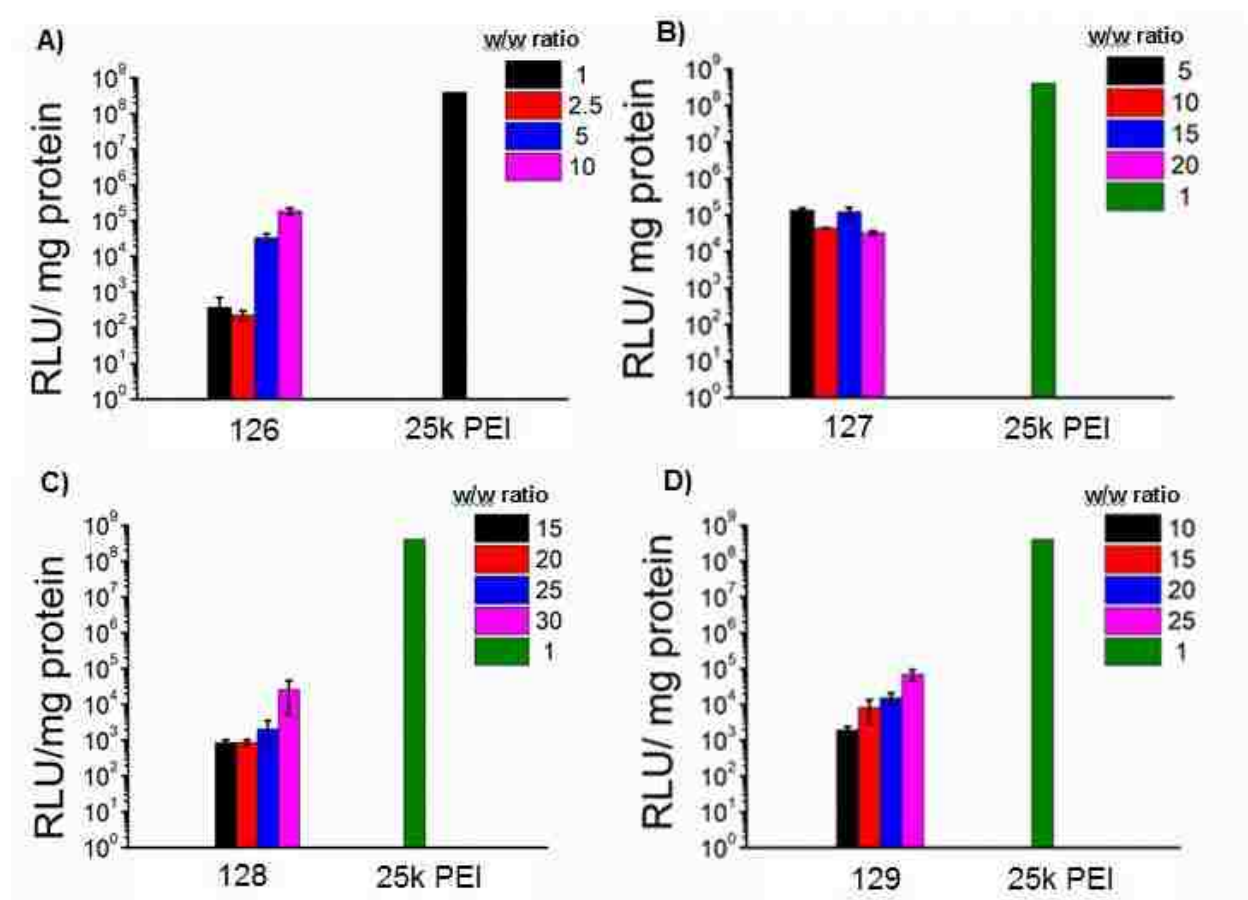
Figure 5.10. Cell transfection of pCMV-Luc in DMEM using pH-responsive cationic block copolypeptoid derived from PNMeOEt-*b*-PNPgG (126, 127, Table 5.2) and AEE-PNMeOEt-*b*-PNPgG (128, 129, Table 5.1) as gene carriers.

5.3.4. Cytotoxicity of Cationic Block Copolypeptoid/DNA Polyplexes

The cytotoxicity of polyplexes based on pH-responsive and non-pH responsive cationic diblock copolypeptoids were evaluated in HeLa cells under serum-free and serum containing conditions. As shown in Figure 5.11, polyplexes formed with non-pH

responsive samples displayed cytotoxicity profiles with very differing cell viability percentages. In DMEM (serum-free) (Figure 5.11, A) and DMEM/10% FBS (serum-containing) (Figure 5.11, B) polyplexes generated with 126 (guanidinum end group) exhibited cell viability percentages significantly higher than 127 (ammonium end group), by ~35% respectively. This trend was also observed at increased polypeptoid/DNA weight ratios (Figure 5.11). The best toxicity profiles were displayed by polyplexes based on pH responsive copolymers 128 and 129, with cell viability percentages reaching greater than 80%. In the presence of increasing w/w ratios (up to 30:1) exceptional viability was retained with 128 under both serum-free and serum containing conditions (Figure 5.11). In serum-free and serum-containing media, weight ratios higher than 20:1 led to a decline in cell viability for 129, 20% at 25:1 and 35% at 30:1 respectively. The cell viability for polyplexes made with pH-responsive and non-pH responsive diblock copolypeptoids was observed in both serum-free and serum containing conditions (Figure 5.11). However, a direct comparison of cytotoxicity profiles for the pH-responsive and non-pH responsive cationic copolypeptoids cannot be made due to their dissimilar compositions.
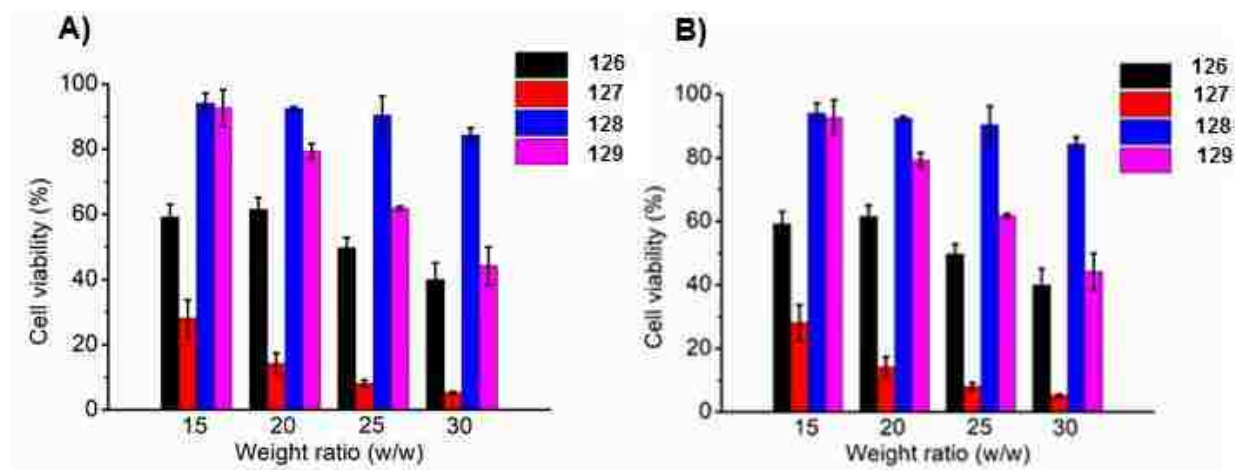
Figure 5.11. (A) Percentage HeLa cell viability after being cultured with polyplexes formed with cationic block copolypeptoid derived from AEEPNPgG-*b*-PNMeOEtG (128, 129, Table 5.1) or PNPgG-*b*-PNMeOEtG (126, 127, Table 5.2) in DMEM or (B) in DMEM/10% FBS for 4 h and characterized by MTT assays.

5.4. Conclusion

In this work, pH responsive cationic block copolypeptoids have been synthesized by sequential ring-opening polymerization of *N*-methyoxyethyl NCA and *N*-propargyl NCA monomers using a mono-protected pH sensitive primary amine initiator and subsequent CuAAC chemistry to conjugate cationic moieties to the sidechains of poly(*N*-propargyl glycine) segment. The resulting cationic block copolypeptoids have been characterized by a combination of ^{1}H NMR and SEC method and further evaluated for their gene delivery capabilities in serum-free and serum containing media. While the polyplexes based on the pH responsive cationic block copolypeptoids exhibited good cytocompatibility with HeLa cells, they exhibited significantly reduced *in vitro* transfection relative to PEI under serum free condition. Additional experiments are required to fully understand the origin of the reduced gene transfection performance.

121

5.5. References

1. Uddin, S., Islam, K. Cationic Polymers and its Uses in Non-viral Gene Delivery Systems: A Conceptual Research. *Trends in Medical Research* **2006**, 1, 86-99.

2. Guan, X., Guo, Z., Wang, T., Lin, L., Chen, J., Tian, H., and Chen, X. A pH-Responsive Detachable PEG Shielding Strategy for Gene Delivery System in Cancer Therapy *Biomacromolecules* **2017**, 18, 1342−1349.

3. Suk, J., Xu, Q., Kim, N., Hanes, J., Ensign, L. PEGylation as a strategy for improving nanoparticle-based drug and gene delivery *Advanced. Drug Delivery Reviews* **2016**, 99, 28−51.

4. Harris, M., Martin, N., Modi, M. Pegylation *Clinical. Pharmacokinetics* **2001**, 40, 539−551.

5. He, H., Yugang, B., Jinhui, W., Qiurong, D., Lipeng, Z., Fenghua, M., Zhiyuan, Z., Lichen, Y. Reversibly Cross-Linked Polyplexes Enable Cancer-Targeted Gene Delivery via Self-Promoted DNA Release and Self-Diminished Toxicity, *Biomacromolecules* **2015**, 16, 1390-1400.

6. Zhu, D., Yan, H., Liu, X., Xiang, J., Zhou, Z., Tang, J., Liu, X., and Shen, Y. Intracellularly Disintegratable Polysulfoniums for Efficient Gene Delivery *Adv. Funct. Mater.* **2017**, 27, 1-16.

7. Stayton, P.S., El-Sayed, M.E., Murthy, N., Bulmus, V., Lackey, C., Cheung, C., Hoffman, A.S. Smart delivery systems for biomolecular therapeutics *Orthod. Craniofac. Res.* **2005**, 8, 219–225.

8. Yang, Z., Li, Y., Gao, J., Cao, Z., Jiang, Q., Liu, J. pH and redox dual-responsive multifunctional gene delivery with enhanced capability of transporting DNA into the nucleus *Colloids and Surfaces B: Biointerfaces* **2017**, 153, 111–122.

9. Zhu, L., Simpson, J., Xu, X., He, H., Zhang, D., Yin, L. Cationic Polypeptoids with Optimized Molecular Characteristics toward Efficient Nonviral Gene Delivery. *ACS App. Mater. Inter.* **2017**, 9, 23476-23486.

10. Cai, X., Dong, C., Dong, H., Wang, G., Pauletti, G., Pan, X., Wen, H., Mehl. I., Li, Y., Shi, D. "Effective Gene Delivery Using Stimulus-Responsive Catiomer Designed with Redox-Sensitive Disulfide and Acid-Labile Imine Linkers" *Biomacromolecules,* **2012**, 13, 1024-1034.

11. O. Coulembier, L. Mespouille, J.L. Hedrick, R.M. Waymouth, P. Dubois. Metal-free catalyzed ring-opening polymerization of beta-lactones: synthesis of amphiphilic triblock copolymers based on poly(dimethylmalic acid) *Macromolecules* **2006**, 39, 4001-4008.

12. Wang, Y., Ke, C.Y., Beh, C., Liu, S.Q., Goh, S.H., Yang, Y.Y. The self-assembly of biodegradable cationic polymer micelles as vectors for gene transfection *Biomaterials* **2007**, 28, 35, 5358-5368.

13. Sebnem, E., Xin, Z., Guy, D., Christian, G., Jacques, D., Svetlana, K., Vladimir, T., Yves, M., Valery, B. Physicochemical properties of low molecular weight alkylated chitosans: A new class of potential nonviral vectors for gene delivery *Colloids and Surfaces B: Biointerfaces* **2006**, 51, 140–148.

14. Kim, W.; Thévenot, J.; Ibarboure, E.; Lecommandoux, S.; Chaikof, E. L., Self-Assembly of Thermally Responsive Amphiphilic Diblock Copolypeptides into Spherical Micellar Nanoparticles. *Angew. Chem. Int. Ed.* **2010**, 49, 4257-4260.

15. Xie, X.X., Ma, Y.F., Wang, Q.S., Chen, Z.L., Liao, R.R., Pan, Y.C. "Yeast CUP1 Protects HeLa cells against Copper-induced Stress." *Brazilian Journal of Medical and Biological Research*, **2015**, 48, 616-621.

16. Xuan, S., Gupta, S., Li, X., Bleuel, M., Schneider, G. J., Zhang, D. Synthesis and Characterization of Well-defined PEGylated Polypeptoids as Protein-resistant Polymers. *Biomacromolecules* **2017**, *18*, 951-964.

CHAPTER 6. SYNTHESIS, CHARACTERIZATION, AND RING-OPENING POLYMERIZATION OF *N*-THIOCARBOXYANHYDRIDE MONOMERS

6.1. Background and Introduction

Ring-opening polymerization of *N*-carboxyanhydride (NCA) monomers is widely used for the syntheses of polypeptides and polypeptoids.[1-5] For certain monomers such as *N*-allyl and *N*-ethyl NCAs, this method can be unreliable due to the monomer's instability and tendency to undergo spontaneous polymerization.[6] In addition, purification of NCAs must be performed under moisture-free conditions such as by dry solvent column chromatography, distillation, or vacuum sublimation, making the access of pure monomer in large quantities challenging. As a result, there is a strong interest to investigate more stable and robust monomers that can be used for polypeptides and polypeptoid synthesis.
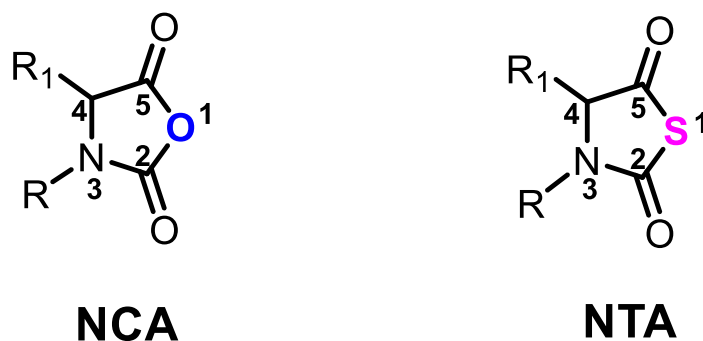
Figure 6.1. Structure of NCA vs. NTA monomer.

Amino acid derived *N*-thiocarboxyanhydrides (NTAs) (Figure 6.1) were first investigated as a substrate for aqueous phase synthesis of polypeptides.[6] NTAs were investigated as an substrate for polymerization by Kricheldorf in 1974. These early

studies showed that polymerization of NTAs tend to terminate at lower conversions relative the polymerization of the corresponding NCAs, producing polypeptides with significantly reduced polymer molecular weights.[7,8] Polymerization of NTAs was revisited by Kricheldorf and coworkers via the polymerizations of sarcosine, DL-phenylalanine, and DL- using primary amine initiators.[9] The observed molecular weights for the polymers obtained from the ROPs of NTAs were considerably lower due to low conversion. Quantitative conversions in the polymerization reactions were only reached in the case of the ROP of sarcosine-NTA at the $[M]_0 : [I]_0 = 20:1$.

Ling and coworkers have recently demonstrated the controlled ROP of N-substituted glycine NTAs using rare earth borohydrides (RE) as initiators to produce high-MW hydrophilic and hydrophobic polypeptoids.[10] In this study sarcosine-NTA (Sar-NTA) and N-butylglycine NTA (NBG-NTA) were investigated. Among RE-$(BH_4)_3(THF)_3$ compounds (RE = Sc, Y, La, Nd, Dy, or Lu) that have been investigated, the borohydride complexes containing "Y" in the case of Sar-NTA and "Lu" in the case of N-butylglycine exhibited the best polymerization control. It was shown that size of atomic radii and electronic structure of RE metals greatly influenced polymerization reactivity. For the first time, polysarcosines (PSars) with M_ns higher than 10 kDa were achieved by the polymerization of Sar-NTA in good yields (>90%). PNBGs with M_ns up to 10.8 kDa were also obtained by the polymerization of Bu-NTA, but with a slight decrease in yields (75-65.3%). In spite the success of using metal hydride in the ROP of NTAs, concerns about toxicity of residual metals in resulting polymers that may limit the biomedical applications has motivated the search of new organic initiator/catalyst systems for NTA polymerization. Ling et al. recently reported a controlled ROP of Sar-NTA using primary

amine-terminated PEG as macroinitiators.[11] Subsequently, the scope of NTAs that can be successfully polymerized in a controlled fashion using primary amine initiators has been further expanded to include Et-NTA and Bu-NTA.[7,8] Degrees of polymerization (DPs) larger than 150 were obtained for PNBGs and high DP up to 287 and 262 were reached for poly(*N*-ethyl glycine) and polysarcosine respectively.

6.2. Ring-opening Polymerization of R-NCAs or R-NTAs by the Normal Amine Mechanism (NAM).

Commonly referred to as the normal amine mechanism (NAM), this process takes advantage of the electrophilic character of NCAs. In this mechanism, organic molecules with sufficient nucleophilicity (i.e., water, alcohol, primary amine, secondary amines, thiols) act as initiators to initiate the polymerization of the R-NCA monomer in a regioselective manner by ring-opening addition to the C5 carbonyl followed by decarboxylation to generate the initiating species bearing a primary amino terminus, from which enchainment ensues by the same sequence of events. The regioselectivity for the nucleophilic addition of amine to C5 over C2 carbonyl is enhanced for R-NCAs bearing electron donating N-substituents relative to NCAs bearing the N-H, further reducing the probability of termination by this pathway relative to propagation. Secondary amines tend to be less nucleophilic than the primary amines which in turn warrants faster initiation relative to propagation, a critical criterion for living polymerization. Due to the reduced electrophilicity of the C5 carbonyl in R-NTA relative to R-NCA and more stable thiocarbamic acid propagating intermediates, nucleophilic addition of amines to R-NTAs and decarboxylation relative to those of R-NCAs precedes much slower. To date, several N-substituted glycine-derived N-

126

thiocarboxyanhydrides (i.e., Me-NTA, Et-NTA and Bu-NTA have only been investigated as substrates for polymerization using primary amine initiators.

6.3. Ring-opening Polymerization by the Activated Monomer Mechanism (AMM).

In addition to polymerization by the NAM pathway, NCAs can also undergo ROP via a different mechanism commonly known as the activated monomer mechanism (AMM) (Scheme 6.1). Initially in this process the deprotonation of NCAs by an organic base, typically primary or secondary amines, produces the anionic substrate **1**, *a.k.a.*, the activated monomer. Once "activated" the negatively charged monomer reacts with another NCA at the C5 carbonyl position by nucleophilic ring-opening addition followed by decarboxylation to form the acylated NCA initiating species **3** (Scheme 6.1).[12,13] Subsequent chain propagation involves further addition of NCA anions to the acylated NCA species **4**. Faster propagation relative to initiation takes place as a result of the increased electrophilicity of **4** compared with NCAs and facile decarboxylation from more electrophilic carboxyamide intermediate **5** in contrast to **2**. Unlike with the NAM pathway, only NCA monomers bearing the *N*-H proton can participate in ring-opening polymerization by AMM. In general, amines with enhanced basicity and reduced nucleophilicity (i.e., sterically hindered secondary or tertiary amines) tend to favor the AMM for the polymerization of NCAs bearing the N-H proton.
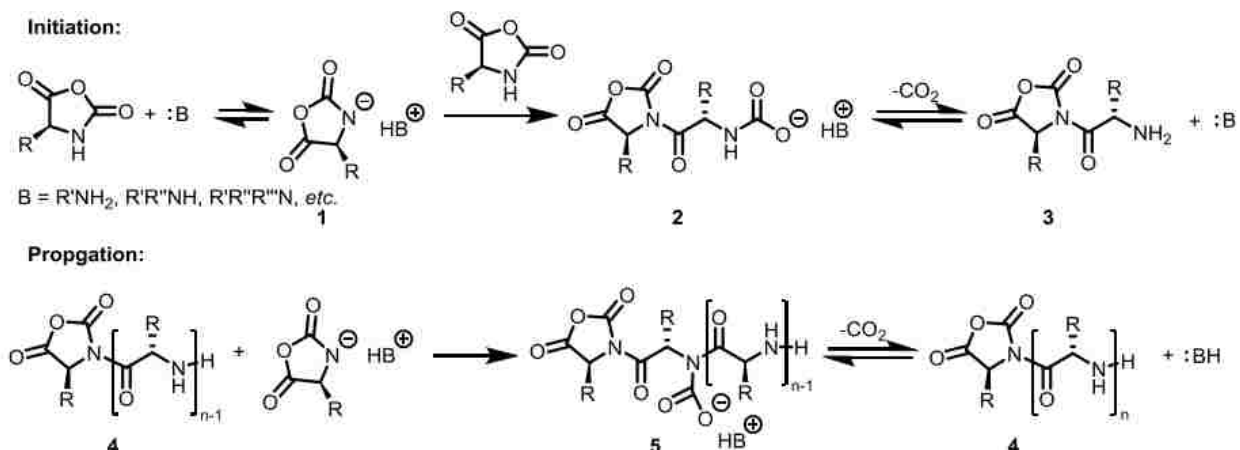
Scheme 6.1 Activated monomer mechanism (AMM) for the ROP of *N*-H bearing NCAs.

Given their labor-intensive synthesis and susceptible nature to spontaneous polymerization, motivation for developing NTAs as alternatives to NCA monomers continues to receive attention from the scientific community. Mechanistically, the polymerization of NTAs should parallel those of NCAs except that carbonyl sulfide gas is lost versus that of carbon dioxide as mentioned in sections 2.3.2 (Scheme 2.3) and 6.2. Research endeavors towards the ROP of Me-NTA have been explored previously by members of our group. Several initiators including benzyl amine, an obvious choice due to known instances that polypeptoids with predictable molecular weights can be obtained from primary amine mediated ROP of R-NCAs via the normal amine mechanism, and 1,1,3,3-tetramethylguanidine (TMG), which have been previously demonstrated to participate in the ROP of R-NCAs were screened. Of the specified initiators investigated it was found that TMG performed the best in the ROP of Me-NTA.[14] From these studies polymerization reactions were observed to reach quantitative conversion in 18 h, nearly threefold faster than previous reports (48 h). Furthermore, polymerization reactions were carried out at ambient temperature versus 60 °C in

128

previous reports. From molecular weight characterization data, it was found that molecular weights increased with increasing monomer to initiator loadings, suggesting that the ROP of Me-NTA exhibits living character.[14] Polysarcosines with relatively narrow PDIs (1.04-1.11) were also obtained.

The success of Me-NTA as a substrate for ROP scientifically has created confidence that other NCA monomers which suffer from poor shelf-life (i.e. Allyl-NCA and Ethyl-NCA) due to sensitivity to moisture and heat can be alternatively derived. Like polysarcosine, polypeptoids produced from these two monomers can be used as potential biomaterials due to their water solubility. My study on *N*-allyl NCAs has shown that this monomer, existing as an oil at room temperature, is highly susceptible to spontaneous polymerization. In view of the enhanced stability of NTA analogs, I set out to investigate the synthesis, characterization, and polymerization of *N*-allyl *N*-thiocarboxyanhydride (Al-NTA) which will be discussed for the rest of the chapter. As stated in chapter 2, the presence of an alkene group allows for introduction of new functionalities to poly(N-allyl glycine) via thiol-ene chemistry, making it a desirable platform to further diversify the polypeptoid structures towards various new technical and biomedical applications.

6.4. Materials and Methods

6.4.1 General Considerations

All chemicals were purchased from Sigma-Aldrich and used as received unless specified. All solvents are regular ACS grade solvents and used directly in the reactions without any special purification step unless specified. ^{1}H and ^{13}C{H} NMR spectra were recorded on a Bruker AV-400 or AV-500 spectrometer. Chemical shifts in ppm were

referenced relative to proton impurities or ^{13}C isotope of deuterated solvents (e.g., CDCl$_3$, CD$_3$CN, THF-d$_8$). SEC-DRI analyses were performed with an Agilent 1200 system equipped with three Phenomenex 5 µm, 300 × 7.8 mm columns [100 Å, 1000 Å and Linear(2)], Wyatt DAWN EOS MALS detector (GaAs 30 mW laser at λ=690 nm) and Wyatt Optilab rEX DRI detector with a 690 nm light source. DMF containing 0.1 M LiBr was used as the eluent at a flow rate of 0.5 mL·min^{-1}. The temperature of the column and detector was 25 °C.

6.4.2 Synthesis of S-Ethoxythiocarbonyl Mercaptoacetic Acid (XAA).

The synthesis route is modified from a published procedure.[15] NaOH (9.31 g, 23.3 mmol) was first dissolved in DI water (233 mL), followed by addition of chloroacetic acid (22.02 g, 23.30 mmol) to afford a homogeneous solution. Potassium ethyl xanthogenate (37.36 g, 23.31 mmol) was then added to the above solution. The mixture was stirred at room temperature overnight, followed by acidification with concentrated HCl to pH ~ 2-3. Next, the resulting cloudy mixture was then extracted with chloroform (3 × 150 mL). The combined organic extract was dried over MgSO$_4$ and concentrated under vacuum. Excess hexanes (500 mL) was then added to the oily residue with vigorous stirring to produce an off-white solid, which was collected by filtration and washed with additional hexanes and dried under vacuum to afford the final product in 91% yield (Appendix Figure C.1).

6.4.3. Synthesis of Allyl *N*-thiocarboxyanhydrosulfide (*N*-Al NTA).

For the following synthesis, the *N*-Allyl glycine hydrochloride used was prepared using the procedure reported for monomer synthesis in chapter 2 (Scheme 2.1). *N*-Allyl glycine hydrochloride (12.5 g, 82.7 mmol), S-ethoxythiocarbonyl mercaptoacetic acid

(14.9 g, 82.7 mmol) and NaOH (6.83 g, 6.83 mmol) were dissolved in 400 mL water and reacted for 24 h at 25 °C. Next the reaction mixture was acidified to a pH of 2 using concentrated hydrochloric acid. The product N-ethoxythiocarbonyl-N-allylglycine (N-Al-XAA) was then extracted several times with ethyl acetate (5 x 100 mL). The organic phase was washed with aqueous citric acid (5 wt %) before concentrating under reduced pressure and drying over $MgSO_4$. The final product was directly used for cyclization without further purification (Appendix Figure C.2).

To a round bottom flask N-Al-XAA (7.70 g, 37.9 mmol) was dissolved in chloroform (300 mL) and cooled in an ice bath (Scheme 6.1). PCl_3 (4.96 mL, 56.8 mmol) was added dropwise in 15 min at 0 °C. The reaction mixture was stirred for additional 10 min at 0 °C before warming to room temperature for the duration of the reaction. After 4 h the reaction was washed by saturated solution of $NaHCO_3$ (3 x 150 mL) and deionized water, the chloroform solution was dried with $MgSO_4$ and concentrated in vacuum. The crude product was purified by flash column chromatography with ethyl acetate and petroleum ether (1:3) to give the final product as a slightly viscous yellow oil in 64.8% yield. HRMS-ESI (m/z): [M + H]+ calculated for $C_6H_7NO_2S$ 158.0281, found 158.0281. ^1H NMR (400 MHz, $CDCl_3$) δ (ppm): 5.81-5.76 (m, 1H, CH_2=CHCH$_2$N-), 5.34-5.27 (m, 2H, CH_2=CHCH$_2$N-), 4.16-4.13 (d, 4H, CH_2=CHCH$_2$N-, -NCH_2CO-). ^{13}C NMR (400 MHz, $CDCl_3$) δ (ppm): 193.78, 164.48, 130.60, 120.03, 59.36, 46.45.

6.4.4. Ring-opening Polymerization of N-Allyl N-Thiocarboxyanhydride using Benzylamine Initiator

A representative polymerization of Allyl NTA monomer was conducted as follows (Scheme 6.2). Inside the glovebox, Allyl NTA (24.8 mg, 0.158 mmol) was dissolved in anhydrous THF (0.284 mL) under nitrogen atmosphere. Predetermined volume of a

stock solution of benzylamine initiator in THF (31.6 µL, 6 µmol, 250 mM) was added to the above solution. The mixture was a clear, homogenous solution. The polymerization was stirred at 60 °C for 48 h. Monomer conversion was tracked by ^{1}H NMR via sampling a reaction aliquot. Isolation of polymers was achieved by precipitation with excess diethyl ether, followed by centrifugation and decanting. Final polymer was vacuum dried for a white solid (10.2 mg, yield: 67%). Characterization of polymer composition and molecular weight was carried out by ^{1}H NMR spectroscopy, SEC, and MALDI-TOF MS.

6.5. Results and Discussion

6.5.1 *N*-Allyl *N*-Thiocarboxyanhydride Monomer

The allyl NTA monomer (Figures 6.1, 6.2, and Appendix Figure C.3) was synthesized by adapting published procedures[2,7,8] and purified by column chromatography in air. Prior to polymerization further purification of the NTA monomer using a DCM solution containing CaH_2 was performed in order to rid any potential residual HCl or other protic species produced during cyclization. It is worth mentioning that the CaH_2 treatment is highly necessary for the complete purification of the final monomer for polymerization purposes. I have found that spectroscopically clean Al-NTA monomers obtained by column chromatography without CaH_2 treatment can result in unsuccessful polymerizations.
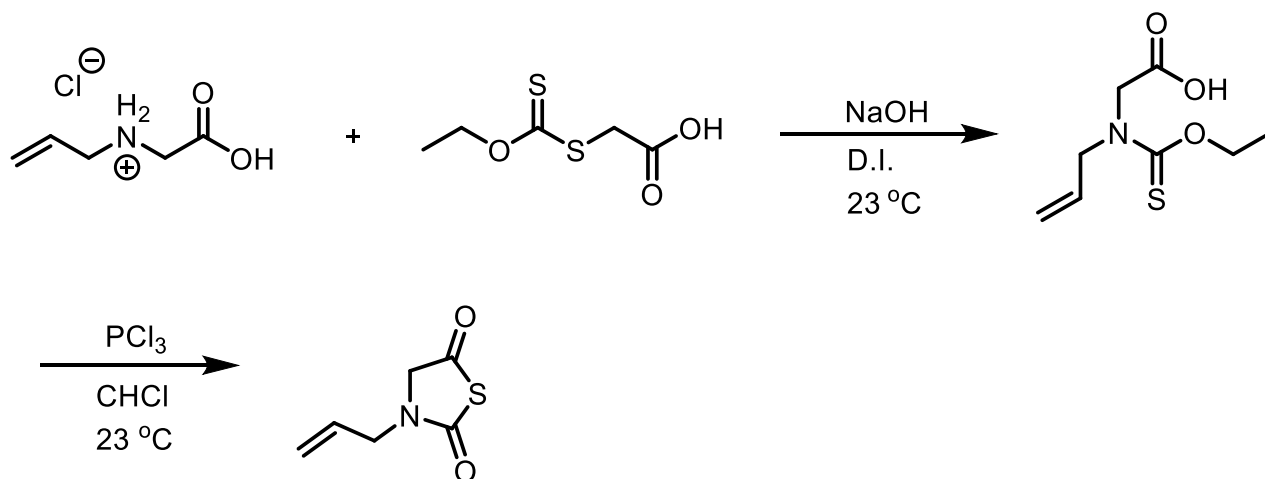
Scheme 6.1. Synthesis of N-Allyl NTA monomer.
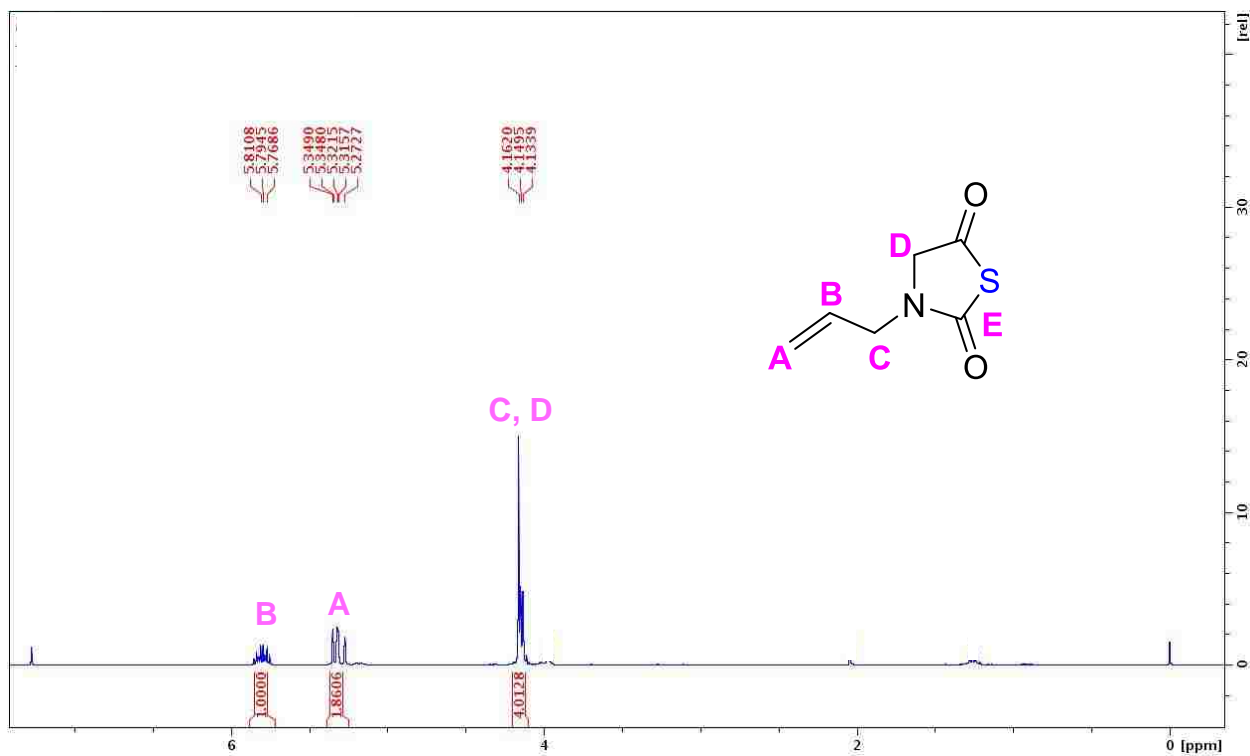
Figure 6.2. ^{1}H NMR spectrum of *N*-Allyl NTA in CDCl$_3$.
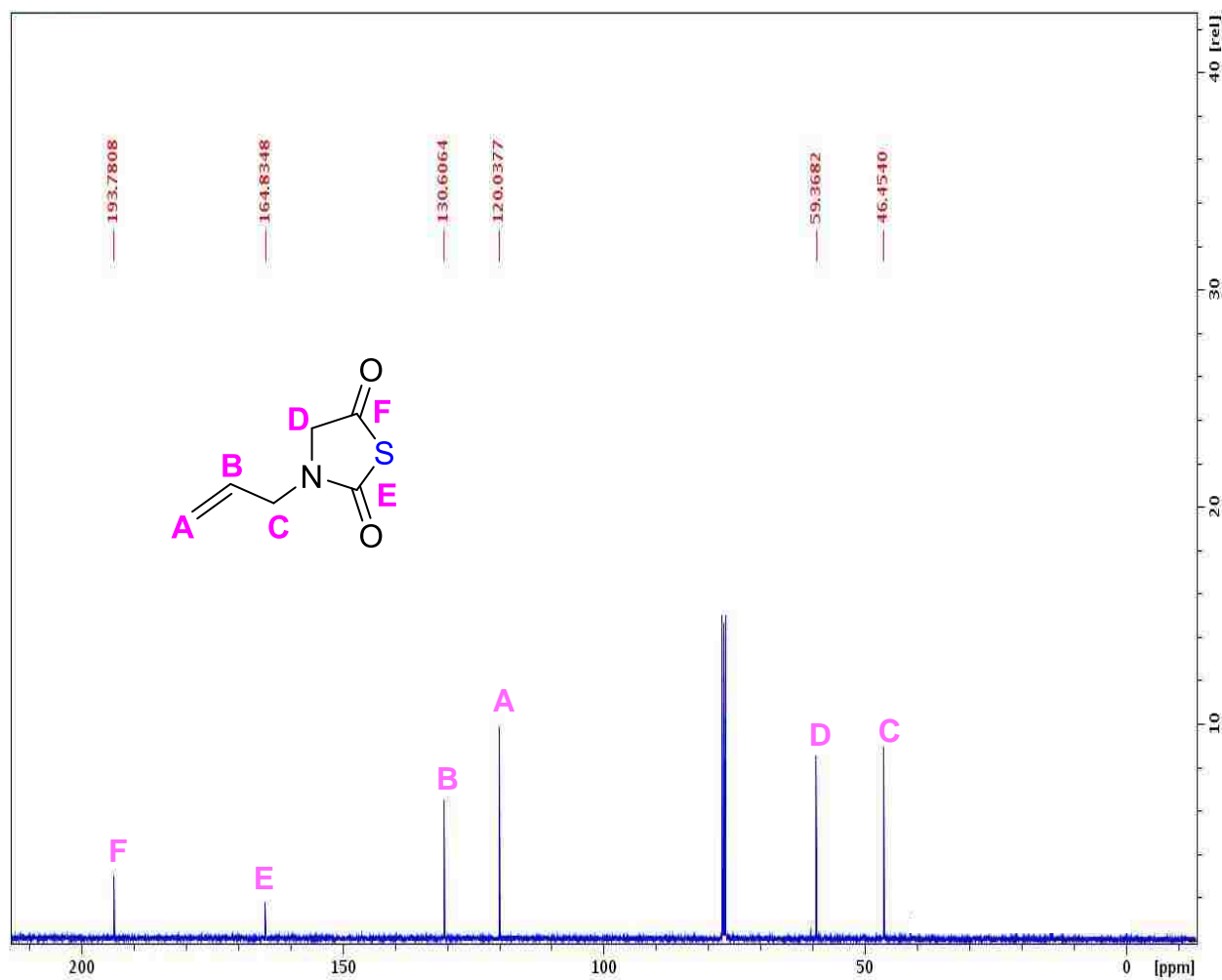
Figure 6.3. ^{13}C {H} NMR spectrum of *N*-Allyl NTA in CDCl$_3$.

 N-thiocarboxyanhydrides are well-known for their enhanced stability and shelf life under both ambient and inert atmospheres (e.g. nitrogen, argon) in contrast to NCAs.[7] Compared with Al-NCA (Appendix Figure C.4), Al-NTA in its neat state is notably more stable in air up to a week before any obvious monomer conversion is noted by FT-IR spectroscopic analysis as shown in figure 6.4. The Al-NTA monomer has a characteristic carbonyl C=O stretching band at 1795 cm^{-1} (Figure 6.4) allowing for the conversion of the monomer to be readily monitored. In solution state (e.g., THF), Al-NTA also exhibits enhanced stability towards air relative to the NCA analog (Appendix

Figure C.5). After 1 week of air exposure conversion of the monomer was observed, as evidenced by the emergence of carbonyl stretching band at 1654-1697 cm^{-1} range (Figure 6.5).
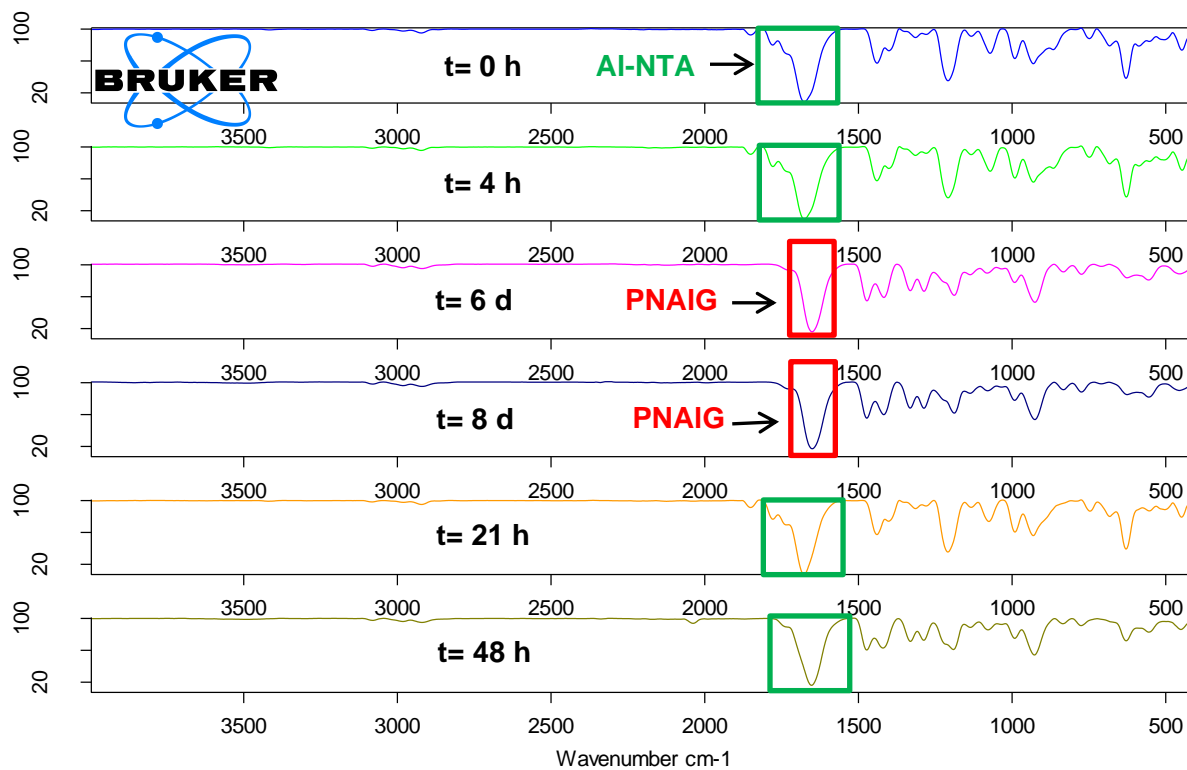
Figure 6.4. FT-IR of *N*-Ally NTA monomer conversion (neat).
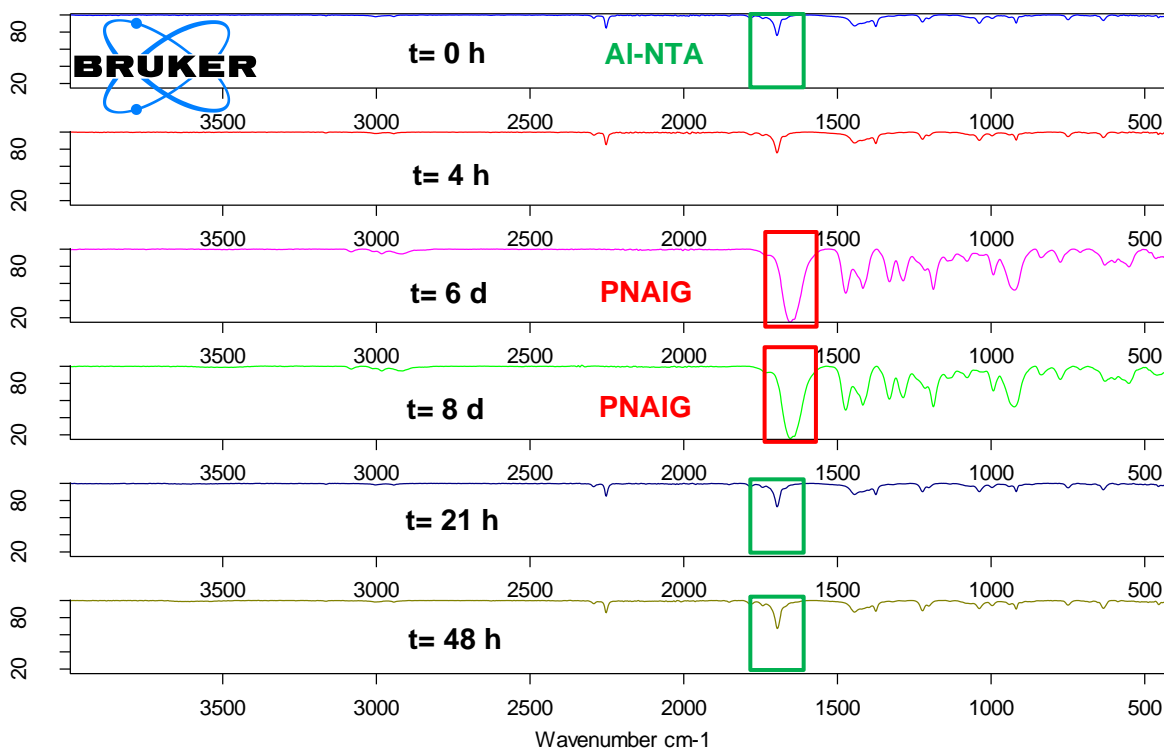
Figure 6.5. FT-IR spectra of *N*-Ally NTA monomer conversion in solution (THF at .5M).

6.5.2. ROP of Allyl NTA with Organo-base Initiators.

Previously, several organo-bases including N-heterocyclic carbene (NHC), 1,8 diazabicycloundec-7-ene (DBU), and 1,1,3,3-tetramethylguanidine (TMG) have been investigated by our group for the ROP of N-substituted NCAs.[16-19] These initiators can either initiate the zwitterionic ROP of N-substituted NCA in a controlled manner or serve as activators for the alcohol based initiators via hydrogen bonding to mediate the ROP.[17] Because of these previous findings I am encouraged to explore the effect of organo-bases in the ROP of NTAs.
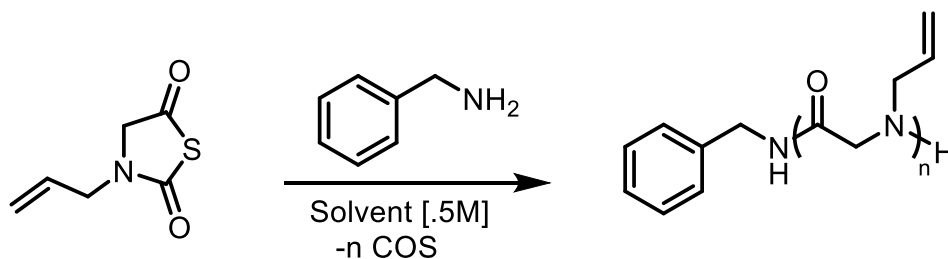
Scheme 6.2. Representative benzylamine mediated ROP of *N*-Allyl *N*-Thiocarboxyanhydride monomer.

Initially benzylamine was examined as an initiator for the ring-opening polymerization of NTA monomers (Scheme 6.2). It was found that benzylamine can effectively initiate the polymerization of Al-NTA to produce poly(N-ally glycine) (PNAIG) polymers in THF solvent at 60 °C. Under this standard condition various initial monomer to initiator ratios ($[M]_0:[I]_0$= 25:1-300:1) were investigated in an effort to examine the molecular weight control in the ROP of *N*-allyl NTA (Table 6.1). All reactions required 48 h to reach quantitative conversions, which are slower compared to ROP of the Al-NCA analogs using primary initiators (Table 6.2 and Figure 6.6 B). MALDI-TOF MS analysis of resulting low molecular PNAIG polymers from Al-NTA confirms that the polymerization with benzylamine proceeds by the normal amine mechanism producing polypeptoids bearing one benzylamide and one secondary amine chain end (Figure 6.8). In comparison to NCAs, the C5 carbonyl in the NTA monomer is less electrophilic due to the reduced electronegativity of the sulfur atom, rendering it less reactive towards nucleophilic addition. Furthermore, elimination of COS from the thiocarbamate propagating intermediate is also slower than the carbamate species in the polymerization of NCA analogs. SEC analysis of the resulting polymers (Figure 6.6 A) exhibited either broad or multimodal distribution with Mn in the 4.2-12.5 kg/mol range and PDIs in the 1.21-1.61 range (Table 6.1). While the polymer molecular weight (M_n)

was found to increase with increasing $[M]_0:[I]_0$ ratio for PNAIGs obtained from Al-NTA (Appendix Figure C.6), the absolute value of M_ns has varying level of deviation from the theoretical prediction based on a living polymerization. This MW outcome is dissimilar to those obtained for polymers from Al-NCA (Appendix Figure C.7). Compared with M_ns for PNAIGs obtained from SEC values determined by ^{1}H NMR were in disagreement, being significantly lower as shown in Table 6.1. The sensitivity of NMR spectroscopy proves highly useful in the structural elucidation of PNAIGs but is limited in terms of determining accurate molecular weight dispersity (MWD). This is accredited to linewidths increase as a consequence of larger molecules present which due to stronger spin-spin relaxation, puts a maximum on the size obtainable by the particular method. As a direct result, when molecules are too large the peaks overlap or become so broad they become undetectable. SEC tends to provide more reliable information about the true molecular weight dispersity (MWD), making it possible to evaluate the level of control of ROP of NCA and NTA.

Table 6.1. Benzylamine initiated ring-opening polymerization of Al-NTA in THF.

$[M]_0:[I]_0$	Time (h)	Mn (theor.) (kg/mol^{-1})	Mn (kg/mol^{-1}) [a]	Mn (kg/mol^{-1}) [b]	PDI [b]	Conv. % [c]	Percent yield
25:1-THF	48	2.5	2.3	4.1	1.21	100%	52.6%
50:1-THF	48	4.9	4.0	6.8	1.21	100%	100%
150:1-THF	48	14.7	8.9	10.8	1.38	64%	50%
300:1-THF	48	29.2	12.9	12.5	1.61	38%	43.5%

(Table cont'd)

[M]$_o$:[I]$_o$	Time (h)	Mn (theor.) (kg/mol^{-1})	Mn (kg/mol^{-1}) [a]	Mn (kg/mol^{-1}) [b]	PDI [b]	Conv. % [c]	Percent yield
25:1-THF	48	2.5	2.3	3.8	1.26	100%	83.4%
50:1-THF	48	4.9	3.8	6.6	1.30	100%	65.8%
150:1-THF	48	14.7	8.2	9.6	1.41	58%	42%
300:1-THF	48	29.2	12.0	11.8	1.53	27%	35.7%

[a]. Experimental chain length determined by integration of the terminal alkene peak relative to the benzyl peaks in their respective ^{1}H NMR spectra in CD$_3$CN. [b]. Experimental molecular weight and polydispersity indices were obtained from SEC-MALS-DRI system in 0.1 M LiBr/DMF solution using dn/dc of 0.0950 g/mol^{-1}. [c]. Obtained via ^{1}H NMR. All Polymerizations were done in THF at [.5M] at 60°C.
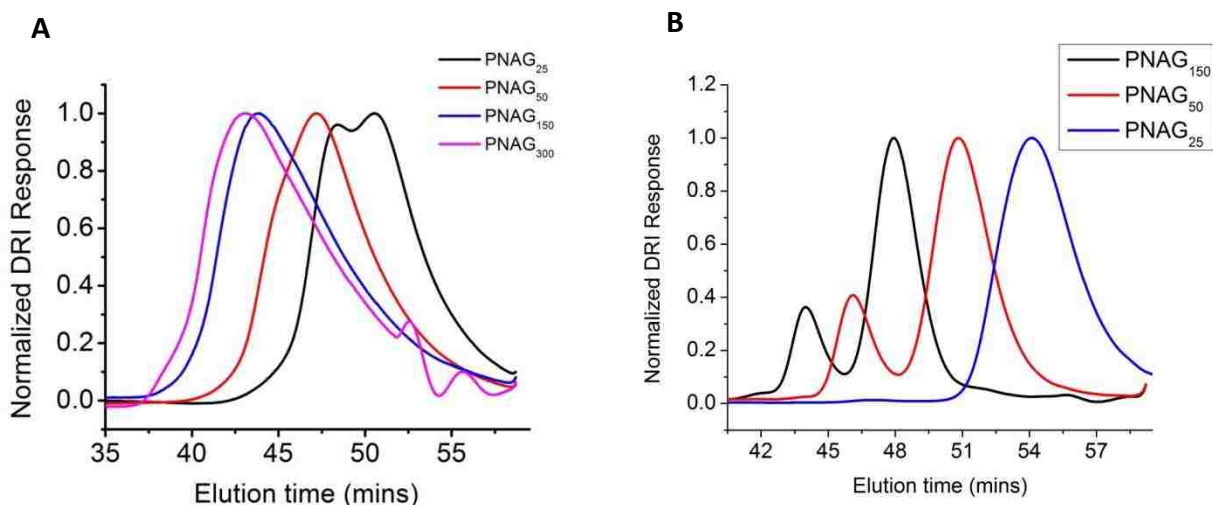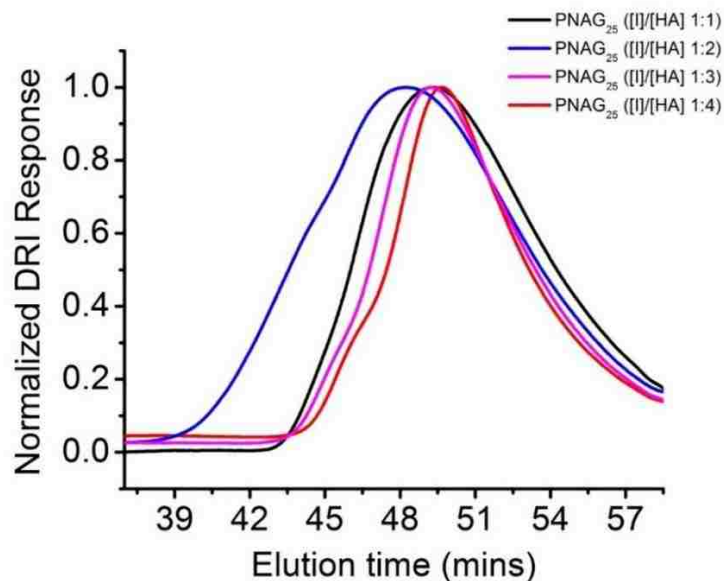

Figure 6.6. A) SEC chromatograms of PNAIGs obtained by benzylamine mediated ROP of Al-NTA under standard conditions (60 °C). B) SEC chromatograms of PNAIGs obtained by benzylamine mediated ROP of Al-NCA under standard conditions (50 °C).
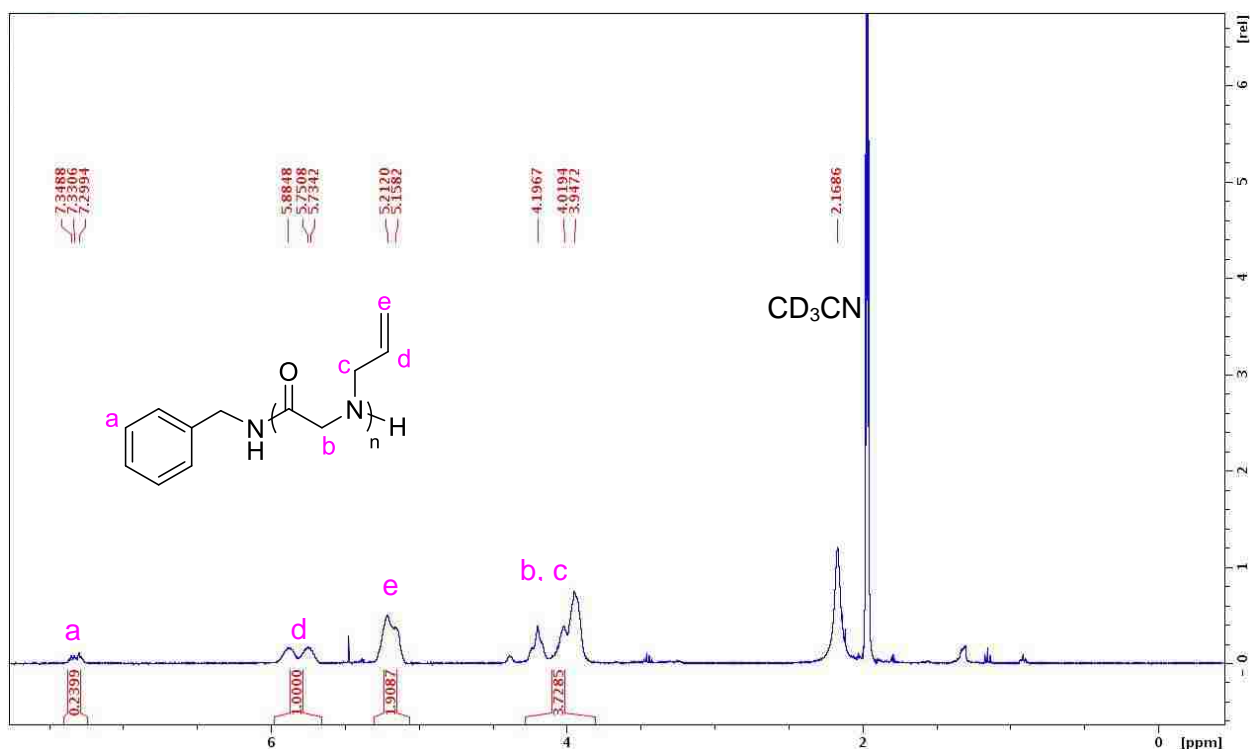
Figure 6.7. ^{1}H NMR spectrum of BnPNAlG in CDCN$_3$.

Table 6.2. Molecular weight parameters for BnNH$_2$ mediated ring-opening polymerization of Al-NCA at 50 ^{o}C in THF.

[M]$_o$:[I]$_o$	Time (h)	Mn (theor.) (kg/mol^{-1})	Mn (kg/mol^{-1}) [a]	Mn (kg/mol^{-1}) [b]	PDI [b]	Conv. % [c]	Percent yield
25:1-THF	18	2.5	1.7	1.5	1.09	100%	85.6%
50:1-THF	24	4.9	3.9	4.5	1.29	100%	100%
150:1-THF	24	14.7	12.5	7.7	1.18	100%	50%
300:1-THF	--	29.2	--	--	--	--	--

[a.] Experimental chain length determined by integration of the terminal alkene peak relative to the benzyl peaks in their respective ^{1}H NMR spectra in CD$_3$CN. [b.] Experimental molecular weight and polydispersity indices were obtained from SEC-MALS-DRI system in 0.1 M LiBr/DMF solution using dn/dc of 0.0950 g/mol^{-1}. [c.] Obtained via FTIR. All Polymerizations were done in THF at [.5M] at 50°C.
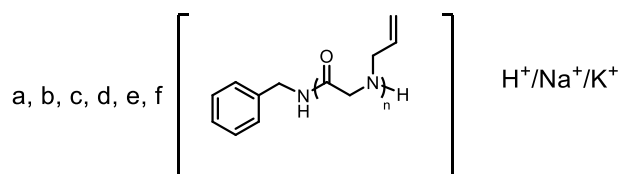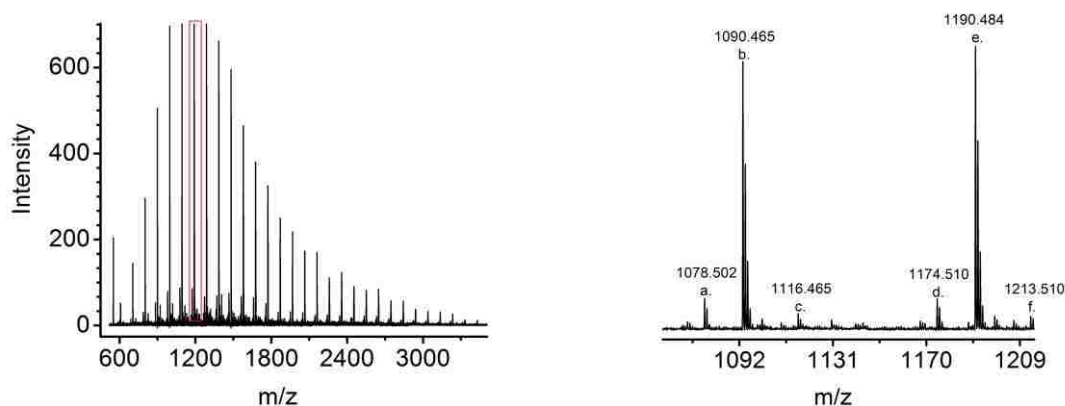
Figure 6.8. MALDI-TOF MS spectra of PNAlGs obtained by benzylamine mediated ROP under standard conditions.

6.5.3. ROP of Allyl NTA with BnNH$_2$/CH$_3$COOH.

Recently, my group member demonstrated that the presence of weak acid such as benzoic acid or acetic acid can improve the conversion during the ROP of amino-acid derived NTAs bearing N-H protons using benzylamine initiators. In addition, it was also shown that polymerization afforded higher conversions when conducted with the concurrent removal of COS under reduced pressure throughout the reaction. The hypothesis is that the hydrogen bonding interaction between the weak acid and thiocarbamate may accelerate the COS elimination relative to H$_2$S elimination (which results in termination), thus improving the polymerization conversion. In addition, COS elimination could be the rate-limiting step in the polymerization of NTAs using primary amine initiators. Inspired by this empirical finding, I set to investigate the effect of acetic

141

acid on the polymerization of Al-NTA. While in the ROP of Al-NTA using primary amine initiators, H_2S elimination is not possible. However, the COS elimination is required for the polymerization to proceed in a normal amine mechanism. It is entirely plausible that the presence of hydrogen bond donor can accelerate the COS release.

I found that introducing acetic acid as a co-catalyst in 2-4 equivalents relative to $BnNH_2$ initiator in the ROP of Al-NTA ($[M]_0$:$[I]_0$= 25:1) significantly reduced the reaction time required for full conversion from 48 h to less than 24 h (Table 6.3). Moderate to quantitative conversions can also be obtained at room temperature with increasing acetic acid loadings (Table 6.4). On contrary this trend is not observed for higher $[M]_0$:$[I]_0$ ratios. Using standard conditions, at the $[M]_0$: $[I]_0$ ratio of 50:1 the acid co-catalyzed (4 eq.) ROP of Al-NTA resulted in ~ 37% monomer conversion after 24 h (Table 6.5). No monomer conversion was detected in the case of higher $[M]_0$:$[I]_0$ ratios. In recollection of possible reasonings mentioned in the discussion pertaining to NAM, I believe this incidence is attributed to the fast acid consumption that would occur in the first circumstance. Under both standard and non-standard conditions, I detected that the load amount of acetic acid influenced the polymerization Al-NTA. By using acid additive the MW and polydispersity of PNAIGs analogues were closer to targeted M_ns with narrower distribution upon increased loadings (Tables 6.3 & 6.4).

Table 6.3. Molecular weight parameters for $BnNH_2/CH_3COOH$ mediated ring-opening polymerization of Al-NTA at 60 °C in THF.

$[M]_o:[I]_o:[HA]_o$	Time (h)	Mn (theor.) (kg/mol^{-1})	Mn (kg/mol^{-1}) [a]	Mn (kg/mol^{-1}) [b]	PDI [b]	Conv. % [c]
25:1:1	22	2.5	1.7	4.4	1.45	76.5%
25:1:2	22	2.5	1.9	5.4	1.62	100%
25:1:3	22	2.5	1.9	3.7	1.22	100%
25:1:4	22	2.5	1.9	3.8	1.18	100%
25:1:1	22	2.5	2.0	3.5	1.25	82%
25:1:2	22	2.5	1.9	3.8	1.14	100%
25:1:3	22	2.5	1.8	3.2	1.17	100%
25:1:4	22	2.5	2.0	3.7	1.17	100%

[a.] Experimental chain length determined by integration of the terminal alkene peak relative to the benzyl peaks in their respective ^1H NMR spectra in CD_3CN. [b.] Experimental molecular weight and polydispersity indices were obtained from SEC-MALS-DRI system in 0.1 M LiBr/DMF solution using dn/dc of 0.0950 g/mol^{-1}. [c.] Obtained via ^1H NMR. All Polymerizations were done in THF at [.5M].

Figure 6.9. SEC chromatograms of PNAIGs obtained by BnNH$_2$/CH$_3$COOH mediated ROP under standard conditions (60 ^{o}C).

Table 6.4. BnNH$_2$/CH$_3$COOH- mediated ring-opening polymerization of Al-NTA at 23 ^{o}C in THF.

[M]$_o$:[I]$_o$:[HA]$_o$	Time (h)	Mn (theor.) (kg/mol^{-1})	Mn (kg/mol^{-1}) [a]	Mn (kg/mol^{-1}) [b]	PDI [b]	Conv. % [c]
25:1:1	24	2.5	1.6	3.5	1.19	60%
25:1:2	24	2.5	2.2	3.2	1.24	77%
25:1:3	24	2.5	1.9	2.9	1.21	84%
25:1:4	24	2.5	2.2	3.8	1.10	88%
25:1:5	24	2.5	2.3	3.5	1.21	81%
25:1:6	24	2.5	2.0	4.1	1.12	100%

(Table cont'd)

[M]$_o$:[I]$_o$:[HA]$_o$	Time (h)	Mn (theor.) (kg/mol^{-1})	Mn (kg/mol^{-1}) [a]	Mn (kg/mol^{-1}) [b]	PDI [b]	Conv. % [c]
25:1:1	24	2.5	2.1	4.5	1.21	89%
25:1:2	24	2.5	2.2	4.2	1.07	91%
25:1:3	24	2.5	2.3	6.2	1.17	100%
25:1:4	24	2.5	2.2	4.1	1.09	91%
25:1:5	24	2.5	2.3	7.1	1.10	59%
25:1:6	24	2.5	2.2	3.2	1.12	100%

[a] Experimental chain length determined by integration of the terminal alkene peak relative to the benzyl peaks in their respective ^{1}H NMR spectra in THF-d$_8$. [b] Experimental molecular weight and polydispersity indices were obtained from SEC-MALS-DRI system in 0.1 M LiBr/DMF solution using dn/dc of 0.0950 g/mol^{-1}. [c] Obtained via ^{1}H NMR. All Polymerizations were done in THF at [.5M].
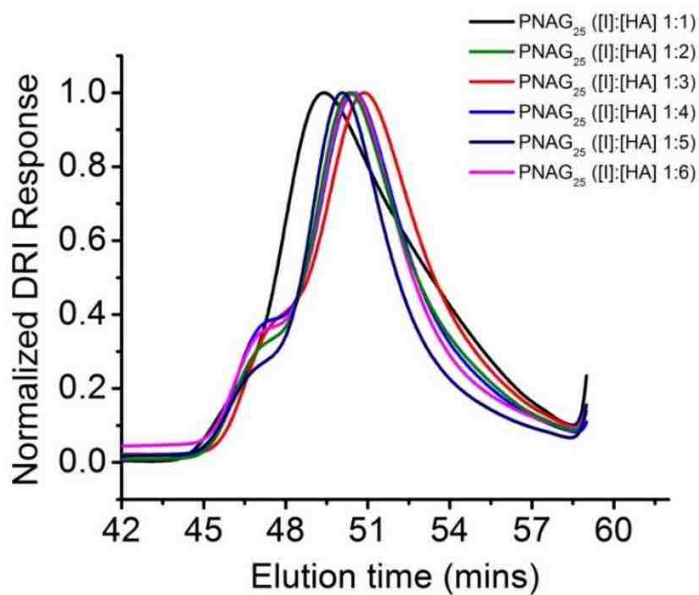
Figure 6.10. SEC chromatograms of PNAlGs obtained by BnNH$_2$/CH$_3$COOH mediated ROP at 23 °C.

Table 6.5. BnNH$_2$/CH$_3$COOH mediated ring-opening polymerization of Al-NTA at 60 °C in THF ([M]$_0$: [I]$_0$ ratios 25-300).

[M]$_0$:[I]$_0$:[HA]$_0$	Time (h)	Mn (theor.) (kg/mol^{-1})	Mn (kg/mol^{-1}) [a]	Mn (kg/mol^{-1}) [b]	PDI [b]	Conv. % [c]
25:1:4	24	2.5	1.6	3.5	1.19	100%
50:1:4	24	2.5	1.7	1.9	1.10	37%
150:1:4	24	2.5	--	--	--	--
300:1:4	24	2.5	--	--	--	--

[a]. Experimental chain length determined by integration of the terminal alkene peak relative to the benzyl peaks in their respective ^{1}H NMR spectra in THF-d$_8$. [b]. Experimental molecular weight and polydispersity indices were obtained from SEC-MALS-DRI system in 0.1 M LiBr/DMF solution using dn/dc of 0.0950 g/mol^{-1}. [c]. Obtained via ^{1}H NMR. All Polymerizations were done in THF at [.5M].

6.5.4. Interfacial ROP (iROP) of Allyl NTA with BnNH$_2$

The interfacial ring-opening polymerization of NTAs using nonpolar solvents have been previously demonstrated by members of our group. Polypeptides derived from the iROP of α-amino-acid derived *N*-thiocarboxyanhydrides (NTAs) in hexanes or heptane suspension using soluble primary amine initiators were successfully obtained under mild conditions (50-80 °C).[20] Polymers of various molecular weight and low-to-moderate molecular weight distribution could be attained with good control. Encouraged by the success of this approach in generating well-defined polypeptides with good control, I was prompted to examine the iROP of Al-NTA using benzylamine.

Benzylamine mediated iROPs of Al-NTA were performed in heptane at 23 °C and 90 °C at various M : I ratios. Compared with solution phase ROPs, iROPs of Al-NTA require significantly longer time periods (7 days), with less than 100% monomer

conversion reached in all cases for polymerizations conducted under heat (Appendix Figure C.8). After several days no monomer conversion was observed for iROPs performed at room temperature, indicating the important role of higher temperatures in driving polymerizations to completion via COS elimination. The type of solvent used also appears to have a major effect on the iROP of Al-NTA, resulting in low monomer conversion as demonstrated by my group member. One plausible explanation for this observed occurrence is the propagating chain's inability to interact with remaining monomer within the suspension due to a difference in solubilities. Another possible reason for low monomer conversion is the fast consumption of initiator. Under both circumstances the final polymer chain length would be limited as a result of loss of reactivity.

6.6. Conclusion

The synthetic route and characterization of a new NTA monomer was successfully demonstrated in this work. Al-NTA offers an air and moisture stable alternative to its NCA counterpart, hence allowing for facile preparation under ambient conditions on a multigram scale. Based on presented evidenced it is concluded that conventional ring-opening polymerization of the NTA monomer with primary amine initiators precede much slower than its NCA analogue under standard conditions. A difference in electronic properties presented by each monomer's heteroatom is primarily responsible for this observed effect.

6.7. References

1. Barz, M., Luxenhofer, R., Zentel, R., Vicent, M. J. Overcoming the PEG-addiction: well-defined alternatives to PEG, from structure–property relationships to better defined therapeutics *Polym. Chem.* **2011**, 2, 1900–1918.

2.   Zhang, D. H., Lahasky, S. H., Guo, L., Lee, C. U., Lavan, M., *Macromolecules* **2012**, 45, 5833–5841.

3.   Knight, A. S., Zhou, E. Y., Francis, M. B., Zuckermann, R. N. Sequence Programmable Peptoid Polymers for Diverse Materials Applications *Adv. Mater.* **2015**, 27, 5665–5691.

4.   Secker, C., Brosnan, S. M., Luxenhofer, R., Schlaad, H. Poly(α-Peptoid)s Revisited: Synthesis, Properties, and Use as Biomaterial *Macromol. Biosci.* **2015**, 15, 881–891.

5.   Gangloff, N., Ulbricht, J., Lorson, T., Schlaad, H., Luxenhofer, R. Peptoids and Polypeptoids at the Frontier of Supra- and Macromolecular Engineering *Chem. Rev.* **2016**, 116, 1753–1802.

6.   Kricheldorf, H. R. α-aminoacid-N-carboxy-anhydrides and related heterocycles: syntheses, properties, peptide synthesis, polymerization; Springer-Verlag: Berlin, 1987.

7.   Kricheldorf, H. R., ÜBer die Polymerisation von α-Aminosäure-N-carboxyanhydriden (1,3-Oxazolidin-2,5-dionen) und α-Aminosäure-N-thiocarboxyanhydriden (1,3-Thiazolidin-2,5-dionen). *Makromol. Chem.* **1974**, 175, 3325-3342.

8.   Kricheldorf, H. R., Bösinger, K., Mechanismus der NCA-Polymerisation, 3. Über die Amin katalysierte Polymerisation von Sarkosin-NCA und -NTA. *Makromol. Chem.* **1976**, 177, 1243-1258.

9.   Kricheldorf, H. R., Sell, M., Schwarz, G. Primary Amine-Initiated Polymerizations of α-Amino Acid N-Thiocarbonic Acid Anhydrosulfide. *J. Macromol. Sci. Pure Appl. Chem.* **2008**, 45, 425-430.

10.   Tao, X., Deng, Y., Shen, Z., and Ling, J. Controlled Polymerization of N-Substituted Glycine N-Thiocarboxyanhydrides Initiated by Rare Earth Borohydrides toward Hydrophilic and Hydrophobic Polypeptoids *Macromolecules* **2014**, 47, 6173−6180.

11.   Tao, X., Deng, C., Ling, J. PEG-Amine-Initiated Polymerization of Sarcosine *N*-thiocarboxyanhydrides Toward Novel Double-Hydrophilic PEG-*b*–Polysarcosine Diblock Copolymers *Macromol. Rapid Commun.* **2014**, 35, 875−881.

12.   Goodman, M., Hutchison, J. The Mechanisms of Polymerization of *N*-Unsubstituted N-Carboxyanhydrides. *Journal of the American Chemical Society* **1966**, 88, 3627-3630.

13. Goodman, M., Hutchison, J. Propagation Mechanism in Strong Base Initiated Polymerization of α-Amino Acid N-Carboxyanhydrides. *Journal of the American Chemical Society* **1965**, 87, 3524-3525.

14. Chan, Brandon. *Peptidomimetic Polymers: Advances in Monomer Design and Polymerization Methods.* Diss. Louisiana State University, **2013**. Web. 13 Nov. 2017.

15. H. R. Kricheldorf, M. Sell, G. Schwarz *J. Macromol. Sci. Part A-Pure Appl. Chem.* **2008**, 45, 425–430.

16. Guo, L., Zhang, D., Cyclic Poly(α-peptoid)s and Their Block Copolymers from N-Heterocyclic Carbene-Mediated Ring-Opening Polymerizations of N-Substituted N-Carboxylanhydrides. *J. Am. Chem. Soc.* **2009**, 131, 18072-18074.

17. Chan, B. A., Xuan, S., Horton, M., Zhang, D., 1,1,3,3-Tetramethylguanidine-Promoted Ring-Opening Polymerization of N-Butyl N-Carboxyanhydride Using Alcohol Initiators. *Macromolecules* **2016**, 49, 2002-2012.

18. Guo, L., Lahasky, S. H., Ghale, K., Zhang, D., N-Heterocyclic Carbene-Mediated Zwitterionic Polymerization of N-Substituted N-Carboxyanhydrides toward Poly(α-peptoid)s: Kinetic, Mechanism, and Architectural Control. J. Am. Chem. Soc. 2012, 134, 9163-9171.

19. Li, A., Lu, L., Li, X., He, L., Do, C., Garno, J. C., Zhang, D. Amidine-Mediated Zwitterionic Ring-Opening Polymerization of N-Alkyl N-Carboxyanhydride: Mechanism, Kinetics, and Architecture Elucidation. *Macromolecules* **2016**, 49, 1163-1171.

20. Cao, J., Siefker, D., Chan, B., Yu, T., Lu, L., Saputra, M., Fronczek, F., Xie, W., Zhang, D. Interfacial Ring-Opening Polymerization of Amino-Acid-Derived *N*-Thiocarboxyanhydrides Toward Well-Defined Polypeptides *ACS Macro Lett.*, **2017**, *6*, 836–840.

CHAPTER 7: SUMMARY AND FUTURE WORK

Poly(α-peptoid)s have emerged as a class of peptidomimetic polymers that are increasingly investigated in the fields of materials science and biomedical science. Development of synthetic methods to increase the structural diversity of polypeptoids is important for the further investigation of these polymers for various biomedical or biotechnological applications. My research efforts focused on diversifying polypetopid structure for different applications and developing new and facile synthetic method to access polypeptoids that can be further derivatized to install other functional groups.

In Chapter 1, the idea of gene therapy was reviewed. Subjects relevant to the practice were discussed including the associated disadvantages and disadvantages. Challenges faced by current practices of gene therapy in this chapter served as motivation for the completed work discussed in succeeding chapters.

In Chapter 2, the background and fundamentals of poly(α-peptoids) have been reviewed. Synthetic strategies used to generate oligomeric and polymeric polypeptoids were discussed. It also highlighted the challenges that should be addressed to further facilitate the development of polypeptoids. This section gave an overview of the previous progress with polypeptoid-based functional materials as well as some fundamental properties of polypeptoids.

In Chapter 3, the motivation, design and performance of cationic polypeptoids as nonviral gene delivery both *in vitro* and *in vivo* was discussed. Transfection efficacy as a correlation of various molecular parameters has been studied in order to determine optimal molecular structural motif for gene transfection. A library of linear cationic polypeptoids comprised of various chain lengths were obtained by a combination of

primary amine-initiated ring-opening polymerization of propargyl-NCA and CuAAC chemistry. Analogues bearing primary amine terminal groups were found to possess excellent gene transfection efficiency under serum free and serum containing conditions.

In Chapter 4, the capacity of cationic copolymers serve as a carrier for genetic materials has been extended to RNA delivery to treat systemic inflammation. Random copolymers containing guanidium terminal groups have been designed, synthesized and characterized. Reduction of systematic inflammation *in vitro* and *in vivo* was achieved using the cationic random copolypeptoids, further demonstrating the potential of polypeptoids in the field of gene therapy. Given the difference of location and biological processes involved in DNA (nucleus) and RNA (cytoplasm) delivery, the generality of peptidomimetics is highlighted in this work.

The studies in Chapter 3 and 4 have revealed the generally reduction of transfection efficiency of cationic polypeptoid carriers in serum-containing environment presumably due to non-specific interaction of the polyplex particles with serum components. In chapter 5, pH-responsive cationic diblock copolypeptoids bearing a non-ionic and hydrophilic segment and a cationic segment has been designed and synthesized to address this challenge. The polymer is expected to condense with genetic materials to form micellar particles, thus shielding them from the challenging environment in serum. The evaluation of pH-responsive and non-pH responsive block copolymers regarding their DNA condensation capability and cytotoxicity has pointed to potential limitations presented by these carriers for gene delivery. Critical micelle concentration experiments also reveal apprehension about the micellar character of the

diblock copolymers. Synthetic approaches that yield polypeptoids which exhibit architecture without compromising transfection efficiencies will have a scientific impact in the discipline of gene therapy.

During the course of my research, the need for polypeptoids that can be further derivatized post-polymerization to increase structural diversity has become apparent. In Chapter 6, the synthesis and characterization of a new *N*-Allyl *N*-thiocarboxyanhydride (Al-NTA) monomer has been studied. NTA monomers are of growing interest due of their enhanced stability against moisture and heat relative to their NCA analogs. While Al-NTAs can undergo ring-opening polymerization in the solution phase using primary amine initiators under relatively mild conditions, control over the molecular weight and molecular weight distribution of the resulting polypeptoids pose an issue. Building from research endeavors put forth in obtaining a well-controlled system, strategies such as use of organic solvents with lower dielectric constants and other organo base initiators toward development of controlled polymerization of Al-NTA under mild conditions to prepare well-defined polypeptoids should be considered for future studies.
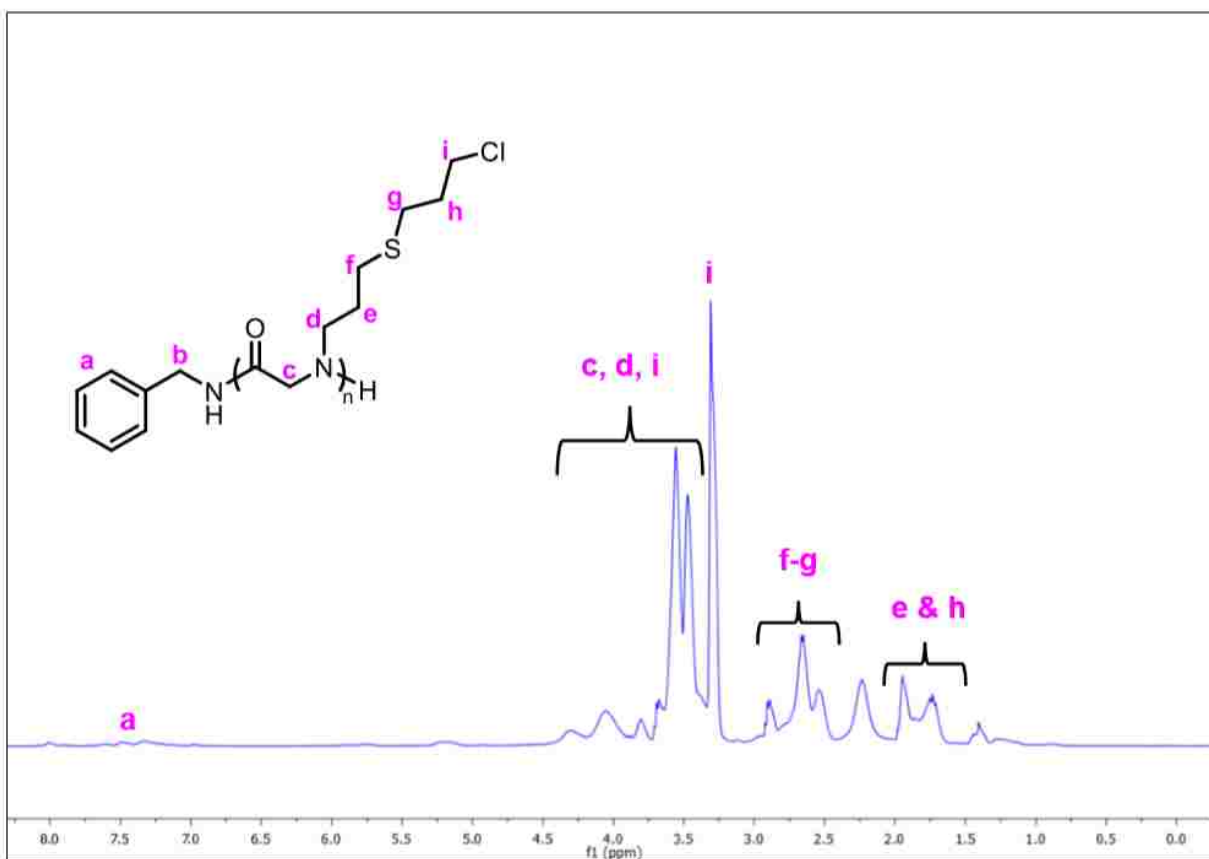
Figure A.1. Representative ^{1}H NMR spectrum of the polypeptoid polymer in CD$_3$CN obtained from grafting CPT to PNAIG polymer via radical thiol-ene chemistry.
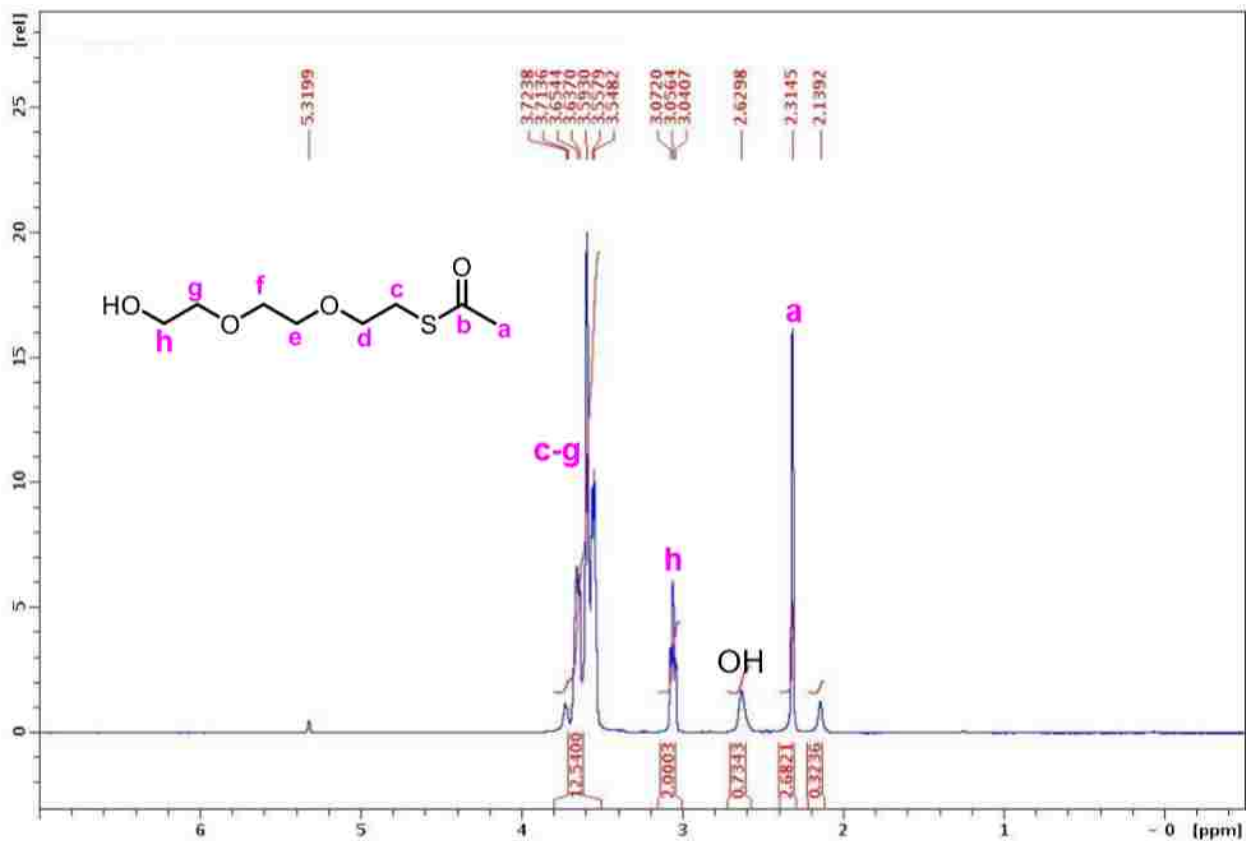
Figure A.2. ^{1}H NMR spectrum of 2-(2-(2-hydroxyethoxy)ethoxy)ethane thioacetate in CD$_2$Cl$_2$.
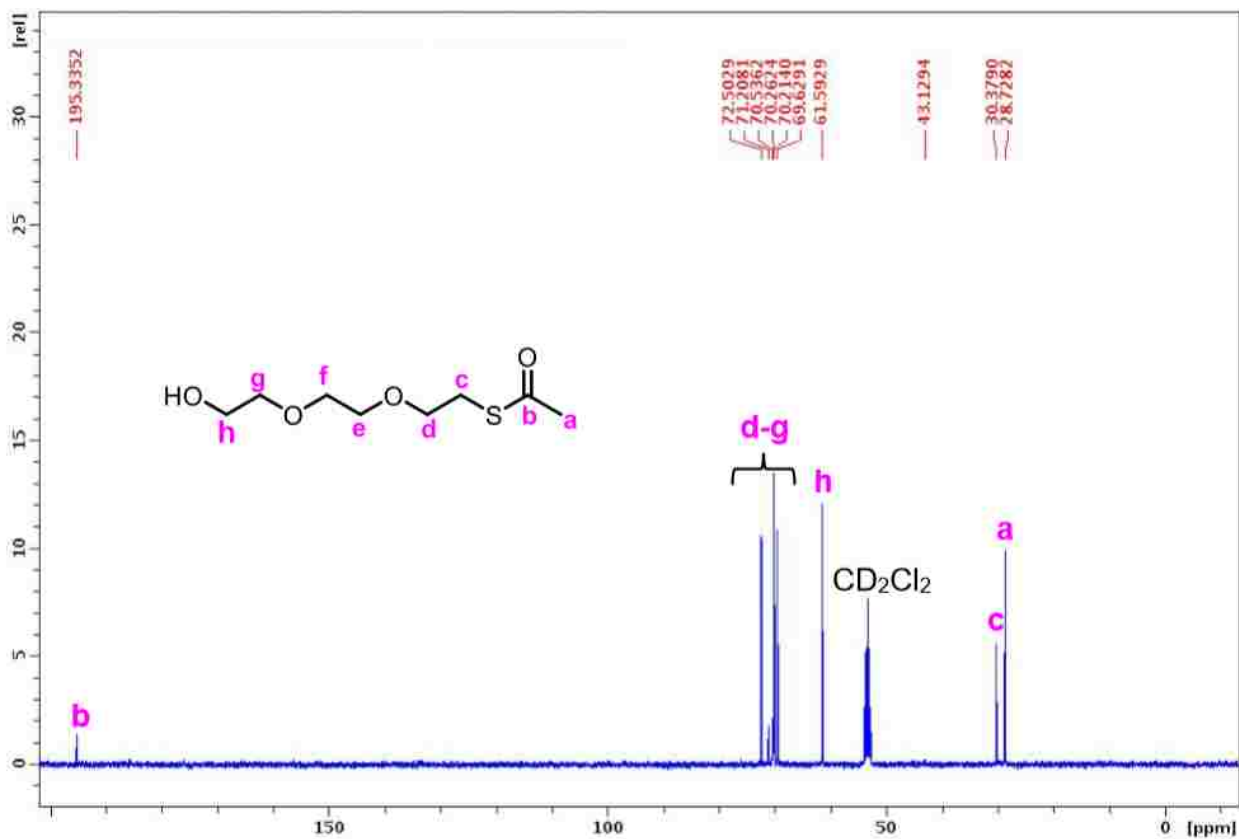
Figure A.3. ^{13}C NMR spectrum of 2-(2-(2-hydroxyethoxy)ethoxy)ethane thioacetate in CD$_2$Cl$_2$.
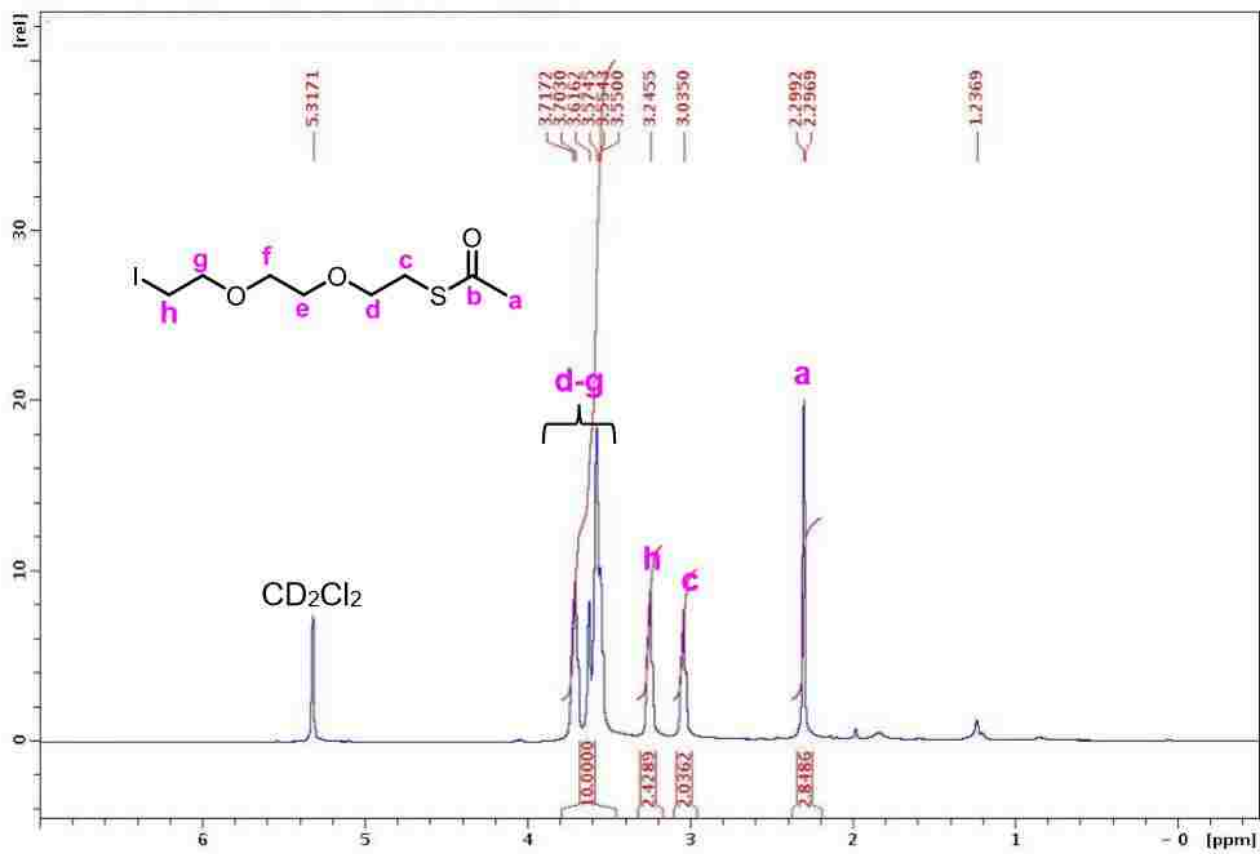
Figure A.4. ^{1}H NMR spectrum of 2-(2-(2-iodoethoxy)ethoxy)ethane thioacetate in CD$_2$Cl$_2$.
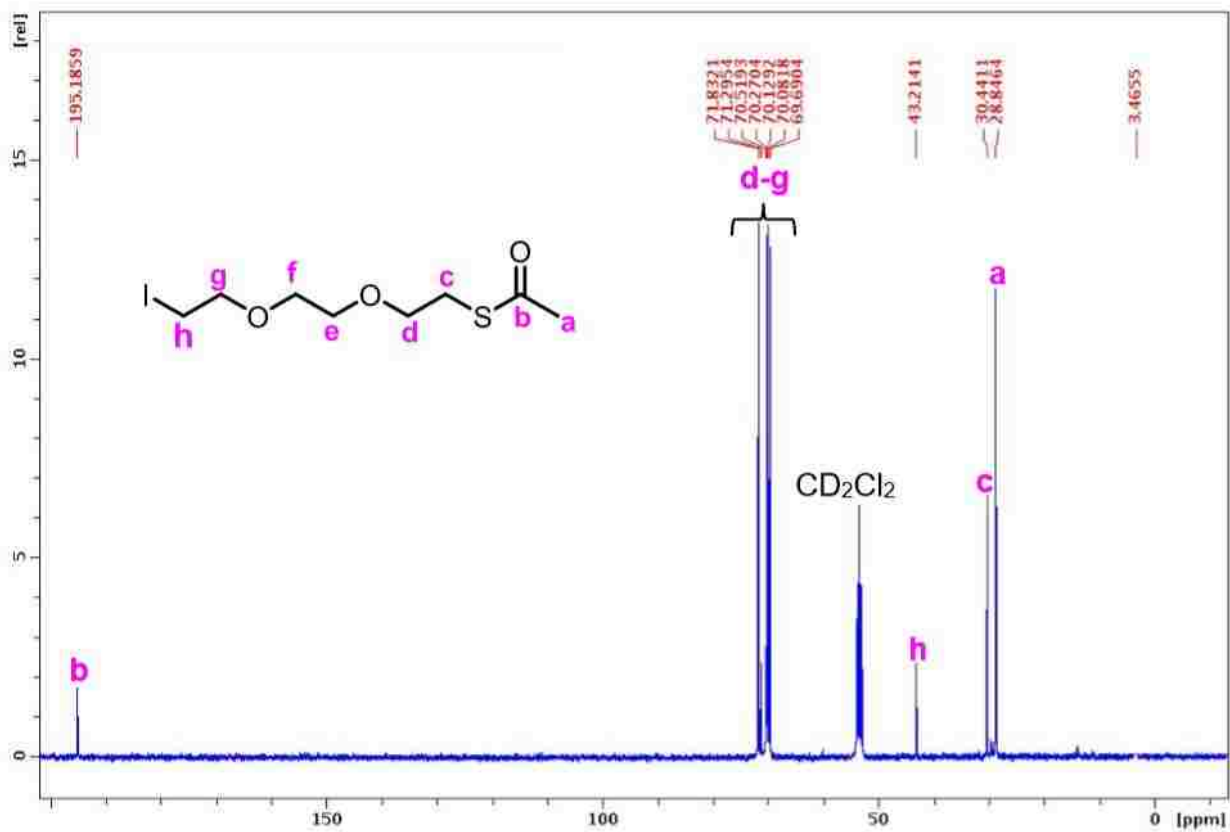
Figure A.5. ^{13}C NMR spectrum of 2-(2-(2-iodoethoxy)ethoxy)ethane thioacetate in CD$_2$Cl$_2$.
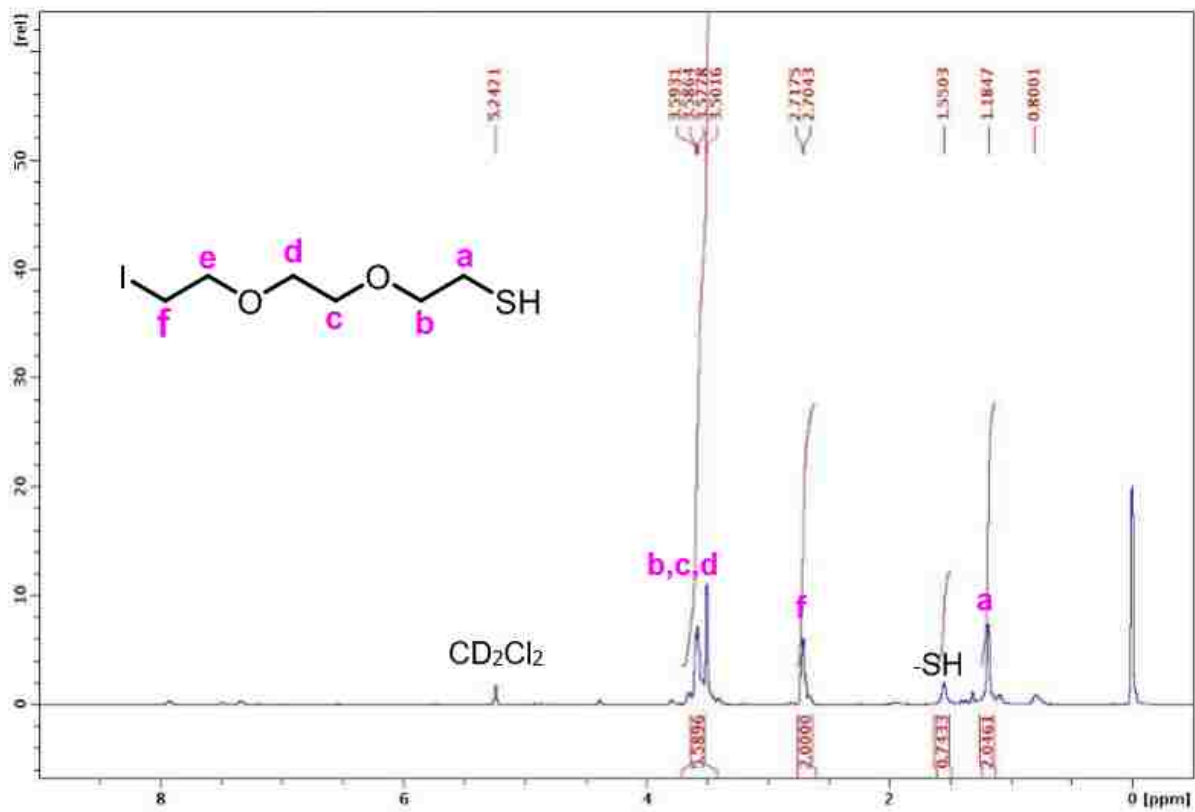
Figure A.6. ^{1}H NMR spectrum of 2-(2-(2-iodoethoxy)ethoxy)ethane thiol in CD$_2$Cl$_2$.
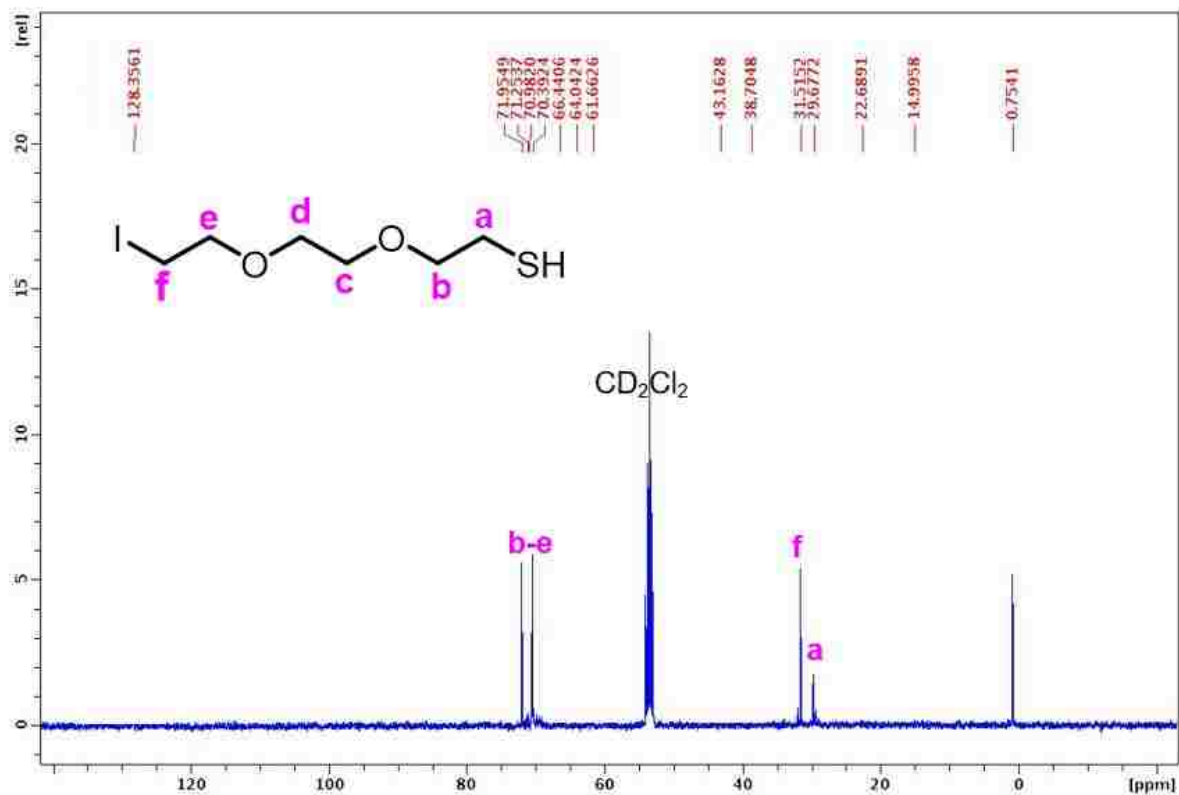
Figure A.7. ^{13}C NMR spectrum of 2-(2-(2-iodoethoxy)ethoxy)ethane thiol in CD$_2$Cl$_2$.
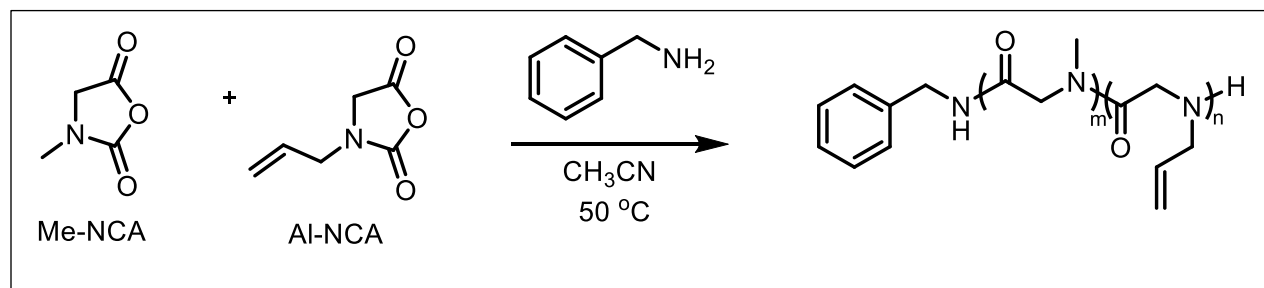
Scheme A.8. Synthesis of PNAlG-r-PNMG Copolymer: Benzylamine-initiated ROP of Al-NCA and Me-NCA in acetonitrile at 50 ^{o}C.

Under inert conditions Al-NCA and Me-NCA were dissolved in anhydrous organic solvents and a measured volume of benzyl amine/THF initiator stock solution was added and allowed to stir at 50 ˚C for approximately 24 h (Scheme A.8). The amount of Me-NCA and Al-NCA monomer used were predetermined in attempt to generate

polymers with varied compositions. Copolypeptoids with PNAIG content as high as 47% were obtained (Table A.9). The monomer conversion was monitored via FT-IR spectroscopy. Copolymer precursors derived from the benzylamine initiated ROP of Al-NCA and Me-NCA were properly characterized by ^{1}H NMR spectroscopy (Table A.9). The copolymer chain length was determined by the integration of methyl protons of PNMG segments and terminal alkene proton of PNAIG segments side chains relative to the aromatic protons of the benzyl end group in the ^{1}H NMR spectrum (Figures A.9-A.10).

Table A.9 Molecular composition of PNAIG-*r*-PNMG random copolymers.

[M1]$_o$:[M2]$_o$:[I]$_o$ [a]	DP (exp.) (^{1}H NMR)	f$_{PNAIG}$ [b]	f$_{PNMG}$ [b]
45:5:1	PNMG$_{39}$-r-PNAIG$_4$	0.09	0.91
20:20:1	PNMG$_{23}$-r-PNAIG$_{20}$	0.47	0.53

[a] Benzylamine-initiated ROP of Al-NCA and Me-NCA in acetonitrile at 50 ^{o}C.for 18-24 h;
[b] Experimental molar fraction of each block in the random copolypeptoids determined via ^{1}H NMR spectroscopic analysis.
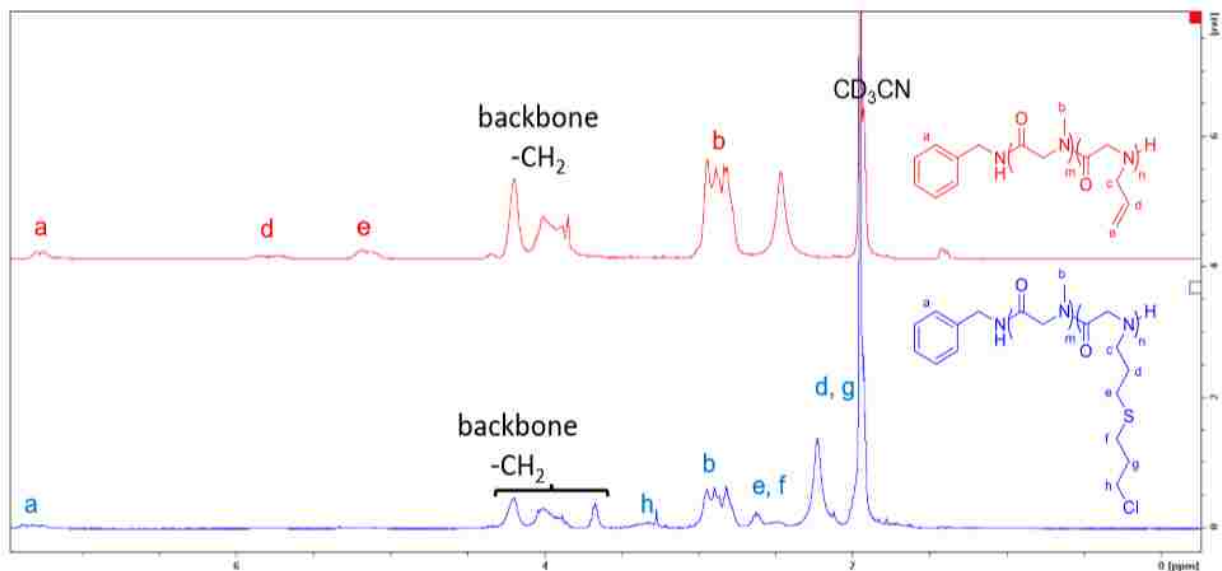
Figure A.10 ^{1}H NMR spectra of PNAlG$_4$-r-PNMeG$_{39}$ random copolymer (red, top) and the resulting polypeptoid obtained (blue, bottom) after radical thiol-ene addition of CPT in CD$_3$CN.
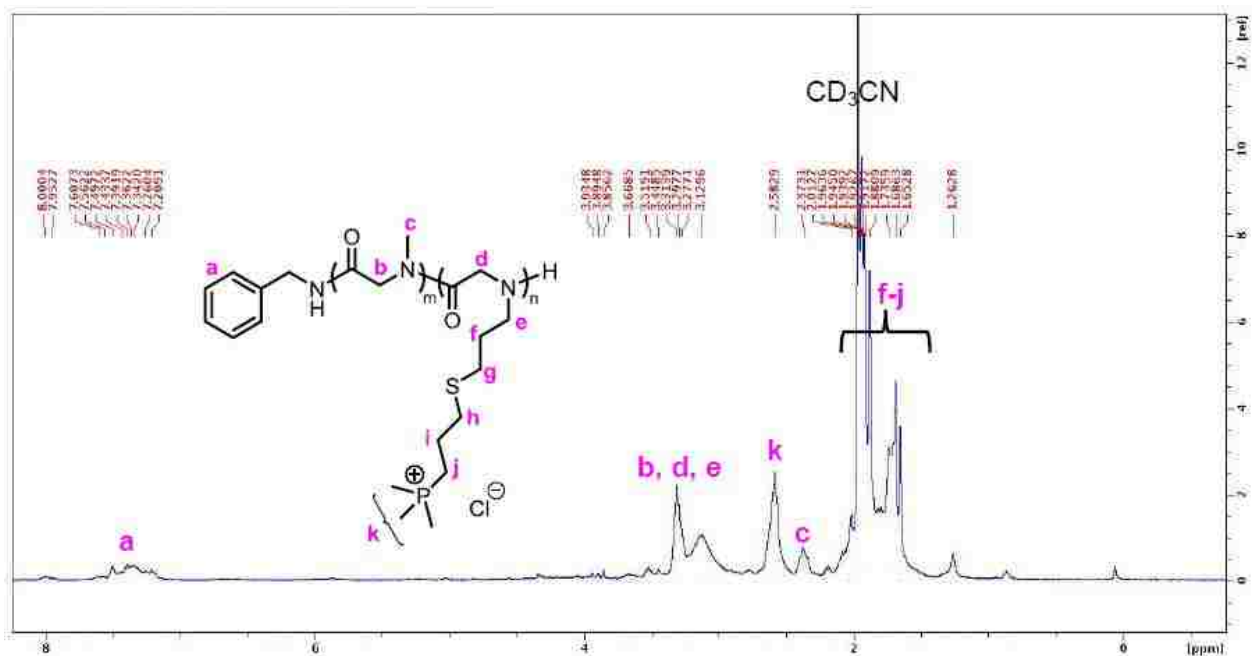
Figure A.11 ^{1}H NMR spectrum of cationic polypeptoid obtained by S$_n$2 substitution reaction between PNAlG$_4$-r-PNMeG$_{39}$-CPT with trimethyl phosphine in CD$_3$CN.
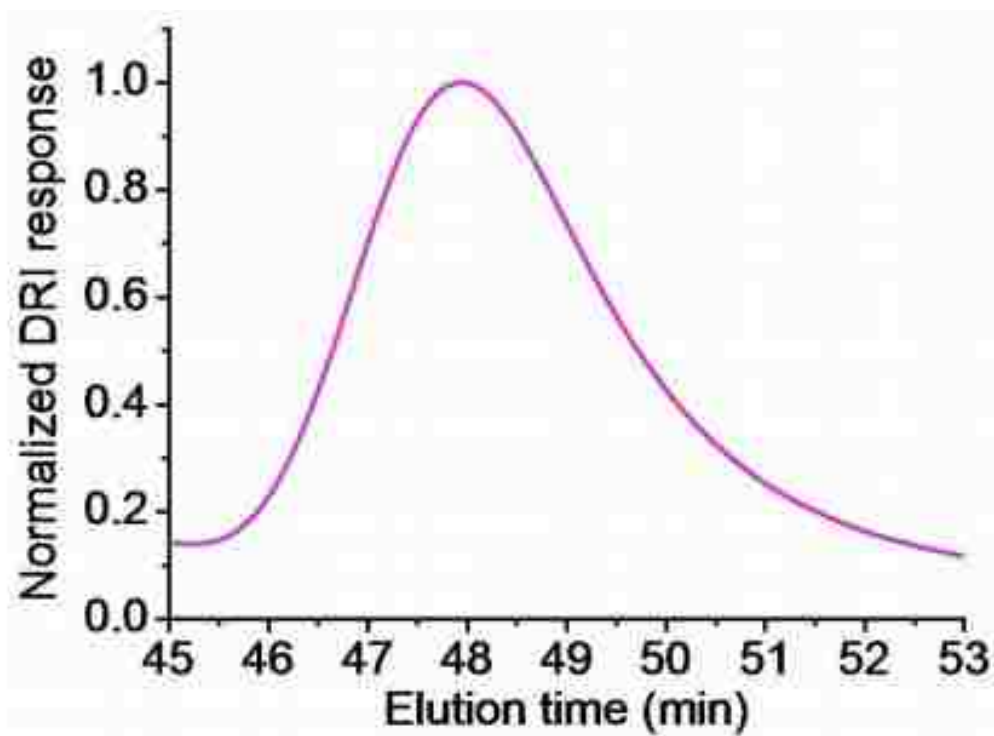
Figure A.12. Normalized SEC chromatogram (0.1 M LiBr/DMF, 25 °C) of the P(NPgG$_{39}$-r-NDeG$_9$) copolypeptoid synthesized via benzylamine-initiated ring-opening copolymerization of Pg-NCA and De-NCA. M_n (5.6 kg/mol) and PDI (1.03) of the copolymer were determined using polystyrene standards.
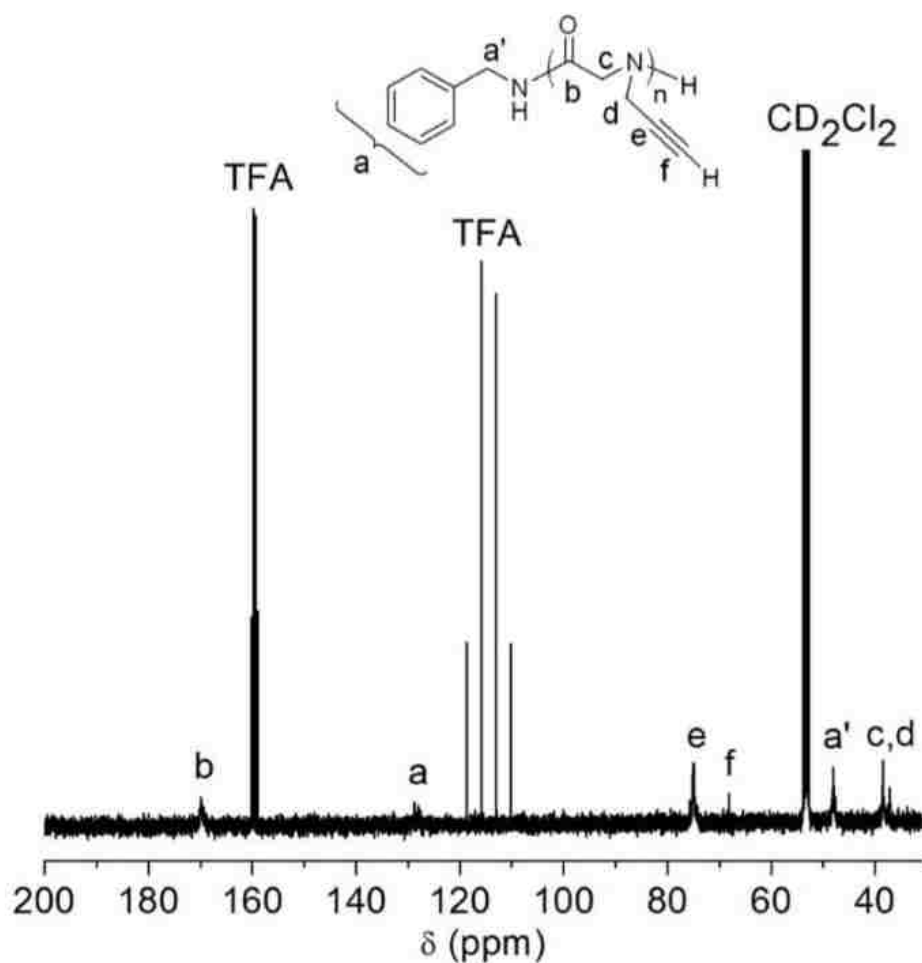
Figure A.13. Representative ^{13}C NMR spectrum of the poly(N-propargyl glycine) homopolymer (PNPgG) in CD$_2$Cl$_2$. ^{13}C NMR (100 MHz, CD$_2$Cl$_2$), δ ppm: 168.9 (−COCH$_2$N−), 128.7−127.5 (C$_6$H$_5$−), 77.5 (−NCH$_2$CC−), 73.0 (−NCH$_2$CC−), 47.1 (C$_6$H$_5$CH$_2$N−), 37.6 (−COCH$_2$N−), 36.6 (−NCH$_2$CC−).

163
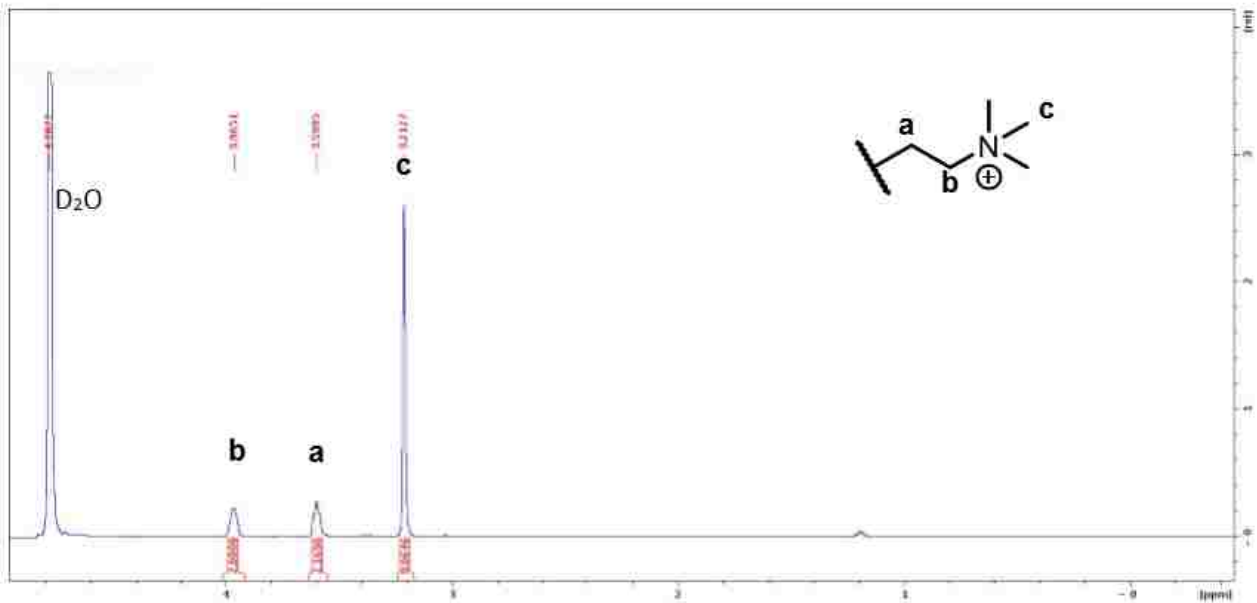
Figure A.14. ^{1}H NMR spectrum of cationic azido compound **1** in D$_2$O.
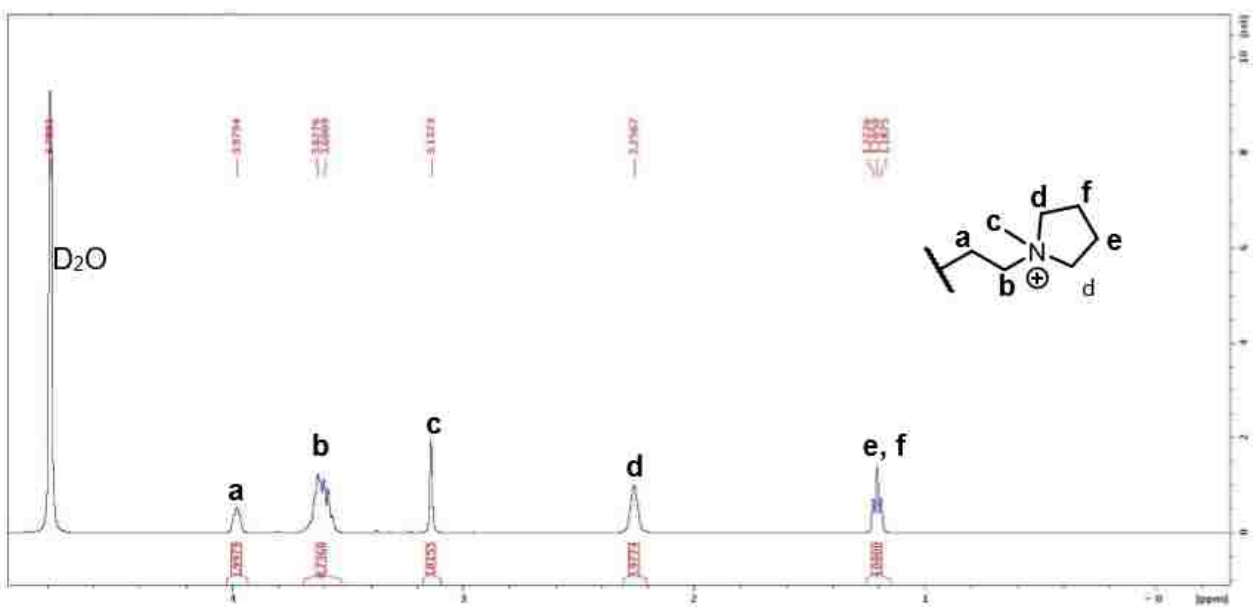
Figure A.15. ^{1}H NMR spectrum of cationic azido compound **8** in D$_2$O.
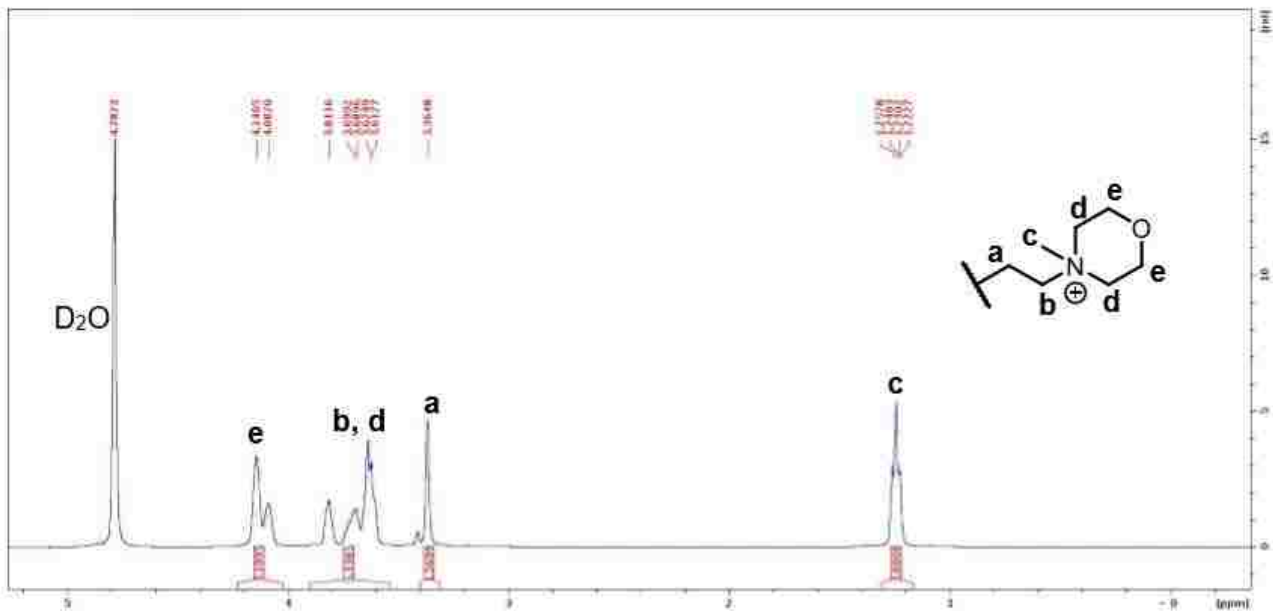
Figure A.16. ^{1}H NMR spectrum of cationic azido compound **10** in D$_2$O.
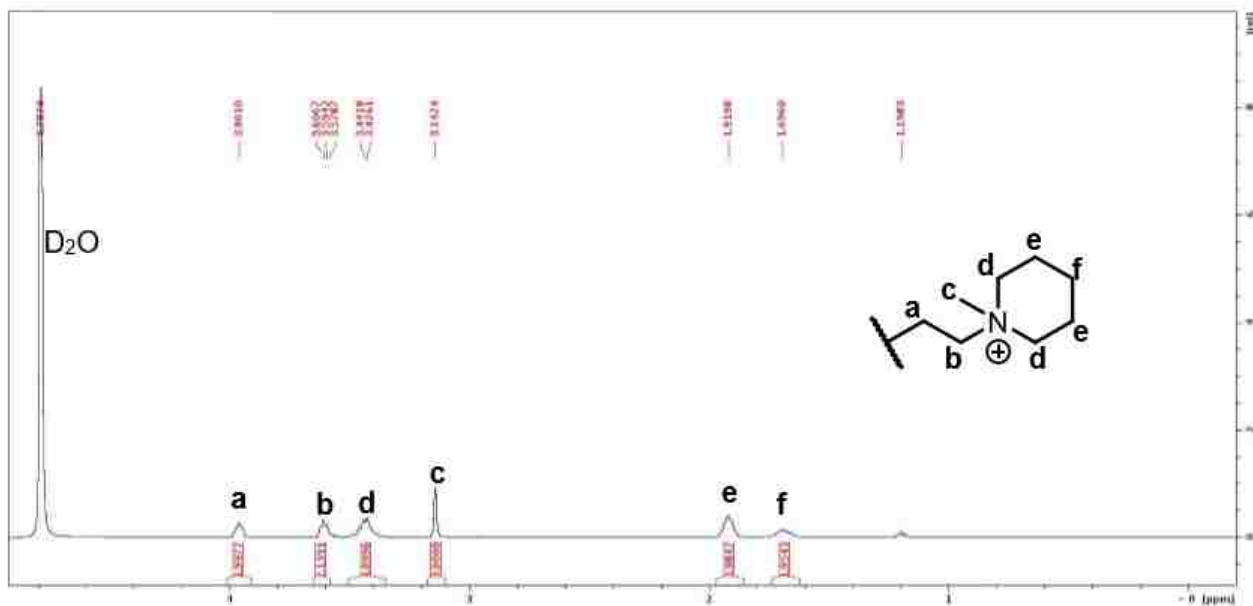
Figure A.17. ^{1}H NMR spectrum of cationic azido compound **7** in D$_2$O.

Route 1:
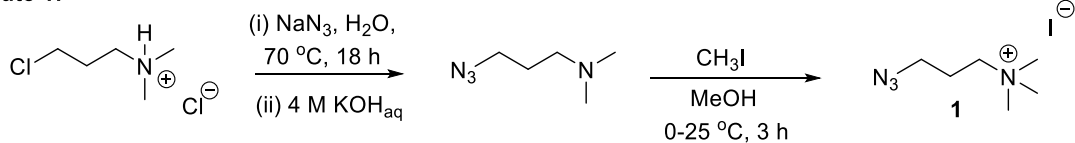
Route 2:
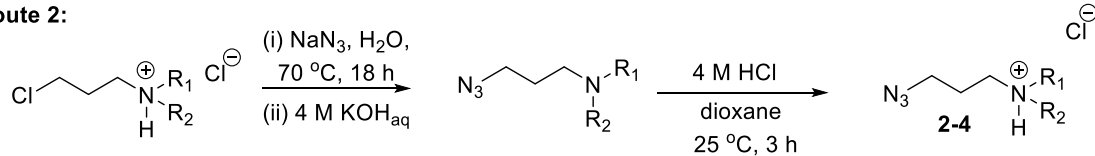
2: R_1, R_2 = CH$_3$
3: R_1 = CH$_3$; R_2 = H
4: R_1= R_2 = H
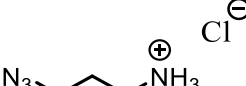
Route 3:
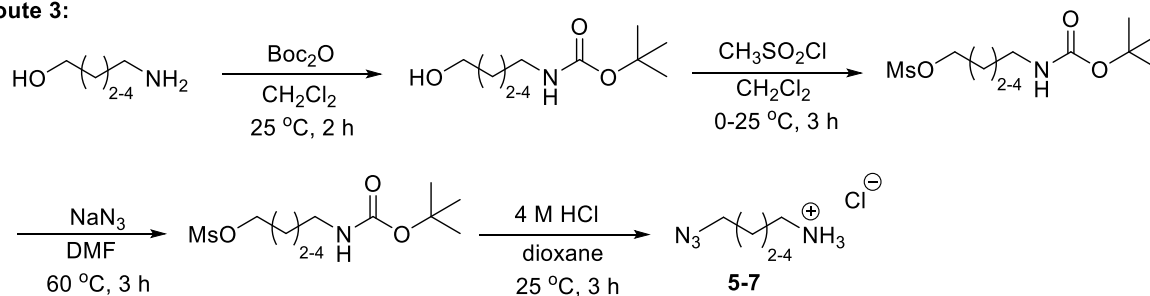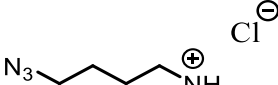
Scheme A.18. A general synthetic scheme of ω-azido-alkyl ammonium derivatives.

1: Yield: 67%, yellow solid. ^{1}H NMR (400 MHz, THF-d$_8$), δ ppm: δ = 3.51-3.48 (t, J= 6.40, 2 H), 3.45-3.41 (t, J= 8.40, 2 H), 3.14 (s, 9 H), 2.13-2.07 (quint, 2 H). ^{13}C{^{1}H} NMR (100 MHz, D$_2$O), δ ppm: 64.1, 53.2, 47.8, 22.4.
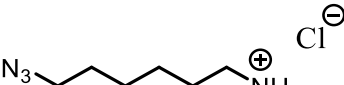
2: Yield: 83%, yellow solid. ^{1}H NMR (D$_2$O): δ = 3.58-3.55 (t, J= 6.40 Hz, 2 H), 3.32-3.28 (t, J= 7.88, 2 H), 2.97 (s, 6 H), 2.11-2.04 (quint, 2 H). ^{13}C{^{1}H} NMR (100 MHz, D$_2$O), δ ppm: 55.4, 48.1, 42.9, 23.6.

3: Yield: ~100%, yellow solid. ^{1}H NMR (D$_2$O): δ = 3.55-3.52 (t, J= 6.44 Hz, 2 H), 3.18-3.14 (t, J= 7.40 Hz, 2 H), 2.76 (s, 3 H), 2.01-1.98 (quint, 2 H). ^{13}C{^{1}H} NMR (100 MHz, D$_2$O), δ ppm: 48.2, 46.8, 32.9, 24.9.

4: N_3 $\overset{\oplus}{NH_3}$ $\overset{\ominus}{Cl}$ Yield: 75%, yellow solid. ^{1}H NMR (D$_2$O): δ = 3.57 (t, J= 6.48, 2 H), 3.16-3.12 (t, J= 7.40, 2 H), 2.03-1.96 (quint, 2 H). ^{13}C{^{1}H} NMR (100 MHz, D$_2$O), δ ppm: 48.3, 37.4, 26.1.

5: N_3 $\overset{\oplus}{NH_3}$ $\overset{\ominus}{Cl}$ Yield: 81%, yellow solid. ^{1}H NMR (D$_2$O): δ = 3.46 (t, J= 6.52, 2 H), 2.78 (t, J= 4.75, 2 H), 1.56 (m, 2 H), 1.33 (quint, 2 H) ^{13}C{^{1}H} NMR (100 MHz, D$_2$O), δ ppm: 49.7, 38.3, 27.4, 24.9.

6: N_3 $\overset{\oplus}{NH_3}$ $\overset{\ominus}{Cl}$ Yield: 100%, yellow solid. ^{1}H NMR (D$_2$O): δ = 3.40 (t, J= 6.79, 2 H), 3.06 (t, J= 4.80, 2 H), 1.75-1.67 (m, 4 H), 1.50 (quint, 2 H) ^{13}C{^{1}H } NMR (100 MHz, D$_2$O), δ ppm: 50.9, 39.4, 27.5, 26.3, 22.9.

7: N_3 $\overset{\oplus}{NH_3}$ $\overset{\ominus}{Cl}$ Yield: 94%, yellow solid. ^{1}H NMR (D$_2$O): δ = 3.39-3.36 (t, J= 6.40, 2 H), 3.05-3.02 (t, J= 6.40, 2 H), 1.66 (m, 4 H), 1.45 (quint, 4 H). ^{13}C{^{1}H } NMR (100 MHz, D$_2$O), δ ppm: 51.1, 39.4, 27.7, 26.6, 25.4, 25.1.
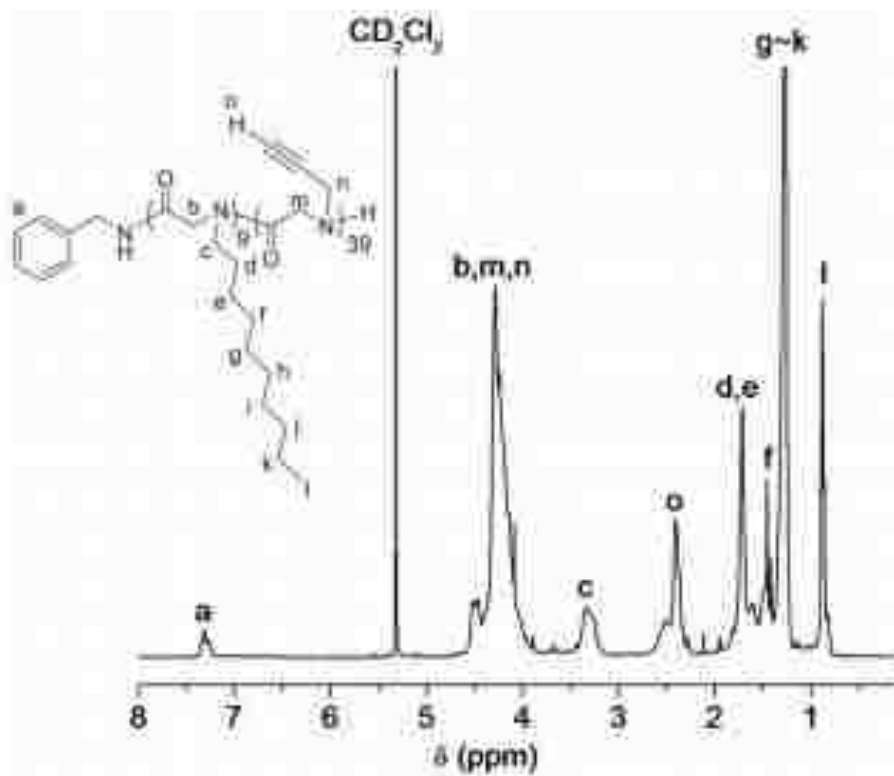
Figure A.19. Representative ^{1}H NMR spectrum of the poly(N-propargyl glycine-r-N-decyl glycine) copolymer P(NPgG$_{39}$-r-NDeG$_9$) in CD$_2$Cl$_2$. The copolymer chain length was determined by the integration of terminal methyl protons (l) of decyl side chains and terminal alkyne proton (o) of propargyl side chains relative to the aromatic protons (a) of the benzyl end group in the ^{1}H NMR spectrum. H NMR (400 MHz, CD$_2$Cl$_2$), δ ppm: 7.23−7.19 ppm (br m, −C$_6$H$_5$, Ha), 4.43−4.15 ppm (br m, Pg/De−COCH$_2$N−, CHCCH$_2$N−, Hb, Hm, Hn), 3.26 ppm (br m, CH$_3$(CH$_2$)$_8$CH$_2$N−, Hc), 2.43−2.28 ppm (br m, CH CCH$_2$−, Ho), 1.63−1.50 ppm (br m, CH$_3$ (CH$_2$) 6 (CH$_2$)$_2$CH$_2$N−, Hd, He), 1.37 ppm (br d, C H$_3$(CH $_2$) 5C H $_2$ (CH $_2$) $_3$ N −, Hf), 1.18 ppm (br s, CH$_3$(CH$_2$)$_5$(CH$_2$)$_4$N−, Hg, Hh, Hi, Hj, Hk), 0.79 ppm (br s, CH$_3$CH$_2$(CH$_2$)$_8$N−, Hl).

168

Figure A.20. Representative $_{13}$C NMR spectrum of the poly(*N*-propargyl glycine-*r*-*N*-decyl glycine) copolymer P(NPgG$_{39}$-*r*-NDeG$_9$) in CD$_2$Cl$_2$. ^{13}C NMR (100 MHz, CD2Cl2), δ ppm: 168.9 (Pg/De−COCH$_2$N−), 127.6 (−C$_6$H$_5$), 78.1 (−CHCCH$_2$−), 73.3 (−CHCCH$_2$−), 48.5 (CH$_3$(CH$_2$)$_8$CH$_2$N−), 47.3 (Pg/De− NCOCH$_2$−), 37.7 (C$_6$H$_5$CH$_2$N−), 36.6 (CH$_3$(CH$_2$)$_7$CH$_2$CH$_2$N−), 31.8 (Pg−CCH$_2$N−), 29.6 and 29.3 (CH$_3$(CH$_2$)$_3$(CH$_2$)$_4$(CH$_2$)$_2$N−), 27.4 and 26.9 (CH$_3$CH$_2$(CH$_2$)$_2$(CH$_2$)$_6$N−), 22.6 (CH$_3$CH$_2$(CH$_2$)$_7$CH$_2$N−), 13.8 (CH$_3$(CH$_2$)$_8$CH$_2$N−).
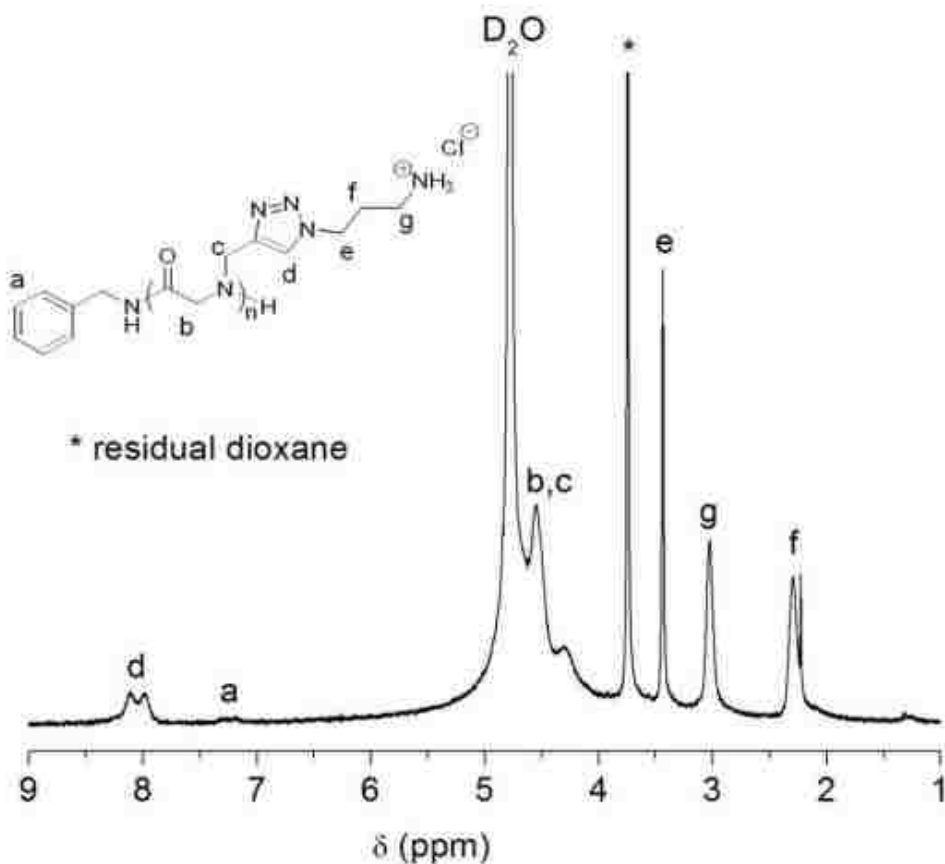
169

Figure A.21. Representative ^{1}H NMR spectrum of **P1** in D$_2$O. M_n was determined by the integration of the triazole proton (d) relative to the aromatic protons (a) of the benzyl end group in the ^{1}H NMR spectrum. ^{1}H NMR (400 MHz, D$_2$O), δ ppm: 8.17 (br. m, −C=C*H*N−, Hd), 7.20 (br. m, −C$_6$*H*$_5$, Ha), 4.58-4.34 (br. m, −COC*H*$_2$N−, −CC*H*$_2$N−, Hb, Hc), 3.65 (s, −NC*H*$_2$(CH$_2$)$_2$N(CH$_3$)$_3$, He), 3.41 (br. s, −N(CH$_2$)$_3$C*H*$_2$N(CH$_3$)$_3$, Hg), 3.14 (br. s, −N(C*H*$_3$)$_3$, Hh); 2.49 (br. s, −NCH$_2$C*H*$_2$CH$_2$N(CH$_3$)$_3$, Hf).
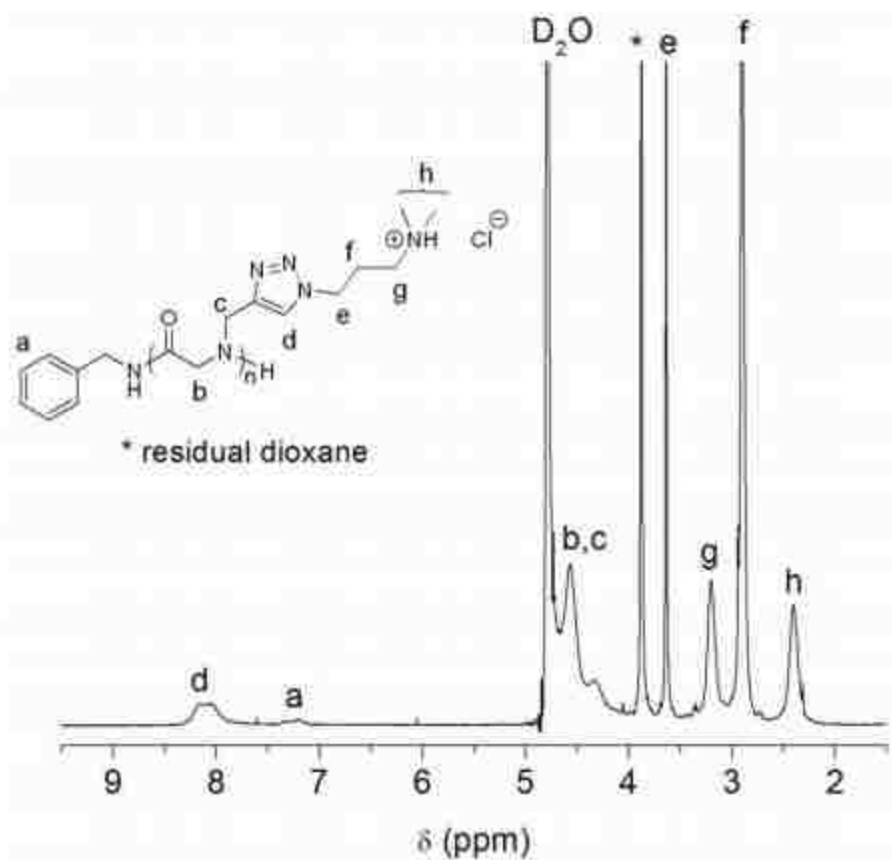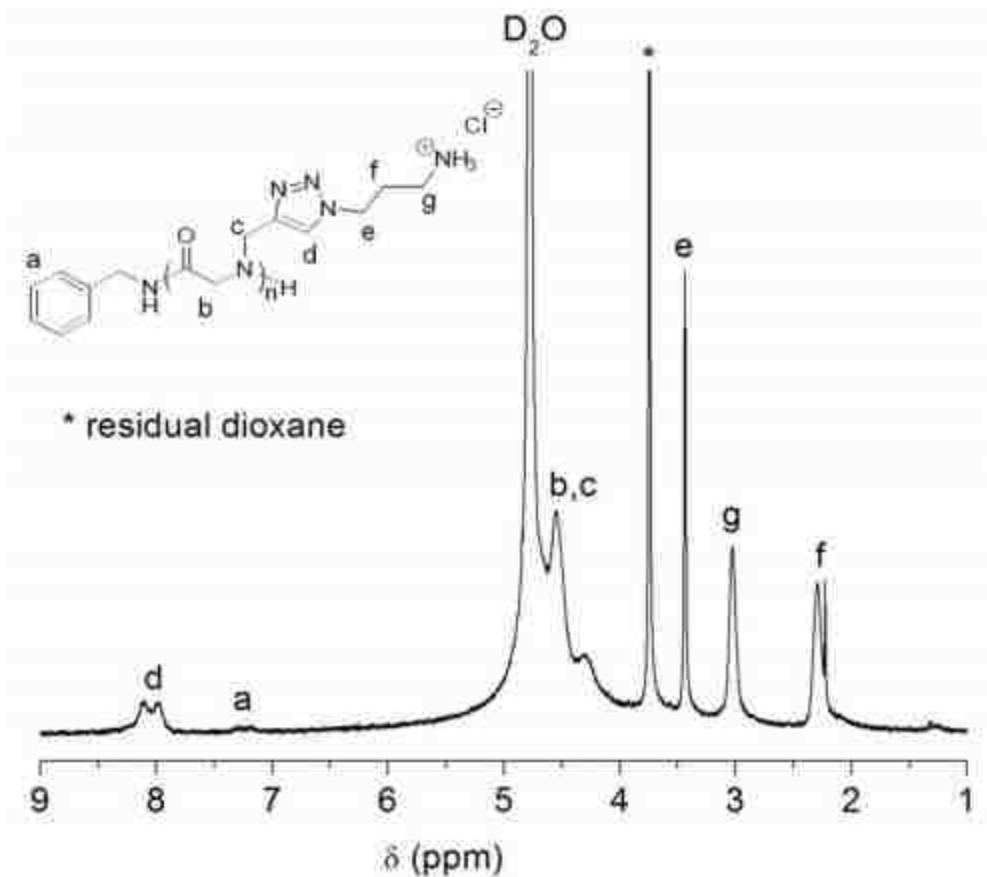
Figure A.22. Representative ^{1}H NMR spectrum of **P2** in D$_2$O. M_n was determined by the integration of the triazole proton (d) relative to the aromatic protons (a) of the benzyl end group in the ^{1}H NMR spectrum. ^{1}H NMR (400 MHz, D$_2$O), δ ppm: 8.04 (br. m, −C=C*H*N−, Hd), 7.20 (br. m, −C$_6$*H$_5$*, Ha), 4.57-4.32 (br. m, −COC*H$_2$*N−, −CC*H$_2$*N−, Hb, Hc), 3.63 (s, −NC*H$_2$*(CH$_2$)$_2$N(CH$_3$)$_2$, He), 3.25 (br. s, −N(CH$_2$)$_2$C*H$_2$*N(CH$_3$)$_2$, Hg), 2.75 (−N(CH$_2$)$_3$N(C*H$_3$)$_2$−, Hh), 2.47 (br. s, −NCH$_2$C*H$_2$*CH$_2$N(CH$_3$)$_2$, Hf).
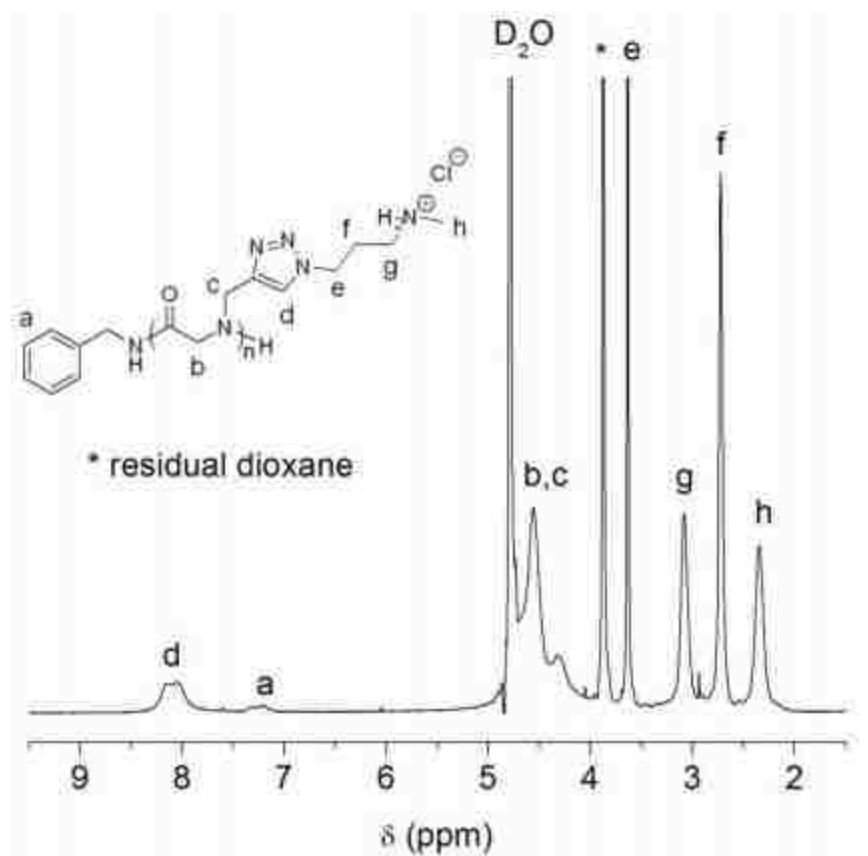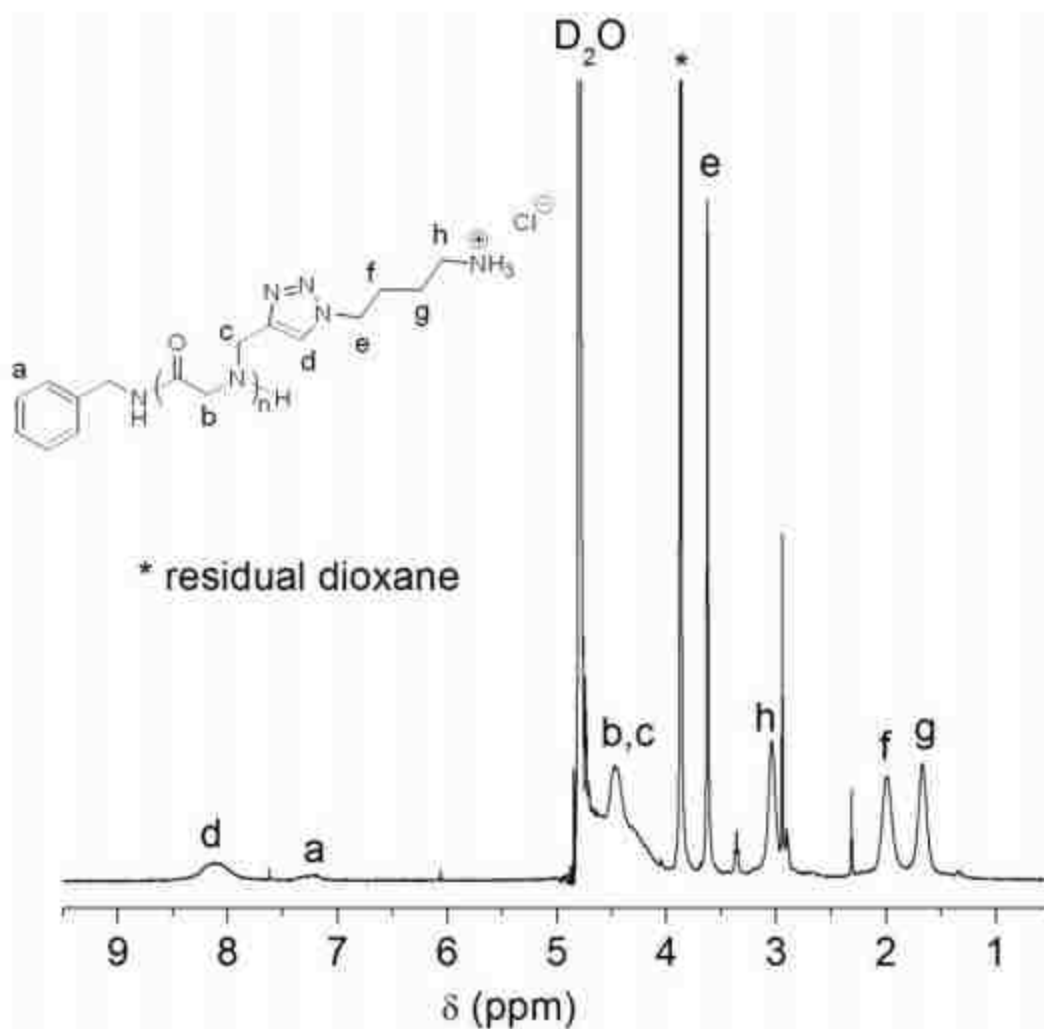
Figure A.23. Representative ^{1}H NMR spectrum of **P3** in D$_2$O. M_n was determined by the integration of the triazole proton (d) relative to the aromatic protons (a) of the benzyl end group in the ^{1}H NMR spectrum. ^{1}H NMR (400 MHz, D$_2$O), δ ppm: 8.15 (br. m, −C=CHN−, Hd), 7.20 (br. m, −C$_6$$H_5$, Ha), 4.56-4.31 (br. m, −COCH_2N−, −CCH_2N−, Hb, Hc), 3.63 (s, −NCH_2(CH$_2$)$_2$NCH$_3$, He), 3.08 (br. s, −N(CH$_2$)$_2$CH_2NCH$_3$−, Hg), 2.72 (br. s, −N(CH$_2$)$_3$NCH_3, Hh), 2.34 (br. s, −NCH$_2$CH_2CH$_2$NCH$_3$, Hf).
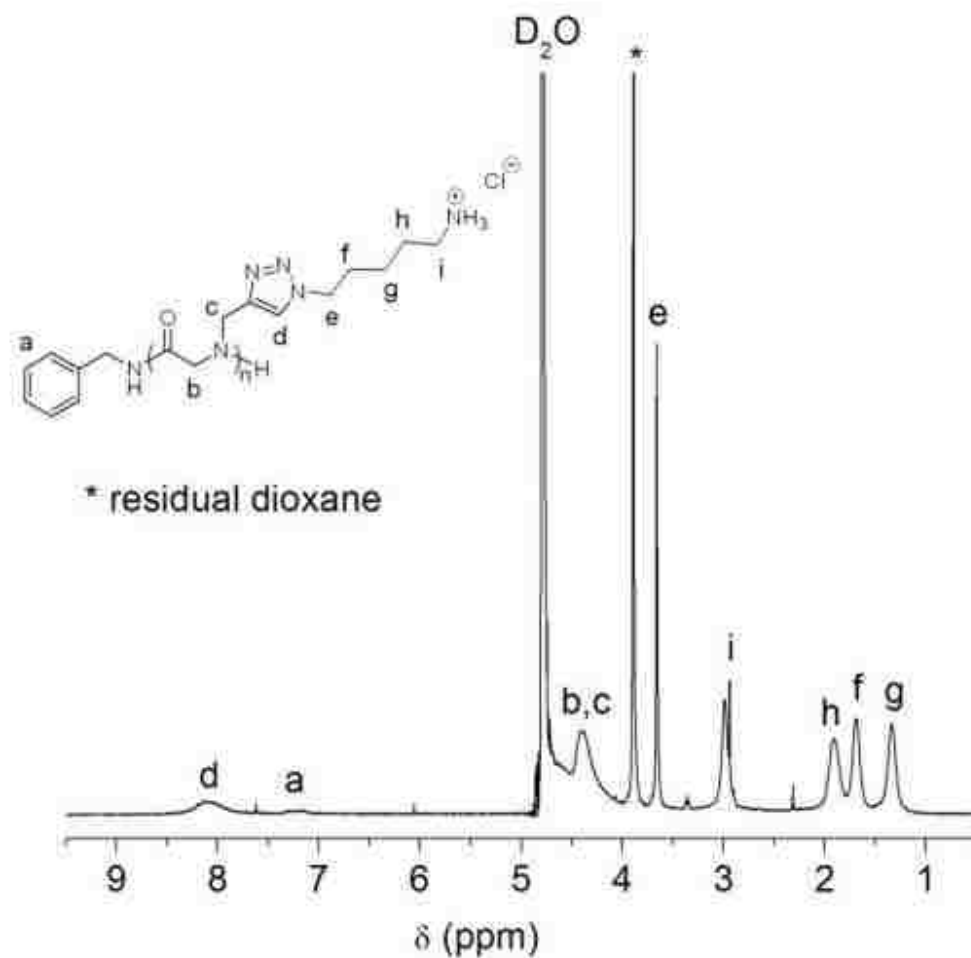
Figure A.24. Representative ^{1}H NMR spectrum of **P4** in D$_2$O. M_n was determined by the integration of the triazole proton (d) relative to the aromatic protons (a) of the benzyl end group in the ^{1}H NMR spectrum. ^{1}H NMR (400 MHz, D$_2$O), δ ppm: 8.10-7.98 (br. m, −C=C*H*N−, Hd), 7.20 (br. m, −C$_6$*H*$_5$, Ha), 4.61- 4.30 (br. m, −COC*H$_2$*N−, −CC*H$_2$*N−, Hb, Hc), 3.43 (s, −NC*H$_2$*(CH$_2$)$_2$NH$_3$, He), 2.98 (br. s, −N(CH$_2$)$_2$C*H$_2$*NH$_3$, Hg), 2.29 (br. s, −NCH$_2$C*H$_2$*CH$_2$NH$_3$, Hf).

Figure A.25. Representative ^{1}H NMR spectrum of **P5** in D$_2$O. M_n was determined by the integration of the triazole proton (d) relative to the aromatic protons (a) of the benzyl end group in the ^{1}H NMR spectrum. ^{1}H NMR (400 MHz, D$_2$O), δ ppm: 8.10-7.98 (br. m, −C=C*H*N−, Hd), 7.20 (br. m, −C$_6$*H*$_5$, Ha), 4.61-4.30 (br. m, −COC*H*$_2$N−, −CC*H*$_2$N−, Hb, Hc), 3.43 (s, −NC*H*$_2$(CH$_2$)$_2$NH$_3$, He), 2.98 (br. s, −N(CH$_2$)$_2$C*H*$_2$NH$_3$, Hg), 2.29 (br. s, −NCH$_2$C*H*$_2$CH$_2$NH$_3$, Hf).
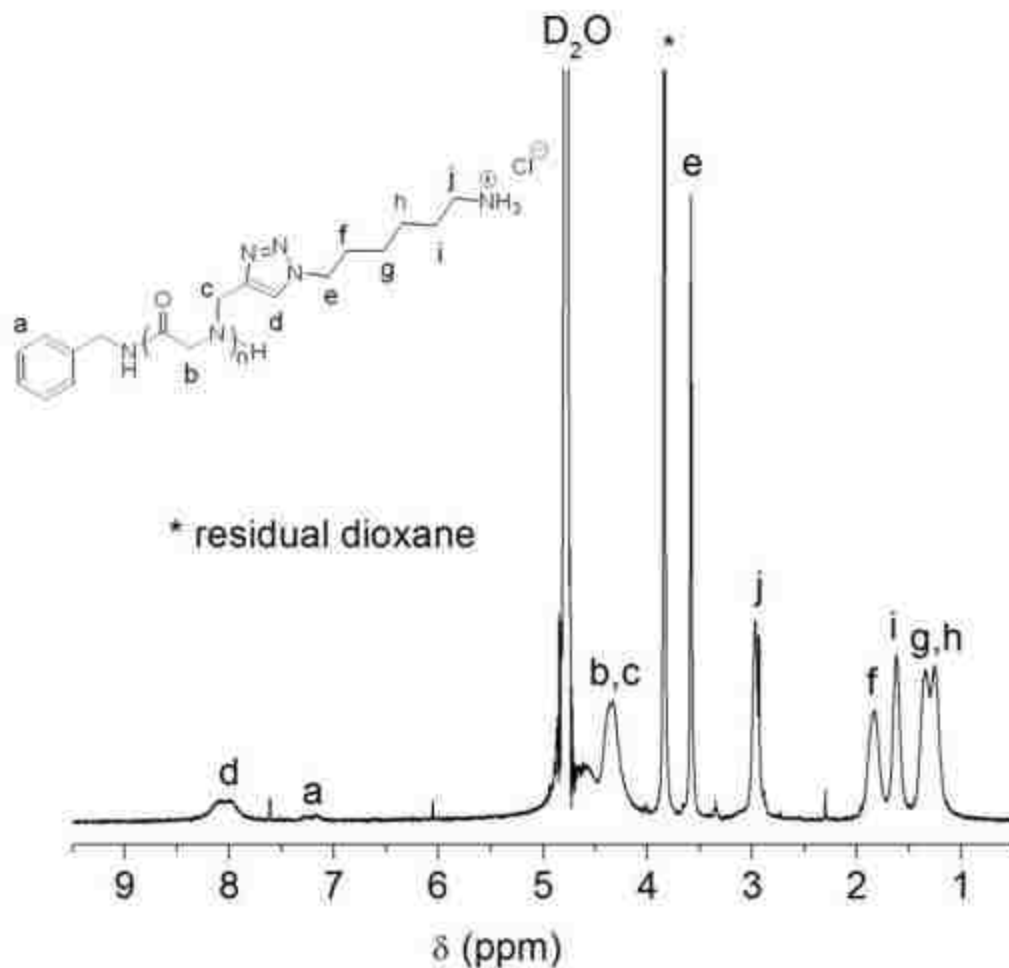
Figure A.26. Representative ^{1}H NMR spectrum of **P6** in D_2O. M_n was determined by the integration of the triazole proton (d) relative to the aromatic protons (a) of the benzyl end group in the ^{1}H NMR spectrum. ^{1}H NMR (400 MHz, D_2O), δ ppm: 8.10-7.98 (br. m, −C=C*H*N−−, Hd), 7.20 (br. m, −C$_6$*H*$_5$, Ha), 4.61-4.30 (br. m, −CO*CH*$_2$N−, −C*CH*$_2$N−, Hb, Hc), 3.43 (s, −NC*H*$_2$(CH$_2$)$_2$NH$_3$, He), 2.98 (br. s, −N(CH$_2$)$_2$C*H*$_2$NH$_3$, Hg), 2.29 (br. s, −NCH$_2$C*H*$_2$CH$_2$NH$_3$, Hf).

Figure A.27. Representative ^{1}H NMR spectrum of **P7** in D$_2$O. M_n was determined by the integration of the triazole proton (d) relative to the aromatic protons (a) of the benzyl end group in the ^{1}H NMR spectrum. ^{1}H NMR (400 MHz, D$_2$O), δ ppm: 8.10-7.98 (br. m, −C=C*H*N−, Hd), 7.20 (br. m, −C$_6$*H$_5$*, Ha), 4.61-4.30 (br. m, −COC*H$_2$*N−, −CC*H$_2$*N−, Hb, Hc), 3.43 (s, −NC*H$_2$*(CH$_2$)$_2$NH$_3$, He), 2.98 (br. s, −N(CH$_2$)$_2$C*H$_2$*NH$_3$, Hg), 2.29 (br. s, −NCH$_2$C*H$_2$*CH$_2$NH$_3$, Hf).

Figure A.28. Representative ^{1}H NMR spectrum of **P8** in D$_2$O. M_n was determined by the integration of the triazole proton (d) relative to the aromatic protons (a) of the benzyl end group in the ^{1}H NMR spectrum. ^{1}H NMR (400 MHz, D$_2$O), δ ppm: 8.10 (br. m, −C=C*H*N−, Hd), 7.20 (br. m, −C$_6$*H*$_5$, Ha), 4.66-4.30 (br. m, −COC*H*$_2$N−, −CC*H*$_2$N−, Hb, Hc), 3.62 (s, −NC*H*$_2$(CH$_2$)$_3$NH$_3$, He), 3.04 (br. m, −N(CH$_2$)$_3$C*H*$_2$NH$_3$, Hh), 1.98 (br. s, −NCH$_2$C*H*$_2$(CH$_2$)$_2$NH$_3$, Hf), 1.66 (br. s, −N(CH$_2$)$_2$C*H*$_2$CH$_2$NH$_3$, Hg).

Figure A.29. Representative ^{1}H NMR spectrum of **P9** in D_2O. M_n was determined by the integration of the triazole proton (d) relative to the aromatic protons (a) of the benzyl end group in the ^{1}HNMR spectrum. ^{1}H NMR (400 MHz, D_2O), δ ppm: 8.12 (br. m, −C=C*H*N−, Ha), 7.18 (br. m, −C$_6$*H*$_5$, Ha), 4.39 (br. m, −COC*H$_2$*N−, −CC*H$_2$*N−, Hb, Hc), 3.65 (s, −NC*H$_2$*(CH$_2$)$_4$NH$_3$, He), 3.02 (br. s, −N(CH$_2$)$_4$C*H$_2$*NH$_3$, Hi), 1.90 (br. s, −N(CH$_2$)$_3$C*H$_2$*CH$_2$NH$_3$, Hh); 1.68 (br. s, −NCH$_2$C*H$_2$*(CH$_2$)$_3$NH$_3$, Hf); 1.33 (br. s, −N(CH$_2$)$_2$C*H$_2$*(CH$_2$)$_2$NH$_3$, Hg).

Figure A.30. Representative ^{1}H NMR spectrum of **P10** in D_2O. M_n was determined by the integration of the triazole proton (d) relative to the aromatic protons (a) of the benzyl end group in the ^{1}H NMR spectrum. ^{1}H NMR (400 MHz, D_2O), δ ppm: 8.01 (br. m, −C=C*H*N−, Hd), 7.22 (br. m, −C$_6$*H*$_5$, Ha), 4.53-4.33 (br. m, −COC*H*$_2$N−, −CC*H*$_2$N−, Hb, Hc), 3.58 (s, −NC*H*$_2$(CH$_2$)$_5$NH$_3$, Hb, Hc), 2.98 (br. s, −N(CH$_2$)$_5$C*H*$_2$NH$_3$, Hj), 1.82 (br. s, −NCH$_2$C*H*$_2$(CH$_2$)$_4$NH$_3$, Hf), 1.62 (br. s, −N(CH$_2$)$_4$C*H*$_2$CH$_2$NH$_3$, Hi); 1.34 (br. s, −N(CH$_2$)$_2$C*H*$_2$(CH$_2$)$_3$NH$_3$, Hg), 1.25 (br. s, −N(CH$_2$)$_3$C*H*$_2$(CH$_2$)$_2$NH$_3$, Hh).

Figure A.31. Representative ^{1}H NMR spectrum of **P11** in D$_2$O. M_n of the charged polymer portion was determined by the integration of the triazole proton (d) relative to the aromatic protons (a) of the benzyl end group in the ^{1}H NMR spectrum. Mn of the uncharged polymer portion was determined by the integration of the methyl protons (l) relative to the aromatic protons (a) of the benzyl end group in the ^{1}H NMR spectrum. ^{1}H NMR (400 MHz, D$_2$O), δ ppm: 8.10-8.01 (br. m, −C=C*H*N−, Ho), 7.32-7.21 (br. m, −C$_6$*H*$_5$, Ha), 4.55-4.33 (br. m, −COC*H$_2$*N−, −CC*H$_2$*N−, Hb, Hm, Hn), 3.46 (s, −NC*H$_2$*(CH$_2$)$_5$NH$_3$, Hp), 3.04 [br. s, (−NC*H$_2$*(CH$_2$)$_8$CH$_3$, −N(CH$_2$C*H$_2$*)(CH$_2$)$_7$CH$_3$), −NCH$_2$C*H$_2$*(CH$_2$)$_4$NH$_3$, −N(CH$_2$)$_5$C*H$_2$*NH$_3$), Hc, Hd, Hq, Hu], 2.31 [br. s, (−N(CH$_2$)$_2$C*H$_2$*(CH$_2$)$_3$NH$_3$, −N(CH$_2$)$_2$ (CH$_2$C*H$_2$*)(CH$_2$)$_2$NH$_3$, −N(CH$_2$)$_4$C*H$_2$*CH$_2$NH$_3$), Hr-Ht], 1.22 (br. m, −N(CH$_2$)$_2$(C*H$_2$*)$_7$CH$_3$, He-Hk), 0.70-0.79 (br. m, −NCH$_2$(CH$_2$)$_8$C*H$_3$, Hl).

Figure A.32. Transfection efficiencies of polyplexes at various polypeptoid/DNA weight ratios in B16F10 (A) and COS-7 (B) cells in the presence of 10% serum, and in HeLa cells (C) under different serum conditions (n = 3). PEI in the presence of 30% serum in HeLa cells (C).

A.33 Experimental

A.34 General Considerations

All chemicals used were purchased from Sigma-Aldrich and used as received unless otherwise noted. THF (Tetrahydrofuran) and DMF (Dimethyl Formamide) used for polymerization and click reactions were purified by passing through alumina columns under argon. All other solvents used in this study were purchased from Sigma without further purification. *N*-propargyl *N*-carboxy anhydride (Pg-NCA) and *N*-decyl *N*-carboxy anhydride (De-NCA) were synthesized by following a reported procedure.[38] Poly(*N*-propargyl glycine) homopolymer (PNPgG) were synthesized by adapting a literature procedure.[39] All ω-azido alkyl ammonium compounds used in the synthesis of cationic polypeptoids were prepared by adapting previous literature procedures.[40-42]

^{1}H and ^{13}C NMR spectra were recorded on Bruker AV-400 and AVIII-400 spectrometers, respectively. The peaks were referenced in parts per million (ppm) relative to proton impurities of deuterated solvents (*e.g.*, D_2O). Size-exclusion chromatography (SEC) was recorded on an Agilent 1200 system (Agilent 1200 series degasser, isocratic pump, auto sampler and column heater) equipped with three Phenomenex 5 μm, 300 × 7.8 mm columns, a Wyatt OptilabrEX differential refractive index (DRI) detector with a 690 nm light source, and a Wyatt DAWN EOS multiangle light scattering (MALS) detector (GaAs 30mW laser at λ = 690 nm). DMF with 0.1 M LiBr was used as the eluent at a flow rate of 0.5 mL/min. The temperature of the column and detector was set at 25 °C.[46] All data analysis was performed using Wyatt Astra V 6.0 software. M_n and the molecular weight distribution index (PDI) of PNPgG were obtained using a d*n*/d*c* of 0.1012 ± 0.0007 g/mol. Copper content was measured on

Varian SpectrAA 220 Atomic Absorption Spectrometer. The flame absorption spectrometry method was used with acetylene/air, lamp current of 4 mA, and slit width of 0.5 nm.

A.35. Monomer Synthesis

All the monomers used in this work were synthesized by adapting reported procedures.[22] *N*-alkyl *N*-carboxyanhydrides (R-NCAs) with propargyl and decyl side chains were synthesized via synthetic routes as shown in Scheme 2.1.

A.36. Polymer Synthesis

All linear homopolypeptoids and random copolypeptoids were synthesized by primary amine-initiated ring opening polymerization of the corresponding *N*-substituted *N*-carboxyany-drides (R-NCAs) in a concerted manner. A representative procedure for the synthesis of P11 was presented. Inside a glovebox, a predetermined volume of $BnNH_2$/THF stock solution (120 µL, 200 mM) was added to a THF solution of Pg-NCA (350 mg, 2.52 mmol, 0.5 M). The reaction mixture was stirred at 50 °C for 18 h under a nitrogen atmosphere. The conversion was determined by the FT-IR spectroscopic analysis of an aliquot of the reaction mixture. The final polymer was isolated by precipitation into hexane and dried under vacuum at room temperature to yield the final polymer as a white solid (230 mg, 96% yield). M_n and PDI of the polymer were determined by SEC. PNPgG homopolymers with various number average degrees of polymerization (DP_n = 28-251) and low PDI were obtained (Table 3.1).

A.37. Representative Synthetic Procedure for the Cationic Polypeptoid Homopolymers

Inside a glovebox, a measured amount of ω-azido hexyl ammonium salt (101 mg, 0.56 mmol) ($[N_3]_0:[\text{propargyl}]_0$ = 2:1) was added into a DMF solution of the PNPgG polymer (27.2 mg, 4 µmol, 0.28 mmol propargyl groups), followed by the addition of a measured volume of DMF solution of CuBr/PMDETA (250 mM, 564 µL, $[\text{Cu}]_0:[\text{PMDETA}]_0:[\text{propargyl}]_0$ = 33:33:100). The reaction mixture was stirred at 50 °C for 18 h. Upon addition of an aqueous solution of EDTA (9.9 mM, 3 mL), the reaction mixture was then dialyzed against deionized (DI) water water for 24-48 h during which the DI water was changed twice a day. The reaction mixture was then lyophilized to yield a light greenish blue powder (70 mg, 91% yield).

A.38. Representative Synthetic Procedure for the Cationic Polypeptoid Copolymer

Inside a glovebox, a measured amount of ω-azido hexyl ammonium salt (82 mg, 0.46 mmol, $[N_3]_0:[\text{propargyl}]_0$ = 2:1) was added into a DMF solution of P(NPgG$_{39}$-r-NDeG$_9$) (33 mg, 6 µmol, 0.23 mmol propargyl groups), followed by the addition of a measured volume of DMF solution of CuBr/PMDETA (250 mM, 460 µL $[\text{Cu}]_0:[\text{PMDETA}]_0:[\text{propargyl}]_0$ = 33:33:100). The reaction mixture was stirred at 50 °C for 18 h. Upon addition of an aqueous solution of EDTA (9.9 mM, 3 mL), the reaction mixture was dialyzed against the DI water for 24-48 h during which the DI water was changed twice a day. The reaction mixture was then lyophilized to yield a light green powder (85 mg, 91% yield).

A.39. Determination of Copper Ion Content in the Cationic Polymers by Flame Atomic Absorption Spectrometry (FAAS)

Cationic polypeptoids (10 mg) were dissolved in DI water (10 mL) at room temperature, and the solution was analyzed by FAAS. The copper ion content was determined by using the copper (II) absorption at 324.8 nm against a calibration curve constructed using a $CuSO_4$ standard.

APPENDIX B: SUPPLEMENTAL DATA FOR CHAPTER 4

B.1. Experimental Section

B.2 Representative Procedure for PNPgG

Inside a glovebox, a fixed volume of $BnNH_2$/THF stock solution (392 μL, 200 mM) was added a THF solution of Pg-NCA (545 mg, 3.92 mmol, 0.5 M). The reaction mixture stirred at 50 °C under a nitrogen atmosphere for 18 h. The conversion was monitored by the FT-IR spectroscopic analysis of an aliquot of the reaction mixture. Isolation of the final polymer was achieved by precipitation into hexane then dried under vacuum at room temperature to yield a white solid (300 mg, 80% yield). M_n and PDI of the final polymer was determined by SEC. PNPgG homopolymers with various number average degrees of polymerization (DP = 28-90) and low polydispersity indices (PDI) were obtained (Table 4.1).

B.3. Representative Synthetic Procedure for P(NPgG-*r*-NDeG)

Under nitrogen, a predetermined volume of $BnNH_2$/THF stock solution (200 mM, 181 μL) was added to a THF solution of Pg-NCA (202 mg, 1.45 mmol, 0.4 M) and De-NCA (88 mg, 0.363 mmol, 0.1 M). The reaction mixture was stirred at 50 °C for 24 h in a glovebox. Monomer conversion was determined by FTIR analysis of an aliquot of the reaction mixture. The final polymer was isolated by precipitation with excess hexane and dried under vacuum at room temperature to yield the polymer as a white solid (180 mg, 86% yield). Determination of copolymer composition (Entry P5, Table 4.1) was done by end-group analysis using ^{1}H NMR spectroscopy. For instance, the integration of terminal alkyne proton of propargyl sidechain at 2.36-2.87 ppm and the terminal

methyl proton of the decyl sidechain at 0.83 ppm relative to the integration of the aromatic protons of the benzyl end group at 7.28 ppm were used to determine the DP of the PNPgG and PNDG segment accordingly. ^{1}H NMR (400 MHz, CD$_2$Cl$_2$), δ ppm: 7.23-7.19 ppm (br. m, −C$_6$H$_5$, H$_a$), 4.43-4.15 ppm (br. m, $^{Pg/De}$−COCH$_2$N−, CHCCH$_2$N−, H$_b$, H$_m$, H$_n$), 3.26 ppm (br. m, CH$_3$(CH$_2$)$_8$CH$_2$N−, H$_c$), 2.43-2.28 ppm (br. m, CHCCH$_2$−, H$_o$), 1.63-1.50 ppm (br. m, CH$_3$(CH$_2$)$_6$(CH$_2$)$_2$CH$_2$N−, H$_d$, H$_e$), 1.37 ppm (br. d, CH$_3$(CH$_2$)$_5$CH$_2$(CH$_2$)$_3$N−, H$_f$), 1.18 ppm (br. s, CH$_3$(CH$_2$)$_5$(CH$_2$)$_4$N−, H$_g$, H$_h$, H$_i$, H$_j$, H$_k$), 0.79 ppm (br. s, CH$_3$CH$_2$(CH$_2$)$_8$N−, H$_l$); ^{13}C{^{1}H} NMR (100 MHz, CD$_2$Cl$_2$), δ ppm: 168.9 ($^{Pg/De}$−COCH$_2$N−), 127.6 (−C$_6$H$_5$), 78.1 (−CHCCH$_2$−), 73.3 (−CHCCH$_2$−), 48.5 (CH$_3$(CH$_2$)$_8$CH$_2$N−), 47.3 ($^{Pg/De}$−NCOCH$_2$−), 37.7 (C$_6$H$_5$CH$_2$N−), 36.6 (CH$_3$(CH$_2$)$_7$CH$_2$CH$_2$N−), 31.8 (^{Pg}−CCH$_2$N−), 29.6 and 29.3 (CH$_3$(CH$_2$)$_3$(CH$_2$)$_4$(CH$_2$)$_2$N−), 27.4 and 26.9 (CH$_3$CH$_2$(CH$_2$)$_2$(CH$_2$)$_6$N−), 22.6 (CH$_3$CH$_2$(CH$_2$)$_7$CH$_2$N−), 13.8 (CH$_3$(CH$_2$)$_8$CH$_2$N−).

B.4. Representative Synthetic Procedure for Polypeptoid Homopolymer (P1)

Inside a glovebox, a measured amount of ω-azido hexyl ammonium salt (51 mg, 0.286 mmol, [N$_3$]$_0$: [propargyl]$_0$ = 2:1) was combined with the PNPgG polymer (23 mg, 3 μmol, 0.239 mmol propargyl groups) in a DMF solution, followed by the addition of a measured volume of DMF solution of CuBr/PMDETA (250 mM, 478 μL, [Cu]$_0$:[PMDETA]$_0$:[propargyl]$_0$ = 33:33:100). The reaction mixture was stirred at 50 °C for 18 h. Upon addition of an aqueous solution of EDTA (9.9 mM, 3 mL), the reaction mixture was then dialyzed against deionized water (DI) for 24-48 h during which the DI water was changed twice a day. The reaction mixture was then lyophilized to yield a light greenish blue powder (60 mg, 91% yield). ^{1}H NMR (400 MHz, D$_2$O), δ ppm: 8.01

(br. m, −C=CHN−, H$_d$), 7.22 (br. m, −C$_6$H$_5$, H$_a$), 4.53-4.33 (br. m, −COCH_2N−, −CCH_2N−, H$_b$, H$_c$), 3.58 (s, −NCH_2(CH$_2$)$_5$NH$_3$, H$_b$, H$_c$), 2.98 (br. s, −N(CH$_2$)$_5$CH_2NH$_3$, H$_j$), 1.82 (br. s, −NCH$_2$CH_2(CH$_2$)$_4$NH$_3$, H$_f$), 1.62 (br. s, −N(CH$_2$)$_4$CH_2CH$_2$NH$_3$, H$_i$); 1.34 (br. s, −N(CH$_2$)$_2$CH_2(CH$_2$)$_3$NH$_3$, H$_g$), 1.25 (br. s, −N(CH$_2$)$_3$CH_2(CH$_2$)$_2$NH$_3$, H$_h$).

B.5. Representative Synthetic Procedure for Polypeptoid Homopolymers (G1-G3)

Using a glovebox, a measured amount of ω-azido hexyl guanidinium salt (96 mg, 0.363 mmol, [N$_3$]$_0$: [propargyl]$_0$ = 2:1) was added to a DMF solution containing the PNPgG polymer (23.7 mg, 4 μmol, 0.242 mmol propargyl groups), followed by the addition of a calculated volume of DMF solution of CuBr/PMDETA (250 mM, 484 μL, [Cu]$_0$:[PMDETA]$_0$:[propargyl]$_0$ = 33:33:100). The reaction mixture was allowed to stir at 50 °C for 18 h. An aqueous solution of EDTA (9.9 mM, 3 mL) was added to the reaction mixture and then dialyzed against DI water for 24-48 h during which the DI water was changed twice a day. The final reaction mixture was then lyophilized to yield a light greenish blue powder (60 mg, 68% yield). ^{1}H NMR (400 MHz, D$_2$O), δ ppm: 8.01 (br. m, −C=CHN−, H$_d$), 7.22 (br. m, −C$_6$H$_5$, H$_a$), 4.53-4.33 (br. m, −COCH_2N−, −CCH_2N−, H$_b$, H$_c$), 3.58 (s, −NCH_2(CH$_2$)$_5$C(NH)$_2$NH$_2$, H$_e$), 2.98 (br. s, −N(CH$_2$)$_5$CH_2C(NH)$_2$NH$_2$, H$_j$), 1.82 (br. s, −NCH$_2$CH_2(CH$_2$)$_4$C(NH)$_2$NH$_2$, H$_f$), 1.62 (br. s, −N(CH$_2$)$_4$CH_2CH$_2$C(NH)$_2$NH$_2$, H$_i$); 1.34 (br. s, −N(CH$_2$)$_2$CH_2(CH$_2$)$_3$C(NH)$_2$NH$_2$, H$_g$), 1.25 (br. s, −N(CH$_2$)$_3$CH_2(CH$_2$)$_2$C(NH)$_2$NH$_2$, H$_h$).

B.6. Representative Synthetic Procedure for Polypeptoid Random Copolymer (GD48)

In a glovebox, a fixed amount of ω-azido hexyl guanidinium salt (117 mg, 0.440 mmol, [N$_3$]$_0$: [propargyl]$_0$ = 2:1) was added into a DMF solution of PNPG$_{39}$-r-PNDG$_9$

(31.0 mg, 5 μmol, 0.22 mmol propargyl groups), succeeded by the addition of a measured volume of CuBr/PMDETA in DMF solution (250 mM, 460 μL [Cu]$_0$:[PMDETA]$_0$:[propargyl]$_0$= 33:33:100). The reaction mixture stirred for 18 h at 50 °C. Upon addition of an aqueous solution of EDTA (9.9 mM, 3 mL), the reaction mixture was dialyzed for 24-48 h against DI water during which the DI water was changed twice a day. The reaction mixture was then lyophilized to yield a light green powder (95 mg, 80% yield). ^{1}H NMR (400 MHz, D$_2$O), δ ppm: 8.10-8.01 (br. m, −C=CHN−, H$_o$), 7.32-7.21 (br. m, −C$_6$$H_5$, H$_a$), 4.55-4.33 (br. m, −COCH_2N−, −CCH_2N−, H$_b$, H$_m$, H$_n$), 3.46 (s, −NCH_2(CH$_2$)$_5$C(NH)$_2$NH$_2$, H$_p$), 3.04 [br. s, (−NCH_2(CH$_2$)$_8$CH$_3$, −N(CH$_2$CH_2)(CH$_2$)$_7$CH$_3$), −NCH$_2$CH_2(CH$_2$)$_4$C(NH)$_2$NH$_2$, −N(CH$_2$)$_5$CH_2C(NH)$_2$NH$_2$, H$_c$, H$_d$, H$_q$, H$_u$], 2.31 [br. s, (−N(CH$_2$)$_2$CH_2(CH$_2$)$_3$C(NH)$_2$NH$_2$, −N(CH$_2$)$_2$ (CH$_2$CH_2)(CH$_2$)$_2$C(NH)$_2$NH$_2$, −N(CH$_2$)$_4$CH_2CH$_2$C(NH)$_2$NH$_2$), H$_r$-H$_t$], 1.22 (br. m, −N(CH$_2$)$_2$(CH_2)$_7$CH$_3$, H$_e$-H$_k$), 0.70-0.79 (br. m, −NCH$_2$(CH$_2$)$_8$CH_3, H$_i$).

B.7. Determination of Copper Ion Content in the Polymers by Flame Atomic Absorption Spectrometry (FAAS)

Polypeptoids (10 mg) were dissolved in deionized water at 1 mg mL^{-1}. The solution was analyzed by FAAS. The copper ion content was then determined by using the copper (II) absorption at 324.8 nm against a calibration curve constructed using a CuSO$_4$ standard.
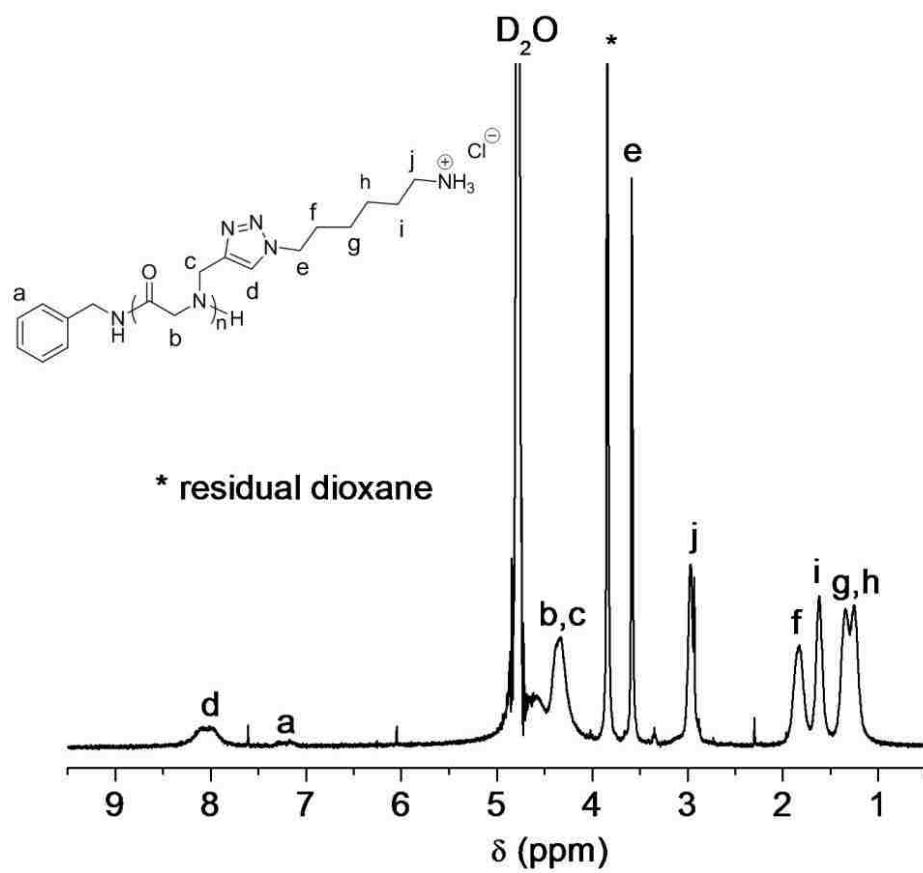
Figure B.7. Representative ^{1}H NMR spectrum of **P54** in D$_2$O.
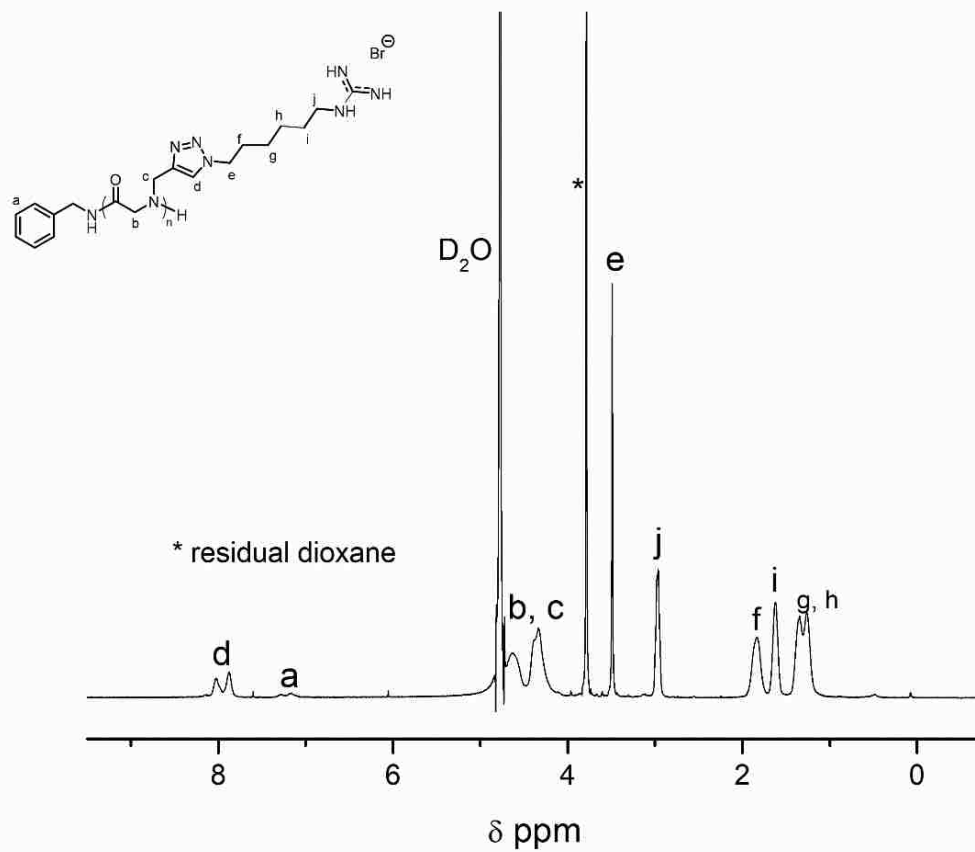
Figure B.8. Representative ^{1}H NMR spectrum of **G30** in D$_2$O.
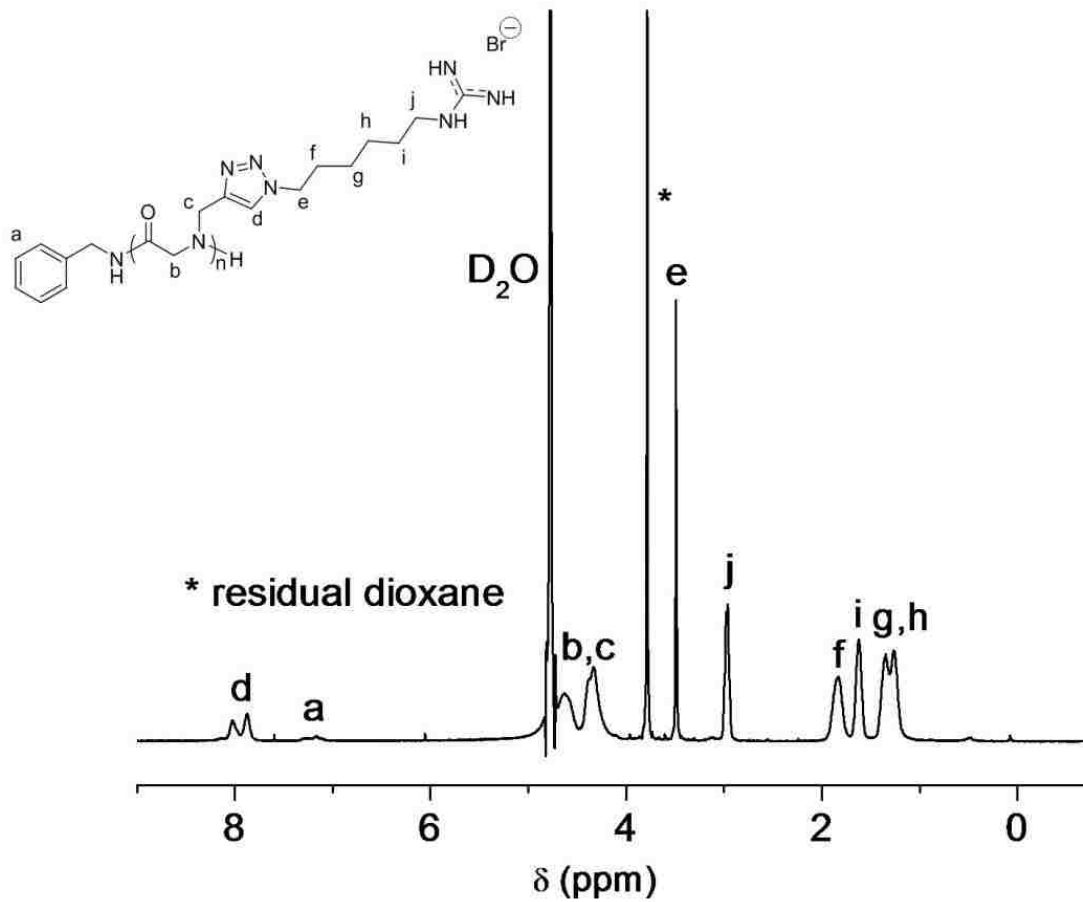
Figure B.9. Representative ^{1}H NMR spectrum of **G54** in D$_2$O.
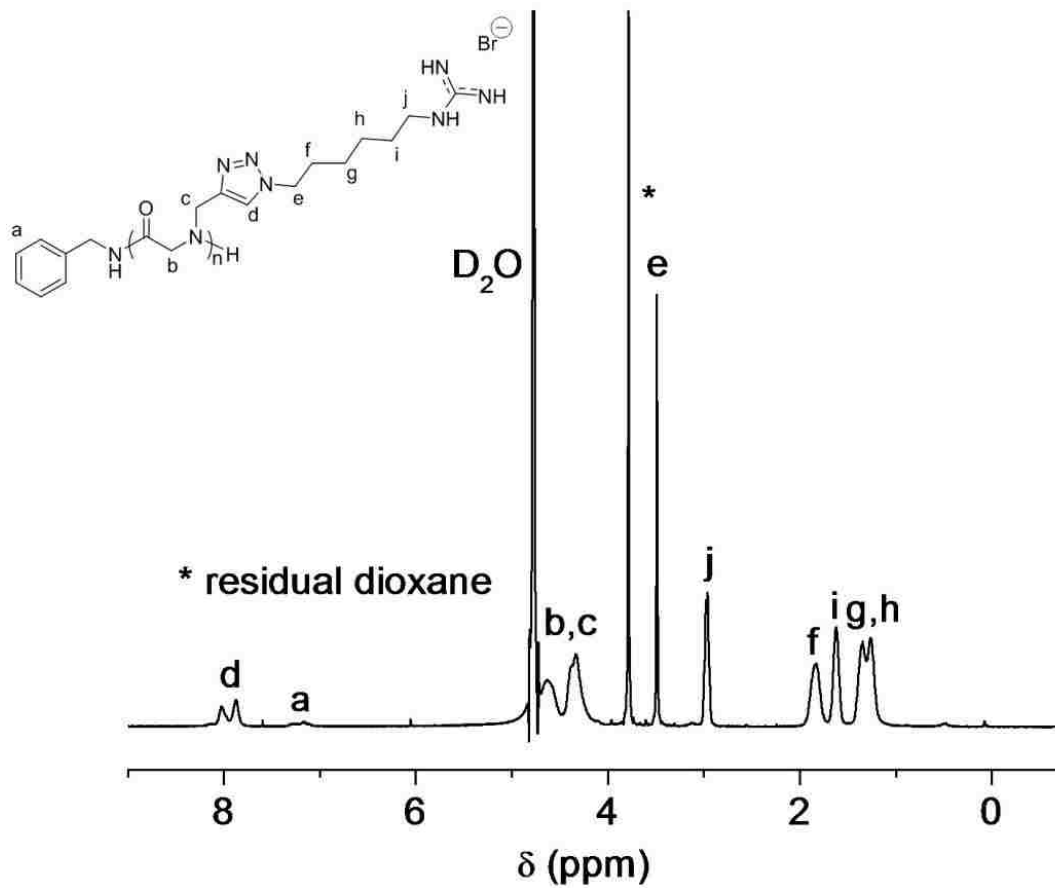
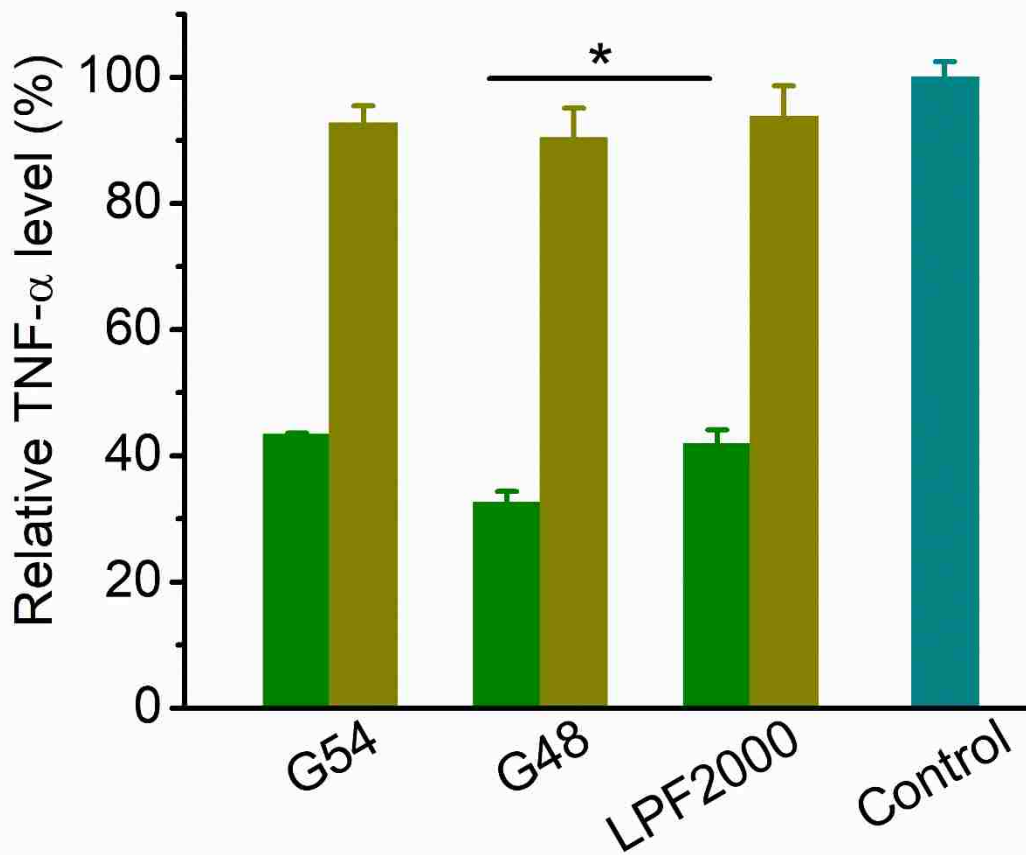Figure B.10. Representative ^{1}H NMR spectrum of **G103** in D$_2$O.
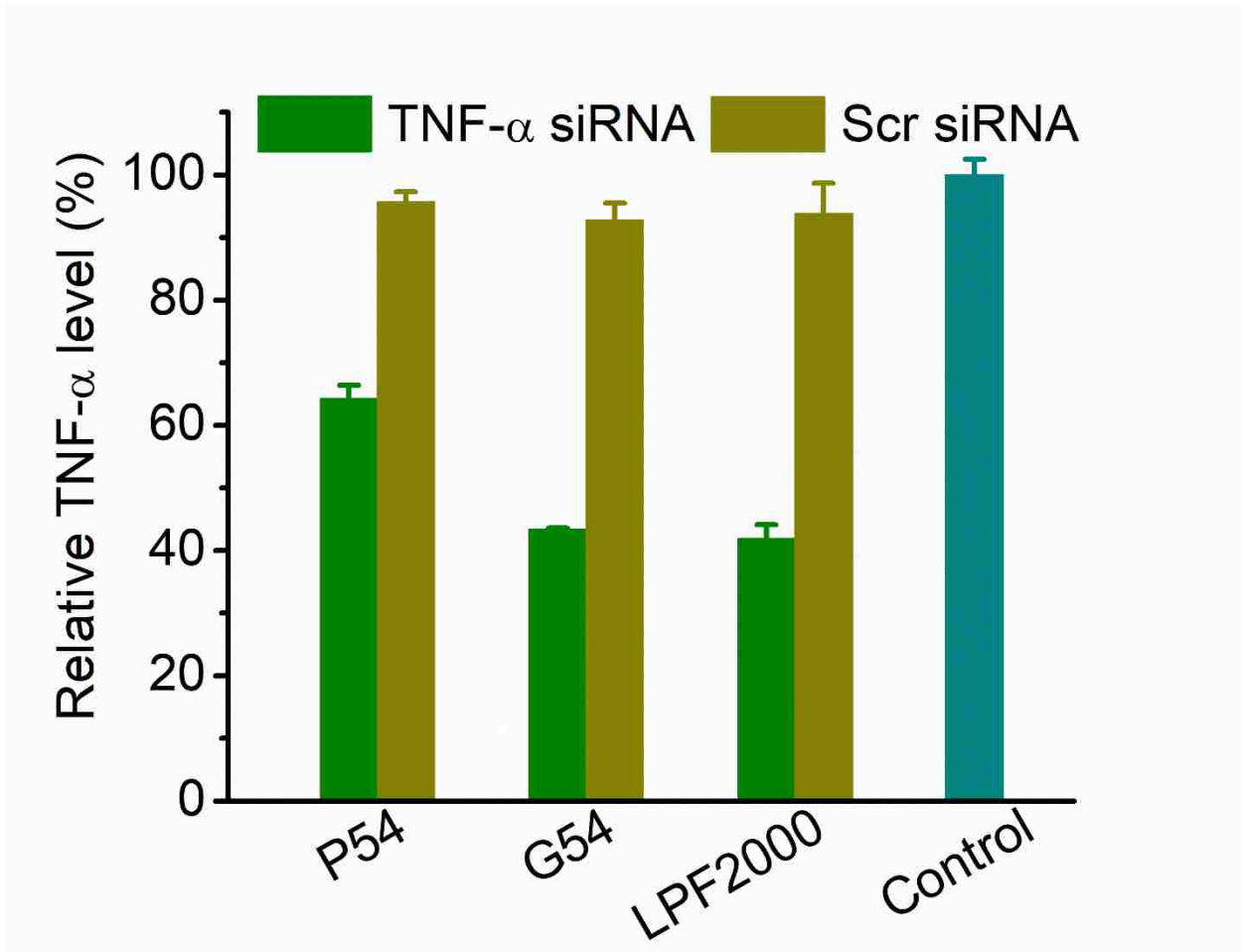
Figure B.11. TNF-α levels of RAW 264.7 cells following treatment with polypeptoids/TNF-α siRNA polyplexes for 4 h at 0.2 μg/well siRNA in DMEM containing 10% FBS, incubation in fresh media for 20 h, and subsequent LPS stimulation at 100 ng/mL for 5 h (n = 3).
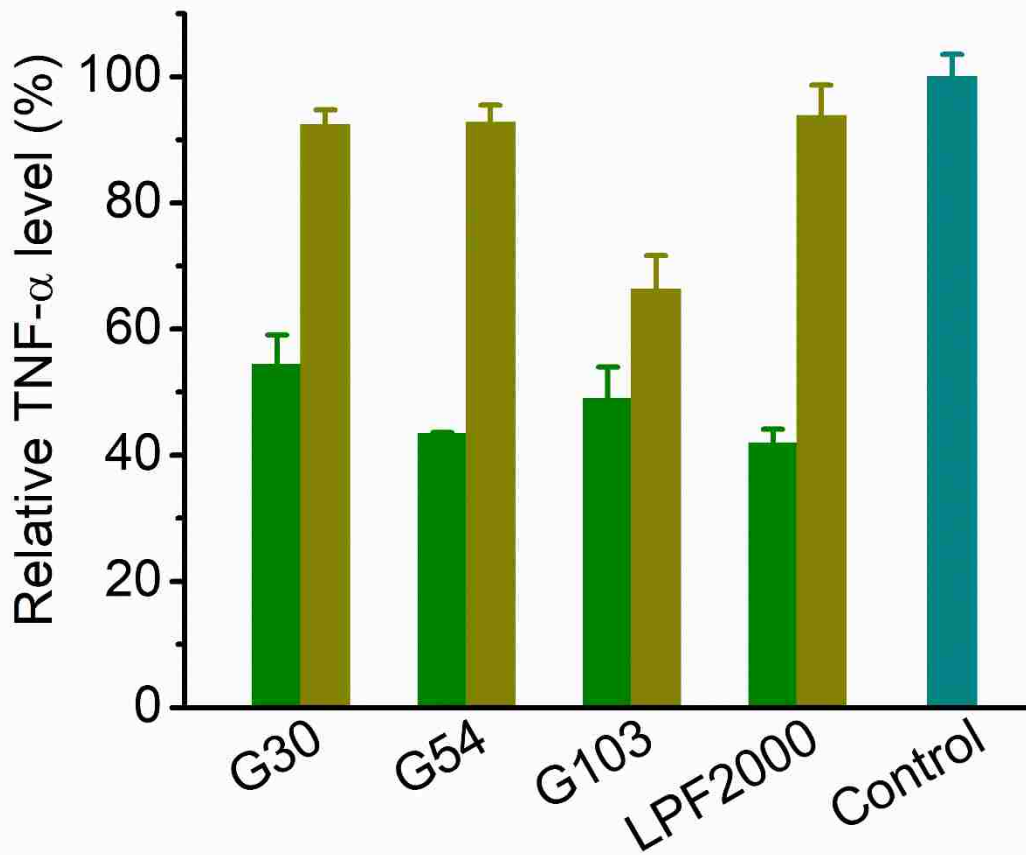
Figure B.12. TNF-α levels of RAW 264.7 cells following treatment with polypeptoids/TNF-α siRNA polyplexes for 4 h at 0.2 μg/well siRNA in DMEM containing 10% FBS, incubation in fresh media for 20 h, and subsequent LPS stimulation at 100 ng/mL for 5 h (n = 3).

Figure B.13. TNF-α levels of RAW 264.7 cells following treatment with polypeptoids/TNF-α siRNA polyplexes for 4 h at 0.2 μg/well siRNA in DMEM containing 10% FBS, incubation in fresh media for 20 h, and subsequent LPS stimulation at 100 ng/mL for 5 h (n = 3).
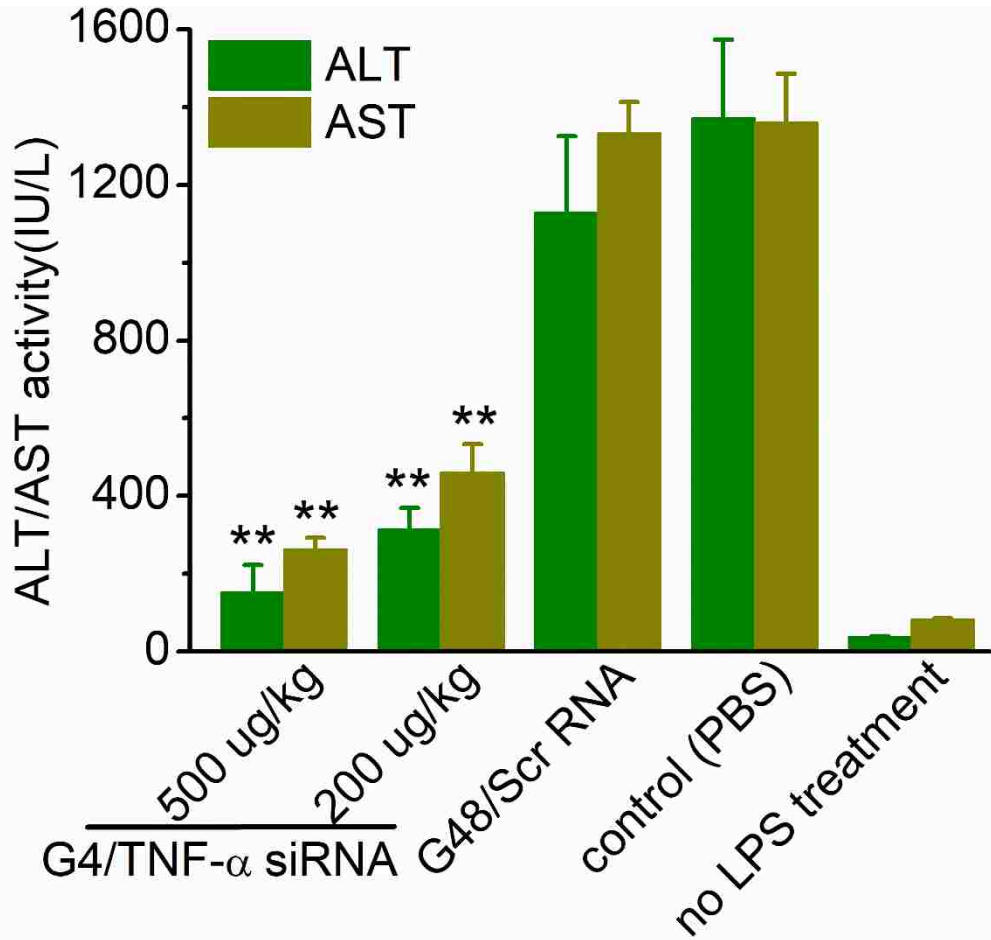
Figure B.14. Systemically administered G4/TNF-α siRNA polyplexes mediate anti-inflammatory effect against LPS/D-GalN-induced hepatic failure: serum ALT and AST levels.
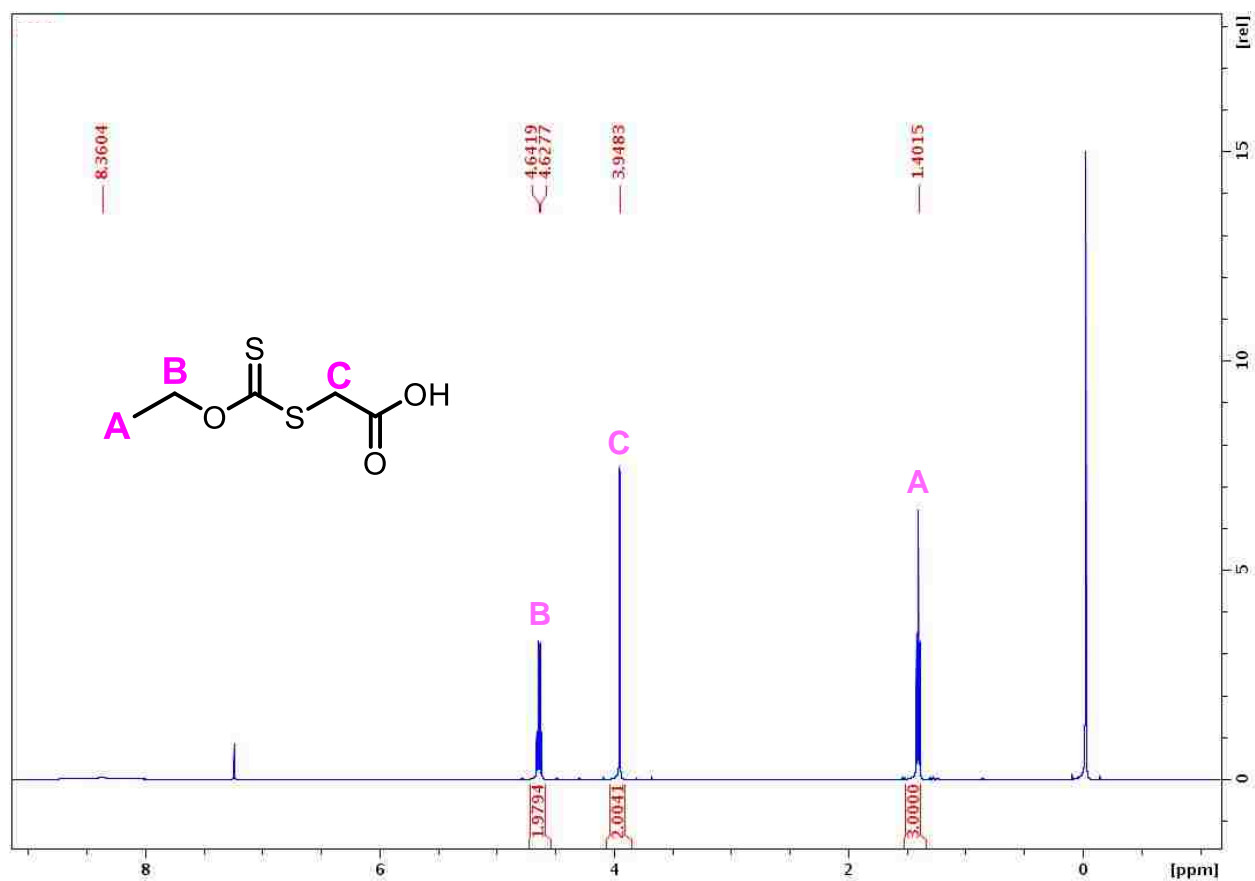
Figure C.1. ^{1}H NMR spectrum of XAA in CDCl$_3$.
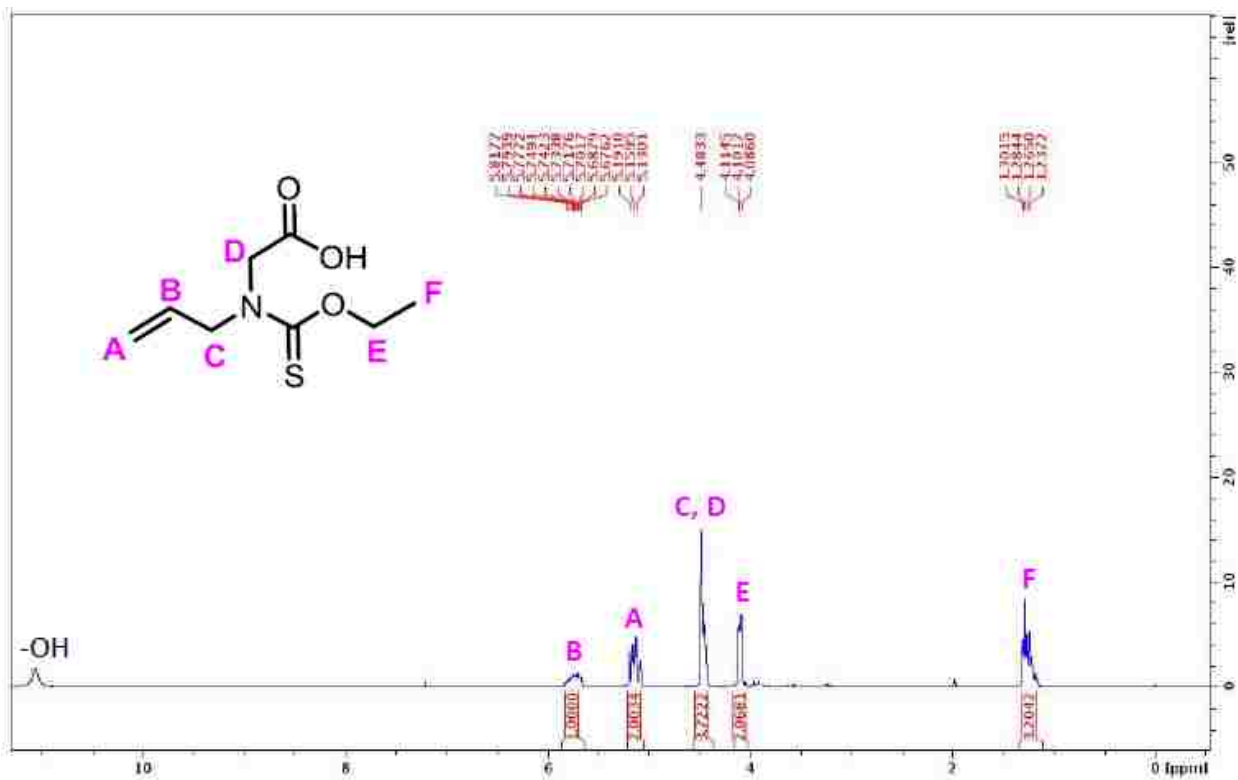
Figure C.2. ^{1}H NMR spectrum of N-ethoxythiocarbonyl-N-allylglycine (N-Al-XAA) in CDCl$_3$.
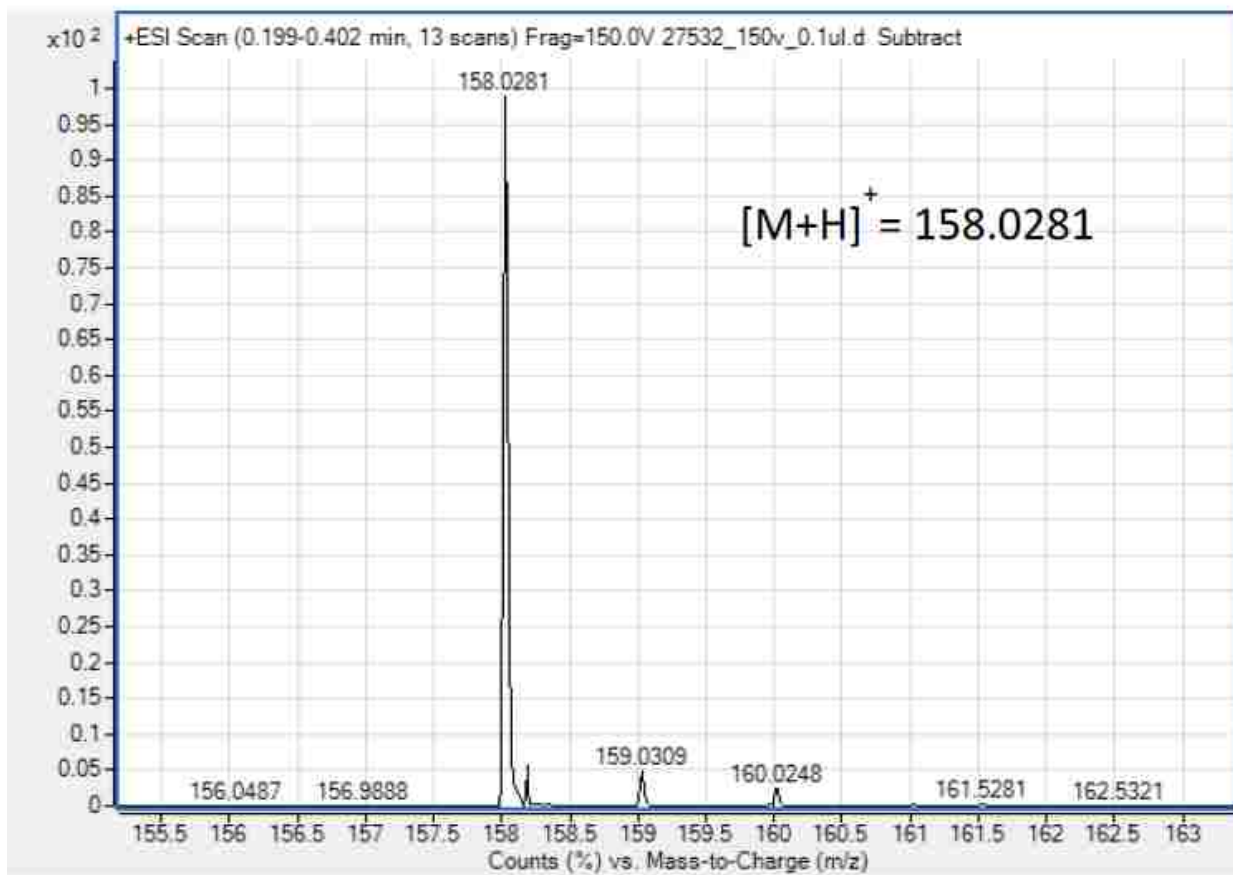
Figure C.3. High resolution ESI-MS of N-Allyl NTA monomer.
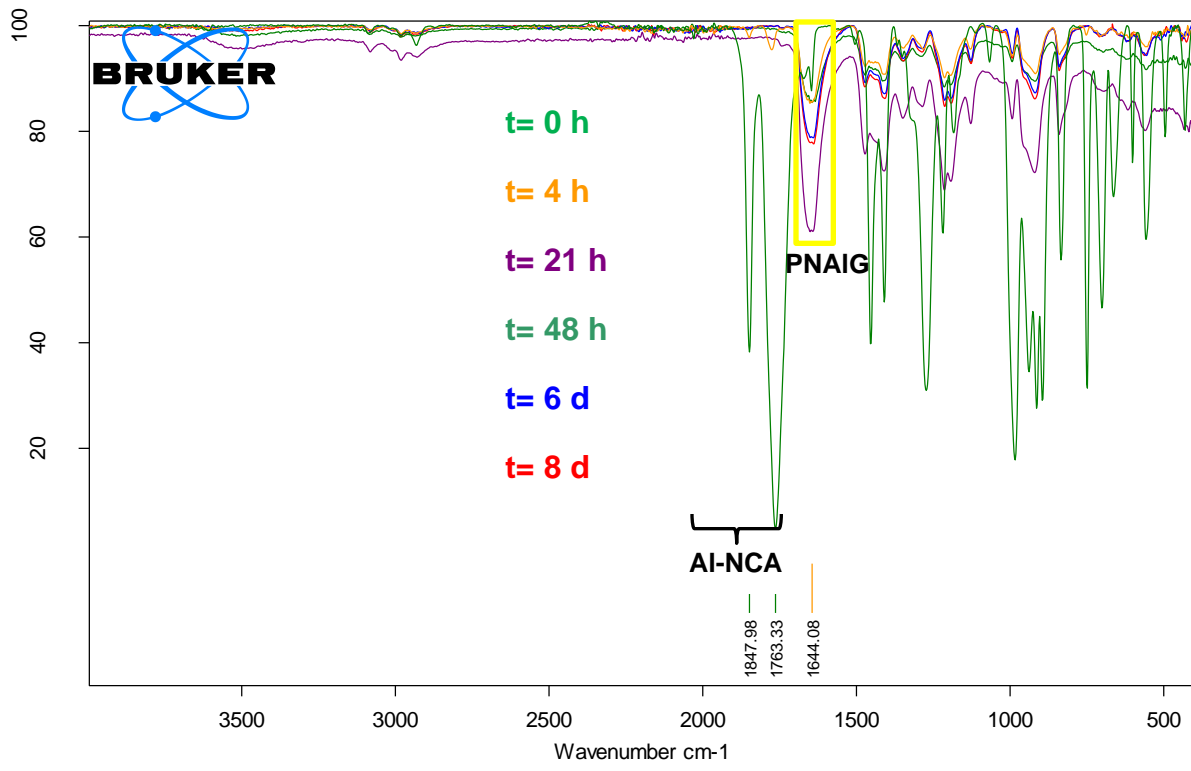
Figure C.4. FT-IR spectra of Al-NCA monomer conversion over time (in neat).
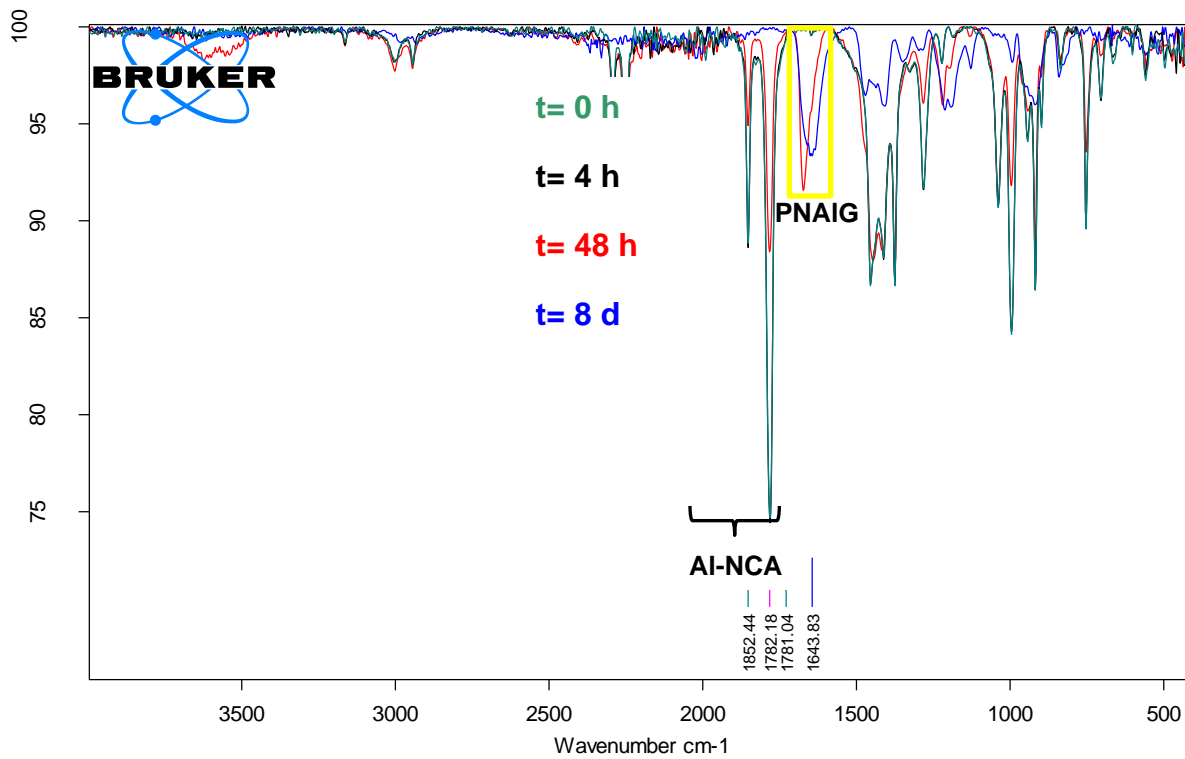
Figure C.5. FT-IR spectra of Al-NCA monomer conversion over time in THF at 0.5M.
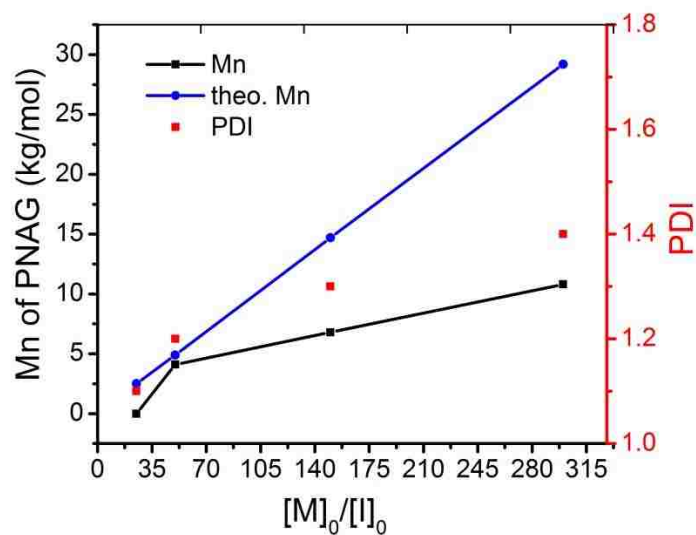
Figure C.6. Plot of Mn versus $[M]_0{:}[I]_0$ and PDI for the BnNH$_2$ mediated ROP of Allyl NTA in THF at 60 $^{\circ}$C.
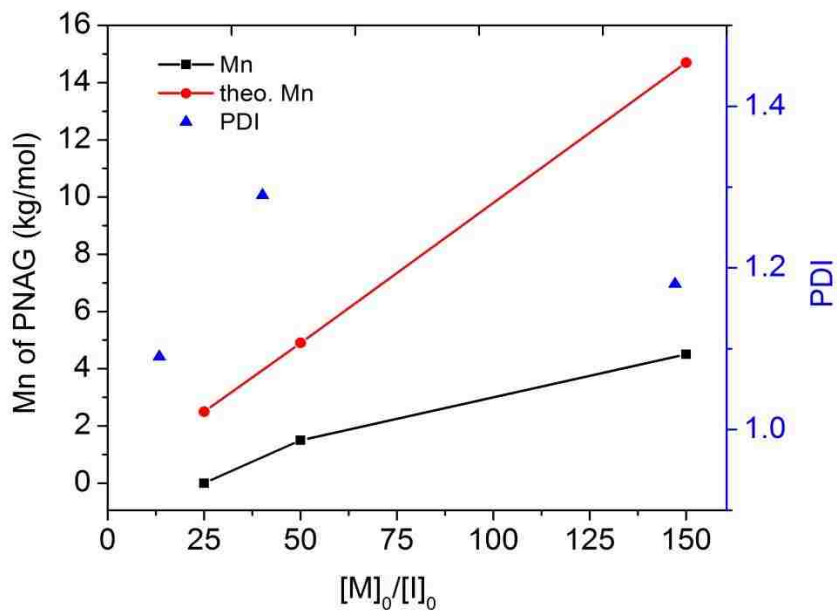
Figure C.7. Plot of Mn versus $[M]_0{:}[I]_0$ and PDI for the BnNH$_2$ mediated ROP of Allyl NTA in THF at 50 $^{\circ}$C.
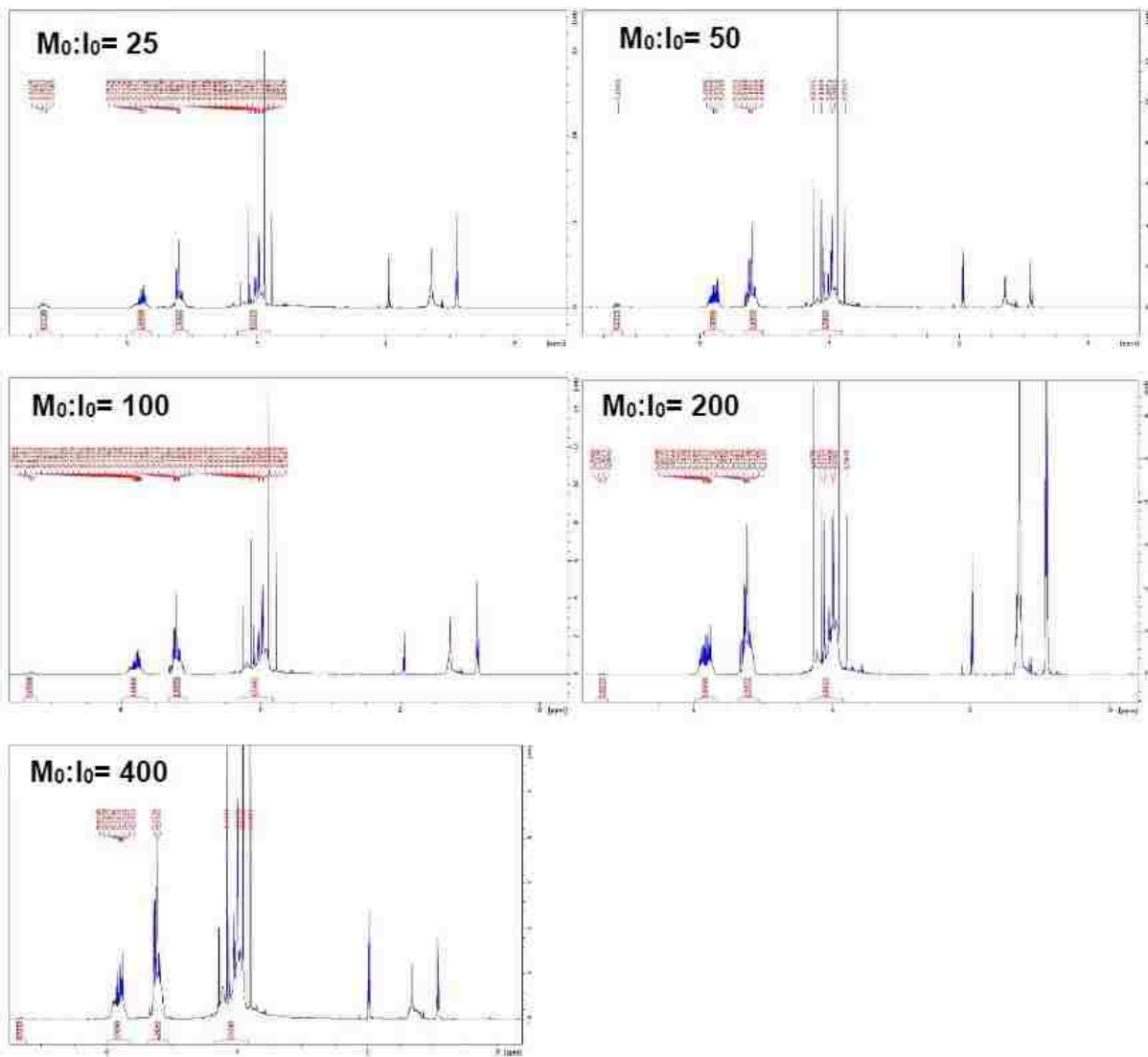
Figure C.8. ^{1}H NMR spectra of Benzylamine mediated iROPs with Al-NTA at 90 ºC in CDCN$_3$ (M$_0$:I$_0$= 25-400). Final polymer chain length cannot be accurately determined by end-group analysis method due to severe overlap of monomer and polymer peaks.

APPENDIX D: COPYRIGHT RELEASE

**JOHN WILEY AND SONS LICENSE
TERMS AND CONDITIONS**

Dec 05, 2017

This Agreement between Dr. Jessica Simpson ("You") and John Wiley and Sons ("John Wiley and Sons") consists of your license details and the terms and conditions provided by John Wiley and Sons and Copyright Clearance Center.

License Number	4242620694207
License date	Dec 05, 2017
Licensed Content Publisher	John Wiley and Sons
Licensed Content Publication	Advanced Functional Materials
Licensed Content Title	Intracellularly Disintegratable Polysulfoniums for Efficient Gene Delivery
Licensed Content Author	Dingcheng Zhu,Huijie Yan,Xin Liu,Jiajia Xiang,Zhuxian Zhou,Jianbin Tang,Xiangrui Liu,Youqing Shen
Licensed Content Date	Mar 10, 2017
Licensed Content Pages	1
Type of use	Dissertation/Thesis
Requestor type	University/Academic
Format	Electronic
Portion	Figure/table
Number of figures/tables	1
Original Wiley figure/table number(s)	Scheme 2
Will you be translating?	No
Title of your thesis / dissertation	Synthesis, Characterization, and Assessment of Cationic Polypeptoids Towards Gene Delivery and Development of Air Stable N-Substituted N-Thiocarboxyanhydrides
Expected completion date	May 2018
Expected size (number of pages)	215
Requestor Location	Dr. Jessica Simpson 2225 College Drive Apt 184-1 ARLINGTON, LA 70808 United States Attn: Dr. Jessica Simpson
Publisher Tax ID	EU826007151
Billing Type	Invoice
Billing Address	Dr. Jessica Simpson 2225 College Drive Apt 184-1 ARLINGTON, LA 70808 United States Attn: Dr. Jessica Simpson

ELSEVIER LICENSE
TERMS AND CONDITIONS

Dec 05, 2017

This Agreement between Dr. Jessica Simpson ("You") and Elsevier ("Elsevier") consists of your license details and the terms and conditions provided by Elsevier and Copyright Clearance Center.

License Number	4242630084189
License date	Dec 05, 2017
Licensed Content Publisher	Elsevier
Licensed Content Publication	Colloids and Surfaces B: Biointerfaces
Licensed Content Title	pH and redox dual-responsive multifunctional gene delivery with enhanced capability of transporting DNA into the nucleus
Licensed Content Author	Zhe Yang,Yingqin Li,Jinbiao Gao,Zhong Cao,Qing Jiang,Jie Liu
Licensed Content Date	1 May 2017
Licensed Content Volume	153
Licensed Content Issue	n/a
Licensed Content Pages	12
Start Page	111
End Page	122
Type of Use	reuse in a thesis/dissertation
Portion	figures/tables/illustrations
Number of figures/tables/illustrations	1
Format	electronic
Are you the author of this Elsevier article?	No
Will you be translating?	No
Original figure numbers	Figure 1A
Title of your thesis/dissertation	Synthesis, Characterization, and Assessment of Cationic Polypeptoids Towards Gene Delivery and Development of Air Stable N-Substituted N-Thiocarboxyanhydrides
Expected completion date	May 2018
Estimated size (number of pages)	215
Requestor Location	Dr. Jessica Simpson 2225 College Drive Apt 184-I

ARLINGTON, LA 70808 United States Attn: Dr. Jessica Simpson |
| Publisher Tax ID | 98-0397604 |
| Total | 0.00 USD |

Terms and Conditions

206

ACS Publications
Most Trusted. Most Cited. Most Read.

Title: Cationic Polypeptoids with Optimized Molecular Characteristics toward Efficient Nonviral Gene Delivery

Author: Lipeng Zhu, Jessica M. Simpson, Xin Xu, et al

Publication: Applied Materials

Publisher: American Chemical Society

Date: Jul 1, 2017

Copyright © 2017, American Chemical Society

PERMISSION/LICENSE IS GRANTED FOR YOUR ORDER AT NO CHARGE

This type of permission/license, instead of the standard Terms & Conditions, is sent to you because no fee is being charged for your order. Please note the following:

- Permission is granted for your request in both print and electronic formats, and translations.
- If figures and/or tables were requested, they may be adapted or used in part.
- Please print this page for your records and send a copy of it to your publisher/graduate school.
- Appropriate credit for the requested material should be given as follows: "Reprinted (adapted) with permission from (COMPLETE REFERENCE CITATION). Copyright (YEAR) American Chemical Society." Insert appropriate information in place of the capitalized words.
- One-time permission is granted only for the use specified in your request. No additional uses are granted (such as derivative works or other editions). For any other uses, please submit a new request.

BACK | CLOSE WINDOW

ELSEVIER LICENSE
TERMS AND CONDITIONS

Dec 12, 2017

This Agreement between Dr. Jessica Simpson ("You") and Elsevier ("Elsevier") consists of your license details and the terms and conditions provided by Elsevier and Copyright Clearance Center.

License Number	4246621331779
License date	Dec 12, 2017
Licensed Content Publisher	Elsevier
Licensed Content Publication	Carbohydrate Polymers
Licensed Content Title	Modified-epsilon-polylysine-grafted-PEI-β-cyclodextrin supramolecular carrier for gene delivery
Licensed Content Author	Pin Lv,Cheng Zhou,Yulin Zhao,Xiali Liao,Bo Yang
Licensed Content Date	Jul 15, 2017
Licensed Content Volume	168
Licensed Content Issue	n/a
Licensed Content Pages	9
Start Page	103
End Page	111
Type of Use	reuse in a thesis/dissertation
Portion	figures/tables/illustrations
Number of figures/tables/illustrations	1
Format	both print and electronic
Are you the author of this Elsevier article?	No
Will you be translating?	No
Original figure numbers	Scheme 1
Title of your thesis/dissertation	Synthesis, Characterization, and Assessment of Cationic Polypeptoids Towards Gene Delivery and Development of Air Stable N-Substituted N-Thiocarboxyanhydrides
Expected completion date	May 2018
Estimated size (number of pages)	215
Requestor Location	Dr. Jessica Simpson 2225 College Drive Apt 184-I ARLINGTON, LA 70808 United States Attn: Dr. Jessica Simpson
Publisher Tax ID	98-0397604
Total	0.00 USD

Terms and Conditions

208

License Number	4317831363484
License date	Mar 28, 2018
Licensed Content Publisher	Royal Society of Chemistry
Licensed Content Publication	Polymer Chemistry
Licensed Content Title	Synthesis and characterization of thermo-responsive polypeptoid bottlebrushes
Licensed Content Author	Samuel H. Lahasky,Lu Lu,Wayne A. Huberty,Jinbao Cao,Li Guo,Jayne C. Garno,Donghui Zhang
Licensed Content Date	Oct 30, 2013
Licensed Content Volume	5
Licensed Content Issue	4
Type of Use	Thesis/Dissertation
Requestor type	academic/educational
Portion	figures/tables/images
Number of figures/tables/images	1
Format	electronic
Distribution quantity	1000
Will you be translating?	no
Order reference number	
Title of the thesis/dissertation	Synthesis, Characterization, and Assessment of Cationic Polypeptoids Towards Gene Delivery and Development of Air Stable N-Substituted N-Thiocarboxyanhydrides
Expected completion date	May 2018
Estimated size	215
Requestor Location	Dr. Jessica Simpson 2225 College Drive Apt 184-I ARLINGTON, LA 70808 United States Attn: Dr. Jessica Simpson
Billing Type	Invoice
Billing Address	Dr. Jessica Simpson 2225 College Drive Apt 184-I ARLINGTON, LA 70808 United States Attn: Dr. Jessica Simpson
Total	0.00 USD

209

PERMISSION/LICENSE IS GRANTED FOR YOUR ORDER AT NO CHARGE

This Agreement between Dr. Jessica Simpson ("You") and Elsevier ("Elsevier") consists of your license details and the terms and conditions provided by Elsevier and Copyright Clearance Center

License Number	4317850742698
License date	Mar 28, 2018
Licensed Content Publisher	Elsevier
Licensed Content Publication	European Polymer Journal
Licensed Content Title	Alkyne-X modification of polypeptoids
Licensed Content Author	Christian Secker, Joshua W. Robinson, Helmut Schlaad
Licensed Content Date	Jan 1, 2015
Licensed Content Volume	62
Licensed Content Issue	n/a
Licensed Content Pages	6
Start Page	394
End Page	399
Type of Use	reuse in a thesis/dissertation
Intended publisher of new work	other
Portion	figures/tables/illustrations
Number of figures/tables/illustrations	1
Format	electronic
Are you the author of this Elsevier article?	No
Will you be translating?	No
Title of your thesis/dissertation	Synthesis, Characterization, and Assessment of Cationic Polypeptoids Towards Gene Delivery and Development of Air Stable N-Substituted N-Thiocarboxyanhydrides
Expected completion date	May 2018
Estimated size (number of pages)	215
Requestor Location	Dr. Jessica Simpson 2225 College Drive Apt 104-I ARLINGTON, LA 70808 United States Attn: Dr. Jessica Simpson
Publisher Tax ID	98-0397604
Total	0.00 USD
Terms and Conditions	

211

VITA

Jessica Simpson was born and raised in Marietta, Georgia. She received her Bachelor of Science degree in Chemistry from Fort Valley State University in 2012. Jessica joined Professor Donghui Zhang's group in Spring of 2013 to start her graduate research at Louisiana State University. Her research interests focuses on the development and characterization of cationic polypeptoid towards biological applications, particularly nonviral gene delivery. A new NTA monomer was developed by Jessica. She anticipates graduating with her Ph.D. degree in May 2018.